

ABSTRACT

CHEN, CHIH-YUAN. Synthetic Metallobacteriochlorins with Site-specific Isotopic Substitution for Probing Photosynthetic Function. (Under the direction of Professor Jonathan S. Lindsey).

Bacteriochlorophylls – natural pigments for absorption of near-infrared (NIR) light – underlie light-absorption and energy transduction in photosynthetic bacteria. Understanding photosynthetic function including the capture and utilization of light is essential for applications ranging from artificial photosynthesis to photomedicine (photodynamic therapy, imaging, and diagnostics). Previous synthetic limitations have largely precluded access to bacteriochlorin model compounds suitable for probing photosynthetic function. A recently developed *de novo* synthesis of stable bacteriochlorins employs the self-condensation of a dihydrodipyrin–acetal, which is prepared from simple precursors such as a pyrrole-2-carboxaldehyde and an α,β -unsaturated ketone–acetal. The success of the *de novo* synthesis to synthetic bacteriochlorins has opened the door to the study of fundamental properties and pursuit of a range of photochemical applications. However, accessibility to metallobacteriochlorins has remained limited.

Access to metallobacteriochlorins is essential for investigation of a wide variety of fundamental photochemical processes, yet relatively few synthetic metallobacteriochlorins have been prepared. Members of a set of synthetic bacteriochlorins bearing 0–4 carbonyl groups (1, 2, or 4 carboethoxy substituents, or an annulated imide moiety) were examined under two conditions: (i) standard conditions for zincation of porphyrins [$\text{Zn}(\text{OAc})_2 \cdot 2\text{H}_2\text{O}$ in DMF at 60–80 °C], and (ii) treatment in THF with a strong base (e.g., NaH or LDA) followed by a metal reagent MX_n . Zincation of bacteriochlorins that bear 2–4 carbonyl groups proceeded under the former method whereas those with 0–2 carbonyl groups

proceeded with NaH or LDA/THF followed by Zn(OTf)₂. The scope of metalation (via NaH or LDA in THF) is as follows: (a) for bacteriochlorins that bear two electron-releasing aryl groups, M = Cu, Zn, Pd, and InCl (but not Mg, Al, Ni, Sn, or Au); (b) for bacteriochlorins that bear two carboethoxy groups, M = Ni, Cu, Zn, Pd, Cd, InCl, and Sn (but not Mg, Al or Au); and (c) a bacteriochlorin with four carboethoxy groups was metalated with Mg (other metals were not examined). Altogether, 15 metallochlorins were isolated and characterized. The availability of diverse metallochlorins should prove useful in a variety of fundamental photochemical studies and applications.

The concise *de novo* synthesis enables site-specific incorporation of isotopes about the bacteriochlorin macrocycle; for a singly substituted dihydrodipyrin–acetal, the corresponding bacteriochlorin contains a pair of isotopic substitutions located at positions symmetrically disposed by 180° rotation about the normal to the plane of the macrocycle. With successful methods for preparing metallochlorins in hand, a series of synthetic metallochlorins have been prepared that bear minimal substituents (to minimize spectral complexity) and incorporate ¹³C/¹⁵N isotopes in the inner resonance frame of bacteriochlorin π-system. In total, 24 isotopically substituted bacteriochlorins were synthesized. The Cu chelates of the isotopologues have been examined by IR and resonance Raman spectroscopies with the aim of assigning the vibrations of the macrocycle. The π-cation radicals of the Zn chelates of the isotopologues have been examined via electron paramagnetic resonance spectroscopy with the aim of elucidating the spin density in the macrocycle. Together, the vibrational and spin-density characteristics should aid in probing photosynthetic function of bacteriochlorophylls in natural systems.

Another challenge in probing photosynthetic function involves reconstructing/mimicking the natural photosynthetic reaction complex that conveys photochemical activities. The desired photochemical features may be best elicited with multicomponent architectures that support efficient excited-state energy and/or electron transfer, yet few such arrays containing bacteriochlorins (the core chromophore of bacteriochlorophylls) are known. The thesis also outlines three synthetic approaches toward bacteriochlorins, surveys all known bacteriochlorin arrays, and compares molecular design strategies for light-harvesting arrays containing bacteriochlorins versus (the better known) porphyrins.

© Copyright 2014 Chih-Yuan Chen

All Rights Reserved

Synthetic Metallobacteriochlorins with Site-specific Isotopic Substitution for Probing
Photosynthetic Function

by
Chih-Yuan Chen

A dissertation submitted to the Graduate Faculty of
North Carolina State University
in partial fulfillment of the
requirements for the degree of
Doctor of Philosophy

Chemistry

Raleigh, North Carolina

2014

APPROVED BY:

Jonathan S. Lindsey
Committee Chair

Jerry L. Whitten

Daniel L. Comins

David A. Shultz

DEDICATION

This thesis is dedicated to the memory of Dr. Tong-Ing Ho.

BIOGRAPHY

Chih-Yuan Chen was born in Taipei, Taiwan on January 24, 1979 to Ching-Chuan Chen and Mei-Hua Lin. Chih-Yuan earned a B.S. degree in chemistry from National Tsing Hua University in July 2001. Subsequently he joined Dr Tong-Ing Ho's group at National Taiwan University. The thesis titled "Electrogenerated Chemiluminescence of Stilbene Intramolecular Charge Transfer Systems" earned Chih-Yuan a M.S. degree in Chemistry in July 2003.

Upon graduation, he joined Chemical Infantry Division, ROC Army as a corporal for the mandatory military service in Taiwan. Being assigned to establish a web-based database server during the service, Chih-Yuan received a "Sixth Army Corps Exemplar Medal" in 2004.

In 2005, Chih-Yuan returned to Dr Tong-Ing Ho's group where he worked as a teaching assistant/lecturer. On December 14 2005, Dr. Tong-Ing Ho deceased at age of 55 by brain tumor. Chih-Yuan turned to work at Taiwan Semiconductor Manufacturing Company (TSMC) as a process engineer in photolithography. The work at TSMC earned Chih-Yuan an "Outstanding Contribution Award" in 2007.

Starting from 2009, Chih-Yuan started his PhD studies and joined Dr. Jonathan S. Lindsey's group at North Carolina State University. The focus of his research work is the synthetic bacteriochlorins for photophysical/photochemical studies.

ACKNOWLEDGMENTS

My deepest gratitude to those who never stop helping me in work, in life,

Advisor

Jonathan S. Lindsey

Lab members & Collaborators

Masahiko Taniguchi, Chandrashaker Vanampally

Michael Krayner, Olga Mass

David F. Bocian, Dewey Holten

Committee members

Jerry L. Whitten, Daniel L. Comins, David A. Shultz

Cynthia L. Hemenway, Hanna Gracz

Family & friends

Ching-Chuang Chen, Mei-Hua Lin

Chih-Hsiang Chen, Chih-Hao Chen

Chun-Yu Lin, Yi-Li Kuo

Le Li, Yu-An Chen

Yan-Ting Chen, Chien-You Chen

Yi-Ting Chen, You-Ting Chen

TABLE OF CONTENTS

	Page #
LIST OF FIGURES	viii
LIST OF SCHEMES.....	x
LIST OF CHARTS	xi
LIST OF TABLES.....	xii
LIST OF EQUATIONS	xiii
Chapter 1 General Introduction	1
Introduction.....	1
Absorption Properties and Four-orbital Model.....	2
Study of Properties of Bacteriochlorins.....	11
References.....	14
Chapter 2 Synthesis and Physicochemical Properties of Metallobacteriochlorins.....	16
Introduction.....	16
Results and Discussion	20
(I) Bacteriochlorin Synthesis	20
(II) Bacteriochlorin Metalation.....	24
1. Literature Methods for Metal Insertion.Introduction.....	24
2. Metal Insertion Studies	28

(III) Structural and Physicochemical Characteristics	40
1. Structural Analysis.....	40
2. Spectral Properties	43
3. Photophysical Properties.....	48
4. Electrochemical and Molecular Orbital Characteristics	52
Conclusions and Outlook	55
Experimental Section	58
References.....	86
Chapter 3 Rational Synthesis of 24 Bacteriochlorin Isotopologues Each Containing a Symmetrical Pair of ¹³ C or ¹⁵ N Atoms in the Inner Core of the Macrocycle	96
Introduction.....	96
Results and Discussion	101
(I) Retrosynthetic Analysis	102
(II) Synthesis.....	103
(III) Chemical Characterization	112
Conclusions.....	119
Experimental Section	120
References.....	164
Chapter 4 Tapping the Near-Infrared Spectral Region with Bacteriochlorin Arrays	172
Introduction.....	172

Bacteriochlorin building blocks.....	175
Bacteriochlorin-containing dyads.....	177
Energy transfer in porphyrin versus hydroporphyrin arrays.....	187
Outlook.....	188
References.....	189

LIST OF FIGURES

Figure 1.1.	Representative absorption spectra of a porphyrin (hematin), chlorin (chlorophyll <i>a</i>), and bacteriochlorin (bacteriochlorophyll <i>a</i>)	3
Figure 1.2.	(a) The HOMO and LUMO of tetrapyrroles; (b) energy diagram thereof in porphyrins, chlorins and bacteriochlorins; and (c) energy diagram of each transition and the mixed transitions under electron correlation	5
Figure 2.1.	Summary of metalation of synthetic bacteriochlorins	39
Figure 2.2.	ORTEP drawing of (A) free base bacteriochlorin BC0, (B) free base bacteriochlorin BC0-2M, and (C) copper bacteriochlorin CuBC0-2T	41
Figure 2.3.	Comparison of core structural parameters across porphyrin, chlorin, and bacteriochlorin macrocycles	42
Figure 2.4.	Absorption spectra in toluene at room temperature of bacteriochlorins (Zn series)	44
Figure 2.5.	Absorption spectra in toluene at room temperature of bacteriochlorins (BC0-2T series).....	44
Figure 2.6.	The effect of the number of electron-withdrawing (carbonyl) groups on the redox potentials and frontier MO energies	53
Figure 3.1.	ESI-Mass spectra of ZnBC-NA, ZnBC- ¹³ C ^{1,11} and ZnBC- ¹³ C ^{4,14}	117
Figure 3.2.	ORTEP drawing of 10-NA	151
Figure 3.3.	Calculated titration curves for NH ₄ OAc solutions (67, 100, 200 equiv) versus 0–120 equiv of HCl	155
Figure 3.4.	¹ H NMR spectra of {H ₂ BC} and {ZnBC} at 298 K.....	160

Figure 4.1.	Absorption spectra of magnesium tetrapyrroles MgOEP, Chl <i>a</i> , Chl <i>b</i> , and Bchl <i>a</i>	173
Figure 4.2.	Routes to bacteriochlorins for incorporation in dyads	177
Figure 4.3.	Bacteriochlorin–bacteriochlorin dyads (naturally derived constituents)	178
Figure 4.4.	Intramolecular folding-up of bacteriochlorin dimer 2b (R = CO ₂ Me) with linker provided by the 17-propionate and ethylene groups	179
Figure 4.5	Bacteriochlorin–chlorin dyads (naturally derived constituents) linked at the (A) 17-17 or (B) 17-3 positions	181
Figure 4.6.	Hybrid dyads containing a naturally derived bacteriochlorin and a synthetic, electron-acceptor moiety	182
Figure 4.7.	Dyads built around naturally derived bacteriochlorin-imides	183
Figure 4.8.	Synthetic bacteriochlorin–quinone dyads	184
Figure 4.9.	Bacteriochlorin–chlorin dyads prepared via <i>de novo</i> synthesis	185
Figure 4.10.	Normalized absorption spectra and fluorescence spectra for (A) dyad 20a, (B) benchmark bacteriochlorin monomer and (C) benchmark chlorin monomer in toluene at room temperature.....	186

LIST OF SCHEMES

Scheme 1.1.	The <i>de novo</i> synthesis of a bacteriochlorin from a dihydrodipyrin acetal.	11
Scheme 2.1.	Synthesis of bacteriochlorins bearing two carboethoxy groups.	23
Scheme 2.2.	Metalation during macrocycle formation.....	28
Scheme 3.1.	Representative isotopologue of bacteriochlorophyll	99
Scheme 3.2.	Retrosynthesis of isotopically substituted bacteriochlorins.....	102
Scheme 3.3.	Synthesis of isotopically substituted pyrrole-2-carboxaldehyde	103
Scheme 3.4.	Syntheses of α - ^{13}C -substituted pyrrole-2-carboxaldehydes	105
Scheme 3.5	Synthesis of isotopically substituted α,β -unsaturated ketone-acetal	107
Scheme 3.6.	Synthesis of various isotopically substituted nitroethylpyrroles	108
Scheme 3.7.	Synthesis of isotopically substituted bacteriochlorins	110
Scheme 3.8.	Proposed route for the loss of ^{15}N upon McMurry reaction	119

LIST OF CHARTS

Chart 1.1.	Structures of bacteriochlorophylls	1
Chart 1.2.	Structures of tetrapyrrole macrocycles.	2
Chart 2.1.	Synthetic bacteriochlorins examined herein	21
Chart 2.2.	Metal chelates of naturally derived bacteriochlorins	26
Chart 2.3.	Metal chelates of synthetic bacteriochlorins	26
Chart 2.4.	A zinc dicyanobacteriochlorin	28
Chart 2.5.	Demethoxylated byproduct upon attempted palladiation	36
Chart 3.1.	Natural bacterial photosynthetic pigments.....	97
Chart 3.2.	Representative structures of synthetic isotopically substituted bacteriochlorins.....	98
Chart 3.3.	Isotopically substituted synthetic bacteriochlorins	101
Chart 3.4.	Structure of EtOBC-NA.....	112

LIST OF TABLES

Table 1.1.	Summary of calculations on electronic spectra of bacteriochlorins.	9
Table 2.1.	Preparative methods for metalation of bacteriochlorins.	25
Table 2.2.	Survey of Metalation (BC0-2T).....	31
Table 2.3.	Zinc Metalation of Synthetic Bacteriochlorins.	33
Table 2.4.	Survey of Metalation of Bacteriochlorin BC2-2M-MeO.....	35
Table 2.5.	Survey of Magnesiumation of Bacteriochlorins	37
Table 2.6.	Spectral Properties of Bacteriochlorins	45
Table 2.7.	Photophysical, Redox, and Molecular-Orbital Properties of Bacteriochlorins	49
Table 2.8.	Summary of Crystal Data for BC0, BC0-2M, and CuBC0-2T.....	63
Table 3.1.	NMR chemical shifts of {H ₂ BC} and {ZnBC}	114
Table 3.2.	Summary of Crystal Data for 10-NA.....	149
Table 3.3.	Procedures for pyrrole-2-carboxaldehyde 5 → nitrohexanone-pyrrole 2.....	153
Table 3.4.	Calculated pH values of buffered solutions	157
Table 3.5.	Selected peaks from the ESI-mass spectrum of ZnBC- ¹³ C ^{4,14}	162
Table 3.6.	Isotopic pattern for ZnBC-NA	163

LIST OF EQUATIONS

Equation 1.1	4
Equation 1.2	4
Equation 1.3	6
Equation 1.4	6
Equation 1.5	7
Equation 2.1	29

CHAPTER 1

General Introduction: Bacteriochlorophylls and Bacteriochlorins

Introduction

Naturally occurring bacteriochlorophylls are essential constituents in bacterial photosynthesis.¹ Bacteriochlorophylls *a-e* and *g* are named in order of discovery, and differ in molecular structure. Bacteriochlorophyll *a*, *b* or *g* contains a bacteriochlorin macrocycle, whereas bacteriochlorophyll *c*, *d* or *e* contains a chlorin macrocycle (Chart 1.1). Both bacteriochlorins and chlorins are related to porphyrins, which collectively are called tetrapyrroles. Tetrapyrroles are classified by the reduction level of the macrocycle. A porphyrin has a fully unsaturated tetrapyrrolic macrocycle. A chlorin has one reduced (pyrroline) ring in the macrocycle, while a bacteriochlorin features two reduced (pyrroline) rings at opposite positions in the macrocycle (Chart 1.2).

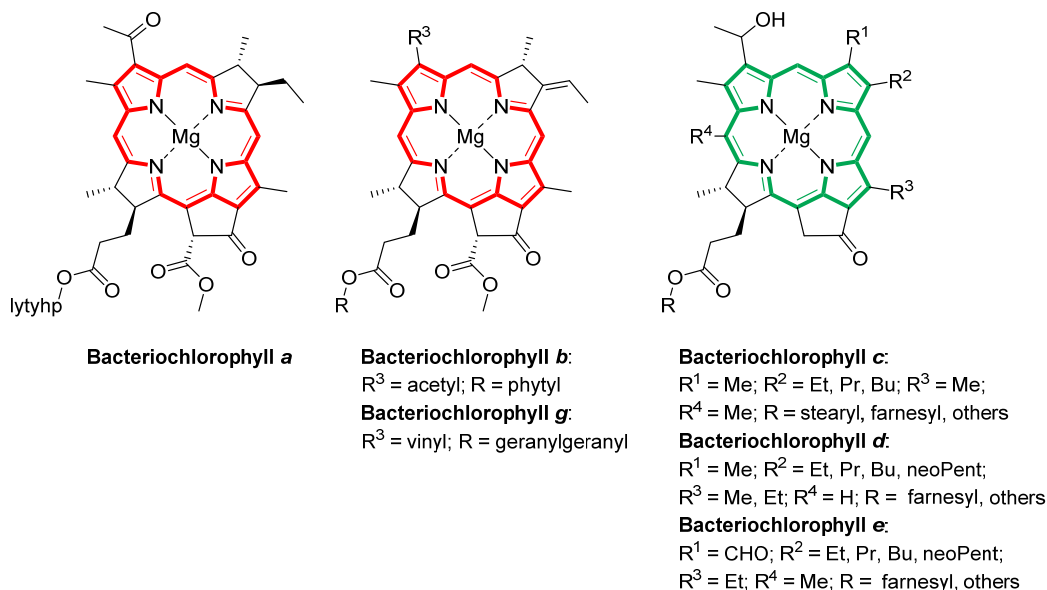


Chart 1.1. Structures of bacteriochlorophylls.

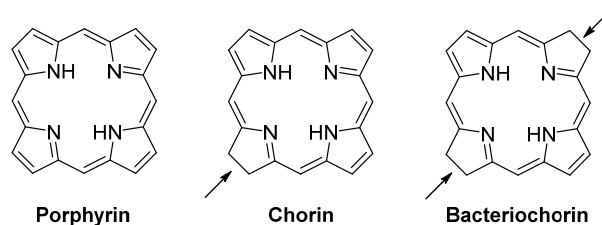


Chart 1.2. Structures of tetrapyrrole macrocycles.

A porphyrin has 18 π -electrons in the conjugated system, if one does not count the lone pairs on two nitrogens in the pyrrole rings and two double bonds in the pyrroline rings. Reduction of one or two pyrrole rings in a tetrapyrrole macrocycle does not alter the conjugated system, yet does significantly change the absorption properties. A detailed discussion of the absorption properties of tetrapyrroles is described in the following section.

Absorption Properties and Four-orbital Model

Each tetrapyrrole macrocycle class exhibits a characteristic absorption spectrum. Porphyrins absorb dominantly in the UV region (B or Soret band) and weakly in the visible region (Q band). Chlorins have two strong absorptions: one in the violet-blue region (B band), while the others in the red region (Q_y band). A more subtle absorption (Q_x band) in chlorins lies between the B and Q_y bands. Bacteriochlorins have an intense, characteristic absorption in the near-infrared region (Q_y band) as well as a strong absorption (B band) in the violet-blue region. Bacteriochlorins also have a medium-intense Q_x band in the visible region. The typical absorption spectrum of each macrocycle is demonstrated by hematin, chlorophyll *a*, and bacteriochlorophyll *a* (Bchl *a*) for porphyrin, chlorin, and bacteriochlorin,

respectively and are shown in Figure 1.1. These characteristic colors of tetrapyrroles make blood red and grass green and therefore tetrapyrroles are often called “the colors of life.”²

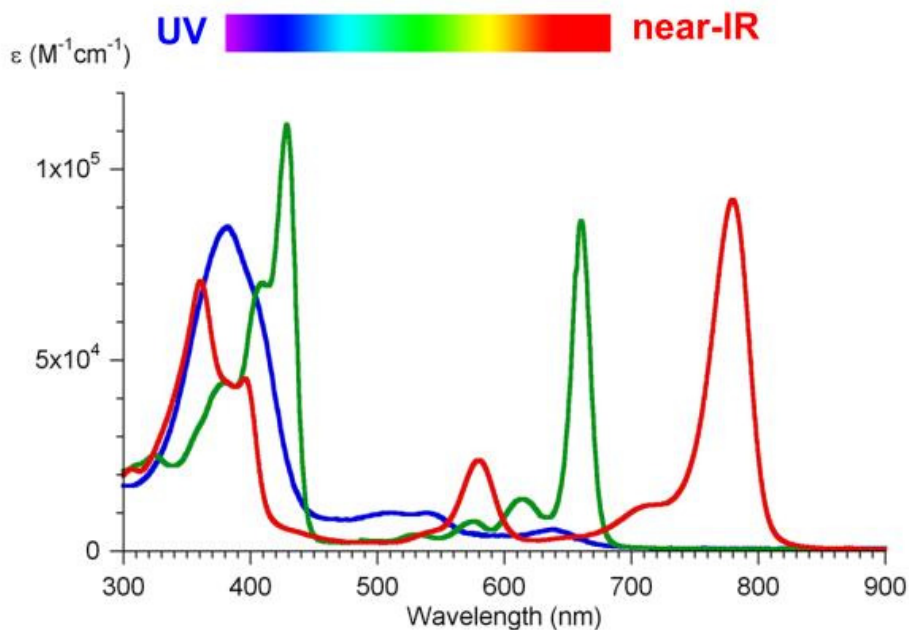


Figure 1.1. Representative absorption spectra of a porphyrin (hematin, blue), chlorin (chlorophyll *a*, green), and bacteriochlorin (Bchl *a*, red).

The difference in absorption properties of tetrapyrroles can be explained by Gouterman’s “four-orbital model.”³⁻⁵ The model was first developed to explain the absorption spectra of porphyrins and then extended to those of chlorins and bacteriochlorins. The model utilized four MOs of a D_{4h} porphyrin (a metalloporphyrin) calculated from the Hückel model: two nearly degenerate HOMOs (b_1 and b_2 in Gouterman’s notation) and two degenerate LUMOs (c_1 and c_2) as shown in Figure 1.2 (a). The four orbitals then give rise to

four singlet, one-electron transitions: $(b_1 \rightarrow c_1)_y$, $(b_1 \rightarrow c_2)_x$, $(b_2 \rightarrow c_1)_x$ and $(b_2 \rightarrow c_2)_y$, where the subscripted x and y indicate the polarization direction of the transitions [Figure 1.2 (b)]. The first two high-energetic transitions from b_2 were preliminarily assigned to the B bands. The latter two were then assigned to the Q bands. However, the B and Q transitions were calculated to have identical transition dipole moments, obviously inconsistent with a porphyrin absorption spectrum.

The assumptions were made by Gouterman that (1) b_1 and b_2 are degenerate, and (2) electron correlation needs to be accounted for. Four transitions would mix pairwise under the same symmetry. The x-polarized transitions $(b_1 \rightarrow c_2)_x$ and $(b_2 \rightarrow c_1)_x$ are mixed to give B_x and Q_x bands (Equation 1.1). Similarly, the y-polarized transitions $(b_1 \rightarrow c_1)_y$ and $(b_2 \rightarrow c_2)_y$ are mixed to give B_y and Q_y bands [Equation 1.2 and Figure 1.2 (c)]. The two resulting $B_{(x,y)}$ excited states are still degenerate under the D_{4h} symmetry but have a higher energy level and an enhanced transition dipole moment. The two degenerate $Q_{(x,y)}$ excited states have a lowered energy level and a weakened transition dipole moment. By such assumptions, the four-orbital model qualitatively explains the strong B bands in the UV region and the weak Q bands in the visible region in the spectra of a metalloporphyrin.

$$\left. \begin{matrix} B_x \\ Q_x \end{matrix} \right\} = [(b_1 \rightarrow c_2)_x \mp (b_2 \rightarrow c_1)_x](2)^{-1/2} \quad (\text{Equation 1.1})$$

$$\left. \begin{matrix} B_y \\ Q_y \end{matrix} \right\} = [(b_1 \rightarrow c_1)_y \pm (b_2 \rightarrow c_2)_y](2)^{-1/2} \quad (\text{Equation 1.2})$$

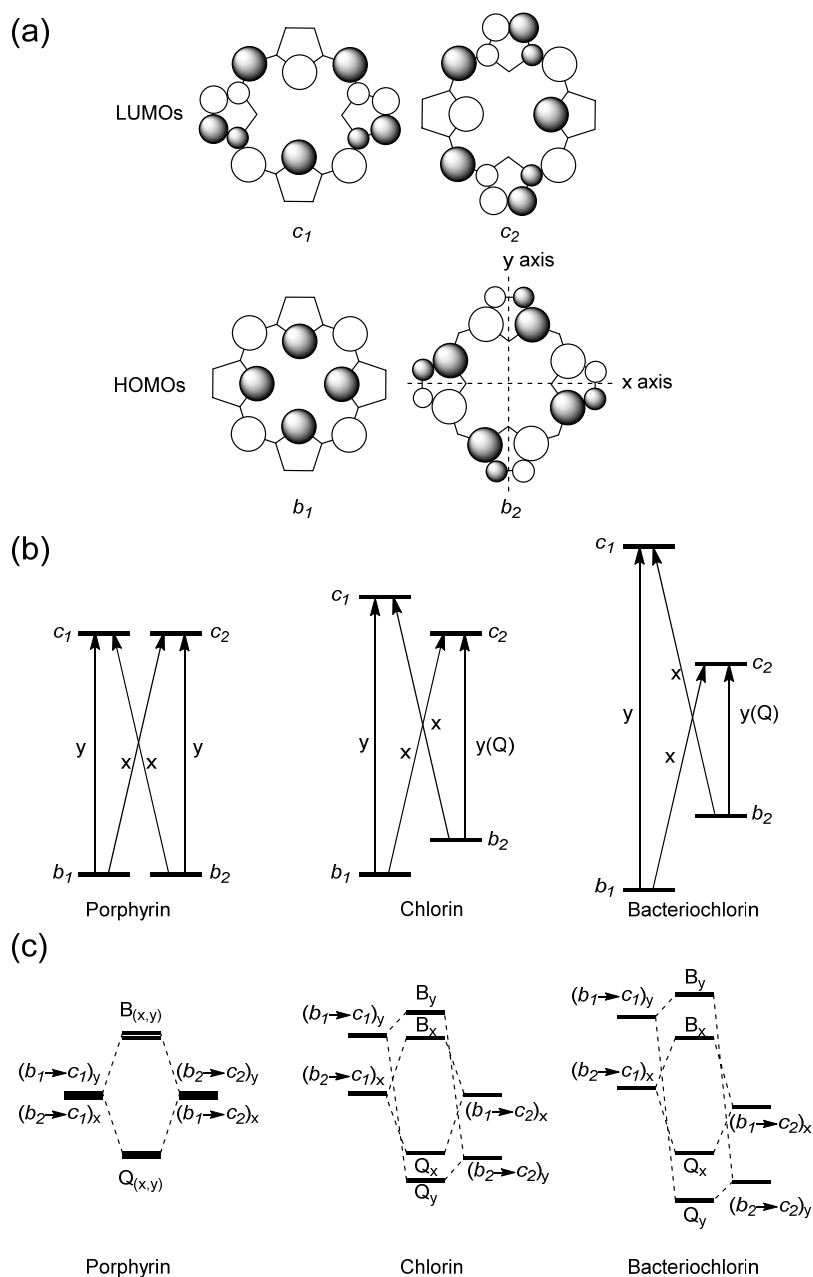


Figure 1.2. (a) The HOMO and LUMO of tetrapyrroles; (b) energy diagram thereof in porphyrins, chlorins and bacteriochlorins; and (c) energy diagram of each transition and the mixed transitions under electron correlation. Note that the nonrealistic energy diagram only reflects the relative energy positions.

The model can also be used to explain the absorption spectra of free base porphyrins as well as chlorins and bacteriochlorins, where the orbitals are shifted from degeneracy. The cases of chlorins and bacteriochlorins are discussed here. The reduced ring in a chlorin alters the π conjugation system and thus raises the energies of the corresponding Hückel molecular orbitals. In the case the reduced ring is chosen to place in the x axis as convention, both energies of b_2 and c_1 orbitals are raised most as shown in Figure 1.2 (b). The energies of the transitions also change accordingly. Of four transitions, the energies of the y-polarized transitions $(b_1 \rightarrow c_1)_y$ and $(b_2 \rightarrow c_2)_y$ split drastically [Equation 1.3, 1.4 and Figure 1.2 (c)]. Considering the electron correlation, the mixing of transitions results in (1) the Q_y band is heavily weighted on the $(b_2 \rightarrow c_2)_y$ transition, while the B_y band is heavily weighted on the $(b_1 \rightarrow c_1)_y$ transition; (2) the energy of the Q_y transition is lowered from that of $(b_2 \rightarrow c_2)_y$, while that of B_y is raised from that of $(b_1 \rightarrow c_1)_y$; and (3) the transition strength of the Q_y excited state is restored at the expense of weakening that of the B_y excited state (Equation 1.5). On the other hand, the energies of the x-polarized transitions $(b_1 \rightarrow c_2)_x$ and $(b_2 \rightarrow c_1)_x$ remain degenerate to some extent. Therefore, the B_x and Q_x bands in a chlorin retain a similar wavelength and intensity (strong B and weak Q) as for those of porphyrins. Therefore, the four-orbital model again qualitatively explains the enhanced Q_y bands in the spectra of chlorins.

$$B_y = \cos \eta (b_1 \rightarrow c_1)_y + \sin \eta (b_2 \rightarrow c_2)_y \quad (\text{Equation 1.3})$$

$$Q_y = +\sin \eta (b_1 \rightarrow c_1)_y - \cos \eta (b_2 \rightarrow c_2)_y \quad (\text{Equation 1.4})$$

$$\frac{\mu^2(Q_y)}{\mu^2(B_y)} = \frac{1 - \sin 2\eta}{1 + \sin 2\eta} \quad (\text{Equation 1.5})$$

A more extreme case is demonstrated by a bacteriochlorin, where the two reduced rings drastically alter the energies of all the four orbitals. Both transition pairs in x and y directions are shifted from degeneracy. As a result, both Q_x and Q_y transitions are shifted to longer wavelength. Both Q_x and Q_y transition are enhanced; moderately in the Q_x bands and strongest in the Q_y band. Also, the B bands in some bacteriochlorins are resolved to give a short wavelength and weakened B_x band as compared to that of a porphyrin or chlorin.

Although Gouterman's four-orbital model qualitatively explains the characteristic absorption property of each tetrapyrrole class, accurate predictions in terms of excitation energy, transition configurations and structural correlations require more elaborate calculations. The early *ab initio* calculations faced challenges concerning electron correlations owing to the large size of π -conjugation (24 π -electrons) in the macrocycles. Calculations concerning molecular structures and potential energy surfaces of porphyrins and hemes have been reviewed.^{6,7} Calculations on hydrophyrins (chlorins or bacteriochlorins) are limited and most are focused on spectral properties. One reason for such a distinction is that there are only a few obtainable compounds in these two latter classes. Most calculations on electronic spectra of bacteriochlorins were chiefly based on natural bacteriochlorophylls or fictive models (e.g., simplest bacteriochlorin model as the structure shown in Chart 1.2). The calculation method, excitation energy (Q_y) and main transition configurations are summarized in Table 1.1. The experimental values for the simplest *de novo* synthetic bacteriochlorins (see the following section; HBC and Zn-HBC, Scheme 1.1, R^2 , R^3 and R^5 =

H), Bchl *a* and bacteriopheophorbide *a* (Bphe *a*, a free base Bchl *a*) are also listed for comparison.

For excitation energy, the SAC-CI, INDO/S and MRMP methods underestimated, while the DFT/CIS and TDDFT methods overestimated, the Q_y excited state. The methods that incorporated solvation in general lowered the excitation energy. On the other hand, DFT/MRCI, INDO/Sm (modified INDO/S) and screened potential methods gave values in good agreement with the the experimental values.

For the main transition configurations of the Q_y states, the results were generally in keeping with those from the four-orbital model. The calculated HOMO–1, HOMO, LUMO and LUMO+1 characteristically resemble those from the Hückel model. The calculation shows that the HOMO→LUMO [or (b₂→c₂)_y in Gouterman's notation] transition contributes to the excited S₁ wavefunction with 70–90% in bacteriochlorins. The second largest contributions are due to HOMO–1→LUMO+1 [or (b₁→c₁)_y in Gouterman's notation] transition.

Table 1.1. Summary of calculations on electronic spectra of bacteriochlorins.

Method	Model ^a	Excitation energy (Q _v)/eV	Main configuration ^b	Reference
SAC-CI	BC	1.47	72, 19	(8)
INDO/S	BC	1.43	not given	(9)
MRMP	BC	1.43	not given	(10)
DFT/CIS	BC	2.04	71, 27	(11)
TDDFT	BC	2.10	77, 23	(12)
TDDFT	BC (PCM) ^c	2.01	83, 17	(12)
DFT/MRCI	BC	1.79	70, 13	(13)
INDO/Sm ^d	BC	1.65, 1.70 ^e	94, 0	(9), (14)
experimental	HBC	1.74	--	(15)
experimental	Bphe <i>a</i>	1.64	--	(15)
MRMP	MgBC	1.50	not given	(10)
MRMP	ZnBC	1.56	not given	(10)
TDDFT	MgBC	2.06, 2.03 ^e	(95, 93), 0	(16), (17)
TDDFT	ZnBC	1.96–2.07 ^g	not given	(18)
TDDFT	Bchl <i>b</i>	1.80	not given	(19)
Screened potential	MBC ^f	1.76	94, 0	(20)
INDO/Sm ^d	MgBC	1.67	97, 0	(14)
experimental	Zn-HBC	1.71	--	(15)
experimental	Bchl <i>a</i>	1.59	--	(15)

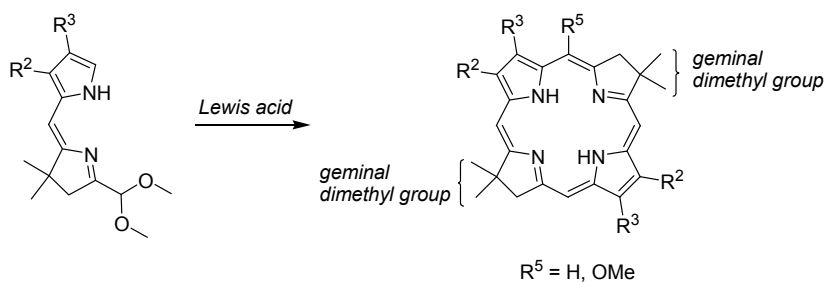
^a(M)BC: structure as shown in Chart 1.1 with the indicated central metal; HBC and Zn-HBC: *de novo* synthetic bacteriochlorins (Scheme 1.1, R², R³ and R⁵ = H). ^bWt% of (HOMO→LUMO) and (HOMO–1→LUMO+1) transitions. ^cWater solvation model included. ^dINDO/S with parameterization modified by the authors. ^eEnergies depending on the geometry optimization methods. ^fMetal not specified. ^gEnergies depending on the solvation model.

Mezentseva *et al.* calculated the excitation energies of a series of bacteriochlorophyll derivatives by ZINDO/S, which gave a very accurate result (percentage error: -0.81–0.16%).²¹ Korppi-Tommola *et al.* used methods including ZINDO/S CIS, PM3 CIS, PM3 CISD, *ab initio* CIS, time-dependent HF and TDDFT to calculate more than 18 tetrapyrrole macrocycles and found that ZINDO/S CIS (with geometry optimization by B3LYP/6-31G*) gave the best estimated excitation energies.²² Burda *et al.* calculated selected photosynthetic pigments to elucidate the structure-transition energy relationship between different π -conjugated systems.²³ Bocian *et al.* calculated a series of *de novo* synthetic bacteriochlorins bearing various substituents on the 2,3,12,13-positions (see below) and found a greater dependence of the Q_y excitation energy on the LUMO rather than the HOMO.²⁴

In summary, Gouterman's four-orbital model qualitatively explains the characteristic absorption properties of tetrapyrroles. The characteristic Q_y absorption of bacteriochlorins originates from relaxation of quasi-degeneracy of two HOMOs and two LUMOs. Modern calculations found that the HOMO→LUMO transition contributes 70–90% to the Q_y state of the bacteriochlorin while the HOMO-1→LUMO+1 transition contributes the rest. The predicted excitation energy varies with the method utilized for calculation. While constrained by the available experimental data, the spectra-structure correlations of bacteriochlorins that have been revealed so far are based on a handful of natural bacteriochlorophylls and a series of *de novo* synthetic bacteriochlorins.

Study of Properties of Bacteriochlorins

Properties of porphyrins have been extensively investigated in part due to the ready availability and versatile synthetic malleability of the macrocycle. Interests in photosynthesis and pursuit of next-generation energy conversion approaches prompt the understanding of properties of chlorophylls, as well as that of synthetic chlorin analogues. Properties of bacteriochlorins, however, have been less investigated owing to limited accessibility. The study of the properties of bacteriochlorins had been mainly based on natural analogues, that is, derivatives of bacteriochlorophylls. A systematic study of the structure-property relationship of bacteriochlorins was not possible until the development of a *de novo* synthesis.²⁵ The *de novo* synthesis utilizes the self-condensation of a dihydrodipyrin-acetal, which is prepared from simple precursors to afford diverse synthetic bacteriochlorins bearing a variety of substituents (Scheme 1.1). The resulting bacteriochlorins contain a geminal dimethyl group in each pyrrole ring to afford stability toward adventitious dehydrogenation. A large number of synthetic chlorins and bacteriochlorins have been prepared for various purposes including the study of fundamental properties, tuning of spectral properties, and pursuit of a range of photochemical applications.^{26,27}



Scheme 1.1. The *de novo* synthesis of a bacteriochlorin from a dihydrodipyrin-acetal.

Interests in understanding properties of bacteriochlorins face limitations. One of which is the limited accessibility to metallobacteriochlorins. Bacteriochlorophylls contain magnesium as the central metal. In special environments, some bacteria use Zn instead of Mg in photosynthesis.¹ Thus, only Mg and Zn are used as the central metal in bacteriochlorophylls. Artificially, a variety of metals including Pd, Co, Ni, Cu, Zn, Cd, Mn have been inserted to Bphe *a*.¹⁵ However, the *de novo* synthetic bacteriochlorins prepared heretofore were the free base species. No broadly applicable methods for metalating synthetic bacteriochlorins have been developed. In Chapter 2, we will continue the topic of metallobacteriochlorins. We discuss the influence of the central metal on properties of bacteriochlorins. We describe the development and application of new methods for metalating a series of synthetic bacteriochlorins. We then report the spectral and photophysical features of a set of metallobacteriochlorins.

Another ostensible limitation, which we have turned to an advantage in our spectroscopic studies, is the symmetry of the *de novo* synthetic bacteriochlorins. Such a synthetic route precludes access to an AB-type bacteriochlorin (a bacteriochlorin bearing distinct substituents on pyrrolic β -positions). However, the nature of the self-condensation gives a symmetric “A₂”-type bacteriochlorin bearing substituents and skeletal atoms from a single A-dihydrodipyrin-acetal. This symmetric property allows the isotopic substitution of a dihydrodipyrin-acetal to be carried through to the spectroscopically homologous positions of a bacteriochlorin. We then exploit this symmetry correspondence to build a series of isotopically substituted metallobacteriochlorins bearing pairs of ¹³C or ¹⁵N atoms in the inner π conjugated system. Such metallobacteriochlorins were used for spectroscopic studies

including electron paramagnetic resonance (EPR), IR and resonance Raman spectroscopies. The synthesis and spectral properties of the isotopically substituted metallobacteriochlorins are described in Chapter 3.

Photosynthesis is not carried out by a single pigment molecule alone but instead stems from the combined action of hundreds of molecules. Accordingly, understanding the interaction of bacteriochlorins with other entities is of utmost importance. Such studies require an architecture that fixes a bacteriochlorin in a suitable orientation and/or position with respect to other chromophores. Only a few such architecture containing bacteriochlorins are known. In Chapter 4, we review those bacteriochlorin-containing arrays and wish to give insights to such studies in the future.

References

- (1) Blankenship R. E. *Molecular Mechanisms of Photosynthesis*; Blackwell Science: Oxford, 2002.
- (2) Milgrom, L. R. *Colors of Life*; Oxford University Press: New York, 1997.
- (3) Gouterman, M. in *The Porphyrins*; Vol. IV, Dolphin, D. Ed., Academic Press: New York, 1978, pp 1–165.
- (4) Gouterman, M. *J. Mol. Spectrosc.* **1961**, *6*, 138-163.
- (5) Gouterman, M. *J. Mol. Spectrosc.* **1963**, *11*, 108-127.
- (6) Ghosh, A. *Acc. Chem. Res.* **1998**, *31*, 189–198.
- (7) Ghosh A. In *The Porphyrin Handbook*; Kadish, K. M., Smith, K. M., Guilard, R., Eds.; Academic Press: San Diego, CA, 2000;; Vol. 7, pp 1–38.
- (8) Hasegawa, J.; Ozeki, Y.; Hada. M.; Nakatsuji H. *J. Phys. Chem. B* **1998**, *102*, 1320–1326.
- (9) Kuzmitsky, V. A.; Volkovich, D. I. *J. Appl. Spectrosc.* **2008**, *75*, 27–35.
- (10) Hashimoto, T.; Choe, Y.-K.; Nakano, H.; Hirao, K. *J. Phys. Chem. A* **1999**, *103*, 1894–1904.
- (11) Parusel, A. B. J.; Ghosh, A. *J. Phys. Chem. A* **2000**, *104*, 2504–2507.
- (12) Petit, L.; Quartarolo, A.; Adamo, C.; Russo, N. *J. Phys. Chem. B* **2006**, *110*, 2398–2404.
- (13) Parusel, A. B. J.; Grimme, S. *J. Porphyrins Phthalocyanines* **2001**, *5*, 225–232.
- (14) Volkovich, D. I.; Gladkov, L. L.; Kuzmitsky, V. A.; Solovyov, K. N. *J. Appl. Spectrosc.* **2011**, *78*, 155–164.

- (15) Chen, C.-Y.; Sun, E.; Fan, D.; Taniguchi, M.; McDowell, B. E.; Yang, E.; Diers, J. R.; Bocian, D. F.; Holten, D.; Lindsey, J. S. *Inorg. Chem.* **2012**, *51*, 9443–9464.
- (16) Wan, L.; Qi, D.; Zhang, Y. *J. Mol. Graphics Model.* **2011**, *30*, 15–23.
- (17) Lanzo, I.; Russo, N.; Sicilia, E. *J. Phys. Chem. B* **2008**, *112*, 4123–4130.
- (18) Petit, L.; Adamo, C.; Russo, N. *J. Phys. Chem. B* **2005**, *109*, 12214–12221.
- (19) Sundholm, D. *Phys. Chem. Chem. Phys.* **2003**, *5*, 4265–4271.
- (20) Sekino, H.; Kobayashi, H. *J. Chem. Phys.* **1987**, *86*, 5045–5052.
- (21) Mezentseva, A. A.; Burlyaeva, E. V.; Mironov, A. F. *Russ. J. Phys. Chem. B* **2008**, *2*, 525–530.
- (22) (a) Linnanto, J.; Korppi-Tommola J. *J. Phys. Chem. A* **2001**, *105*, 3855–3866; (b) Linnanto, J.; Korppi-Tommola J. *J. Comput. Chem.* **2004**, *25*, 123–137; (c) Linnanto, J.; Korppi-Tommola J. *J. Phys. Chem. A* **2004**, *108*, 5872–5882; for a review, see (d) Linnanto, J.; Korppi-Tommola, J. *Phys. Chem. Chem. Phys.* **2006**, *8*, 663–687.
- (23) Vokáčová, Z.; Burda, J. V. *J. Phys. Chem. A* **2007**, *111*, 5864–5878.
- (24) Yang, E.; Kirmaier, C.; Krayner, M.; Taniguchi, M.; Kim, H.-J.; Diers, J. R.; Bocian, D. F.; Lindsey, J. S.; Holten, D. *J. Phys. Chem. B* **2011**, *115*, 10801–10816.
- (25) Kim, H.-J.; Lindsey, J. S. *J. Org. Chem.* **2005**, *70*, 5475–5486.
- (26) Taniguchi, M.; Cramer, D. L.; Bhise, A. D.; Kee, H. L.; Bocian, D. F.; Holten, D.; Lindsey, J. S. *New J. Chem.* **2008**, *32*, 947–958.
- (27) Krayner, M.; Ptaszek, M.; Kim, H.-J.; Meneely, K. R.; Fan, D.; Secor, K.; Lindsey, J. S. *J. Org. Chem.* **2010**, *75*, 1016–1039.

CHAPTER 2

Synthesis and Physicochemical Properties of Metallobacteriochlorins

Preamble. The contents of this chapter have been published⁹⁵ together with contributions from the following individuals/groups: Erjun Sun for synthesis of **BC2-2H** series; Dazhong Fan for synthesis/survey of **BC0-2T** series; Masahiko Taniguchi for single-crystal X-ray analysis; Eunkyung Yang/Dewey Holten for photophysical property studies; James R. Diers/David F. Bocian for electrochemical studies.

Introduction

Naturally occurring chlorophylls and bacteriochlorophylls are essential constituents in plant and bacterial photosynthesis. Both types of hydroporphyrins contain magnesium as the central metal.¹ The introduction of different metals in tetrapyrrole macrocycles can alter the electronic,² axial-ligation,³ and photophysical⁴⁻⁶ properties of the coordination complex. The effect of metals can be seen by comparing the properties of metalloporphyrins containing magnesium, zinc, copper, or palladium, each of which is a divalent metal. Magnesium is five or six coordinate, and gives a reasonable yield of fluorescence ($\Phi_f \sim 0.1$), a long-lived excited singlet state ($\tau \sim 10$ ns), and a good yield of intersystem crossing to the triplet state.⁴ Zinc is four or five coordinate, and gives a lower yield of fluorescence ($\Phi_f \sim 0.03$), a shorter excited singlet state ($\tau \sim 2$ ns), and a higher yield of intersystem crossing to the triplet state.⁴ Copper is four coordinate and gives essentially no detectable fluorescence, a very short-lived nominal excited singlet state, and highly temperature-dependent properties of two excited-

states borne from the coupling of the porphyrin triplet with the unpaired metal electron.⁵ Palladium is four coordinate and gives no detectable fluorescence, a near unity yield of intersystem crossing, and a short-lived excited triplet state.⁶

A further distinction caused by metals concerns the change in optical properties. The introduction of a metal in a porphyrin typically increases the symmetry (e.g., D_{2h} to D_{4h}) and causes the spectral features in the visible region (500–650nm) to collapse from primarily four bands (due to partially overlapping x and y transitions) to a two-banded spectrum (wherein the x and y transitions are degenerate).⁷ The two visible bands are the Q(0,0) and Q(1,0) transitions. (Weaker additional vibronic overtone bands also contribute to the spectra with or without a metal ion.) The resulting absorption of the metalloporphyrin occurs at shorter wavelength than for that of the free base porphyrin. For a chlorin, insertion of a metal does not alter the symmetry but does typically cause a hypsochromic shift in the position of the long-wavelength absorption band. An example is provided by chlorophyll *a* and pheophytin *a* (the free base of chlorophyll *a*) which absorb at 662 and 667 nm, respectively.¹ For a bacteriochlorin, insertion of a metal also does not alter the symmetry but typically causes a bathochromic shift in the position of the long-wavelength absorption band. An example is provided by bacteriochlorophyll *a* (Bchl *a*) and bacteriopheophytin *a* (Bphe *a*), which absorb at 772 and 749 nm, respectively.¹ The ability to shift the absorption to longer wavelength upon metalation is quite attractive given the multiple motivations for access to chromophores with strong absorption in the near-infrared (NIR) spectral region. The relatively low energy of photons in the NIR region (1.76–1.23 eV, 700–1000 nm) enables photochemical studies in an energy regime that has been comparatively unexplored versus studies of organic

photochemistry in the ultraviolet (6.17–3.09 eV, 200–400 nm) or visible regions (3.09–6.17 eV, 400–700 nm). Applications of NIR-active bacteriochlorins include light-harvesting,⁸ optical imaging^{9,10} and photodynamic therapy¹¹ of soft tissues, and fluorescent markers in clinical diagnostics.¹² In addition, selected photosynthetic organisms are now known to employ zinc-containing analogues of bacteriochlorophylls (rather than the expected magnesium).¹³ For all of these reasons, fundamental studies of diverse metallobacteriochlorins are warranted.

Despite the range of physical behavior that can be elicited with metalloporphyrins, relatively few metallobacteriochlorins have been prepared, and most that have been prepared are derived from Bchl *a*.^{14,15} While data from the naturally derived macrocycles are quite valuable, lack of access to diverse synthetic metallobacteriochlorins has precluded wide-ranging studies of effects of peripheral substituents on spectral and photophysical properties, an approach that has been extensively pursued with porphyrins and chlorins. We have been working to develop a rational, *de novo* synthesis of bacteriochlorins.¹⁶⁻¹⁹ The resulting bacteriochlorins bear a geminal dimethyl group in each reduced, pyrroline ring to resist adventitious oxidants that otherwise could result in dehydrogenation. We recently characterized the photophysical properties of a large set of free base bacteriochlorins²⁰ derived from this synthetic approach, and also examined several indium(III) chelates thereof,²¹ but relatively few metal chelates of the synthetic bacteriochlorins have heretofore been prepared.

The metalation of bacteriochlorins – an ostensibly simple reaction – has proved more difficult than for porphyrins and chlorins. As one illustration, treatment of a chlorin–

bacteriochlorin dyad with zinc acetate in CHCl_3 /methanol at room temperature for four hours afforded selective metalation of the chlorin; the resulting zinc chlorin – free base bacteriochlorin dyad was isolated in nearly quantitative yield.⁹ As a second illustration, conditions that afford smooth zincation of the chlorin pheophytin *a* ($\text{Zn}(\text{OTf})_2$ in methanol or acetonitrile at room temperature) upon application to Bphe *a* resulted in decomposition rather than metalation.²² The origin of the difficulty of metalation of bacteriochlorins remains unclear, but has been attributed to a number of factors. The factors include (1) nucleophilicity, which decreases with increased saturation of the macrocycle (porphyrin > chlorin > bacteriochlorin),²² and (2) acidity of the N-H protons, which decreases with increasing electron-richness of the ligand (porphyrin > chlorin > bacteriochlorin).²³ A factor that complicates interpretation is that many bacteriochlorins examined in metalation studies to date are derived from natural ligands of somewhat limited stability. In short, the dearth of bacteriochlorins that withstand a broad range of reaction conditions has impeded a thorough investigation of these issues.

In this chapter, we first summarize methods that have been used to date for metalation of bacteriochlorins, and identify correlations between methods and structural features of the bacteriochlorins. We then describe the development and application of a new method for metalation of synthetic bacteriochlorins. Finally, we report the spectral and photophysical features of a set of metallochlorins. While no metalation procedure has yet been developed that is generically applicable to all bacteriochlorins, the present work should expand the availability of a variety of metallochlorins that have heretofore been inaccessible.

Results and Discussion

(I) Bacteriochlorin Synthesis. The metalation studies were carried out on a series of synthetic macrocycles that spanned a range from electron-deficient to electron-rich bacteriochlorins. The most electron-deficient bacteriochlorin (**BC4-MeO**) contains four carboethoxy groups (denoted by “4”) and a methoxy group at the 5-position (denoted by “MeO”), which is followed by the bacteriochlorin-imide **BC3-2E** with three carbonyl groups and two ethyl groups. Bacteriochlorins with two carboethoxy and two alkyl groups **BC2-2E**, **BC2-2H**, and **BC2-2H-MeO** (E = ethyl, H = heptyl) are in the middle of the range, followed by **BC2-2M-MeO** with two carboethoxy and two mesityl groups. The most electron-rich bacteriochlorin (**BC0-2T**) bears electron-donating, *p*-tolyl groups at the 2- and 12-positions. This feature makes **BC0-2T** an appropriate benchmark to gauge the scope of the metalation for electron-rich bacteriochlorins. Additionally, the unsubstituted bacteriochlorin **BC0** lacking any β -pyrrole substituents provides a benchmark for comparison with diverse substituted bacteriochlorins (Chart 2.1). The term here denotes 1, 2, or 4 carboethoxy substituents and/or the 2 substituted acyl moieties of the annulated imide ring.

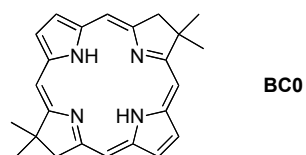
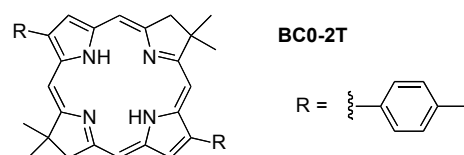
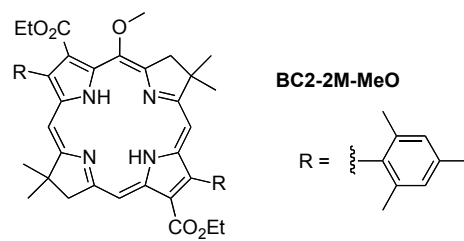
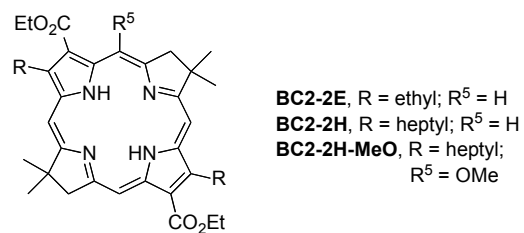
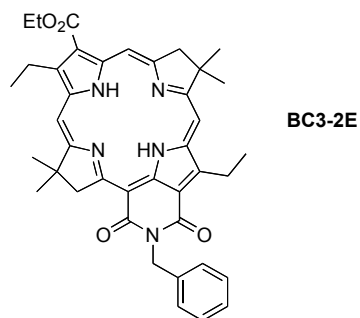
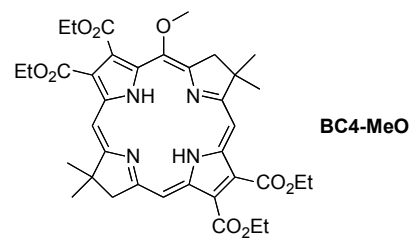
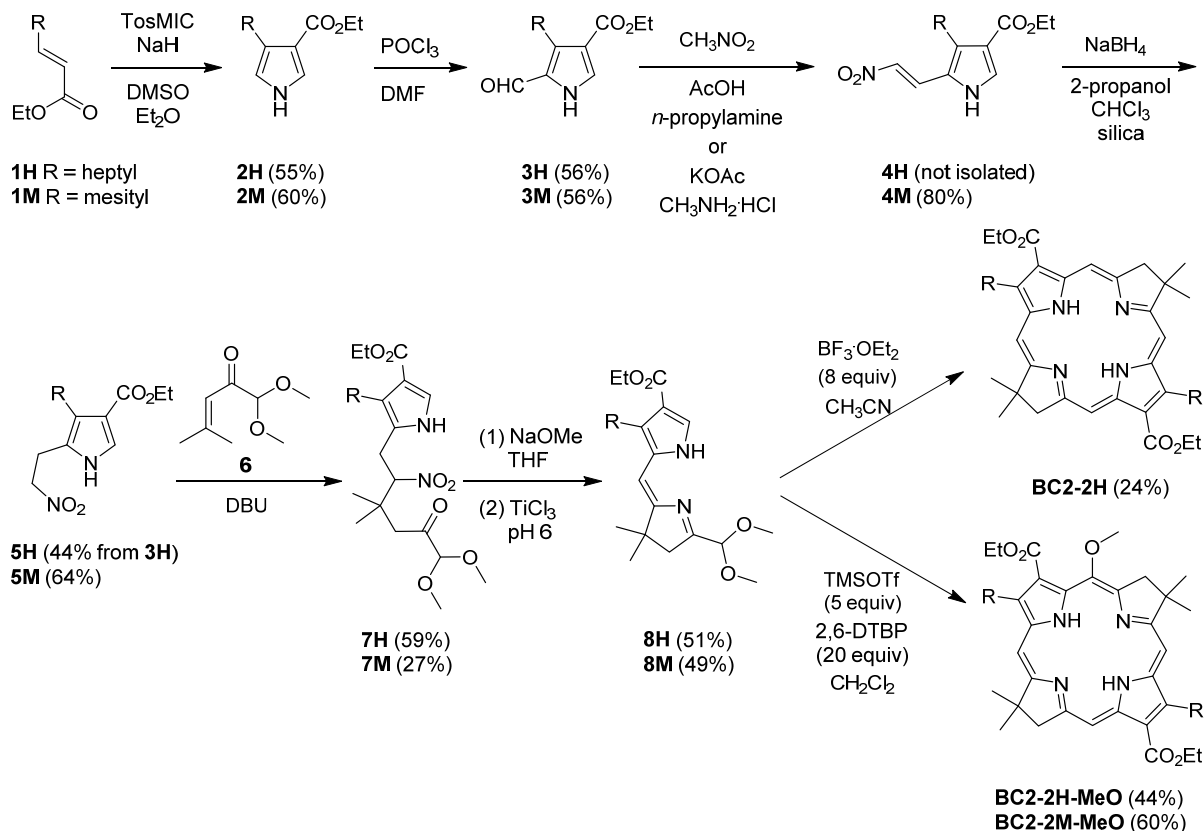


Chart 2.1. Synthetic bacteriochlorins examined herein.

These bacteriochlorins thus comprise a far broader range of substituents than has heretofore been examined, and all members of the set differ from the naturally occurring bacteriopheophytins in the following ways: (i) absence of an isocyclic ring (ring E), (ii) presence of a geminal dimethyl group rather than *trans*-dialkyl substituents in each pyrroline ring, and (iii) absence of alkyl (sp^3 -hybridized) groups on adjacent β -pyrrole carbons, which could induce nonplanarity. On the other hand, within the set of bacteriochlorins in Chart 2.1, some are sparsely substituted (i.e., lack 2 or 4 β -pyrrole substituents), those with mesityl substituents are sterically hindered, and the set encompasses molecules with 0-4 carbonyl groups. Collectively, the bacteriochlorins present a rich test of the generality of metalation methods.

The syntheses of bacteriochlorins **BC4-MeO**,¹⁸ **BC3-2E**,²⁴ **BC2-2E**,¹⁸ **BC0-2T**,¹⁶ and **BC0**¹⁸ have been reported. The syntheses of **BC2-2H**, **BC2-2H-MeO**, and **BC2-2M-MeO** are shown in Scheme 2.1. The general approach relies on installation of the desired β -pyrrole substituents at the earliest stage of the synthesis.¹⁸ Thus, treatment of α,β -unsaturated ester **1H** (R = heptyl) or **1M** (R = mesityl)²⁵ with *p*-toluenesulfonyl methylisocyanide (TosMIC) via the van Leusen method²⁶ afforded the corresponding pyrrole **2H** or **2M**. Formylation²⁷ gave pyrrole-2-carboxaldehyde **3H** or **3M** wherein the formyl group is positioned adjacent to the heptyl or mesityl moiety, respectively. Treatment of **3H** or **3M** to sequential nitroaldol (Henry) condensation^{17,28} and reduction²⁹ gave the nitrovinylpyrrole **4M** (**4H** was not isolated) and 2-(2-nitroethyl)pyrrole **5H** or **5M**, respectively. Michael addition³⁰ with the α,β -unsaturated ketone-acetal **6**^{16,19} gave the nitrohexanone-pyrrole **7H** or **7M**, which upon McMurry-type reductive cyclization¹⁷

afforded the dihydrodipyririn-acetal **8H** or **8M**. Macrocycle formation was carried out by self-condensation at room temperature via two catalytic conditions:¹⁸ TMSOTf/2,6-di-*tert*-butylpyridine (DTBP) in CH₂Cl₂ with **8H** or **8M** afforded **BC2-2H-MeO** or **BC2-2M-MeO**, whereas BF₃·OEt₂ in CH₃CN with **8H** gave **BC2-2H**. The new compounds (**2**, **3**, **5**, **7** and **8** in the **H** and **M** series) were characterized by melting point, ¹H NMR spectroscopy, ¹³C NMR spectroscopy, and ESI-MS; compounds **2H**, **3H**, **5H**, **7H** and **8M** also were verified by elemental analysis. Bacteriochlorins **BC2-2H**, **BC2-2H-MeO**, and **BC2-2M-MeO** were characterized by ¹H NMR spectroscopy, ¹³C NMR spectroscopy, absorption spectroscopy, MALDI-MS and ESI-MS.



Scheme 2.1. Synthesis of bacteriochlorins bearing two carboethoxy groups.

Bacteriochlorin **BC2-2M-MeO** contains mesityl groups at the 2- and 12-positions. The location of the β -pyrrole substituents in the macrocycle is set at the stage of formylation of the pyrrole (2M \rightarrow 3M). It is noteworthy that Vilsmeier formylation²⁷ of 3-mesitylpyrrole, obtained by decarboxylation³¹ of pyrrole 2M, affords the 2-formyl-4-mesitylpyrrole and the isomeric 2-formyl-3-mesitylpyrrole in 4:1 ratio. The availability of 2-formyl-4-mesitylpyrrole enabled synthesis of a bacteriochlorin that contains mesityl groups at the 3- and 13-positions.⁹⁵

(II) Bacteriochlorin Metalation. 1. Literature Methods for Metal Insertion. A classic method for metalation of porphyrins entails treatment of the free base macrocycle with a metal acetate (or metal acac) in a somewhat polar solvent at elevated temperature.^{32,33} For porphyrins, the use of high temperatures often is acceptable because most porphyrins are stable at high temperature and in solution exposed to air. However, many bacteriochlorins do not survive at high temperatures even if the reactions are run anaerobically.³⁴ There are two general methods for metalation of bacteriochlorins: (1) direct metalation of a free base bacteriochlorin with a metal salt (MX_2) in a solvent at temperatures ranging from room temperature to >100 °C to obtain the Zn(II), Cu(II), Pd(II), Ni(II) or Cd(II) bacteriochlorin (Table 2.1, entries 1-5);^{23,35-48} and (2) transmetalation wherein a Cd(II) chelate of a bacteriochlorin is formed *in situ* in acetone and then treated with a metal chloride at room temperature to obtain the target metallochlorin (entry 6).^{23,39-41} Strell and Urumow first prepared a variety of metallochlorins via the transmetalation method,⁴⁹ which was subsequently applied by Scheer and coworkers²³ to bacteriochlorophylls.

Table 2.1. Preparative methods for metalation of bacteriochlorins.

Entry	Metal salt	Conditions	Bacteriochlorin ^a
1	Zn(OAc) ₂ or Zn(OAc) ₂ ·2H ₂ O	Reflux in diverse solutions ^b	I , ²³ II , ^{35,36} III , ³⁷ IV , ³⁸ V , ³⁸ VI , ³⁹ VII , ^{40,41} VIII , ⁴² IX ⁴³
2	Cu(OAc) ₂ or CuO ₂	MeOH or AcOH at rt or reflux; CHCl ₃ /MeOH at reflux	I , ²³ II , ⁴⁴ VI , ³⁹ IX ⁴⁵
3	Pd(OAc) ₂	MeOH at rt	I , ⁴⁶ VII ⁴¹
4	NiCl ₂ ·6H ₂ O ^c or NiCl ₂	DMF at reflux	X , ⁴⁷ XI , ⁴⁸ XII ⁴⁸
5	Cd(OAc) ₂	DMF at reflux	I , ²³ VI , ³⁹ VII ^{40,41}
6 ^d	MnCl ₂ ·2H ₂ O, CoCl ₂ , NiCl ₂ , CuCl ₂ , ZnCl ₂ , PdCl ₂	Acetone at rt	I , ²³ VI , ³⁹ VII ^{40,41}

^aThe free base analogue of the structures shown in Charts 2.2 and 2.3 were used unless noted otherwise. ^b1,2-Dichloroethane/EtOH, pyridine, AcOH, DMF, CHCl₃/MeOH, CH₂Cl₂/MeOH, or CHCl₃/pyridine (6:1). ^cIncomplete metalation and partial dehydrogenation (to porphyrin) were observed. ^dTransmetalation from the cadmium complex.

The bacteriochlorins that have been prepared via these methods are displayed in Charts 2.2 and 2.3. Examination of structural features of the naturally derived bacteriochlorins (**I-VII**) subjected to metalation reveals the presence of at least one if not two carbonyl (ketone, aldehyde, amide, or imide) groups, whereas some of the synthetic bacteriochlorins (**VIII-XII**) lack such electron-withdrawing groups. The electron-richness of the macrocycle is believed to be an important feature that affects the rate of metalation and the propensity of the metallo-bacteriochlorin toward protolytic demetalation.

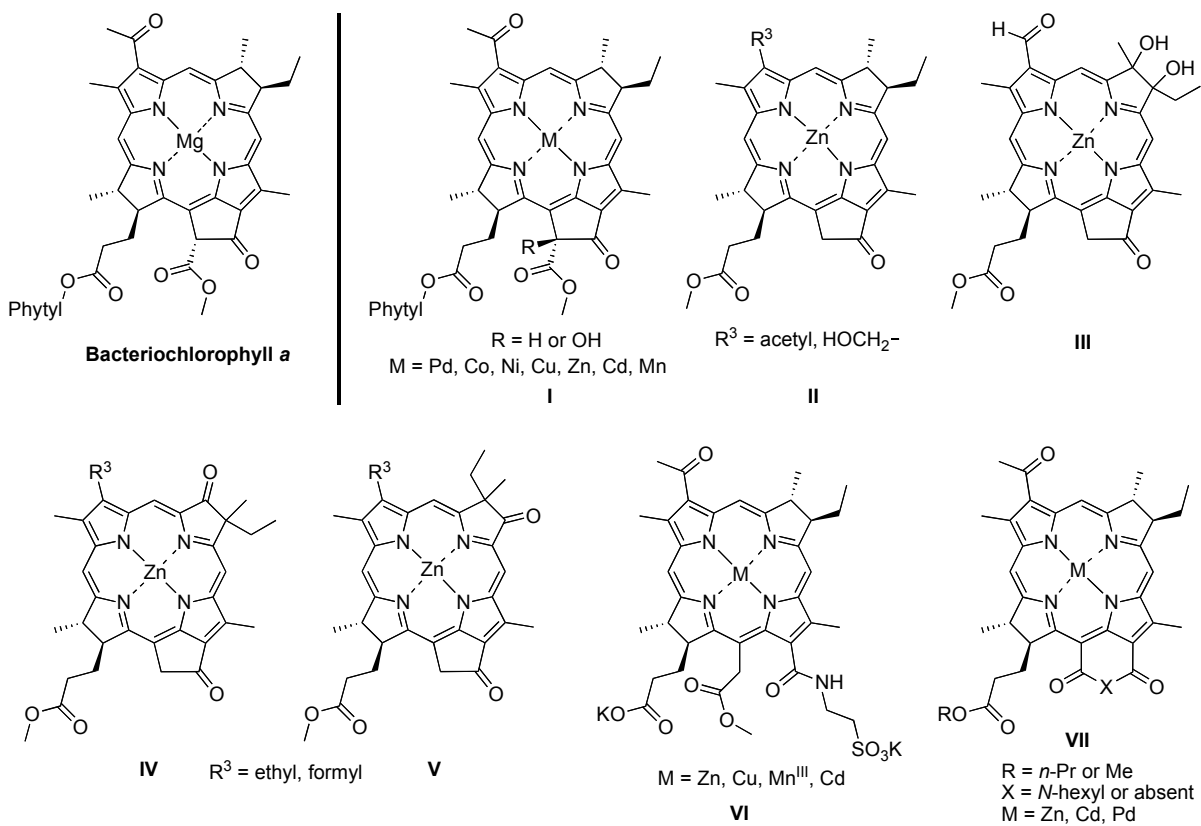


Chart 2.2. Metal chelates of naturally derived bacteriochlorins.

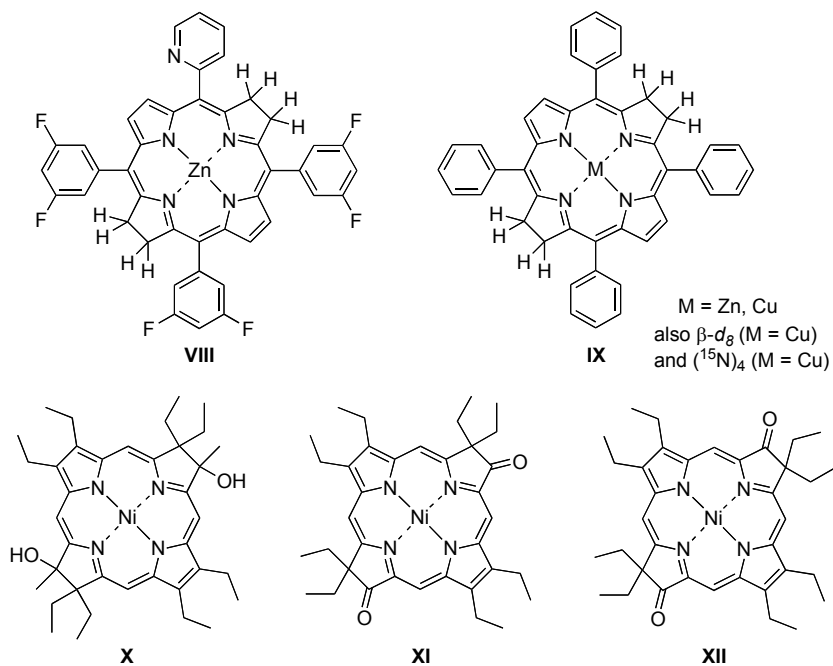


Chart 2.3. Metal chelates of synthetic bacteriochlorins.

In addition to the aforementioned general methods, several more specialized procedures have been reported for the preparation of metallochlorins. (1) Wasielewski employed a hindered Grignard reagent and a non-nucleophilic base to magnesiate Bphe *a* and thereby reconstitute Bchl *a*.⁵⁰ (2) Eschenmoser treated octaethylporphyrinogen with nickel acetate in refluxing xylene and obtained nickel octaethylbacteriochlorin; the process entails metalation, tautomerization, and $2e^-/2H^+$ oxidation (converting the hexahydroporphyrin to a tetrahydroporphyrin).^{51,52} (3) Stolzenberg applied the method of Arnold (formation and isolation of the dilithium derivative of a tetrapyrrole macrocycle followed by transmetalation with a metal reagent^{53,54}) with tetra-*p*-tolylbacteriochlorin to prepare the oxotitanyl chelate.⁵⁵ (4) Chen caused a nickel tetrabromoporphyrin to undergo scission of the two β -pyrrole carbons on opposing rings and thereby form a “bacteriophin,” which exhibits an absorption spectrum comparable to that of a bacteriochlorin.⁵⁶ An alternative approach to metallochlorins might be envisaged as the simple hydrogenation of a metalloporphyrin. Whereas tetrahydrogenation of a free base porphyrin affords the free base bacteriochlorin, tetrahydrogenation of a zinc porphyrin affords the zinc isobacteriochlorin rather than the zinc bacteriochlorin.⁵⁷

Through our recent work concerning the *de novo* synthesis of bacteriochlorins, two reactions were found unexpectedly to yield metallochlorins: (1) Pd-catalyzed cyanation of a free base 3,13-dibromobacteriochlorin with $Zn(CN)_2$ gave the corresponding zinc(II)-3,13-dicyano-8,8,18,18-tetramethylbacteriochlorin (Chart 2.4),⁵⁸ and (2) self-condensation of a dihydrodipyrin-acetal in CH_3CN containing $InCl_3$ afforded the corresponding indium bacteriochlorin²¹ (Scheme 2.2). The formation of the zinc chelate in

the former case might result from direct metalation of the electron-deficient 3,13-dicyanobacteriochlorin, and the latter case is thus far restricted to indium given that the metal reagent must provide acid catalysis for the condensation and also engender chelation during the course of the reaction. In general, no broadly applicable method for metalating synthetic bacteriochlorins has been developed to date.

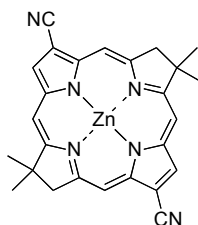
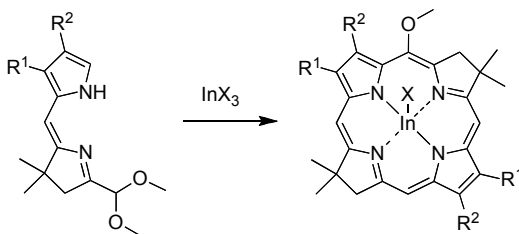


Chart 2.4. A zinc dicyanobacteriochlorin.



Scheme 2.2. Metalation during macrocycle formation.

2. Metal Insertion Studies. *Survey of Methods for an Electron-Rich Bacteriochlorin.* We examined the metalation of the di-*p*-tolylbacteriochlorin, **BC0-2T**, under four conditions.

(1) Treatment of **BC0-2T** with $\text{Zn}(\text{OAc})_2$, $\text{Cu}(\text{OAc})_2 \cdot \text{H}_2\text{O}$, $\text{Ni}(\text{OAc})_2 \cdot 4\text{H}_2\text{O}$, $\text{Pd}(\text{OAc})_2$, $\text{Pd}(\text{O}_2\text{CCF}_3)_2$ or $\text{Co}(\text{OAc})_2$ in $\text{CHCl}_3/\text{MeOH}$ at room temperature or reflux did not afford the metal chelate as determined by LD-MS and absorption spectroscopy. More

forcing conditions employing elevated temperature in two different solvent systems (ClCH₂CH₂Cl/MeOH and DMF) with Pd(O₂CCF₃)₂ (used in porphyrin metalation)⁵⁹ also showed only starting material.

(2) The standard “acac” conditions³⁴ with Zn(acac)₂ in refluxing benzene did not afford **ZnBC0-2T**.⁹⁵

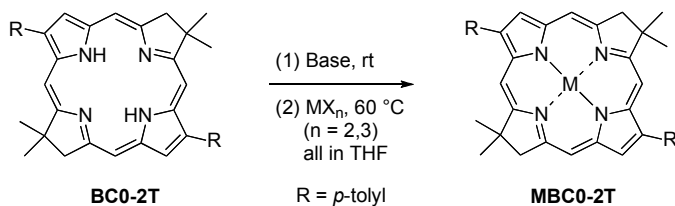
(3) Use of Cd(OAc)₂ in DMF at 130 °C, the initial step in the transmetalation method,²³ afforded a byproduct (M + 14; by LD-MS analysis) that was consistent with an analogue of **BC0-2T** wherein one of the pyrroline methylene units is oxidized to form a ketone (e.g., a putative oxobacteriochlorin). No bacteriochlorin chelate was formed.

(4) A room-temperature method for magnesium insertion into porphyrins employs MgI₂ and a non-coordinating base (e.g., diisopropylamine, DIEA) in a non-coordinating solvent (e.g., CH₂Cl₂).⁶⁰ An extension of this method, using ZnI₂ and DIEA in CH₂Cl₂ at reflux (~40 °C) for 12 h, afforded **ZnBC0-2T** in 30% yield as determined by absorption spectroscopy.

A base may be essential for metalation, to facilitate deprotonation of the bacteriochlorin and/or remove the acid liberated upon metalation (Equation 2.1). We examined a wide variety of bases and metal reagents at slightly elevated temperature. Ultimately we found that treatment of **BC0-2T** with NaH in THF at room temperature for 1 hour followed by Zn(OTf)₂ and heating to 60 °C for 12 h afforded the desired **ZnBC0-2T** (Table 2.2, entry 1). The development of this method is described in ref 95 (supporting information).



The method was applied to other metal reagents. Thus, use of PdBr_2 or $\text{Cu}(\text{OAc})_2$ afforded **PdBC0-2T** or **CuBC0-2T**, respectively (entries 2 and 3). The base LDA, which has comparable strength to that of NaH (pK_a of conjugate acid ~ 35),⁶¹ also was found to be effective. One key difference between NaH and LDA is that typically the former affords a heterogeneous reaction whereas the latter affords a homogeneous reaction. Use of LDA afforded **ZnBC0-2T** and **CuBC0-2T** from the same reagents as with NaH (entries 4 and 5). On the other hand, InCl_3 gave no insertion with NaH but did afford the $\text{ClIn}(\text{III})$ complex (**ClInBC0-2T**) upon use of LDA (entry 6). For examination of a variety of indium reagents, see ref 95 (supporting information). No metallobacteriochlorins were obtained under any condition explored with metal reagents based on MgX_2 ($X = \text{Cl, Br, I, OH, OTf}$), Al_2O_3 , AlX_3 ($X = \text{acac, Cl, Br}$), NiX_2 ($X = \text{acac, Cl, Br, I}$), SnX_2 ($X = \text{OH, OAc, acac, Br, I}$), or AuX_3 ($X = \text{Cl, Br, I}$). In summary, a few metals can be inserted into the electron-rich bacteriochlorin **BC0-2T** with use of NaH or LDA in THF. It warrants consideration that the alkali metal of the base (e.g., Na or Li) is likely not a spectator but instead plays a role in coordination of the deprotonated bacteriochlorin. In this regard, the overall metalation reflects in part a competition between two cations (acids) and two anionic ligands (bases). In-depth study of the nature of reaction intermediates, the role of counterions, and delineation of the kinetics and thermodynamics of reaction are beyond the scope of the present chapter.

Table 2.2. Survey of Metalation (BC0-2T).

Entry	Base	Metal Reagent	Time ^a	Product	Yield ^b
1	NaH	Zn(OTf) ₂	12 h	ZnBC0-2T	80%
2	NaH	PdBr ₂	0.5 h	PdBC0-2T	78%
3	NaH	Cu(OAc) ₂	3 h	CuBC0-2T	80%
4	LDA	Zn(OTf) ₂	2 h	ZnBC0-2T	quantitative
5	LDA	Cu(OAc) ₂	0.5 h	CuBC0-2T	56%
6	LDA	InCl ₃	1 h	ClInBC0-2T^c	85%

^aThe reaction conditions entail (1) treatment of **BC0-2T** (1.1 mg, 4.0 mM) in THF at room temperature with NaH (100 equiv = 400 mM) for 1 h or LDA (10 equiv = 40 mM) for 5 min, (2) addition of the metal reagent (30–80 mM, see ref 95, supporting information), and (3) heating at 60 °C for the indicated period. ^bThe crude mixtures were monitored by TLC and LD-MS. The yields were determined by absorption spectroscopy.

Zincation of Bacteriochlorins Bearing 0-4 Carbonyl Substituents. To better understand the scope of the metalation method (MX_n/NaH or LDA), we examined the set of bacteriochlorins shown in Chart 2.1 and isolated the corresponding metal chelates. For comparison, the standard “porphyrin metalation conditions” of Zn(OAc)₂·2H₂O in DMF were also examined. The unsubstituted bacteriochlorin **BC0** afforded **ZnBC0** in 80% isolated yield upon treatment with NaH/THF and Zn(OTf)₂ (Table 2.3, entry 1) whereas no reaction was observed with the standard porphyrin metalation conditions of Zn(OAc)₂·2H₂O

in DMF (entry 2). Treatment of diester-bacteriochlorin **BC2-2H** with the NaH/THF method for 6 h at 60 °C gave the zinc chelate in 31% yield (entry 3) whereas Zn(OAc)₂·2H₂O in DMF at 80 °C for 3 days gave some metalation but extensive byproducts interfered with isolation (entry 4). Essentially identical results were observed with the 5-methoxy analogue, namely **BC2-2H-MeO** (entries 5 and 6). Treatment of diester-bacteriochlorin **BC2-2M-MeO** with the NaH/THF method for 5 h at 60 °C gave the zinc chelate in 54% yield (entry 7) whereas use of LDA/THF for 3 h at 60 °C gave **ZnBC2-2M-MeO** in quantitative yield as determined by absorption spectroscopy (entry 8).

The remaining bacteriochlorins with 2-4 carbonyl groups (**BC2-2E**, **BC3-2E**, **BC4-MeO**) were each treated to the standard porphyrin zincation conditions [Zn(OAc)₂·2H₂O in DMF] at 60 °C for 16 h, and examined for metalation (by absorption spectroscopy and MALDI-MS). If metalation was less than quantitative, the reaction mixture was then heated at elevated temperature. Thus, **BC2-2E**, **BC3-2E**, and **BC4-MeO** were successfully metalated upon subsequent heating at 80 °C for 24, 7 and 3 h, respectively (entries 9-11). The differences in yield are attributed to purification procedures, given that each reaction appeared to go to completion.

In summary, bacteriochlorins bearing three or four carbonyl groups undergo zincation upon standard porphyrin metalation conditions, whereas those with no such electron-withdrawing groups do not, and instead require use of a strong base (NaH or LDA). Bacteriochlorins bearing two carboethoxy substituents undergo metalation via both the NaH or LDA/THF method and the DMF method, the conversion efficiency and ease of isolation depending on the nature of the set of bacteriochlorin substituents.

Table 2.3. Zinc Metalation of Synthetic Bacteriochlorins.

Entry	Substrate	Conditions ^a	Temp./Time	Product(s)	Isolated Yield
1	BC0	NaH/THF, Zn(OTf) ₂	60 °C/16 h	ZnBC0	80%
2	BC0	DMF, Zn(OAc) ₂ ·2H ₂ O	80 °C/24 h	no reaction	–
3	BC2-2H	NaH/THF, Zn(OTf) ₂	60 °C/6 h	ZnBC2-2H	31%
4	BC2-2H	DMF, Zn(OAc) ₂ ·2H ₂ O	80 °C/3 days	ZnBC2-2H and byproduct	–
5	BC2-2H-MeO	NaH/THF, Zn(OTf) ₂	60 °C/6 h	ZnBC2-2H-MeO	50%
6	BC2-2H-MeO	DMF, Zn(OAc) ₂ ·2H ₂ O	80 °C/3 days	ZnBC2-2H-MeO and byproduct	–
7	BC2-2M-MeO	NaH/THF, Zn(OTf) ₂	60 °C/5 h	ZnBC2-2M-MeO	54%
8	BC2-2M-MeO	LDA/THF, Zn(OTf) ₂	60 °C/3 h	ZnBC2-2M-MeO	Quantitative ^b
9	BC2-2E	DMF, Zn(OAc) ₂ ·2H ₂ O	^c 80 °C/24 h	ZnBC2-2E	86%
10	BC3-2E	DMF, Zn(OAc) ₂ ·2H ₂ O	^c 80 °C/7 h	ZnBC3-2E	54%
11	BC4-MeO	DMF, Zn(OAc) ₂ ·2H ₂ O	^c 80 °C/3 h	ZnBC4-MeO	97%

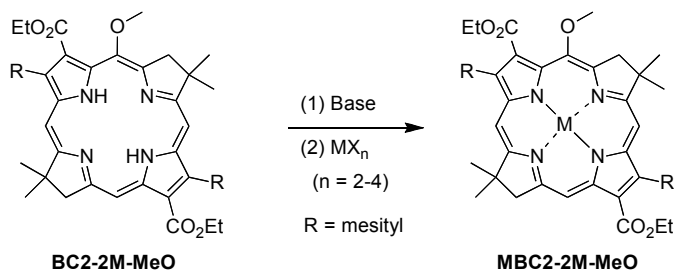
^aThe reaction conditions entail: (a) treatment of bacteriochlorin (4 mM) in THF at room temperature with NaH (150 equiv = 600 mM) for 1 h or LDA (10 equiv = 40 mM) for 5 min, followed by Zn(OTf)₂ (30 equiv) and heating as indicated; or (b) treatment of bacteriochlorin (4 mM) in DMF with Zn(OAc)₂·2H₂O (30 equiv) and heating as indicated. ^bYield determined by absorption spectroscopy. ^cAfter an initial period of 60 °C for 16 h.

Scope of Metalation of Diester-Bacteriochlorins. The diester-bacteriochlorin **BC2-2M-MeO** was readily zincated upon treatment with NaH or LDA in THF followed by Zn(OTf)₂ (Table 2.3, entries 7 and 8). We sought to examine the range of metal chelates that could be prepared with this substrate versus that lacking ester substituents (i.e., **BC0-2T**) as examined in Table 2.1. Thus, metalation of **BC2-2M-MeO** was monitored by TLC, absorption spectroscopy, and MALDI-MS. Metal reagents that provided the best yield in the metalation of **BC0-2T** were examined for **BC2-2M-MeO** and also gave reasonable yields (Table 2.4, entries 1-5). In addition to insertion of Zn(II), Cu(II), Pd(II) and In(III), treatment with NiCl₂, CdCl₂ and SnCl₂ also gave the corresponding metal chelates (Table 2.4, entries 6-8). For insertion of SnCl₂ as well as SnCl₄, only partial metalation was observed despite supplemental reagents or prolonged reaction time (entries 8 and 9). Here, the reaction failed with Mg(OTf)₂, Al(OTf)₂, and AuCl₃.

Surprisingly, when **BC2-2M-MeO** was treated with NaH and PdBr₂, the reaction mixture showed a peak at [M – 30] in comparison to the starting material by MALDI-MS (Table 2.4, entry 2). The absorption spectrum showed a hypsochromically shifted Q_x band and a bathochromically shifted Q_y band; the positions of the resulting bands were typical for the absence of a methoxy group.^{16,20} The reaction at the multimilligram scale afforded a product that upon isolation and characterization (by ¹H NMR spectroscopy, absorption spectroscopy, MALDI-MS and ESI-MS) proved indeed to be the free base bacteriochlorin that lacks the 5-methoxy group (**BC2-2M**, Chart 2.5). A Ni-catalyzed process for reductive cleavage of aryl methyl ethers has recently been reported.⁶² The proposed mechanism

included reductive elimination from a nickel(II) hydride intermediate. Herein, palladium(II) hydride generated from PdBr₂ and NaH might account for demethoxylation.

Table 2.4. Survey of Metalation of Bacteriochlorin BC2-2M-MeO.



Entry	Base	Metal Reagent	Time ^a	Product	Yield ^b
1	NaH	Cu(OAc) ₂	8 h	CuBC2-2M-MeO	39%
2	NaH	PdBr ₂	2 h	BC2-2M	29% ^c
3	LDA	Cu(OAc) ₂	20 h	CuBC2-2M-MeO	42%
4	LDA	InCl ₃	28 h	ClInBC2-2M-MeO	59%
5	LDA	PdBr ₂	3 h	PdBC2-2M-MeO	71%
6	NaH	NiCl ₂	3 h	NiBC2-2M-MeO	78%
7	NaH	CdCl ₂	3 h	CdBC2-2M-MeO	78%
8	NaH	SnCl ₂	1 h	Cl₂SnBC2-2M-MeO	53% ^d
9	NaH	SnCl ₄	2 h	Cl₂SnBC2-2M-MeO	31% ^e

^aThe reaction conditions (0.60 mg of **BC2-2M-MeO**) entail (1) treatment of **BC2-2M-MeO** (4.0 mM) in THF at room temperature with NaH (600 mM) for 1 h or LDA (40 mM) for 5 min, followed by (2) addition of the metal reagent and heating at 60 °C for the indicated period. ^bThe crude mixtures were monitored by TLC and MALDI-MS. The yields were determined by absorption spectroscopy (assuming equal molar absorptivity of the respective free base and metallo-bacteriochlorins at the Q_y(0,0) band). ^cIsolated yield based on 7.8 mg of **BC2-2M-MeO**. ^dThe free base bacteriochlorin also was present (24% yield). ^eThe free base bacteriochlorin also was present (69% yield).

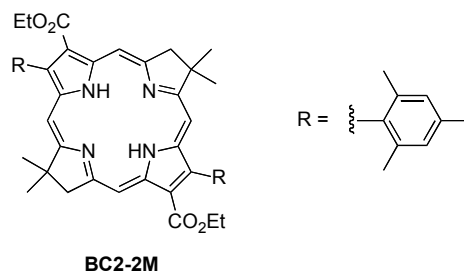


Chart 2.5. Demethoxylated byproduct upon attempted palladiation.

Magnesium of Ester-Bacteriochlorins. Magnesium tetrapyrroles (e.g., chlorophylls, bacteriochlorophylls) are ubiquitous, a fact thrown into sharp relief given the historical difficulties that have surrounded the chemical insertion of magnesium into the free base macrocycles.⁶⁰ The biosynthetic incorporation of magnesium (into protoporphyrin IX) is endergonic.⁶³ Magnesium porphyrins are class IV metalloporphyrins³² and as such readily demetalate upon exposure to weak acids such as silica gel and acetic acid. Failure to magnesiate **BC2-2M-MeO** with $\text{Mg}(\text{OTf})_2$ and NaH in THF, while not unexpected, also pointed toward the use of other reaction conditions and/or more electron-deficient bacteriochlorins. As stated above, porphyrins (and many chlorins) can be magnesiated upon use of MgX_2 ($\text{X} = \text{Br}$ or I) under non-coordinating slightly basic conditions (e.g., in CH_2Cl_2 containing triethylamine (TEA)).⁶⁰

Application of the condition for magnesiation of porphyrins⁶⁰ (MgI_2 in CH_2Cl_2 containing TEA) to the tetraester-bacteriochlorin **BC4-MeO** did not yield any magnesium chelate after 16 h (Table 2.5, entry 1). A large excess of magnesium reagent only resulted in the decomposition of **BC4-MeO** (Table 2.5, entry 2). Returning to the conditions identified for zincation in Table 2.2, **BC4-MeO** in THF was treated with NaH followed by MgI_2 (Table 2.5, entries 3 and 4). After heating at 60 °C for 24 h, the Q_x band was found at 612 nm

(versus 548nm for **BC4-MeO**; all in CH₂Cl₂) and a peak at [M + 22] was found upon MALDI-MS, indicating formation of the magnesium chelate. However, the crude mixture contained a significant amount of unknown impurities as examined by TLC and absorption spectroscopy. Increasing the amount of NaH to 300 equivalents considerably reduced the impurities and the reaction was completed within 3 h. The magnesium chelate was found to be quite unstable, decomposing in CH₂Cl₂ solution within 2 h at room temperature, but could be handled by avoiding chlorinated solvents and by performing chromatography on basic alumina. Although the tetraester-bacteriochlorin **BC4-MeO** was successfully magnesiated, **BC3-2E** and **BC2-2E** each gave no reaction under similar conditions (entries 5 and 6).

Table 2.5. Survey of Magnesiation of Bacteriochlorins.^a

Entry	Substrate	Condition	Base ^b	Metal reagent	Result ^c
1	BC4-MeO	40 °C, 16 h	[TEA] = 80 mM	40 mM	No reaction
2	BC4-MeO	40 °C, 5 h	[TEA] = 80 mM	120 mM	Decomposition
3	BC4-MeO	60 °C, 24 h	[NaH] = 0.6 M	120 mM	MgBC4-MeO and byproducts
4	BC4-MeO	60 °C, 3 h	[NaH] = 1.2 M	120 mM	MgBC4-MeO
5	BC3-2E	60 °C, 40 h	[NaH] = 1.2 M	120 mM	No reaction
6	BC2-2E	60 °C, 30 h	[NaH] = 0.6 M	120 mM	No reaction

^aThe reaction procedure entails treatment of substrate (4 mM) in CH₂Cl₂ (with TEA) or THF (with NaH) followed by MgI₂ at the indicated temperature for the indicated time. ^bThe quantity is given in concentration units for ease of comparison even though not all material may be dissolved. ^cThe crude mixture was checked by TLC, absorption spectroscopy, and MALDI-MS.

A summary of our observations concerning metalation of synthetic bacteriochlorins is shown in Figure 2.1. The chief results are as follows: (1) Bacteriochlorins lacking any electron-withdrawing groups, including unsubstituted **BC0**, afford a limited set of metal chelates upon treatment with a strong base (NaH or LDA) in THF. (2) The same strong-base conditions accommodate a broader scope of metal chelates upon application to a bacteriochlorin bearing two carboethoxy substituents. (3) Bacteriochlorins bearing 2–4 carbonyl (carboethoxy, imide) substituents can be zincated with the standard “porphyrin metalation conditions” of $\text{Zn}(\text{OAc})_2 \cdot 2\text{H}_2\text{O}$ in hot DMF. (4) Where direct comparisons were made for the bacteriochlorins bearing two carboethoxy substituents, treatment with a strong base (NaH or LDA) afforded more rapid and cleaner metalation than use of $\text{Zn}(\text{OAc})_2 \cdot 2\text{H}_2\text{O}$ in hot DMF. (5) A bacteriochlorin bearing 4 carboethoxy substituents could be magnesiated under the strong base conditions, but the resulting magnesium chelate exhibited limited stability. (6) *Ortho*-aryl substituents are known to slow substantially the rate of metalation of *meso*-tetraarylporphyrins,⁶⁴ yet no adverse effect was observed upon application of the preparative procedures with the dimesitylbacteriochlorin (**BC2-2M-MeO**).

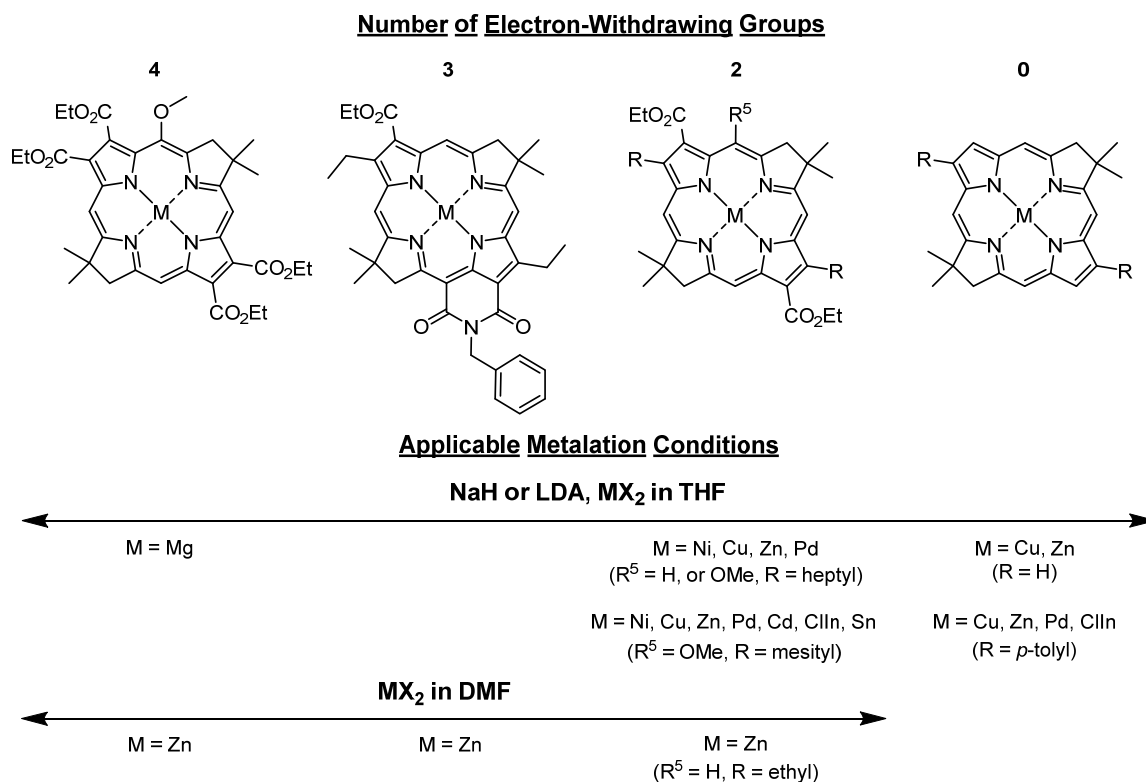


Figure 2.1. Summary of metalation of synthetic bacteriochlorins.

Isolation and Characterization of Metallobacteriochlorins. A number of reactions were carried out at the multimilligram scale to obtain sufficient metallobacteriochlorin for physicochemical studies. Thus, eight zinc bacteriochlorins (Tables 2.2 and 2.3), three copper chelates (**CuBC2-2M-MeO**, **CuBC0-2T**, **CuBC0**), two palladium chelates (**PdBC2-2M-MeO**, **PdBC0-2T**), and one indium chelate (**ClInBC0-2T**) were isolated and characterized. Upon purification, the metallobacteriochlorins were stable under dry conditions in the absence of light for an extended period. Each metallobacteriochlorin was characterized by ¹H NMR spectroscopy (except for Cu bacteriochlorins), absorption spectroscopy, MALDI-MS or LD-MS, and ESI-MS. The magnesium chelate (**MgBC4-MeO**) was only partially

characterized owing to limited stability. The availability of these various metallobacteriochlorins enabled the physicochemical studies described in the following sections.

(III) Structural and Physicochemical Characteristics. 1. Structural Analysis.

The single-crystal X-ray structures of bacteriochlorins **BC0**, **BC0-2M**, and **CuBC0-2T** are shown in Figure 2.2. Note that **BC0-2M** contains 3,13-dimesityl groups whereas **CuBC0-2T** contains 2,12-di-*p*-tolyl groups. While a sizable number of photosynthetic proteins containing bacteriochlorophylls have been examined by X-ray crystallography, relatively few single-crystal X-ray studies have been carried out of bacteriochlorins. These include synthetic free base bacteriochlorins,⁶⁵ synthetic metallobacteriochlorins,^{42,52,66} and naturally derived (free base) bacteriopheophorbides.⁶⁷

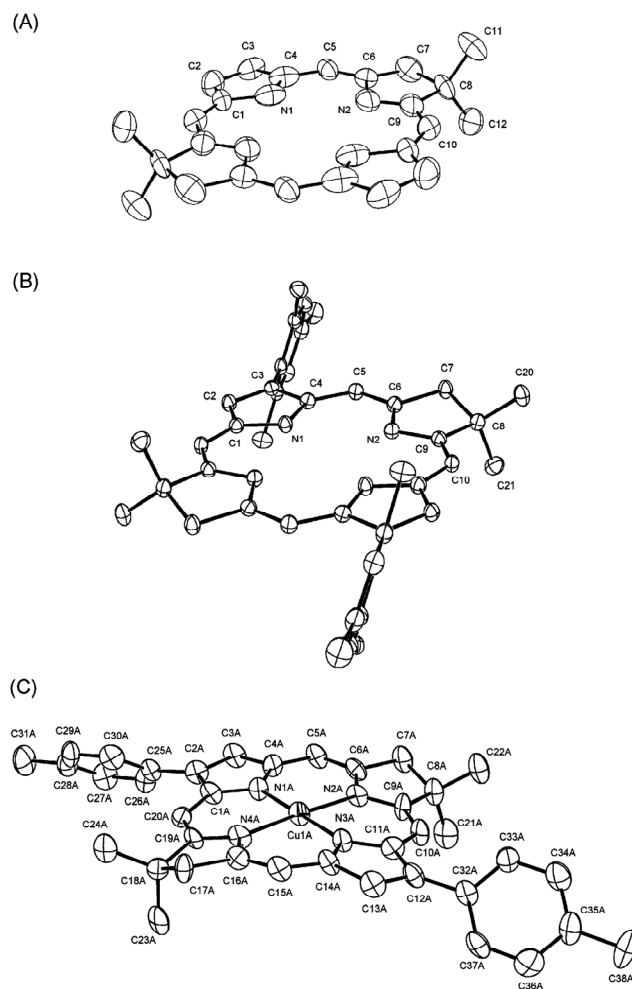


Figure 2.2. ORTEP drawing of (A) free base bacteriochlorin **BC0**, (B) free base bacteriochlorin **BC0-2M**, and (C) copper bacteriochlorin **CuBC0-2T** (one molecule from the unit cell). Ellipsoids are displayed at the 50% probability level and hydrogen atoms are omitted for clarity. The large spherical ellipsoids of **BC0** result from the high R factor value due to the weakly diffracting crystal.

The core shape of porphyrin (**porphine**), chlorin (**FbC**), and bacteriochlorins (**BC0**) macrocycles are shown in Figure 2.3. The core shape of porphine is close to square,⁶⁸ while that of chlorin **FbC** is slightly kite-shaped due to the presence of one pyrroline ring (D) and

three pyrrole rings (A, B, and C).^{69,70} The core shape of bacteriochlorin **BC0** is slightly rectangular. The two pyrrole rings and two pyrroline rings that constitute a bacteriochlorin alternate upon circumambulating the macrocycle; thus, the two pyrroline rings occupy opposite corners, as do the two pyrrole rings. The core size can be evaluated by the comparison of the average distances between each of the nitrogen atoms and their centroid.⁷¹ The order of average nitrogen-centroid distances is porphine (2.055 Å) < chlorin (2.074 Å) < bacteriochlorin (2.096 Å).

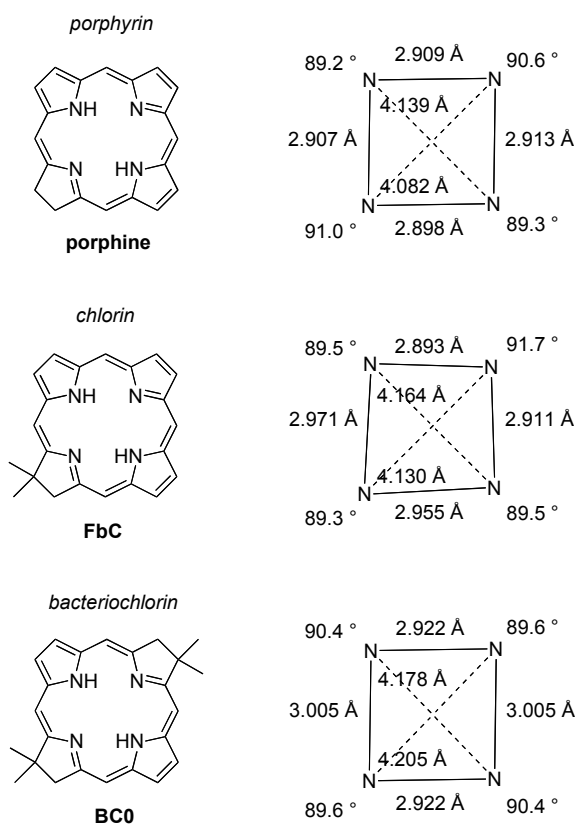


Figure 2.3. Comparison of core structural parameters across porphyrin, chlorin, and bacteriochlorin macrocycles.

The core shape of the copper bacteriochlorin **CuBC0-2T** is shown in ref 95 (supporting information). Copper bacteriochlorin **CuBC0-2T** is fairly planar, with the copper atom located on the least-square plane defined by the four nitrogen atoms. The average copper–centroid distance is 2.005 Å, which is shorter than that of free base bacteriochlorins **BC0** and **BC0-2M** (~2.095 Å).

2. Spectral Properties. The ground-state electronic absorption spectra of the metallochlorins and the free base bacteriochlorins in toluene are shown in Figure 2.4 (**Zn** series) and Figure 2.5 (**BC0-2T** series). The spectral data including the position, intensity, and full-width at half maximum (fwhm) of the long-wavelength absorption band (Q_y); the shift ($\Delta\lambda$) in the position of the Q_y band with respect to the free base bacteriochlorins; and intensity ratios of the Q_y to B_y bands (I_{Q_y}/I_{B_y} ratio) are listed in Table 2.6. Table 2.6 also gives spectral data for the native bacteriochlorins. In general, the absorption spectra of the synthetic metallochlorins resemble that of Bchl *a*, just as the spectra of the synthetic free base bacteriochlorins resemble that of the native free-base (Mg-less) analogue Bphe *a*.

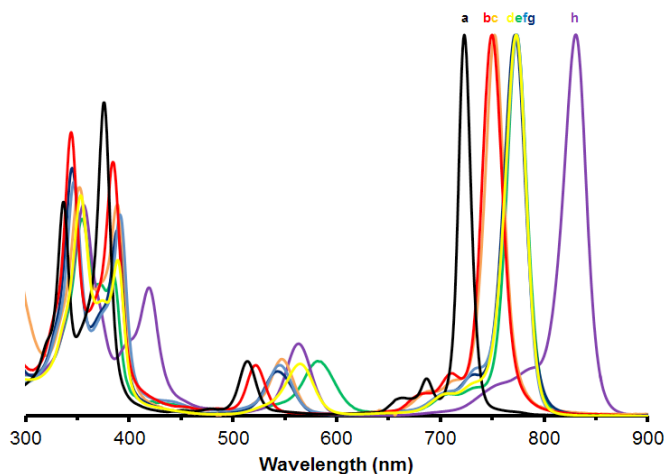


Figure 2.4. Absorption spectra in toluene at room temperature of bacteriochlorins (normalized at the Q_y bands). The labels in the graph are as follows: (a) **ZnBC0** (black), (b) **ZnBC0-2T** (red), (c) **ZnBC2-2H-MeO** (orange), (d) **ZnBC2-2M-MeO** (yellow), (e) **ZnBC4-MeO** (green), (f) **ZnBC2-2E** (blue), (g) **ZnBC2-2H** (dark blue), and (h) **ZnBC3-2E** (purple).

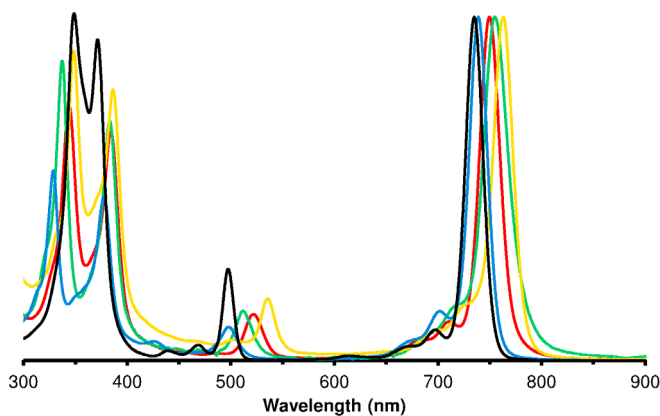


Figure 2.5. Absorption spectra in toluene at room temperature of bacteriochlorins (normalized at the Q_y bands). The labels in the graph are as follows: (a) **BC0-2T** (black), (b) **PdBC0-2T** (blue), (c) **ZnBC0-2T** (red), (d) **CuBC0-2T** (green), and (e) **ClInBC0-2T** (orange).

Table 2.6. Spectral Properties of Bacteriochlorins.^a

Compound	B _y (0,0) ^b abs λ (nm)	B _x (0,0) ^b abs λ (nm)	Q _x (0,0) abs λ (nm)	Q _y (0,0) abs λ (nm)	Q _y (0,0) abs fwhm (nm)	Q _y (0,0) em λ (nm)	Q _y (0,0) em fwhm (nm)	ΔQ _x ^c Δλ (nm)	ΔQ _y ^c Δλ (nm)	I _{Q_y} /I _{B_y}
<i>Zn-BCs</i>										
ZnBC0-2T	344	384	521	749	23	756	26	22	13	1.3
ZnBC2-2M-MeO	353	389	565	773	25	780	26	27	15	1.6
ZnBC4-MeO	354	385	581	774	22	782	27	31	15	2.0
ZnBC3-2E	356	419	564	830	27	835	23	20	12	1.7
ZnBC2-2E	347	391	546	773	24	778	25	25	12	1.6
ZnBC2-2H	347	391	547	775	23	780	24	26	13	1.2
ZnBC2-2H-MeO	353	389	548	750	26	758	26	26	10	1.3
ZnBC0	336	375	514	723	14	725	18	25	10	1.7
<i>Pd-BCs</i>										
PdBC0-2T	330	379	499	739	21	745	25	0	3	1.7
PdBC2-2M-MeO	337	382	538	758	20	765	23	0	0	2.8
<i>Cu-BCs</i>										
CuBC0-2T	337	383	512	755	29	--	--	13	18	1.2
CuBC2-2M-MeO	348	390	556	780	37	--	--	18	22	1.5
CuBC0	332	378	507	728	19	--	--	18	15	1.7

Table 2.6. Continued

<i>FbBCs</i>										
BC0-2T	351	374	499	736	20	742	23	0	0	1.0
BC2-2M-MeO	361	383	538	758	22	765	23	0	0	1.0
BC4-MeO^d	361	368	550	759	20	763	23	0	0	1.2
BC3-2E^d	358	408	544	818	24	823	24	0	0	1.3
BC2-2E^d	354	383	521	761	20	764	21	0	0	0.9
BC2-2H	354	383	521	762	20	766	21	0	0	0.9
BC2-2H-MeO	357	379	522	740	18	746	21	0	0	1.1
BC0^d	340	365	489	713	12	716	16	0	0	0.9
<i>In-ClBCs</i>										
ClInBC0-2T^e	350	388	539	763	23	769	31	40	27	1.1
<i>MgBCs</i>										
MgBC4-MeO	360	380	599	776	31	780	33	49	17	0.9
<i>Native BCs</i>										
BChl a	363	396	581	781	28	789	29	49	21	1.4
BPhe a ^d	362	389	532	758	31	768	27	0	0	0.7

^aIn toluene at room temperature. ^bThe nominal B_x(0,0) and B_y(0,0) absorption bands may alternate order with compound and have mixed x and y polarization. ^cThe shift of the band relative to that of the free base analogue. ^dData from ref 20. ^eData from ref 21.

The spectrum of each bacteriochlorin exhibits four absorption bands generally categorized as $B_y(0,0)$, $B_x(0,0)$, $Q_x(0,0)$, and $Q_y(0,0)$ from short to long wavelength. ($B_y(0,0)$ and $B_x(0,0)$ may reverse positions depending on the bacteriochlorin and have mixed x and y polarizations.) In general, the B bands of all bacteriochlorins examined herein fall in the region 330 to 419 nm. The Q bands of the **BC0-2T** series including the free base and all metal chelates lie at shorter wavelength (Q_x 499 to 536 nm; Q_y 737 to 763 nm) versus those of the **BC2-2M-MeO** series (Q_x 524 to 556 nm; Q_y 758 to 779 nm). For the **Zn** series, the Q bands are located at longer wavelength compared to the corresponding free base bacteriochlorins. The shifts in Q_x bands (19–34 nm) are generally more significant than those of Q_y bands (12–16 nm). The Q_y bands of the synthetic bacteriochlorins are quite intense. For **BC0-2T**, the long-wavelength maximum (732 nm) has a molar absorptivity of $\sim 120,000 \text{ M}^{-1} \text{ cm}^{-1}$.¹⁶

Within the same bacteriochlorin series, the extent of the Q_x band shift increases in order of $\text{Pd} < \text{Cu} < \text{Zn} (< \text{ClIn})$ chelates, while that of Q_y increases in order of $\text{Pd} < \text{Zn} < \text{Cu} (< \text{ClIn})$. Each bacteriochlorin features a sharp Q_y band with fwhm in the range of 20–24 nm, except for the Cu chelates which exhibit broadened Q_y band in the range of 29–40 nm. The intensity ratios of the Q_y to B_y bands of the metallochlorins increase inversely with the increase of the wavelength shift ($\Delta\lambda$) with respect to the free base bacteriochlorins in order of $(\text{ClIn}) < \text{Cu} < \text{Zn} < \text{Pd}$. For the **Zn** series, the intensity ratios of the Q_y to B_y bands fall in the range of 1.3–1.9.

The fluorescence spectrum of each zinc bacteriochlorin is dominated by a $Q_y(0,0)$ band that is only modestly (5–10 nm) shifted to longer wavelength than the $Q_y(0,0)$

absorption band and has a comparable spectral width (Table 2.6). This behavior is analogous to that observed for free base bacteriochlorins (Table 2.6 and ref 20). Similar fluorescence spectra are found for the indium chelates, as we have reported previously,²¹ and for the palladium bacteriochlorins. However, compared to the zinc and free base bacteriochlorins, the fluorescence intensities are much weaker for the indium complexes and weaker still for the palladium complexes as described in the following.

3. Photophysical Properties. Table 2.7 lists the photophysical properties of the zinc and palladium bacteriochlorins, along with representative data for the free base and indium analogues. The table also gives data for the native chromophores Bchl *a* and Bphe *a* in toluene. In comparing exact values of the photophysical characteristics of the zinc and free base bacteriochlorins, one must take into account that some of the zinc chelates may be axially ligated because they, like a few Fb complexes, were studied in THF rather than toluene for greater solubility (as indicated in Table 2.7 footnotes).

The zinc bacteriochlorins exhibit fluorescence quantum yields (Φ_f) generally in the range 0.08–0.20 with an average value of 0.13 that is comparable to that (0.15) for the free base analogues studied here or previously.²⁰ The exception is $\Phi_f = 0.033$ for the bacteriochlorin–imide **ZnBC3-2E**, which like that (0.040)²⁰ for the free base analogue is reduced due to the lower energy ($Q_y > 800$ nm; Table 2.6) of the singlet excited state resulting in more facile nonradiative internal conversion. The lifetimes (τ_s) of the singlet excited state for the zinc bacteriochlorins are in the range 2.2–4.4 ns, with an average value of 3.3 ns. These lifetimes are also similar to those for the free base analogues (3.3–4.4 ns; average 3.8 ns). The typical yield of intersystem crossing to the triplet excited state (Φ_{isc}) for

the zinc bacteriochlorins is ~ 0.7 , which is somewhat greater than the average value of ~ 0.5 for the free base analogues due to a modest effect of the metal ion on spin-orbit coupling. The typical Φ_f and τ_S values for the indium chelates (0.02 and ~ 0.3 ns)²¹ are reduced and the Φ_{isc} values (~ 0.9) increased from those for the zinc chelates due to greater heavy metal enhancement of spin-orbit coupling.

Table 2.7. Photophysical, Redox, and Molecular-Orbital Properties of Bacteriochlorins.^a

Compound	τ_S (ns)	Φ_f	Φ_{isc}	τ_T^c (μ s)	E_{ox}^b (V)	E_{red}^b (V)	HOMO (eV)	LUMO (eV)
<u>Zn-BCs</u>								
ZnBC0-2T	2.9	0.11	0.83	161	-0.04	-1.60	-4.26	-2.20
ZnBC2-2M-MeO	2.9	0.12	0.71	120	+0.45	-1.38	-4.55	-2.51
ZnBC4-MeO	4.4	0.13	0.80	38	+0.16	-1.10	-4.87	-2.92
ZnBC3-2E	2.2	0.033	0.28	94	+0.02	-1.12	-4.78	-2.94
ZnBC2-2E	2.6	0.08	0.71	149	-0.12	-1.42	-4.48	-2.53
ZnBC2-2H	3.5	0.14	0.60	191	0.00	-1.42	-4.47	-2.52
ZnBC2-2H-MeO	4.3	0.20	0.70	187	-0.14	-1.47	-4.48	-2.46
ZnBC0	3.4	0.10	0.67	151	-0.12	-1.68	-4.30	-2.16
<u>Pd-BCs</u>								
PdBC0-2T	0.35	0.020	>0.99	12	+0.43	-1.14	-4.36	-2.26
PdBC2-2M-MeO	0.015	0.006	>0.99	5.8	+0.29	-1.29	-4.63	-2.54
<u>Cu-BCs</u>								
CuBC0-2T				0.5 ns ^c	-0.04	-1.53	-4.25	-2.25
CuBC2-2M-MeO				1.7 ns ^c	+0.18	-1.32	-4.53	-2.55
CuBC0				0.3 ns ^c	-0.04	-1.60	-4.27	-2.18
<u>FbBCs</u>								
BC0-2T^d	3.3	0.18	0.55	163	+0.21	-1.49	-4.40	-2.22
BC2-2M-MeO	3.9	0.15	0.35	52	+0.38	-1.29	-4.65	-2.48
BC4-MeO^d	4.3	0.16	0.24	46	+0.57	-1.05	-5.00	-2.95
BC3-2E^d	1.9	0.04	0.51	85	+0.45	-0.98	-4.91	-2.99

Table 2.7. Continued.

BC2-2E^d	3.3	0.14	0.55	110	+0.29	-1.32	-4.68	-2.58
BC2-2H	3.3	0.10	0.45	110	+0.29	-1.33	-4.59	-2.52
BC2-2H-MeO	4.4	0.17	0.49	86	+0.28	-1.43	-4.60	-2.45
BC0^d	3.9	0.14	0.24	169	+0.45	-0.99	-4.46	-2.20
<i>In-ClBCs</i>								
ClInBC0-2T^e	0.21	0.016	0.9	44	+0.31	-1.25	-4.52	-2.52
<i>MgBCs</i>								
MgBC4-MeO	5.4	0.16	0.60	90			-4.86	-2.94
<i>Native BCs</i>								
BChl <i>a</i>	3.1	0.12	0.30	50			-4.75	-2.86
BPhe <i>a^d</i>	2.7	0.10	0.57	25			-4.87	-2.84

^aIn toluene at room temperature except as follows: the τ_T values for all compounds and the Φ_f , Φ_{isc} , and τ_S values for **BC2-2H**, **BC2-2H-MeO**, **ZnBC0**, **ZnBC2-2H**, **ZnBC2-2H-MeO** and **MgBC4-MeO** were determined in tetrahydrofuran. ^bFirst oxidation (E_{ox}) and first reduction (E_{red}) potentials measured in 0.1 M tetrabutylammonium hexafluorophosphate in which the ferrocene couple has an $E_{1/2}$ of 0.19 V. ^cDecay of the tripdouplet/quartet excited-state manifold in nanoseconds. ^dData from ref 20. ^eData from ref 21.

The heavy metal effect (and potential d-orbital contribution) is greater still for the palladium bacteriochlorins, resulting in essentially quantitative singlet-to-triplet intersystem crossing. The consequence for **PdBC2-2M-MeO** is a very low fluorescence yield ($\Phi_f = 0.006$) and singlet lifetime ($\tau_S = 15$ ps). The two values are somewhat greater for **PdBC0-2T** for reasons that are not clear. Enhanced spin-orbit coupling also results in a progressive shortening of the lifetime of the lowest triplet excited state (τ_T) from a typical value of ~ 100 μ s for the zinc and free base bacteriochlorins to ~ 30 μ s for the indium chelates and to ~ 10 μ s for the palladium chelates.

In the case of copper bacteriochlorins (**CuBC0**, **CuBC0-2T**, **CuBC2-2M-MeO**), interactions involving the unpaired metal electron associated with the d^9 configuration of Cu(II) transform the macrocycle singlet excited state into a “singdoublet” and split the macrocycle triplet excited state into “tripdoublet” and “quartet” excited states that are close in energy, in analogy to copper porphyrins.⁷ Normal fluorescence is not expected (and none is found in the case of **CuBC2-2M-MeO**). Transient absorption studies of **CuBC0**, **CuBC0-2T**, and **CuBC2-2M-MeO** indicate essentially complete decay to the ground state with time constants of 0.3, 0.5, and 1.7 ns in THF. This time evolution likely represents deactivation of the tripdoublet/quartet excited-state manifold via a ring-to-metal charge-transfer state that has been implicated in the excited-state dynamics of copper porphyrins,⁷² but which now lies at lower energy in the corresponding bacteriochlorins due to the greater ease of macrocycle oxidation.

Zinc tetrapyrroles (generally porphyrins and chlorins until the present) are often exploited in photophysical and photochemical applications compared to the corresponding magnesium complexes due to a reduced propensity for demetalation. In the case of porphyrins, a sacrifice is a shorter singlet excited-state lifetime (e.g., ~2 versus ~6 ns) and fluorescence yield (~0.03 versus ~0.13). Here we have found that the zinc bacteriochlorin **ZnBC4-MeO** has Φ_f , τ_S , Φ_{isc} , and τ_T values comparable to those of the corresponding magnesium bacteriochlorin **MgBC4-MeO**. In this regard, compared to the native magnesium bacteriochlorin, Bchl *a* (Table 2.6),⁷³⁻⁷⁵ the zinc bacteriochlorins generally have similar Φ_f , comparable or greater τ_S , comparable Φ_{isc} , and longer τ_T values. This comparison is similar to that for the free base bacteriochlorins relative to the native metal-free bacteriochlorin Bphe

a (Table 2.6).²⁰ In summary, the synthetic zinc bacteriochlorins (and the indium and palladium analogues), like the free base bacteriochlorins, exhibit photophysical characteristics suitable for a range of applications in solar-energy conversion and photomedicine.

4. Electrochemical and Molecular Orbital Characteristics. The redox properties (reduction potentials) and energies of the frontier MOs of the bacteriochlorins are listed in Table 2.7. Only the potentials for the first oxidation (E_{ox}) and reduction (E_{red}) (which are both reversible) are presented in the table, as these are most germane for the discussion below. It should be noted, however, that the molecules also exhibit redox processes corresponding to second oxidations and reductions. Differences in the E_{ox} and E_{red} values among the the different metallobacteriochlorins and free base analogues generally parallel those for porphyrin systems.² In prior work on a large number of chlorins,⁷⁶ good correlations were found between the E_{ox} and the HOMO energy and between the E_{red} and the LUMO energy. Such a correlation is generally found in Table 2.7 and in Figure 2.6, which plots the redox potentials and MO energies versus the number of electron-withdrawing groups on the bacteriochlorin.

Comparison of HOMO and LUMO energies of compounds **BC0**, **BC0-2T**, and **BC3-2E** listed in Table 2.7 with the values for their counterparts studied previously²⁰ that contain a 5-methoxy group shows that the 5-methoxy group shifts the MO energies by a relatively small amount (≤ 0.08 eV). When there is a shift in the MO energies, the shift is to slightly more negative values, indicating that the compound should be slightly harder to oxidize and easier to reduce. The data in Table 2.7 and Figure 2.6 further show that an increasing

number of electron-withdrawing groups on the bacteriochlorin (affording greater ease of metalation) is reflected in a more positive E_{ox} (harder to oxidize) and a less negative E_{red} (more difficult to reduce). The one compound that is an outlier is **BC0**. Along the same set of compounds, an increasing number of electron-withdrawing groups is reflected in shifts in the HOMO energy to more negative values (harder to oxidize) and the LUMO energy to more negative values (easier to reduce). Here, compound **BC0** is not an outlier and has essentially the same MO energies as compound **BC0-2T**. Thus, the fact that **BC0** is an outlier in the redox data may be in part a solvation (electrolyte) effect.

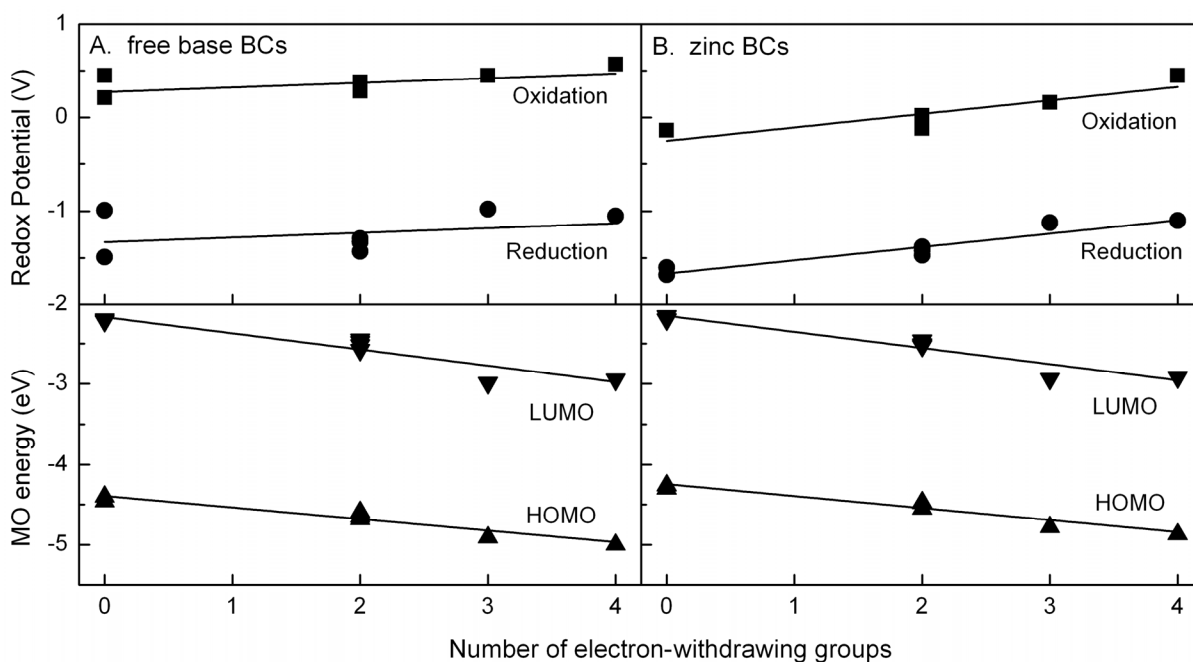


Figure 2.6. The effect of the number of electron-withdrawing (carbonyl) groups on the redox potentials and frontier MO energies.

As expected, an increasing number of electron-withdrawing groups shifts the redox potentials and MO energies so as to make it harder to remove an electron (or electron density) and easier to add an electron (or electron density). Because metalation involves replacing two protons of the free base with a divalent metal ion, and a pair of protons is typically more electropositive than the metal ion, metalation effectively involves a net addition of electron density to the macrocycle. This property results in the correlation between the ease of metalation and the redox and MO energies.

The above comparisons are made for a set of bacteriochlorins that differ in the number and types of substituents at the same macrocycle positions. These changes cause shifts in the energies and electron densities of the HOMO and LUMO, but do not alter the identities of these two orbitals. The finding of such correlations, or even the interpretation if they are found, may be more difficult if the set of molecules differ in the sites of macrocycle substitution, and particularly if different macrocycles are involved. For example, depending on the substituent pattern, in progressing from porphyrin to chlorin (and then to bacteriochlorin), the HOMO may change from the $a_{2u}(\pi)$ orbital that has substantial electron density at the central nitrogens (and metal ion once incorporated) to the $a_{1u}(\pi)$ -like orbital that has far less electron density or even nodes at these positions. Such a switch would need to be taken into account in assessing relationships between the ease (kinetics and thermodynamics) of metalation versus the MO and redox properties.

Conclusions and Outlook

The ability to prepare synthetic metallobacteriochlorins is essential for biomimetic studies pertaining to the roles of bacteriochlorophylls in bacterial photosynthesis and to probe the electronic interplay of peripheral substituents and central metal on photophysical properties. In this regard, the metalation of bacteriochlorins over the years has in some cases proceeded uneventfully and in other cases proved extremely difficult. In general, the reaction course for metalation of tetrapyrrole macrocycles has been interpreted in terms of a variety of parameters, including macrocycle conformation, molecular rigidity (ability to distort from a planar conformation to accommodate the incoming metal ion), nucleophilicity of the nitrogens toward the incoming metal ion, and solvent interactions that entail deprotonation of the pyrrolic NH bonds as well as coordination to the metal ion.²² Related to the ease of preparing a metal chelate is the stability of the resulting metal chelate toward demetalation. The difficulty of metalation upon moving to hydroporphyrins (porphyrin < chlorin < bacteriochlorin) has been attributed to the diminution of ligand nucleophilicity that accompanies saturation of the pyrrole rings.²² On the other hand, a careful study by Saga *et al.* of identically substituted macrocycles revealed that the ease of zinc demetalation decreased along the series porphyrin ~> chlorin >> bacteriochlorin.⁷⁷ In contrast to porphyrins, where the availability of collections of diverse macrocycles in ample quantities have enabled systematic studies of metalation and demetalation chemistry, comparable studies with bacteriochlorins to assess kinetics and thermodynamics have largely remained out of reach.

A *de novo* route to bacteriochlorins has provided a suite of macrocycles that differ in number and type of substituents. The macrocycles provide the foundation for initiation of systematic studies of metalation methods. While a full matrix defined by metalation conditions, metal types, metal ligands, and bacteriochlorin substrates has not been performed, attempts to metalate the set of synthetic bacteriochlorins examined herein has led to the following observations:

- The difficulty of metalation of tetrapyrrole macrocycles decreases for bacteriochlorins with increasing number of electron-withdrawing groups.
- Metalation of a bacteriochlorin occurs upon treatment with a strong base (e.g., NaH or LDA) in THF followed by MX_n : (a) for bacteriochlorins that bear electron-releasing groups, $\text{M} = \text{Cu}, \text{Zn}, \text{Pd}, \text{and InCl}$; (b) for bacteriochlorins that bear two carboethoxy (electron-withdrawing) groups, $\text{M} = \text{Ni}, \text{Cu}, \text{Zn}, \text{Pd}, \text{Cd}, \text{InCl}, \text{and Sn}$ (but not Al or Au); and (c) a bacteriochlorin with four carboethoxy groups was metalated with Mg.
- Bacteriochlorins that bear ≥ 2 carbonyl groups typically can be zincated by standard porphyrin metalation conditions [$\text{Zn}(\text{OAc})_2 \cdot 2\text{H}_2\text{O}$ in DMF at 60–80 °C]

Scheer has suggested that the rate-determining step of bacteriochlorin metalation consists of deprotonation of the pyrrole N-H protons.²³ The use of a very strong base overcomes this limitation, and resembles the method developed by Arnold for preparing early transition metal chelates of porphyrins. The Arnold method entails formation and isolation of the dilithium derivative of the porphyrin as the reactive species for transmetalation upon treatment with a metal reagent.^{53,54} Such method has been applied by

Stolzenberg with tetra-*p*-tolylbacteriochlorin to prepare the oxotitanyl chelate.⁵⁵ The deprotonation of the N-H protons would be facilitated with increasing number of electron-withdrawing groups located on the pyrrole units, as observed here.

In comparing the above results with other types of tetrapyrrole macrocycles, it warrants emphasis that the (up to four) carbonyl groups were located exclusively in the pyrrole (rings A and C) and not in the pyrroline (rings B and D) units of the bacteriochlorins. By contrast, studies of chlorins can incorporate groups in the pyrrole (rings A and C), pyrroline (ring B), and pyrroline (ring D) units. In porphyrins, both pyrrole and pyrroline groups are present yet facile tautomerization typically precludes localization of a substituent in a particular heterocycle.

The studies reported herein concerning metalation of diverse synthetic bacteriochlorins – an ostensibly simple reaction – provide access to a number of the corresponding metallochlorins. One area of particular interest is the examination of dyadic (and larger) arrays comprised of free base and metallochlorins. In this regard, a review of all covalently linked arrays that contain one or more bacteriochlorins reveals only ~20 dyads prepared to date, and most of the bacteriochlorins incorporated therein have been free base species.⁸ Thus, the study of heterometalated arrays, an approach that has been widely used to probe photosynthetic-like mechanisms in synthetic multipigment architectures,⁷⁸ has largely resided outside the scope of experimentation for bacteriochlorins (but has been accessible via computational means⁷⁹). The straightforward access described herein should open the door to the study of fundamental properties, tuning NIR spectral

properties, and pursuit of a range of photochemical applications of synthetic metallobacteriochlorins.

Experimental Section

A. General Methods. ^1H NMR (400 MHz) spectra and ^{13}C NMR spectra (100 MHz) were collected at room temperature in CDCl_3 unless noted otherwise. Absorption spectra were collected in toluene at room temperature. NaH (60% dispersion in mineral oil) and LDA (2.0 M solution in heptanes/THF/ethylbenzene) were provided by Aldrich. Bacteriochlorins were analyzed by laser desorption mass spectrometry in the absence of a matrix (LD-MS) (e.g., the **BC0-2T** series) or in the presence of the matrix POPOP (MALDI-MS).⁸⁰ Silica gel (40 μm average particle size) was used for column chromatography. All solvents were reagent grade and were used as received unless noted otherwise. THF was freshly distilled from sodium/benzophenone ketyl. Anhydrous MeOH was reagent grade and was used as received. Electrospray ionization mass spectrometry (ESI-MS) and fast atom bombardment mass spectrometry (FAB-MS) data are reported for the molecular ion or protonated molecular ion. The concentration of bases and metal reagents is typically given in mM quantities for clarity although not all material may be dissolved.

B. Survey of Metalation. Each reaction was carried out in a conical microreaction vial equipped with a conical stir bar and fitted with a Teflon septum. A bulk solution of the bacteriochlorin was prepared (~6 mg of bacteriochlorin in ~10 mL of THF) and divided without dilution into the microreaction vials. The concentration of the bulk solution was determined by 1000-fold dilution into an absorption cuvette, relying on the known molar

absorption coefficient of representative bacteriochlorins (**BC0-2T** has $\lambda_{737\text{ nm}} = 130,000\text{ M}^{-1}\text{cm}^{-1}$; ¹⁶ **BC2-2M-MeO** has $\lambda_{758\text{ nm}} = 120,000\text{ M}^{-1}\text{cm}^{-1}$) in toluene.

The reaction mixtures were checked by TLC and absorption spectroscopy, the latter again by 1000-fold dilution into an absorption cuvette. The yield was determined spectroscopically assuming equal absorptivity in the Q_y band for both the free base bacteriochlorin and the metallochlorin. If the metalation was found to go to completion, the reaction mixture was quenched by the addition of saturated aqueous NaHCO_3 solution and extraction with CH_2Cl_2 or ethyl acetate. The resulting mixture was concentrated and checked by LD-MS or MALDI-MS. The results are reported in Tables 2.2, 2.4 and 2.5, and in ref 95 (supporting information).

C. Noncommercial Compounds. Compounds **1M**,²⁵ **6**,^{16,19} **BC0**,¹⁸ **BC4-MeO**,¹⁸ **BC3-2E**,²⁴ **BC2-2E**¹⁸ and **BC0-2T**¹⁶ were prepared as described in the literature.

D. Purification. The NaH was received as a 60% dispersion in mineral oil. The reaction could be carried out with the NaH as received, without a pre-wash with hexanes to remove the mineral oil, in which case the mineral oil would be removed from the metallochlorin upon column chromatography or crystallization. In general, however, it was preferable to remove the mineral oil from NaH, under argon, by washing with hexanes, prior to treatment with the free base bacteriochlorin.

Typically the crude reaction mixture upon metalation is relatively clean, the dominant impurities consisting of hydrocarbons (e.g., derived from NaH) and any unwanted free base bacteriochlorin. Initially, we attempted purification by flash chromatography on silica gel. During the course of elution, an intense colored band gradually split into multiple colored

bands, which reflected the decomposition of the macrocycles. Absorption spectroscopy analysis of each collected band indicated the fastest eluting band was usually the desired metallobacteriochlorin whereas the slower eluting bands consisted of impurities. Chromatography with longer retention times afforded an increase in impurities. A basicified eluant [hexanes/CH₂Cl₂ (1:1 to 3:1) containing 1–2 % of TEA] and passage over a short column (ca. 10 cm length, 2 cm diameter) diminished the decomposition but at the expense of resolution. The poor resolution impeded removal of hydrocarbons and unreacted free base bacteriochlorin. Attempts to perform purification on alumina columns or the very traditional sugar columns (widely employed for chlorophyll isolation)⁸¹ also gave the same issue of balance between retention time and purity.

Greater success at purification was achieved by forcing the reaction to completion with prolonged reaction time, thereby affording a mixture that contains only a small amount of the free base bacteriochlorin. The crude mixture was then subjected to chromatography on silica gel [hexanes/CH₂Cl₂ (1:1) to CH₂Cl₂] to remove impurities. At small scale, the chromatography could be performed in a Pasteur pipette. The resulting product was concentrated to dryness. The method of subsequent purification of the resulting solid depended on the solubility of the free base bacteriochlorin and metallobacteriochlorin.

For the **BC4-MeO**, **BC3-2E**, **BC2-2E**, **BC0-2T** and **BC0** series, free base bacteriochlorins were soluble in hexanes whereas the metallobacteriochlorins derived therefrom were insoluble in hexanes. Accordingly, the crude solid was treated with hexanes, sonicated in a benchtop sonication bath, centrifuged, and the supernatant discarded. Repetition once or twice resulted in a solid product that consisted of the

metallobacteriochlorin in pure form.

For the **BC2-2E**, **BC2-2E-MeO**, and **BC2-2M-MeO** series, both free base bacteriochlorins and the metallobacteriochlorins derived therefrom were soluble in hexanes. Accordingly, the crude solid was dissolved in methanol and treated with hexanes. Two intensely colored phases typically form, and can be separated with the aid of illumination to identify the interface. Thus, the hexanes phase (upper layer) was removed as this phase was highly enriched in free base bacteriochlorins yet also contained some metallobacteriochlorin. The methanol phase typically contained the desired metallobacteriochlorin in pure form.

The zinc bacteriochlorins, except those that contain ≥ 3 electron-withdrawing substituents (**ZnBC4-MeO** and **ZnBC3-2E**) tend to demetalate if exposed to prolonged chromatography on silica gel. In most cases, the workup entailed a short column chromatography or washing the solid metallobacteriochlorin product with hexanes to remove hydrocarbons (derived from NaH) or other impurities. In the case of palladium metalation with LDA, an isopropylamine-like byproduct was always found in the crude mixture by ^1H NMR spectroscopy; in the case of **BC2-2M-MeO** such impurity could be removed by size-exclusion chromatography.

E. X-ray Crystallographic Data Collection and Processing. The samples were mounted on a nylon loop with a small amount of NVH immersion oil. All X-ray measurements were made on a Bruker-Nonius X8 Apex2 CCD diffractometer at a temperature of 173 K (**BC0** and **CuBC0-2T**) or 110 K (**BC0-2M**). The frame integration was performed using SAINT+.⁸² The resulting raw data were scaled and absorption-

corrected by multi-scan averaging of symmetry equivalent data using SADABS.⁸³ The data are shown in Table 2.8.

F. X-ray Crystallographic Structure Solution and Refinement. The structures were solved by direct methods using SIR92.⁸⁴ All non-hydrogen atoms were obtained from the initial E-map. The hydrogen atom positions were placed at idealized positions and were allowed to ride on the parent carbon atom. The structural model was fit to the data using full matrix least-squares based on F^2 . The model required 100 restraints to keep the anisotropic displacement parameters from going non-positive definite. The calculated structure factors included corrections for anomalous dispersion from the usual tabulation. The structure was refined using the XL program from the SHELXTL package,⁸⁵ and graphic plots were produced using the version of ORTEP included in the NRCVAX crystallographic program suite.⁸⁶

G. Optical and Photophysical Characterization. Static absorption (Varian Cary 100 or Shimadzu UV-1800) and fluorescence (Spex Fluorolog Tau 2 or PTI Quantamaster 40) measurements were performed at room temperature, as were all other studies. The fluorescence quantum yield (Φ_f), singlet excited-state lifetimes (τ_S) and triplet yields (Φ_T) measurements utilized dilute (μM) Ar-purged toluene and methanol solutions. The triplet lifetimes measurements (τ_T) utilized Ar-purged 2-methyltetrahydrofuran (2-MeTHF) solutions. Samples for Φ_f measurements had an absorbance ≤ 0.1 at the excitation wavelength to minimize front-face effects and similarly low absorbance in the $Q_y(0,0)$ band to minimize inner-filter effects.

Table 2.8. Summary of Crystal Data for **BC0**, **BC0-2M**, and **CuBC0-2T**.

	BC0	BC0-2M	CuBC0-2T
Formula	C ₂₄ H ₂₆ N ₄	C ₄₂ H ₄₆ N ₄	C ₃₈ H ₃₆ CuN ₄
Formula Weight (g/mol)	370.49	606.85	612.25
Crystal Dimensions (mm)	0.12 × 0.10 × 0.02	0.30 × 0.26 × 0.10	0.20 × 0.16 × 0.10
Crystal Color and Habit	green prism	dark green prism	red plate
Crystal System	rhombohedral	triclinic	monoclinic
Space Group	R -3	P -1	P 2 ₁ /c
Temperature, K	173	110	173
<i>a</i> , Å	20.4174(6)	7.2455(3)	17.3789(11)
<i>b</i> , Å	20.4174	10.4695(3)	35.432(2)
<i>c</i> , Å	12.4782(4)	12.0705(5)	16.9880(12)
α, °	90.00	71.0943(16)	90.0
β, °	90.00	85.586(2)	90.017(5)
γ, °	120.00	74.8557(17)	90.0
<i>V</i> , Å ³	4504.9(2)	836.12(5)	10460.8(12)
<i>Z</i>	9	1	14
μ, (cm ⁻¹)	0.074	0.07	0.765
2Φmax (°)	44.04	61.28	41.3
Number of reflections measured	20677	31993	47168
Unique reflections measured	1237	4362	10634
R ₁ ^a	0.1146	0.065	0.0662
wR ₂ ^b	0.3003	0.056	0.1533
R ₁ (all data) ^a	0.1434	0.067	0.1344
wR ₂ (all data) ^b	0.3304	0.066	0.1930
GOF	0.095	1.96	1.126

$$^a R_1 = \sum (|F_o| - |F_c|) / \sum F_o, \quad ^b wR_2 = [\sum (w(F_o^2 - F_c^2)^2) / \sum (w F_o^4)]^{1/2}$$

Static emission measurements employed 2-4 nm excitation- and detection-monochromator bandwidths and 0.2-nm data intervals. Emission spectra were corrected for detection-system spectral response. Fluorescence quantum yields were determined relative to several different standards. These standards are (i) chlorophyll *a* in deoxygenated toluene ($\Phi_f = 0.325$),⁸⁷ which is the value measured in benzene;⁸⁸ (ii) free base *meso*-tetraphenylporphyrin (**FbTPP**) in nondegassed toluene, for which $\Phi_f = 0.070$ was established with respect to the zinc chelate **ZnTPP** in nondegassed toluene ($\Phi_f = 0.030$),⁸⁹ consistent with prior results on **FbTPP**;⁹⁰ and (iii) 8,8,18,18-tetramethylbacteriochlorin⁹¹ in Ar-purged toluene, for which $\Phi_f = 0.14$ was established with respect to chlorophyll *a* in benzene and **FbTPP** in toluene.

Fluorescence lifetimes were obtained using time-correlated-single-photon-counting detection on an apparatus with an approximately Gaussian instrument response function with a full-width-at-half-maximum of ~ 1 ns (Photon Technology International LaserStrobe TM-3). Samples were excited in the Soret or Q regions using excitation pulses at 337 nm from a nitrogen laser or in the blue to green spectral regions from a dye laser pumped by the nitrogen laser.

The Φ_{isc} values (triplet yields) were obtained using transient absorption spectroscopy. The extent of bleaching of the ground-state Q_x bands due to the formation of the lowest singlet excited state was measured immediately following a 130 fs flash in the $Q_y(0,0)$ band and compared with that due to the formation of the lowest triplet excited state at the asymptote of the singlet excited-state decay.^{20,92}

H. Electrochemistry. The electrochemical studies were performed in butyronitrile (Burdick and Jackson) using previously described instrumentation.⁹³ The supporting electrolyte was 0.1 M tetrabutylammonium hexafluorophosphate (Aldrich; recrystallized three times from methanol and dried at 110 °C in vacuo). The electrochemical cell was housed in a Vacuum Atmospheres glovebox (Model HE-93) equipped with a Dri-Train (Model 493). The $E_{1/2}$ values were obtained with square wave voltammetry (frequency 10 Hz) under conditions where the ferrocene couple has a potential of +0.19 V.

I. Density Functional Theory Calculations. Calculations were performed with Spartan '08 for Windows version 1.2.0 in parallel mode⁹⁴ on a PC equipped with an Intel i7-975 cpu, 24 GB ram, and three 300 GB, 10k rpm hard drives. The calculations employed the hybrid B3LYP functional and 6-31G* basis set. The equilibrium geometries were fully optimized using the default parameters of the Spartan program.

J. Synthesis Procedures.

3-(Ethoxycarbonyl)-4-heptylpyrrole (2H). Following the van Leusen method,²⁶ a solution of α,β -unsaturated ester **1H** (12.3 g, 58.0 mmol) and TosMIC (12.6 g, 64.5 mmol) in diethyl ether/DMSO (300 mL, 2:1) was slowly added via an addition funnel to a suspension of NaH (5.0 g, 60% in oil suspension, 0.12 mol) in 100 mL of diethyl ether. The resulting exotherm caused the mixture to reflux. The reaction mixture was stirred at room temperature for 16 h. Water was added carefully, and the mixture was extracted with diethyl ether. The organic layer was concentrated and dried (Na_2SO_4). Column chromatography (silica, CH_2Cl_2) afforded a light yellow solid (8.3 g, 55%): mp 54–56 °C; ^1H NMR (300 MHz) δ 0.88 (t, $J = 6.6$ Hz, 3H), 1.26–1.35 (m, 9H), 1.33 (t, $J = 7.2$ Hz, 2H), 1.58 (m, 2H), 2.71 (t, $J = 7.2$ Hz,

2H), 4.27 (q, $J = 7.2$ Hz, 2H), 6.52 (m, 1H), 7.37 (m, 1H), 8.78 (brs, 1H); ^{13}C NMR (75 MHz) δ 14.1, 14.5, 22.7, 26.3, 29.3, 29.7, 30.6, 32.0, 59.4, 114.1, 116.8, 124.6, 126.4, 165.8; ESI-MS obsd 260.1614, calcd 260.1621 [(M + Na) $^+$, M = C₁₄H₂₃NO₂]; Anal. Calcd for C₁₄H₂₃NO₂: C, 70.85; H, 9.77; N, 5.90. Found: C, 70.90; H, 9.81; N, 5.48.

4-(Ethoxycarbonyl)-2-formyl-3-heptylpyrrole (3H). Following a general procedure,²⁷ the Vilsmeier reagent was prepared by treatment of dry DMF (30 mL) with POCl₃ (4.6 mL, 49 mmol) at 0 °C and stirring of the resulting mixture for 10 min. In a separate flask, a solution of **2H** (10.7 g, 45.1 mmol) in DMF (150 mL) was treated with the freshly prepared Vilsmeier reagent at 0 °C. The resulting mixture was stirred at 0 °C for 1 h and then 2 h at room temperature. The reaction mixture was treated with a mixture of saturated aqueous sodium acetate/CH₂Cl₂ [400 mL, 1:1 (v/v)] and stirred for 1 h. The water phase was separated and extracted with CH₂Cl₂. The combined organic phase was washed with saturated NaCl, dried (Na₂SO₄), and concentrated. Column chromatography (silica, CH₂Cl₂) afforded a light brown solid (6.7 g, 56%): mp 45–47 °C; ^1H NMR (300 MHz) δ 0.88 (t, $J = 6.4$ Hz, 3H), 1.27–1.37 (m, 9H), 1.36 (t, $J = 7.2$ Hz, 2H), 1.66 (m, 2H), 3.04 (t, $J = 7.2$ Hz, 2H), 4.31 (q, $J = 7.6$ Hz, 2H), 7.63 (m, 1H), 9.60 (brs, 1H), 9.69 (s, 1H); ^{13}C NMR δ 14.1, 14.4, 22.7, 24.3, 29.2, 29.6, 31.9, 32.3, 60.0, 116.5, 130.4, 131.5, 140.1, 164.1, 178.8; ESI-MS obsd 266.1746, calcd 266.1751 [(M + H) $^+$, M = C₁₅H₂₃NO₃]; Anal. Calcd for C₁₅H₂₃NO₃: C, 67.90; H, 8.74; N, 5.28. Found: C, 67.86; H, 8.76; N, 5.17.

4-(Ethoxycarbonyl)-3-heptyl-2-(2-nitroethyl)pyrrole (5H). Following a general procedure,¹⁷ a stirred mixture of **3H** (5.8 g, 22 mmol), potassium acetate (1.7 g, 18 mmol), and methylamine hydrochloride (1.2 g, 18 mmol) in absolute ethanol (8 mL) was treated with

nitromethane (3.0 mL, 55 mmol). The mixture was stirred for 2 h, whereupon water was added. The reaction mixture was filtered, and the filtered material was washed with water and a small amount of cold ethanol. The filtered material was dried under high vacuum to afford a yellow solid, which was used directly in the next step. The crude solid material was dissolved in CHCl₃/2-propanol (3:1, 250 mL). Silica (24 g) and NaBH₄ (1.5 g, 40 mmol) were added,²⁹ and the mixture was stirred at room temperature under argon for 2 h. The reaction mixture was filtered, and the filtrate was concentrated. The resulting crude solid was dissolved in CH₂Cl₂. The organic solution was washed (water, brine), dried (Na₂SO₄), and concentrated to afford a pale brown solid (3.0 g, 44%): mp 93–95 °C; ¹H NMR (300 MHz) δ 0.88 (t, *J* = 6.4 Hz, 3H), 1.28–1.35 (m, 9H), 1.33 (t, *J* = 7.2 Hz, 2H), 1.49 (m, 2H), 2.63 (t, *J* = 7.8 Hz, 2H), 3.25 (t, *J* = 6.3 Hz, 2H), 4.27 (q, *J* = 7.2 Hz, 2H), 4.54 (t, *J* = 6.3 Hz, 2H), 7.31 (d, *J* = 3.0 Hz, 1H), 8.39 (brs, 1H); ¹³C NMR δ 14.2, 14.5, 22.8, 23.4, 25.0, 29.4, 30.0, 31.9, 32.1, 59.6, 75.3, 114.8, 123.5, 123.7, 124.2, 165.5; ESI-MS obsd 311.1951, calcd 311.1965 [(M + H)⁺, M = C₁₆H₂₆N₂O₄]; Anal. Calcd for C₁₆H₂₆N₂O₄: C, 61.91; H, 8.44; N, 9.03. Found: C, 62.52; H, 8.48; N, 8.81.

6-(4-(Ethoxycarbonyl)-3-heptylpyrrol-2-yl)-1,1-dimethoxy-4,4-dimethyl-5-nitrohexan-2-one (7H). Following a general procedure,³⁰ a mixture of **5H** (2.8 g, 9.0 mmol) and **6** (4.2 g, 27 mmol, 3 equiv) was treated with DBU (4.2 mL, 27 mmol). The reaction mixture was stirred under argon at room temperature for 16 h. A saturated solution of cold aqueous NH₄Cl was added. The mixture was extracted with ethyl acetate, and the organic layer was washed with brine, dried (Na₂SO₄), and concentrated. Column chromatography [silica, CH₂Cl₂/ethyl acetate (9:1)] afforded a pale brown solid (2.5 g, 59%): mp 78–82 °C;

^1H NMR (300 MHz) δ 0.88 (t, $J = 6.8$ Hz, 3H), 1.15 (s, 3H), 1.25 (s, 3H), 1.28–1.33 (m, 9H), 1.32 (t, $J = 7.2$ Hz, 2H), 1.51 (m, 2H), 2.61 (m, 2H), 2.60, 2.75 (AB, $J = 18.7$ Hz, 2H), 3.00 (ABX, $^3J = 2.3$ Hz, $^2J = 15.5$ Hz, 1H), 3.27 (ABX, $^3J = 11.7$ Hz, $^2J = 15.5$ Hz, 1H), 3.43 (s, 3H), 3.44 (s, 3H), 4.25 (q, $J = 7.2$ Hz, 2H), 4.36 (s, 1H), 5.11 (ABX, $^3J = 2.3$ Hz, $^3J = 11.7$ Hz, 1H), 7.26 (d, $J = 8.8$ Hz, 1H), 8.46 (brs, 1H); ^{13}C NMR (75 MHz) δ 14.2, 14.5, 22.8, 24.2, 24.3, 24.6, 25.0, 29.4, 30.0, 31.8, 32.1, 36.6, 45.0, 55.3, 59.4, 94.7, 104.9, 114.7, 123.5, 123.7, 124.1, 165.2, 203.7; ESI-MS obsd 469.2893, calcd 469.2908 [(M + H) $^+$, M = C₂₄H₄₀N₂O₇]; Anal. Calcd for C₂₄H₄₀N₂O₇: C, 61.52; H, 8.60; N, 5.98. Found: C, 61.84; H, 8.68; N, 5.82.

8-(Ethoxycarbonyl)-2,3-dihydro-1-(1,1-dimethoxymethyl)-7-heptyl-3,3-dimethyldipyrin (8H). Following a general procedure,¹⁷ in a first flask a solution of **7H** (2.2 g, 4.7 mmol) in freshly distilled THF (13 mL) at 0 °C was treated with NaOMe (7.6 g, 24 mmol). The mixture was stirred and degassed by bubbling argon through the solution for 45 min. In a second flask purged with argon, TiCl₃ (20 mL, 20 wt % in 3% HCl solution, 34 mmol), THF (70 mL), and NH₄OAc (20.0 g, 261 mmol) were combined under argon, and the mixture was degassed by bubbling with argon for 45 min. Then, the first flask mixture was transferred via cannula to the buffered TiCl₃ mixture. The resulting mixture was stirred under argon at room temperature for 16 h. The mixture was extracted with ethyl acetate. The organic extract was washed (saturated aqueous NaHCO₃), dried (Na₂SO₄) and concentrated. Column chromatography (silica, CH₂Cl₂) afforded a yellow oil (1.0 g, 51%): ^1H NMR (300 MHz) δ 0.87 (t, $J = 6.4$ Hz, 3H), 1.23 (s, 6H), 1.23–1.36 (m, 11H), 1.50–1.58 (m, 2H), 2.63 (s, 2H), 2.77 (q, $J = 7.2$ Hz, 2H), 3.44 (s, 6H), 4.25 (q, $J = 7.2$ Hz, 2H), 5.03 (s, 1H), 5.86 (s, 1H), 7.42 (d, $J = 3.0$ Hz, 1H), 10.84 (brs, 1H); ^{13}C NMR δ 14.1, 14.4, 22.6, 24.6,

29.14, 29.20, 29.5, 31.7, 31.9, 40.2, 48.2, 54.5, 59.1, 102.5, 104.6, 114.2, 124.6, 125.2, 128.6, 159.8, 165.4, 174.6; ESI-MS obsd 419.2884, calcd 419.2904 [(M + H)⁺, M = C₂₄H₃₈N₂O₄].

3-(Ethoxycarbonyl)-4-mesitylpyrrole (2M). Following the van Leusen method,²⁶ a suspension of TosMIC (12.0 g, 61.5 mmol) and the known α,β -unsaturated ester **1M**²⁵ (12.8 g, 58.6 mmol) in anhydrous Et₂O/DMSO (2:1) (281 mL) was added dropwise under argon into a stirred suspension of NaH (3.07 g, 60% dispersion in mineral oil, 76.8 mmol) in anhydrous THF (118 mL). After stirring for 2.5 h, water (260 mL) was carefully added. The mixture was extracted with diethyl ether and CH₂Cl₂. The combined extract was dried (Na₂SO₄) and filtered. The filtrate was concentrated to afford a yellow oil. Chromatography [silica, ethyl acetate/hexanes (1:9 → 1:3)] gave a white solid (9.13 g, 60%): mp 164–165 °C; ¹H NMR (300 MHz) δ 1.08 (t, *J* = 7.2 Hz, 3H), 2.03 (s, 6H), 2.30 (s, 3H), 4.07 (q, *J* = 7.2 Hz, 2H), 6.54–6.56 (m, 1H), 6.89 (s, 2H), 7.53–7.55 (m, 1H), 8.47 (br, 1H); ¹³C NMR (75 MHz) δ 14.3, 21.0, 21.3, 59.5, 117.9, 124.6, 127.7, 129.7, 130.6, 132.3, 136.3, 137.7, 165.2; FAB-MS obsd 257.1414, calcd 257.1416 (C₁₆H₁₉NO₂).

4-(Ethoxycarbonyl)-2-formyl-3-mesitylpyrrole (3M). Following a general procedure,²⁷ a solution of **2M** (19.8 g, 77.0 mmol) in DMF (24.6 mL) and CH₂Cl₂ (400 mL) at 0 °C under argon was treated dropwise with freshly distilled POCl₃ (8.50 mL, 92.7 mmol). After 1 h, the ice bath was removed. The flask was allowed to warm to room temperature with stirring for 18 h. The reaction mixture was cooled to 0 °C, whereupon 2.5 M aqueous NaOH (350 mL) was added. The mixture was extracted with CH₂Cl₂. The organic phase was washed [10% (w/w) aqueous acetic acid and saturated brine], dried (Na₂SO₄), and concentrated. The residue was triturated with hexanes and filtered to afford a pale yellow

solid (11.2 g, 56%): mp 214–216 °C; ^1H NMR δ 1.06 (t, $J = 7.2$ Hz, 3H), 2.00 (s, 6H), 2.30 (s, 3H), 4.14 (q, $J = 7.2$ Hz, 2H), 6.84–6.86 (m, 1H), 6.91 (s, 2H), 9.64–9.92 (br, 1H), 10.25 (s, 1H); ^{13}C NMR δ 13.7, 20.7, 21.0, 60.3, 121.2, 123.8, 127.6, 130.4, 133.4, 136.8, 137.1, 163.5, 182.2; ESI-MS obsd 286.1439, calcd 286.1438 [(M + H) $^+$, M = C₁₇H₁₉NO₃].

4-(Ethoxycarbonyl)-3-mesityl-2-(2-nitrovinyl)pyrrole (4M). Following a general procedure,²⁸ a stirred solution of acetic acid (0.69 mL, 13 mmol) in methanol (1.75 mL) under argon at 0 °C was treated dropwise with *n*-propylamine (0.95 mL, 12 mmol). The resulting *n*-propylammonium acetate solution was stirred at 0 °C for 5 min, then added dropwise to a stirred solution of **3M** (5.90 g, 20.7 mmol) in nitromethane (3.38 mL, 90.0 mmol) and freshly distilled THF (20 mL) at 0 °C. The resulting mixture was stirred at 0 °C. After 15 min, the cooling bath was removed, and stirring was continued at room temperature. The color changed from yellow to dark red during the course of reaction. After 3 h, CH₂Cl₂ (100 mL) was added, and the organic phase was washed with water and brine. The organic layer was dried (Na₂SO₄) and concentrated to afford a dark viscous mixture. Filtration through a silica pad (ethyl acetate) afforded a dark brown solid (5.44 g, 80%): mp 68–70 °C; ^1H NMR δ 1.03 (t, $J = 7.2$ Hz, 3H), 2.01 (s, 6H), 2.30 (s, 3H), 4.11 (q, $J = 7.2$ Hz, 2H), 6.81 (d, $J = 2.8$ Hz, 1H), 6.89 (s, 2H), 7.56 (d, $J = 14.0$ Hz, 1H), 8.71 (d, $J = 14.0$ Hz, 1H), 8.91–9.07 (br, 1H); ^{13}C NMR δ 13.4, 20.7, 21.0, 60.5, 120.1, 123.2, 126.4, 127.6, 128.2, 128.4, 130.8, 134.2, 136.8, 136.9, 164.1; ESI-MS obsd 329.1501, calcd 329.1501 [(M + H) $^+$, M = C₁₈H₂₀N₂O₄].

4-(Ethoxycarbonyl)-3-mesityl-2-(2-nitroethyl)pyrrole (5M). Following a general procedure,²⁹ a solution of **4M** (5.42 g, 16.5 mmol) in CHCl₃ (150 mL) and isopropanol (50

mL) was treated with silica (19.8 g). The resulting suspension was treated in one portion with NaBH₄ (1.25 g, 33.0 mmol) under vigorous stirring. After 20 min, a further portion of NaBH₄ (355 mg, 9.38 mmol) was added in one batch. After 20 min, TLC analysis showed complete consumption of the vinylpyrrole. The mixture was filtered, and the filter cake was washed with CH₂Cl₂. The filtrate was concentrated, and the resulting dark oil was filtered through a bed of silica (hexanes/ethyl acetate, 3:1) to afford a brown solid (3.48 g, 64%): mp 108–110 °C; ¹H NMR δ 0.91 (t, *J* = 7.2 Hz, 3H), 1.99 (s, 6H), 2.29 (s, 3H), 3.63 (t, *J* = 6.1 Hz, 2H), 3.98 (q, *J* = 7.2 Hz, 2H), 4.77 (t, *J* = 6.1 Hz, 2H), 6.42 (d, *J* = 2.5 Hz, 1H), 6.86 (s, 2H), 8.52 (br, 1H); ¹³C NMR δ 13.6, 20.7, 21.0, 25.8, 59.2, 74.7, 111.5, 116.0, 124.7, 127.3, 132.4, 133.2, 136.0, 137.2, 165.2; ESI-MS obsd 331.1651, calcd 331.1652 [(M + H)⁺, M = C₁₈H₂₂N₂O₄].

6-[4-(Ethoxycarbonyl)-3-mesitylpyrrol-2-yl]-1,1-dimethoxy-4,4-dimethyl-5-nitro-2-hexanone (7M). Following a general procedure,³⁰ a mixture of **5M** (3.48 g, 10.5 mmol) and **6** (4.99 g, 31.3 mmol) was treated with DBU (4.49 mL, 30.0 mmol). CH₂Cl₂ (5 mL) was added to the reaction mixture to dissolve completely the nitroethylpyrrole compound **5M**. The reaction mixture was stirred at room temperature for 7 h, diluted with ethyl acetate (100 mL), and washed with aqueous NH₄Cl solution and brine. The organic layer was dried (Na₂SO₄) and concentrated. The resulting oil was chromatographed [silica, ethyl acetate/hexanes (1:2)] to afford a brown solid (1.37 g, 27%): mp 131–134 °C; ¹H NMR δ 0.90 (t, *J* = 7.2 Hz, 3H), 1.22 (s, 3H), 1.33 (s, 3H), 1.94 (s, 3H), 1.99 (s, 3H), 2.28 (s, 3H), 2.67, 2.76 (AB, ²*J* = 18.6 Hz, 2H), 3.34 (ABX, ³*J* = 11.8 Hz, ²*J* = 14.6 Hz, 1H), 3.83 (ABX, ³*J* = 2.5 Hz, ²*J* = 14.6 Hz, 1H), 3.42 (s, 3H), 3.43 (s, 3H), 3.94–4.07 (m, 2H), 4.41 (s, 1H),

5.22 (ABX, $^3J = 2.5$ Hz, $^3J = 11.8$ Hz, 1H), 6.36 (d, $J = 2.5$ Hz, 1H), 6.85 (s, 2H), 8.23–8.30 (br, 1H); ^{13}C NMR δ 13.9, 20.7, 20.9, 21.2, 23.8, 24.2, 27.1, 36.7, 44.7, 55.1, 59.2, 95.2, 104.6, 111.8, 116.2, 124.8, 127.27, 127.39, 132.8, 133.2, 136.0, 137.3, 137.6, 165.2, 203.3; ESI-MS obsd 489.2591, calcd 489.2595 [(M + H) $^+$, M = C₂₆H₃₆N₂O₇].

8-(Ethoxycarbonyl)-1-(1,1-dimethoxymethyl)-3,3-dimethyl-7-mesityl-2,3-dihydrodipyrin (8M). Following a general procedure,¹⁷ a solution of **7M** (1.37 g, 2.81 mmol) in anhydrous THF (12.0 mL) under argon was treated with NaOMe (0.45 g, 8.3 mmol). The reaction mixture was bubbled with argon for 15 min and then stirred for 1 h at room temperature (first flask). In a second flask, TiCl₃ [8.6 wt % TiCl₃ in 28 wt % HCl, 13.3 mL, 9.7 mmol] and THF (27 mL) were combined. The mixture was bubbled with argon for 30 min. Then, NH₄OAc (11.2 g, 145 mmol) was slowly added under argon bubbling to buffer the mixture to pH 6.0 (pH paper). The mixture in the first flask containing the nitronate anion of **7M** was transferred via a cannula to the buffered TiCl₃ mixture in the second flask. The resulting mixture was stirred overnight at room temperature. Then the mixture was poured into a vigorously stirred solution of saturated aqueous NaHCO₃ (300 mL). After 10 min, the mixture was extracted with ethyl acetate. The organic layers were combined, washed with water, dried (Na₂SO₄), and concentrated. Filtration through a alumina pad (alumina, hexanes/ethyl acetate, 3:1) afforded a dark brown solid (0.60 g, 49%): mp 148–150 °C; ^1H NMR δ 0.93 (t, $J = 7.2$ Hz, 3H), 1.28 (s, 6H), 2.04 (s, 6H), 2.30 (s, 3H), 2.67 (s, 2H), 3.47 (s, 6H), 4.01 (q, $J = 7.2$ Hz, 2H), 5.05 (s, 1H), 6.56 (d, $J = 2.5$ Hz, 1H), 6.87 (s, 2H), 6.97 (s, 1H), 11.18–11.31 (br, 1H); ^{13}C NMR δ 13.8, 20.9, 21.1, 29.1, 40.7, 48.4, 54.7, 59.0, 102.6, 106.3, 111.5, 117.8, 124.4, 127.3, 133.3, 135.5, 135.8, 137.4, 163.4,

165.6, 176.8; Anal. Calcd for C₂₆H₃₄N₂O₄: C, 71.21; H, 7.81; N, 6.39. Found: C, 71.46; H, 7.98; N, 6.31.

3,13-Bis(ethoxycarbonyl)-2,12-diheptyl-8,8,18,18-tetramethylbacteriochlorin (BC2-2H). Following a general procedure,¹⁸ a solution of **8H** (340 mg, 0.81 mmol, 18 mM) in anhydrous CH₃CN (45 mL) was treated with BF₃·O(Et)₂ (0.80 mL, 6.5 mmol, 140 mM). The reaction mixture was stirred at room temperature for 16 h. Excess TEA (1.2 mL) was added to the reaction mixture. The reaction mixture was concentrated, and the residue was chromatographed (silica, CH₂Cl₂). A single purple band was isolated and concentrated to afford the title compound as a purple solid (70 mg, 24%): ¹H NMR δ -1.41 (brs, 2H), 0.89–0.92 (m, 6H), 1.31–1.71 (m, 22H), 1.94 (s, 12H), 2.09–2.18 (m, 4H), 4.10 (t, *J* = 7.8 Hz, 4H), 4.42 (s, 4H), 4.78 (q, *J* = 7.2 Hz, 4H), 8.64 (s, 2H), 9.66 (s, 2H); ¹³C NMR δ 14.3, 14.8, 22.9, 27.5, 29.5, 30.4, 31.1, 32.1, 33.4, 46.0, 52.0, 60.9, 94.8, 98.7, 119.4, 134.0, 135.1, 140.5, 160.6, 166.7, 171.1; λ_{abs} (toluene) 353, 383, 520, 761 nm; λ_{em} (λ_{exc} 522 nm) 768 nm; MALDI-MS obsd 710.5; ESI-MS obsd 711.4830, calcd 711.4844 [(M + H)⁺, M = C₄₄H₆₂N₄O₄].

3,13-Bis(ethoxycarbonyl)-2,12-diheptyl-5-methoxy-8,8,18,18-tetramethylbacteriochlorin (BC2-2H-MeO). Following a general procedure,¹⁸ a solution of **8H** (430 mg, 1.1 mmol, 18 mM) in anhydrous CH₂Cl₂ (60 mL) was treated first with 2,6-DTBP (4.70 mL, 21.2 mmol, 360 mM) and second with TMSOTf (0.956 mL, 5.30 mmol, 90 mM). The reaction mixture was stirred at room temperature for 16 h. The reaction mixture was concentrated, and the residue was chromatographed (silica, CH₂Cl₂). The second green band was isolated and concentrated to afford the title compound as a purple solid (160 mg,

44%): ^1H NMR δ -1.84 (brs, 1H), -1.56 (brs, 1H), 0.87–0.89 (m, 6H) 1.31–1.71 (m, 22H), 1.94 (d, J = 4.0 Hz, 12H), 2.15 (m, 4H), 3.78 (t, J = 7.6 Hz, 2H), 4.12 (t, J = 7.6 Hz, 2H), 4.22 (s, 3H), 4.36 (s, 2H), 4.40 (s, 2H), 4.78 (q, J = 6.8 Hz, 4H), 8.53 (s, 1H), 8.65 (s, 1H), 9.60 (s, 1H); ^{13}C NMR δ 14.10, 14.11, 14.59, 14.68, 22.68, 22.70, 26.6, 27.3, 29.23, 29.37, 29.9, 30.2, 30.9, 31.1, 31.81, 31.91, 32.8, 33.3, 45.6, 45.9, 47.9, 51.7, 60.7, 61.7, 64.3, 93.8, 95.5, 97.6, 118.5, 124.6, 127.9, 132.5, 134.31, 134.36, 134.9, 135.2, 140.3, 155.7, 160.5, 166.6, 167.9, 168.9, 171.3; λ_{abs} (toluene) 358, 379, 522, 740 nm; λ_{em} (λ_{exc} 521 nm) 744 nm; MALDI-MS obsd 740.1; ESI-MS obsd 741.4938, calcd 741.4949 [(M + H) $^+$, M = C₄₅H₆₄N₄O₅].

3,13-Bis(ethoxycarbonyl)-2,12-dimesityl-5-methoxy-8,8,18,18-tetramethylbacteriochlorin (BC2-2M-MeO). Following a general procedure,¹⁸ a solution of **8M** (600 mg, 1.24 mmol) in anhydrous CH₂Cl₂ (69 mL) was treated first with 2,6-di-*tert*-butylpyridine (4.75 mL, 24.8 mmol) and second with TMSOTf (1.21 mL, 6.21 mmol). The resulting mixture was stirred at room temperature for 19 h. The reaction mixture was concentrated and chromatographed (silica, CH₂Cl₂/ethyl acetate, 1:1) to afford a pink greenish solid (290 mg, 60%): ^1H NMR δ -1.15 (brs, 1H), -0.90 (brs, 1H), 1.19 (t, J = 7.2 Hz, 3H), 1.25 (t, J = 7.2 Hz, 3H), 1.92 (s, 6H), 1.93 (s, 6H), 2.00 (s, 6H), 2.08 (s, 6H), 2.48 (s, 3H), 2.53 (s, 3H), 3.63 (s, 3H), 4.19 (s, 2H), 4.26 (s, 2H), 4.42 (q, J = 7.2 Hz, 2H), 4.47 (q, J = 7.2 Hz, 2H), 7.72 (s, 2H), 7.78 (s, 2H), 8.12 (s, 1H), 9.61 (s, 1H), 9.63 (s, 1H); ^{13}C NMR δ 13.8, 13.9, 21.0, 21.24, 21.34, 21.38, 29.1, 30.9, 31.1, 45.8, 47.4, 51.4, 60.43, 60.49, 62.7, 96.9, 97.3, 97.5, 120.4, 121.5, 127.43, 127.8, 132.1, 134.2, 134.74, 134.80, 135.1, 135.8, 136.2, 136.7, 137.34, 137.47, 137.56, 139.5, 155.7, 162.0, 165.6, 166.2, 171.7; λ_{abs}

(toluene) 361, 382, 538, 758 nm ($\lambda_{758 \text{ nm}} = 120,000 \text{ M}^{-1} \text{ cm}^{-1}$); λ_{em} (λ_{exc} 538 nm) 763 nm; ESI-MS obsd 781.4322, calcd 781.4323 [(M + H)⁺, M = C₄₉H₅₆N₄O₅].

3,13-Bis(ethoxycarbonyl)-2,12-dimesityl-8,8,18,18-tetramethylbacteriochlorin

(BC2-2M). Following Procedure A (see next section), a solution of **BC2-2M-MeO** (7.8 mg, 10 μmol , 4 mM) in freshly distilled THF (2.5 mL) under argon was treated with NaH (60 mg, 1.5 mmol, 60% dispersion in mineral oil) at room temperature for 30 min. PdBr₂ (80 mg, 0.30 mmol) was then added to the mixture, and the flask was heated at 60 °C for 2 h. The reaction was monitored by absorption spectroscopy and TLC [silica, hexanes/ethyl acetate (3:1)]. The reaction mixture was diluted with CH₂Cl₂ and washed with saturated aqueous NaHCO₃. The organic layer was dried (Na₂SO₄) and filtered. The filtrate was concentrated and chromatographed [alumina, hexanes/CH₂Cl₂ (2:1) with 1% TEA] to yield a pink solid (2.2 mg, 29%): ¹H NMR (300 MHz) δ -1.22 (brs, 2H), 1.25 (t, $J = 7.2$ Hz, 6H), 1.95 (s, 12H), 1.99 (s, 12H), 2.54 (s, 6H), 4.25 (s, 4H), 4.46 (q, $J = 7.2$ Hz, 4H), 7.18 (s, 4H), 8.26 (s, 2H), 9.68 (s, 2H); λ_{abs} (toluene) 357, 383, 524, 765 nm; λ_{em} (λ_{exc} 524 nm) 770 nm; MALDI-MS obsd 750.9; ESI-MS obsd 751.4218 calcd 751.4206 [(M + H)⁺, M = C₄₈H₅₄N₄O₄].

K. Metalation of Bacteriochlorins

Procedure A (NaH/THF):

Zn(II)-8,8,18,18-Tetramethyl-2,12-di-*p*-tolylbacteriochlorin (ZnBC0-2T). A solution of **BC0-2T** (16.5 mg, 30.0 μmol , 4 mM) in THF (7.5 mL) under argon was treated with NaH (180 mg, 4.50 mmol) at room temperature for 1 h. The color of the resulting heterogeneous reaction mixture changed from light green to red. Then Zn(OTf)₂ (327 mg, 0.900 mmol) was added to the mixture, and the flask was heated to 60 °C for 12 h under

argon. TLC analysis [silica, hexanes/CH₂Cl₂ (1:1)] showed the disappearance of **BC0-2T** and the presence of only one spot. The reaction mixture was diluted with CH₂Cl₂ and washed with saturated aqueous NaHCO₃ solution. The organic layer was dried (Na₂SO₄) and filtered. The filtrate was concentrated, and the residue was chromatographed on a short column [silica, hexanes/CH₂Cl₂/TEA (49:49:2), v/v/v] to afford a black-red solid (16.2 mg). The crude solid was treated with hexanes, sonicated in a benchtop sonication bath, centrifuged, and the supernatant discarded (as this consisted of unreacted **BC0-2T** and hydrocarbon impurities). Repetition twice afforded a black-red powder (12.1 mg, 66%): ¹H NMR (THF-*d*₈) δ 1.93 (s, 12H), 2.55 (s, 6H), 4.45 (s, 4H), 7.51 (d, *J* = 8.0 Hz, 4H), 8.06 (d, *J* = 8.0 Hz, 4H), 8.62 (s, 2H), 8.63 (s, 2H), 8.76 (s, 2H); λ_{abs} (toluene) 344, 385, 523, 750 nm; λ_{em} (λ_{exc} 523 nm) 760 nm; LD-MS obsd 612.3; FAB-MS obsd 612.2233, calcd 612.2231 (C₃₈H₃₆N₄Zn).

Procedure B (LDA/THF):

Zn(II)-8,8,18,18-Tetramethyl-2,12-di-*p*-tolylbacteriochlorin (ZnBC0-2T). A solution of **BC0-2T** (11.0 mg, 20.0 μmol, 4 mM) in THF (5 mL) under argon was treated with a 2.0 M LDA solution (100 μL, 200 μmol) at room temperature for 5 min. The color of the resulting homogeneous reaction mixture rapidly changed from light green to red. Then Zn(OTf)₂ (14.1 mg, 40.0 μmol) was added to the mixture, and the flask was heated to 60 °C for 2-3 h under argon. TLC analysis [silica, hexanes/CH₂Cl₂ (1:1)] showed the disappearance of **BC0-2T** and the presence of only one spot, and the absorption spectrum did not show the Q_x band of **BC0-2T**. The reaction mixture was diluted with CH₂Cl₂ and washed with saturated aqueous NaHCO₃ solution. The organic layer was dried (Na₂SO₄) and

filtered. The filtrate was concentrated. The resulting solid was treated with hexanes, sonicated in a benchtop sonication bath, centrifuged, and the supernatant discarded (as this consisted of unreacted **BC0-2T** and hydrocarbon impurities). Repetition twice afforded a black-red solid (9.7 mg, 79%) with satisfactory characterization data (¹H NMR spectroscopy, absorption spectroscopy, LD-MS and FAB-MS).

Procedure C (Zn(OAc)₂·2H₂O/DMF):

Zn(II)-2,3,12,13-Tetrakis(ethoxycarbonyl)-5-methoxy-8,8,18,18-tetramethylbacteriochlorin (ZnBC4-MeO). A solution of **BC4-MeO** (5.4 mg, 7.8 μmol, 4 mM) in DMF (2 mL) was treated with Zn(OAc)₂·2H₂O (52 mg, 240 μmol, 30 equiv). The reaction mixture was heated to 60 °C for 16 h and then 80 °C for 3 h. TLC analysis [silica, hexanes/CH₂Cl₂ (1:1)] showed the disappearance of **BC4-MeO** and the presence of only one spot. The reaction mixture was diluted with CH₂Cl₂ and washed with saturated aqueous NaHCO₃ solution. The organic layer was dried (Na₂SO₄) and filtered. The filtrate was concentrated. The crude solid was treated with hexanes, sonicated in a benchtop sonication bath, centrifuged, and the supernatant discarded. Repetition twice afforded a dark blue solid (5.7 mg, 97%): ¹H NMR (300 MHz, THF-*d*₈) δ 1.51–1.61 (m, 12H), 1.92 (s, 6H + 6H), 4.13 (s, 3H), 4.33 (s, 2H + 2H), 4.55–4.68 (m, 8H), 8.92 (s, 1H), 9.12 (s, 1H), 9.64 (s, 1H); λ_{abs} (toluene) 354, 384, 582, 774 nm; λ_{em} (λ_{exc} 582 nm) 781 nm; MALDI-MS obsd 750.9; ESI-MS obsd 773.2121, calcd 773.2135 [(M + Na)⁺, M = C₃₇H₄₂N₄O₉Zn].

Mg(II)-2,3,12,13-Tetrakis(ethoxycarbonyl)-5-methoxy-8,8,18,18-tetramethylbacteriochlorin (MgBC4-MeO). Following a modification of Procedure A, a solution of **BC4-MeO** (5.0 mg, 7.3 μmol, 4 mM) in freshly distilled THF (1.8 mL) was

treated with NaH (52 mg, 2.1 mmol, 60% dispersion in mineral oil washed beforehand with hexanes) and MgI₂ (60 mg, 0.21 mmol). The reaction mixture was heated at 60 °C for 3 h under argon. The reaction was monitored by absorption spectroscopy and MALDI-MS. The reaction mixture was diluted with ethyl acetate and washed with saturated aqueous NaHCO₃ solution. The organic layer was dried (Na₂SO₄) and filtered. The filtrate was concentrated. The crude solid was chromatographed in a Pasteur pipet [basic alumina, ethyl acetate to ethyl acetate/MeOH (95:5)] to afford a blue solid (1.0 mg, 19%): λ_{abs} (CH₂Cl₂) 360, 612, 764 nm; MALDI-MS obsd 711.2, calcd 710.3 (C₃₇H₄₂N₄O₉Mg). Limited stability precluded further analysis.

Zn(II)-8,8,18,18-Tetramethylbacteriochlorin (ZnBC0). Following Procedure A, a solution of **BC0** (4.6 mg, 12 μ mol, 4 mM) in freshly distilled THF (3 mL) was treated with NaH (46 mg, 1.9 mmol, 60% dispersion in mineral oil washed beforehand with hexanes) and Zn(OTf)₂ (131 mg, 0.360 mmol). The reaction mixture was heated at 60 °C for 16 h under argon. The reaction was monitored by absorption spectroscopy and MALDI-MS. The reaction mixture was diluted with CH₂Cl₂ and washed with saturated aqueous NaHCO₃ solution. The organic layer was dried (Na₂SO₄) and filtered. The filtrate was concentrated. The crude solid was treated with hexanes, sonicated in a benchtop sonication bath, centrifuged, and the supernatant discarded. Repetition twice afforded a pink solid (4.3 mg, 80%): ¹H NMR (300 MHz, THF-*d*₈) δ 1.97 (s, 12H), 4.46 (s, 4H), 8.60–8.62 (m, 2H), 8.60 (s, 2H), 8.64–8.66 (m, 2H), 8.64 (s, 2H); λ_{abs} (toluene) 336, 376, 514, 723 nm; λ_{em} (λ_{exc} 514 nm) 725 nm; MALDI-MS obsd 432.2; ESI-MS obsd 432.1280, calcd 432.1292 (C₂₄H₂₄N₄Zn).

Zn(II)-3,13-Bis(ethoxycarbonyl)-2,12-dimesityl-5-methoxy-8,8,18,18-tetramethylbacteriochlorin (ZnBC2-2M-MeO). Following Procedure A, a solution of **BC2-2M-MeO** (9.4 mg, 12 μ mol, 4 mM) in freshly distilled THF (3 mL) was treated with NaH (72 mg, 1.8 mmol, 60% dispersion in mineral oil washed beforehand with hexanes) at room temperature for 30 min. Zn(OTf)₂ (131 mg, 0.360 mmol) was added, and the flask was heated at 60 °C for 5 h under argon. The reaction was monitored by absorption spectroscopy and TLC [silica, hexanes/ethyl acetate (3:1)]. The reaction mixture was diluted with ethyl acetate and washed with saturated aqueous NaHCO₃. The organic layer was dried (Na₂SO₄) and filtered. The crude product was found to contain only hydrocarbon impurities by ¹H NMR spectroscopy. The crude solid was dissolved in methanol and treated with hexanes. Two intensely colored phases formed. The hexanes phase was removed as this phase was highly enriched in **BC2-2M-MeO** yet also contained some metallobacteriochlorin. The methanol phase, which contained the title metallobacteriochlorin, was collected and concentrated to yield a pink solid (5.5 mg, 54%): ¹H NMR (300 MHz, THF-*d*₈) δ 1.14 (t, *J* = 7.2 Hz, 3H), 1.20 (t, *J* = 7.2 Hz, 3H), 1.90 (s, 6H), 1.94 (s, 6H), 1.99 (s, 6H), 2.08 (s, 6H), 2.46 (s, 3H), 2.52 (s, 3H), 3.57 (s, 3H), 4.15 (s, 2H), 4.23 (s, 2H), 4.36 (q, *J* = 7.2 Hz, 2H), 4.40 (q, *J* = 7.2 Hz, 2H), 7.08 (s, 2H), 7.14 (s, 2H), 8.01 (s, 1H), 9.50 (s, 1H), 9.56 (s, 1H); λ_{abs} (toluene) 353, 389, 565, 773 nm; λ_{em} (λ_{exc} 565 nm) 779 nm; MALDI-MS obsd 842.8; ESI-MS obsd 842.3393, calcd 842.3380 (C₄₉H₅₄N₄O₅Zn).

Zn(II)-3,13-Bis(ethoxycarbonyl)-2,12-diheptyl-5-methoxy-8,8,18,18-tetramethylbacteriochlorin (ZnBC2-2H-MeO). Following Procedure A, a solution of **BC2-2H-MeO** (5.9 mg, 8.0 μ mol, 4 mM) in THF (2.0 mL) was treated with NaH (48 mg,

1.2 mmol) at room temperature for 1 h. The color of the reaction mixture changed from light green to red. Then Zn(OTf)₂ (87 mg, 0.24 mmol) was added to the mixture, and the flask was heated to 60 °C for 6 h under argon. TLC analysis [silica, hexanes/ethyl acetate (3:1)] showed the disappearance of the free base bacteriochlorin and the presence of only one spot. The reaction mixture was diluted with CH₂Cl₂ and washed with saturated aqueous NaHCO₃ solution. The organic layer was dried (Na₂SO₄) and filtered. The filtrate was concentrated, and the residue was chromatographed on a short column [silica, hexanes/ethyl acetate/TEA (74:25:1), v/v/v] to afford a black-red solid (3.2 mg, 50%): ¹H NMR (300 MHz, THF-*d*₈) δ 0.86–0.98 (m, 6H) 1.29–1.66 (m, 22H), 1.94 (d, *J* = 4.0 Hz, 12H), 2.12 (m, 4H), 3.72 (t, *J* = 7.6 Hz, 2H), 4.10 (t, *J* = 7.6 Hz, 2H), 4.12 (s, 3H), 4.36 (s, 2H), 4.38 (s, 2H), 4.63 (q, *J* = 6.8 Hz, 4H), 8.43 (s, 1H), 8.58 (s, 1H), 9.58 (s, 1H); λ_{abs} (toluene) 349, 385, 542, 752 nm; λ_{em} (λ_{exc} 542 nm) 757 nm; MALDI-MS obsd 802.1; ESI-MS obsd 802.3995, calcd 802.4006 (C₄₅H₆₂N₄O₅Zn).

Zn(II)-3,13-Bis(ethoxycarbonyl)-2,12-diheptyl-8,8,18,18-tetramethylbacteriochlorin (ZnBC2-2H). Following Procedure A, a solution of **BC2-2H** (5.7 mg, 8.0 μmol, 4 mM) in THF (2.0 mL) was treated with NaH (48 mg, 1.2 mmol) at room temperature for 1 h. The color of the reaction mixture changed from light green to red. Then Zn(OTf)₂ (87 mg, 0.24 mmol) was added to the mixture, and the flask was heated to 60 °C for 6 h under argon. TLC analysis [silica, hexanes/ethyl acetate (3:1)] showed the disappearance of the free base bacteriochlorin and the presence of only one spot. The reaction mixture was diluted with CH₂Cl₂ and washed with saturated aqueous NaHCO₃ solution. The organic layer was dried (Na₂SO₄) and filtered. The filtrate was concentrated,

and the residue was chromatographed on a short column [silica, hexanes/ethyl acetate/TEA (74:25:1), v/v/v] to afford a black-red solid (1.9 mg, 31%): ^1H NMR (300 MHz, THF- d_8) δ 0.88–0.92 (m, 6H), 1.31–1.66 (m, 22H), 1.94 (s, 12H), 2.12 (m, 4H), 4.12 (t, $J = 7.8$ Hz, 4H), 4.39 (s, 4H), 4.66 (q, $J = 7.2$ Hz, 4H), 8.55 (s, 2H), 9.60 (s, 2H); λ_{abs} (toluene) 347, 391, 547, 776 nm; λ_{em} (λ_{exc} 547 nm) 781 nm; MALDI-MS obsd 772.6; ESI-MS obsd 772.3879, calcd 772.3901 ($\text{C}_{44}\text{H}_{60}\text{N}_4\text{O}_4\text{Zn}$).

Zn(II)-3,13-Bis(ethoxycarbonyl)-2,12-diethyl-8,8,18,18-tetramethylbacteriochlorin (ZnBC2-2E). Following Procedure C, a solution of **BC2-2E** (5.0 mg, 8.8 μmol , 4 mM) in DMF (2.2 mL) was treated with $\text{Zn}(\text{OAc})_2 \cdot 2\text{H}_2\text{O}$ (58 mg, 260 μmol , 30 equiv). The reaction mixture was heated to 60 °C for 16 h and then 80 °C for 24 h under argon. The reaction was monitored by absorption spectroscopy and MALDI-MS. The reaction mixture was diluted with CH_2Cl_2 and washed with saturated aqueous NaHCO_3 solution. The organic layer was dried (Na_2SO_4) and filtered. The filtrate was concentrated. The crude solid was treated with hexanes, sonicated in a benchtop sonication bath, centrifuged, and the supernatant discarded. Repetition twice afforded a dark blue solid (4.8 mg, 86%): ^1H NMR (THF- d_8) δ 1.64 (t, $J = 6.8$ Hz, 6H), 1.69 (t, $J = 7.6$ Hz, 6H), 1.95 (s, 12H), 4.10 (q, $J = 7.6$ Hz, 4H), 4.39 (s, 4H), 4.66 (q, $J = 6.8$ Hz, 4H), 8.55 (s, 2H), 9.60 (s, 2H); λ_{abs} (toluene) 347, 391, 545, 774 nm; λ_{em} (λ_{exc} 545 nm) 780 nm; MALDI-MS obsd 631.7; ESI-MS obsd 632.2349, calcd 632.2341 ($\text{C}_{34}\text{H}_{40}\text{N}_4\text{O}_4\text{Zn}$).

Zn(II)-15²-N-Benzyl-3-(ethoxycarbonyl)-2,12-diethyl-8,8,18,18-tetramethylbacteriochlorin-13,15-dicarboximide (ZnBC3-2E). Following Procedure C, a

solution of **BC3-2E** (6.9 mg, 11 μ mol, 4 mM) in DMF (2.6 mL) was treated with $\text{Zn}(\text{OAc})_2 \cdot 2\text{H}_2\text{O}$ (69 mg, 320 μ mol, 30 equiv). The reaction mixture was heated to 60 °C for 16 h and then 80 °C for 7 h. The reaction was monitored by absorption spectroscopy and MALDI-MS. The reaction mixture was diluted with CH_2Cl_2 and washed with saturated aqueous NaHCO_3 solution. The organic layer was dried (Na_2SO_4) and filtered. The filtrate was concentrated, and the residue was chromatographed on a short column [silica, $\text{CH}_2\text{Cl}_2/\text{MeOH}$ (98:2)] to afford a purple solid (4.1 mg, 54%): ^1H NMR ($\text{THF-}d_8$) δ 1.60–1.69 (m, 9H), 1.90 (s, 6H), 1.92 (s, 6H), 4.03 (q, $J = 7.7$ Hz, 2H), 4.15 (q, $J = 7.3$ Hz, 2H), 4.33 (s, 2H), 4.65 (q, $J = 7.0$ Hz, 2H), 4.74 (s, 2H), 5.55 (s, 2H), 7.18 (t, $J = 7.3$ Hz, 1H), 7.29 (t, $J = 7.5$ Hz, 2H), 7.76 (d, $J = 7.0$ Hz, 2H), 8.47 (s, 1H), 8.62 (s, 1H), 9.51 (s, 1H); λ_{abs} (toluene) 356, 419, 563, 831 nm; λ_{em} (λ_{exc} 563 nm) 834 nm; MALDI-MS obsd 719.9; ESI-MS obsd 720.2501, calcd 720.2523 [(M + H)⁺, M = $\text{C}_{40}\text{H}_{41}\text{N}_5\text{O}_4\text{Zn}$].

Cu(II)-8,8,18,18-Tetramethylbacteriochlorin (CuBC0). Following Procedure A, a solution of **BC0** (5.0 mg, 14 μ mol, 4 mM) in freshly distilled THF (3.4 mL) was treated with NaH (48 mg, 2.0 mmol, 60% dispersion in mineral oil washed beforehand with hexanes) and $\text{Cu}(\text{OAc})_2$ (74 mg, 0.41 mmol). The reaction mixture was heated at 60 °C for 16 h under argon. The reaction was monitored by absorption spectroscopy and MALDI-MS. The reaction mixture was diluted with CH_2Cl_2 and washed with saturated aqueous NaHCO_3 solution. The organic layer was dried (Na_2SO_4) and filtered. The filtrate was concentrated. The crude solid was treated with hexanes, sonicated in a benchtop sonication bath, centrifuged, and the supernatant discarded. Repetition twice afforded a green solid (2.4 mg,

41%): λ_{abs} (toluene) 336, 376, 514, 723 nm; MALDI-MS obsd 431.1; ESI-MS obsd 431.1300, calcd 431.1291 (C₂₄H₂₄N₄Cu).

Cu(II)-8,8,18,18-Tetramethyl-2,12-di-*p*-tolylbacteriochlorin (CuBC0-2T).

Following Procedure B, a solution of **BC0-2T** (16.5 mg, 30.0 μmol , 4 mM) in THF (7.5 mL) was treated with LDA (0.750 mL, 1.50 mmol, 200 mM) at room temperature for 5 min. Cu(OAc)₂ (54.5 mg, 300 μmol) was added, and the flask was heated at 70 °C for 30 min under argon. TLC analysis [silica, hexanes/CH₂Cl₂ (1:1)] showed the disappearance of **BC0-2T** and the presence of only one spot, and the absorption spectrum did not show the Q_x band of **BC0-2T**. The reaction mixture was diluted with CH₂Cl₂ and washed with saturated brine. The organic layer was treated to the remaining steps of the standard workup procedure to yield a dark powder (10.2 mg, 56%): λ_{abs} (toluene) 337, 383, 512, 755 nm; LD-MS obsd 611.3; FAB-MS obsd 611.2238, calcd 611.2336 (C₃₈H₃₆N₄Cu).

Cu(II)-3,13-Bis(ethoxycarbonyl)-2,12-dimesityl-5-methoxy-8,8,18,18-tetramethylbacteriochlorin (CuBC2-2M-MeO). Following Procedure A, a solution of **BC2-2M-MeO** (6.2 mg, 8 μmol , 4 mM) in freshly distilled THF (2 mL) was treated with NaH (48 mg, 1.2 mmol, 60% dispersion in mineral oil washed beforehand with hexanes) at room temperature for 30 min under argon. Cu(OAc)₂ (43 mg, 0.24 mmol) was added, and the flask was heated at 60 °C for 20 h under argon. The reaction was monitored by absorption spectroscopy and TLC [silica, hexanes/ethyl acetate (3:1)]. The standard workup procedure was employed except for the chromatography procedure [silica, hexanes/ethyl acetate (4:1) with 1% TEA], which yielded a pink solid (5.3 mg, 79%): λ_{abs} (toluene) 348,

390, 556, 779 nm; MALDI-MS obsd 841.3; ESI-MS obsd 841.3381, calcd 841.3385 (C₄₉H₅₄N₄O₅Cu).

Pd(II)-8,8,18,18-Tetramethyl-2,12-di-*p*-tolylbacteriochlorin (PdBC0-2T).

Following Procedure A, a solution of **BC0-2T** (16.5 mg, 30.0 μmol, 4 mM) in THF (7.5 mL) was treated with NaH (120 mg, 3.00 mmol) at room temperature for 1 h. PdBr₂ (240 mg, 90.0 mmol) was then added, and the flask was heated at 60 °C for 0.5 h under argon. TLC analysis [silica, hexanes/CH₂Cl₂ (1:1)] showed the disappearance of **BC0-2T** and the presence of only one spot. The standard workup afforded a black-red powder (9.3 mg, 48%): ¹H NMR δ 1.87 (s, 12H), 2.59 (s, 6H), 4.43 (s, 4H), 7.54 (d, *J* = 8.0 Hz, 4H), 8.01 (d, *J* = 8.0 Hz, 4H), 8.55 (s, 2H), 8.68 (s, 2H), 8.72 (s, 2H); λ_{abs} (toluene) 329, 379, 499, 739 nm; λ_{em} (λ_{exc} 499 nm) 745 nm; LD-MS obsd 653.9; FAB-MS obsd 654.1958, calcd 654.1975 (C₃₈H₃₆N₄Pd).

Pd(II)-3,13-Bis(ethoxycarbonyl)-2,12-dimesityl-5-methoxy-8,8,18,18-tetramethylbacteriochlorin (PdBC2-2M-MeO). Following Procedure B, a solution of **BC2-2M-MeO** (7.8 mg, 10 μmol, 4 mM) in freshly distilled THF (2.5 mL) was treated with LDA (50 μL, 0.1 mmol, 0.2 M) at room temperature for 10 min. PdBr₂ (80 mg, 0.30 mmol) was then added to the mixture, and the flask was heated at 60 °C for 20 h under argon. The reaction was monitored by absorption spectroscopy and TLC [silica, hexanes/ethyl acetate (3:1)]. The reaction mixture was diluted with ethyl acetate and washed with saturated aqueous NaHCO₃ solution. The organic layer was dried (Na₂SO₄) and filtered. The concentrated crude solid was chromatographed [silica, hexanes/ethyl acetate (3:1)], and the only mobile band (pink) was collected. The concentrated mixture was found to contain some

amine-like impurity, which was removed by size-exclusion chromatography (toluene, Bio-Beads S-X1, 200–400 mesh). The collected band (pink) was then chromatographed [silica, hexanes/ethyl acetate (3:1)] to afford a purple solid (3.1 mg, 35%): ^1H NMR (300 MHz) δ 1.12 (t, $J = 7.2$ Hz, 3H), 1.18 (t, $J = 7.2$ Hz, 3H), 1.87 (s, 6H), 1.90 (s, 6H), 2.00 (s, 6H), 2.09 (s, 6H), 2.46 (s, 3H), 2.50 (s, 3H), 3.46 (s, 3H), 4.18 (s, 2H), 4.26 (s, 2H), 4.34 (q, $J = 7.2$ Hz, 2H), 4.38 (q, $J = 7.2$ Hz, 2H), 7.07 (s, 2H), 7.13 (s, 2H), 8.04 (s, 1H), 9.55 (s, 1H), 9.61 (s, 1H); λ_{abs} (toluene) 337, 382, 538, 758 nm; MALDI-MS obsd 884.5; ESI-MS obsd 884.3228, calcd 884.3202 ($\text{C}_{49}\text{H}_{54}\text{N}_4\text{O}_5\text{Pd}$).

In(III)Cl-8,8,18,18-Tetramethyl-2,12-di-*p*-tolylbacteriochlorin (InClBC0-2T).

Following Procedure B, a solution of **BC0-2T** (11.0 mg, 20.0 μmol , 4 mM) in THF (4.5 mL) was treated with LDA in THF (500 μL , 1.00 mmol, 200 mM) at room temperature for 5 min. InCl_3 (44.2 mg, 200 μmol) was added, and the flask was heated at 60 $^\circ\text{C}$ for 1.5 h under argon. TLC analysis [silica, hexanes/THF (1:1)] showed the disappearance of **BC0-2T** and the presence of only one spot, and the absorption spectrum did not show the Q_x band of **BC0-2T**. The reaction mixture was diluted with CH_2Cl_2 and washed with saturated brine. The organic layer was treated to the remaining steps of the standard workup procedure to yield a black-red powder (12.5 mg, 89%): ^1H NMR (THF- d_8) δ 1.84 (s, 6H), 2.09 (s, 6H), 2.56 (s, 6H), 4.48, 4.71 (AB, $^2J = 16.0$ Hz, 4H), 7.55 (d, $J = 8.0$ Hz, 4H), 8.09 (d, $J = 8.0$ Hz, 4H), 8.78 (s, 2H), 8.82 (s, 2H), 8.87 (s, 2H); λ_{abs} (toluene) 350, 389, 539, 764 nm; λ_{em} (λ_{exc} 539 nm) 772 nm; LD-MS obsd 698.2; FAB-MS obsd 698.1688, calcd 698.1667 ($\text{C}_{38}\text{H}_{36}\text{ClInN}_4$).

References

- (1) Scheer, H. In *Chlorophylls and Bacteriochlorophylls. Biochemistry, Biophysics, Functions and Applications*; Grimm, B.; Porra, R. J.; Rüdiger, W.; Scheer, H., Eds., *Advances in Photosynthesis and Respiration*, 2006, Vol. 25; Springer, Dordrecht, The Netherlands, pp 1–26.
- (2) Felton, R. H. in *The Porphyrins*, Vol. 5, Dolphin, D., Ed., Academic Press: New York, 1978, pp 53–125.
- (3) Sanders, J. K. M.; Bampos, N.; Clyde-Watson, Z.; Darling, S. L.; Hawley, J. C.; Kim, H.-J.; Mak, C. C.; Webb, S. J. In *The Porphyrin Handbook*; Kadish, K. M., Smith, K. M., Guillard, R., Eds.; Academic Press: San Diego, CA, 2000; Vol. 3, pp 1–48.
- (4) Gradyushko, A. T.; Tsvirko, M. P. *Opt. Spectroscopy* **1971**, *31*, 291–295.
- (5) Eastwood, D.; Gouterman, M. *J. Mol. Spectroscopy* **1969**, *30*, 437–458.
- (6) Eastwood, D.; Gouterman, M. *J. Mol. Spectroscopy* **1970**, *35*, 359–375.
- (7) Gouterman, M. in *The Porphyrins*, Vol. 3, Dolphin, D., Ed., Academic Press: New York, 1978, pp 1–165.
- (8) Lindsey, J. S.; Mass, O.; Chen, C.-Y. *New J. Chem.* **2011**, *35*, 511–516.
- (9) Kee, H. L.; Nothdurft, R.; Muthiah, C.; Diers, J. R.; Fan, D.; Ptaszek, M.; Bocian, D. F.; Lindsey, J. S.; Culver, J. P.; Holten, D. *Photochem. Photobiol.* **2008**, *84*, 1061–1072.
- (10) Kee, H. L.; Diers, J. R.; Ptaszek, M.; Muthiah, C.; Fan, D.; Lindsey, J. S.; Bocian, D. F.; Holten, D. *Photochem. Photobiol.* **2009**, *85*, 909–920.

- (11) Huang, L.; Huang, Y.-Y.; Mroz, P.; Tegos, G. P.; Zhiyentayev, T.; Sharma, S. K.; Lu, Z.; Balasubramanian, T.; Krayner, M.; Ruzié, C.; Yang, E.; Kee, H. L.; Kirmaier, C.; Diers, J. R.; Bocian, D. F.; Holten, D.; Lindsey, J. S.; Hamblin, M. R. *Antimicrob. Agents Chemother.* **2010**, *54*, 3834–3841.
- (12) (a) Sutton, J. M.; Clarke, O. J.; Fernandez, N.; Boyle, R. W. *Bioconjugate Chem.* **2002**, *13*, 249–263. (b) Singh, S.; Aggarwal, A.; Thompson, S.; Tomé, J. P. C.; Zhu, X.; Samaroo, D.; Vinodu, M.; Gao, R.; Drain, C. M. *Bioconjugate Chem.* **2010**, *21*, 2136–2146.
- (13) (a) Wakao, N.; Yokoi, N.; Isoyama, N.; Hiraishi, A.; Shimada, K.; Kobayashi, M.; Kise, H.; Iwaki, M.; Itoh, S.; Takaichi, S.; Sakurai, Y. *Plant Cell Physiol.* **1996**, *37*, 889–893. (b) Tomi, T.; Shibata, Y.; Ikeda, Y.; Taniguchi, S.; Haik, C.; Mataga, N.; Shimada, K.; Itoh, S. *Biochim. Biophys. Acta* **2007**, *1767*, 22–30.
- (14) Kobayashi, M.; Akiyama, M.; Yamamura, M.; Kise, H.; Wakao, N.; Ishida, N.; Koizumi, M.; Kano, H.; Watanabe, T. *Z. Phys. Chem.* **1999**, *213*, 207–214.
- (15) Kobayashi, M.; Akiyama, M.; Kano, H.; Kise, H. In *Chlorophylls and Bacteriochlorophylls. Biochemistry, Biophysics, Functions and Applications*; Grimm, B.; Porra, R. J.; Rüdiger, W.; Scheer, H., Eds.; Advances in Photosynthesis and Respiration, 2006, Vol. 25; Springer: Dordrecht, The Netherlands, pp 79–94.
- (16) Kim, H.-J.; Lindsey, J. S. *J. Org. Chem.* **2005**, *70*, 5475–5486.
- (17) Krayner, M.; Balasubramanian, T.; Ruzié, C.; Ptaszek, M.; Cramer, D. L.; Taniguchi, M.; Lindsey, J. S. *J. Porphyrins Phthalocyanines* **2009**, *13*, 1098–1110.

- (18) Kraye, M.; Ptaszek, M.; Kim, H.-J.; Meneely, K. R.; Fan, D.; Secor, K.; Lindsey, J. *S. J. Org. Chem.* **2010**, *75*, 1016–1039.
- (19) Mass, O.; Lindsey, J. S. *J. Org. Chem.* **2011**, *76*, 9478–9487.
- (20) Yang, E.; Kirmaier, C.; Kraye, M.; Taniguchi, M.; Kim, H.-J.; Diers, J. R.; Bocian, D. F.; Lindsey, J. S.; Holten, D. *J. Phys. Chem. B* **2011**, *115*, 10801–10816.
- (21) Kraye, M.; Yang, E.; Kim, H.-J.; Kee, H. L.; Deans, R. M.; Sluder, C. E.; Diers, J. R.; Kirmaier, C.; Bocian, D. F.; Holten, D.; Lindsey, J. S. *Inorg. Chem.* **2011**, *50*, 4607–4618.
- (22) Orzel, L.; Kania, A.; Rutkowska-Zbik, D.; Susz, A.; Stochel, G.; Fiedor, L. *Inorg. Chem.* **2010**, *49*, 7362–7371.
- (23) Hartwich, G.; Fiedor, L.; Simonin, I.; Cmiel, E.; Schäfer, W.; Noy, D.; Scherz, A.; Scheer H. *J. Am. Chem. Soc.* **1998**, *120*, 3675–3683.
- (24) Kraye, M.; Yang, E.; Diers, J. R.; Bocian, D. F.; Holten, D.; Lindsey, J. S. *New J. Chem.* **2011**, *35*, 587–601.
- (25) Medina, E.; Moyano, A.; Pericàs, M. A.; Riera, A. *Helv. Chim. Acta* **2000**, *83*, 972–988.
- (26) van Leusen, A. M.; Siderius, H.; Hoogenboom, B. E.; van Leusen, D. *Tetrahedron Lett.* **1972**, *13*, 5337–5340.
- (27) Brückner, C.; Posakony, J. J.; Johnson, C. K.; Boyle, R. W.; James, B. R.; Dolphin, D. *J. Porphyrins Phthalocyanines* **1998**, *2*, 455–465.
- (28) Ptaszek, M.; Bhaumik, J.; Kim, H.-J.; Taniguchi, M.; Lindsey, J. S. *Org. Process Res. Dev.* **2005**, *9*, 651–659.

- (29) Sinhababu, A. K.; Borchardt, R. T. *Tetrahedron Lett.* **1983**, *24*, 227–230.
- (30) Kim, H.-J.; Dogutan, D. K.; Ptaszek, M.; Lindsey, J. S. *Tetrahedron* **2007**, *63*, 37–55.
- (31) Balasubramanian, T.; Strachan, J.-P.; Boyle, P. D.; Lindsey, J. S. *J. Org. Chem.* **2000**, *65*, 7919–7929.
- (32) Buchler, J. W. In *Porphyrins and Metalloporphyrins*; Smith, K. M., Ed.; Elsevier: Amsterdam, 1975; pp 157–231.
- (33) Buchler, J. W. In *The Porphyrins*; Dolphin, D., Ed.; Academic Press: New York, 1978; Vol. 1, pp 389–483.
- (34) Lahiri, G. K.; Summers, J. S.; Stolzenberg, A. M. *Inorg. Chem.* **1991**, *30*, 5049–5052.
- (35) Tamiaki, H.; Yagai, S.; Miyatake, T. *Bioorg. Med. Chem.* **1998**, *6*, 2171–2178.
- (36) Sasaki, S.-I.; Tamiaki, H. *J. Org. Chem.* **2006**, *71*, 2648–2654.
- (37) Kunieda, M.; Yamamoto, K.; Sasaki, S.-I. Tamiaki, H. *Chem. Lett.* **2007**, *36*, 936–937.
- (38) Kunieda, M.; Tamiaki, H. *J. Org. Chem.* **2005**, *70*, 820–828.
- (39) Brandis, A.; Mazor, O.; Neumark, E.; Rosenbach-Belkin, V.; Salomon, Y.; Scherz, A. *Photochem. Photobiol.* **2005**, *81*, 983–993.
- (40) Kozyrev, A. N.; Chen, Y.; Goswami, L. N.; Tabaczynski, W. A.; Pandey, R. K. *J. Org. Chem.* **2006**, *71*, 1949–1960.
- (41) Fukuzumi, S.; Ohkubo, K.; Zheng, X.; Chen, Y.; Pandey, R. K.; Zhan, R.; Kadish, K. M. *J. Phys. Chem. B* **2008**, *112*, 2738–2746.
- (42) Vasudevan, J.; Stibrany, R. T.; Bumby, J.; Knapp, S.; Potenza, J. A.; Emge, T. J.; Schugar, H. J. *J. Am. Chem. Soc.* **1996**, *118*, 11676–11677.

- (43) Fajer, J.; Borg, D. C.; Forman, A.; Felton, R. H.; Dolphin, D.; Vegh, L. *Proc. Natl. Acad. Sci. USA* **1974**, *71*, 994–998.
- (44) Donohoe, R. J.; Frank, H. A.; Bocian, D. F. *Photochem. Photobiol.* **1988**, *48*, 531–537.
- (45) Donohoe, R. J.; Atamian, M.; Bocian, D. F. *J. Phys. Chem.* **1989**, *93*, 2244–2252.
- (46) Scherz, A.; Salomon, Y.; Brandis, A.; Scheer, H. U.S. 6,569,846.
- (47) Hu, S.; Mukherjee, A.; Spiro, T. G. *J. Am. Chem. Soc.* **1993**, *115*, 12366–12377.
- (48) Connick, P. A.; Macor, K. A. *Inorg. Chem.* **1991**, *30*, 4654–4663.
- (49) Strell, M.; Urumow, T. *Liebigs Ann. Chem.* **1977**, 970–974.
- (50) Wasielewski, M. R. *Tetrahedron Lett.* **1977**, *18*, 1373–1376.
- (51) Johansen, J. E.; Piermattie, V.; Angst, C.; Diener, E.; Kratky, C.; Eschenmoser, A. *Angew. Chem.* **1981**, *93*, 273–275.
- (52) Kratky, C.; Waditschatka, R.; Angst, C.; Johansen, J. E.; Plaquevent, J. C.; Schreiber, J.; Eschenmoser, A. *Helv. Chim. Acta* **1985**, *68*, 1312–1337.
- (53) (a) Arnold, J. *J. Chem. Soc., Chem. Commun.* **1990**, 976–978. (b) Brand, H.; Capriotti, J. A.; Arnold, J. *Inorg. Chem.* **1994**, *33*, 4334–4337. (c) Brand, H.; Arnold, J. *Coord. Chem. Rev.* **1995**, *140*, 137–168.
- (54) Berreau, L. M.; Hays, J. A.; Young, V. G., Jr.; Woo, L. K. *Inorg. Chem.* **1994**, *33*, 105–108.
- (55) Stolzenberg, A. M.; Haymond, G. S. *Inorg. Chem.* **2002**, *41*, 300–308.
- (56) Li, K.-L.; Guo, C.-C.; Chen, Q.-Y. *Org. Lett.* **2009**, *11*, 2724–2727.

- (57) Whitlock, H. W., Jr.; Hanauer, R.; Oester, M. Y.; Bower, B. K. *J. Am. Chem. Soc.* **1969**, *91*, 7485–7489.
- (58) Ruzié, C.; Krayner, M.; Balasubramanian, T.; Lindsey, J. S. *J. Org. Chem.* **2008**, *73*, 5806–5820.
- (59) Sharada, D. S.; Muresan, A. Z.; Muthukumaran, K.; Lindsey, J. S. *J. Org. Chem.* **2005**, *70*, 3500–3510.
- (60) (a) Lindsey, J. S.; Woodford, J. N. *Inorg. Chem.* **1995**, *34*, 1063–1069. (b) O’Shea, D. F.; Miller, M. A.; Matsueda, H.; Lindsey, J. S. *Inorg. Chem.* **1996**, *35*, 7325–7338.
- (61) (a) Fraser, R. R.; Mansour, T. S. *J. Org. Chem.* **1984**, *49*, 3443–3444. (b) March, J. *Advanced Organic Chemistry*; 4th Ed., John Wiley & Sons, Inc.: New York, 1992; p 252.
- (62) Alvarez-Bercedo, P.; Martin, R. *J. Am. Chem. Soc.* **2010**, *132*, 17352–17353.
- (63) (a) Reid, J. D.; Hunter, C. N. *J. Biol. Chem.* **2004**, *279*, 26893–26899. (b) Masuda, T. *Photosynth. Res.* **2008**, *96*, 121–143.
- (64) Robinson, L. R.; Hambright, P. *Inorg. Chim. Acta* **1991**, *185*, 17–24.
- (65) (a) Barkigia, K. M.; Fajer, J.; Chang, C. K.; Young, R. *J. Am. Chem. Soc.* **1984**, *106*, 6457–6459. (b) Arasasingham, R. D.; Balch, A. L.; Olmstead, M. M. *Heterocycles* **1988**, *27*, 2111–2118. (c) Pandey, R. K.; Isaac, M.; MacDonald, I.; Medforth, C. J.; Senge, M. O.; Dougherty, T. J.; Smith, K. M. *J. Org. Chem.* **1997**, *62*, 1463–1472. (d) Senge, M. O.; Runge, S. *Acta Cryst.* **1998**, *C54*, 1917–1919. (e) Shea, K. M.; Jaquinod, L.; Khoury, R. G.; Smith, K. M. *Tetrahedron* **2000**, *56*, 3139–3144.

- (66) Barkigia, K. M.; Miura, M.; Thompson, M. A.; Fajer, J. *Inorg. Chem.* **1991**, *30*, 2233–2236.
- (67) (a) Barkigia, K. M.; Fajer, J.; Smith, K. M.; Williams, G. J. B. *J. Am. Chem. Soc.* **1981**, *103*, 5890–5893. (b) Barkigia, K. M.; Gottfried, D. S.; Boxer, S. G.; Fajer, J. *J. Am. Chem. Soc.* **1989**, *111*, 6444–6446. (c) Barkigia, K. M.; Gottfried, D. S. *Acta Cryst.* **1994**, *C50*, 2069–2072.
- (68) Saltsman, I.; Goldberg, I.; Balasz, Y.; Gross, Z. *Tetrahedron Lett.* **2007**, *48*, 239–244.
- (69) Taniguchi, M.; Ptaszek, M.; McDowell, B. E.; Boyle, P. D.; Lindsey, J. S. *Tetrahedron* **2007**, *63*, 3850–3863.
- (70) Taniguchi, M.; Mass, O.; Boyle, P. D.; Tang, Q.; Diers, J. R.; Bocian, D. F.; Holten, D.; Lindsey, J. S. *J. Mol. Structure* **2010**, *979*, 27–45.
- (71) Scheidt, W. R. In *The Porphyrins*; Dolphin, D., Ed., Academic Press: New York, Vol. 3, 1978, pp 463–511.
- (72) (a) Kim, D.; Holten, D.; Gouterman, M. *J. Am. Chem. Soc.* **1984**, *106*, 2793–2798. (b) Yan, X.; Holten, D. *J. Phys. Chem.* **1988**, *92*, 5982–5986.
- (73) Connolly, J. S.; Gorman, D. S.; Seely, G. R. *Ann. N. Y. Acad. Sci.* **1973**, *206*, 649–669.
- (74) Connolly, J. S.; Janzen, A. F.; Samuel, E. B. *Photochem. Photobiol.* **1982**, *36*, 559–563.
- (75) Tait, C. D.; Holten, D. *Photobiochem. Photobiophys.* **1983**, *6*, 201–209.

- (76) Kee, H. L.; Kirmaier, C.; Tang, Q.; Diers, J. R.; Muthiah, C.; Taniguchi, M.; Laha, J. K.; Ptaszek, M.; Lindsey, J. S.; Bocian, D. F.; Holten, D. *Photochem. Photobiol.* **2007**, *83*, 1125–1143.
- (77) Saga, Y.; Miura, R.; Sadaoka, K.; Hirai, Y. *J. Phys. Chem. B* **2011**, *115*, 11757–11762.
- (78) Harvey, P. D. In *The Porphyrin Handbook*; Kadish, K. M., Smith, K. M., Guillard, R., Eds.; Academic Press: San Diego, CA, 2003; Vol. 18, pp 63–250.
- (79) (a) Kobayashi, R.; Amos, R. D. *Chem. Phys. Lett.* **2006**, *420*, 106–109. (b) Erratum, **2006**, *424*, 225. (c) Dreuw, A.; Head-Gordon, M. *J. Am. Chem. Soc.* **2004**, *126*, 4007–4016. (d) Yamaguchi, Y.; Yokoyama, S.; Mashiko, S. *J. Chem. Phys.* **2002**, *116*, 6541–6548.
- (80) Srinivasan, N.; Haney, C. A.; Lindsey, J. S.; Zhang, W.; Chait, B. T. *J. Porphyrins Phthalocyanines* **1999**, *3*, 283–291.
- (81) Svec, W. A. In *The Porphyrins*; Dolphin, D. Ed., Academic Press: New York, Vol. V, 1978, pp 366–369.
- (82) Bruker-Nonius, SAINT+ version 7.07B, **2004**, Bruker-Nonius, Madison, WI 53711, USA.
- (83) Bruker-Nonius, SADABS version 2.10, **2004**, Bruker-Nonius, Madison, WI 53711, USA.
- (84) Altomare, A.; Cascarano, G.; Giacovazzo, C.; Guagliardi, A.; Burla, M. C.; Polidori, G.; Camalli, M. *J. Appl. Cryst.* **1994**, *27*, 435.

- (85) Bruker-AXS, XL, SHELXTL version 6.12, UNIX, **2001**, Bruker-Nonius, Madison, WI 53711, USA.
- (86) Gabe, E. J.; Le Page, Y.; Charland, J.-P.; Lee, F. L.; White, P. S. *J. Appl. Cryst.* **1989**, *22*, 384–387.
- (87) Mass, O.; Taniguchi, M.; Ptaszek, M.; Springer, J. W.; Faries, K. M.; Diers, J. R.; Bocian, D. F.; Holten, D.; Lindsey, J. S. *New J. Chem.* **2011**, *35*, 76–88.
- (88) Weber, G.; Teale, F. W. J. *Trans. Faraday Soc.* **1957**, *53*, 646–655.
- (89) Seybold, P. G.; Gouterman, M. *J. Mol. Spectroscopy* **1969**, *31*, 1–13.
- (90) Gradyushko, A. T.; Sevchenko, A. N.; Solovyov, K. N.; Tsvirko, M. P. *Photochem. Photobiol.* **1970**, *11*, 387–400.
- (91) Taniguchi, M.; Cramer, D. L.; Bhise, A. D.; Kee, H. L.; Bocian, D. F.; Holten, D.; Lindsey, J. S. *New J. Chem.* **2008**, *32*, 947–958.
- (92) Kee, H. L.; Bhaumik, J.; Diers, J. R.; Mroz, P.; Hamblin, M. R.; Bocian, D. F.; Lindsey, J. S.; Holten, D. *J. Photochem. Photobiol. A: Chem.* **2008**, *200*, 346–355.
- (93) Strachan, J.-P.; Gentemann, S.; Seth, J.; Kalsbeck, W. A.; Lindsey, J. S.; Holten, D.; Bocian, D. F. *J. Am. Chem. Soc.* **1997**, *119*, 11191–11201.
- (94) Except for molecular mechanics and semi-empirical models, the calculation methods used in Spartan '08 or '10 have been documented in: Shao, Y.; Molnar, L. F.; Jung, Y.; Kussmann, J.; Ochsenfeld, C.; Brown, S. T.; Gilbert, A. T. B.; Slipchenko, L. V.; Levchenko, S. V.; O'Neill, D. P.; DiStasio, R. A., Jr.; Lochan, R. C.; Wang, T.; Beran, G. J. O.; Besley, N. A.; Herbert, J. M.; Lin, C. Y.; Van Voorhis, T.; Chien, S. H.; Sodt, A.; Steele, R. P.; Rassolov, V. A.; Maslen, P. E.; Korambath, P. P.; Adamson, R.

- D.; Austin, B.; Baker, J.; Byrd, E. F. C.; Dachsel, H.; Doerksen, R. J.; Dreuw, A.; Dunietz, B. D.; Dutoi, A. D.; Furlani, T. R.; Gwaltney, S. R.; Heyden, A.; Hirata, S.; Hsu, C.-P.; Kedziora, G.; Khalliulin, R. Z.; Klunzinger, P.; Lee, A. M.; Lee, M. S.; Liang, W.-Z.; Lotan, I.; Nair, N.; Peters, B.; Proynov, E. I.; Pieniazek, P. A.; Rhee, Y. M.; Ritchie, J.; Rosta, E.; Sherrill, C. D.; Simmonett, A. C.; Subotnik, J. E.; Woodcock, H. L., III; Zhang, W.; Bell, A. T.; Chakraborty, A. K.; Chipman, D. M.; Keil, F. J.; Warshel, A.; Hehre, W. J.; Schaefer, H. F., III; Kong, J.; Krylov, A. I.; Gill, P. M. W.; Head-Gordon, M. *Phys. Chem. Chem. Phys.* **2006**, *8*, 3172–3191.
- (95) Chen, C.-Y.; Sun, E.; Fan, D.; Taniguchi, M.; McDowell, B. E.; Yang, E.; Diers, J. R.; Bocian, D. F.; Holten, D.; Lindsey, J. S. *Inorg. Chem.* **2012**, *51*, 9443–9464.

CHAPTER 3

Rational Synthesis of 24 Bacteriochlorin Isotopologues Each Containing a Symmetrical Pair of ^{13}C or ^{15}N Atoms in the Inner Core of the Macrocycle

Introduction

Bacteriochlorophylls and their free base analogues (bacteriopheophytins) are the chief chromophores that enable energy transduction in photosynthetic bacteria.¹ Consequently, the characterization of the fundamental physicochemical properties of the isolated chromophores, independent of the complexities of the photosynthetic protein assemblies, has been a topic of long-standing interest. Spectroscopic studies have been paramount and include traditional optical methods (absorption and fluorescence) as well as other techniques such as electron paramagnetic resonance (EPR) and resonance Raman (RR) spectroscopies.²⁻⁸ EPR spectroscopy provides a fundamental understanding of the spin-density distribution in the radical species, whereas RR spectroscopy affords information on the vibrational characteristics of the molecule, which may be utilized in normal coordinate analysis. Regardless, spectroscopic interrogation of bacteriochlorophylls is limited in two ways: (1) naturally occurring bacteriochlorophylls are somewhat labile and can undergo dehydrogenation to yield the corresponding chlorins;⁹ (2) the nearly full complement of peripheral substituents around the bacteriochlorin chromophore causes highly rich and congested spectra. Two simplifying methods have been resorted to, including use of porphyrins as surrogates of bacteriochlorophylls, and preparation of synthetic bacteriochlorins that bear stable isotopes at designated sites.

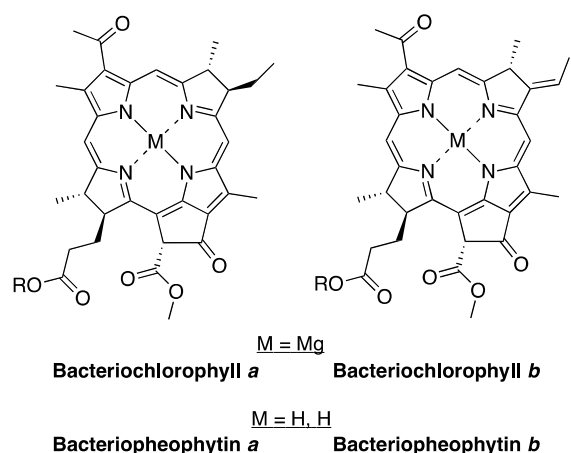


Chart 3.1. Natural bacterial photosynthetic pigments.

Porphyrins have long been exploited as biomimetic analogues of bacteriochlorophylls owing to ready accessibility and versatile synthetic malleability. Nonetheless, use of the porphyrin surrogates ignores the essential structural differences among the respective classes of tetrapyrroles; indeed, the different reduction level of porphyrins versus bacteriochlorins (tetrahydroporphyrins) causes profound changes in physicochemical properties, which are particularly manifested in the spectral properties. To our knowledge, only two synthetic bacteriochlorin core structures and their isotopologues have been prepared for spectroscopic purposes; these include *meso*-tetraphenylbacteriochlorin and octaethylbacteriochlorin species. The *meso*-tetraphenylbacteriochlorin (**TPBC**) scaffold has proved more versatile, with reported isotopologues including the all- ^{15}N (shown in Chart 3.2), all-*meso*- ^{13}C , all-phenyl- d_{20} , and β - d_8 . Fajer *et al.*¹⁰ examined the cation radicals of zinc and free base **TPBC** isotopologues by EPR spectroscopy. Bocian *et al.*¹¹ performed a normal coordinate analysis of **Cu-TPBC** isotopologues based on RR spectroscopic studies. Spiro *et al.*¹²⁻¹⁴ employed

the nickel(II) chelate of an isotopically substituted octaethylbacteriochlorin (**Ni-OEBC**) as well as **M-TPBC** isotopologues for vibrational spectroscopic studies.

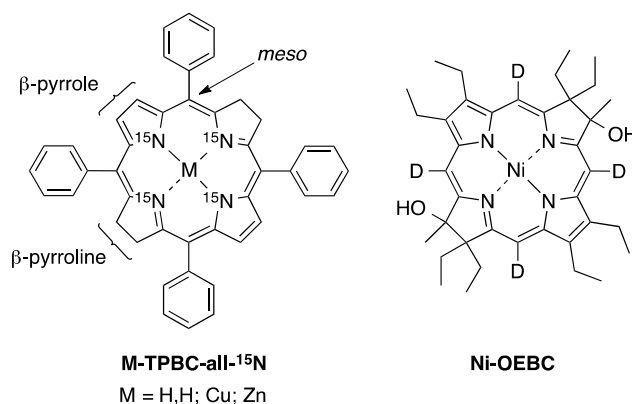
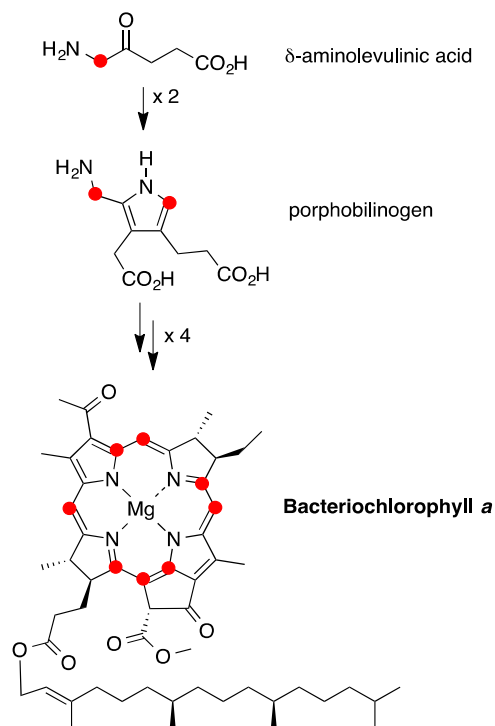


Chart 3.2. Representative structures of synthetic isotopically substituted bacteriochlorins.

The synthetic routes to **M-TPBC** and **Ni-OEBC** relied on hydrogenation of *meso*-tetraphenylporphyrin¹⁵ or transformation of octaethylporphyrin,¹⁶ respectively. The approach is satisfactory for situations wherein the isotopic substitution pattern in the porphyrin gives rise to a distinct and unambiguous pattern in the bacteriochlorin (e.g., **M-TPBC-all-¹⁵N** in Chart 3.2). On the other hand, transformation of a porphyrin that bears a single isotopic atom can result in a mixture of up to four isotopomeric bacteriochlorins. A complementary route toward isotopically substituted bacteriochlorophylls relies on biosynthetic transformations;¹⁷ however, even with the availability of rather advanced precursors (such as δ -aminolevulinic acid or porphobilinogen) that bear site-specific isotopic substitution,^{18,19} the resulting macrocycles bear isotopic atoms at numerous sites (Scheme 3.1). Such bacteriochlorophylls have numerous valuable applications,²⁰ but are not generally well suited for studies aimed at

developing spin-density maps or vibrational force fields because of the spectral complexity arising from multiple isotopic atoms. In this regard, no bacteriochlorins that contain only one or two isotopic atoms have yet been reported.



Scheme 3.1. Representative isotopologue of bacteriochlorophyll ($\bullet = {}^{13}\text{C}$).²⁰

Methods for the synthesis of bacteriochlorins have advanced significantly over the past two decades,²¹ encompassing semisynthesis (beginning with naturally occurring macrocycles),^{9,22,23} derivatization of intact synthetic porphyrins or chlorins,²⁴⁻²⁸ and *de novo* syntheses.²⁹⁻³³ Only the latter enable site-specific control over isotopic placement in the macrocycle framework. The *de novo* routes incorporate a geminal dialkyl group in each

pyrroline ring that stabilizes the tetraporphyrin chromophore toward adventitious dehydrogenation. The route we developed relies on the acid-catalyzed self-condensation of a dihydrodipyrin–acetal.³¹ The synthetic bacteriochlorin has nominal C_{2h} symmetry (assuming a planar macrocycle and the appropriate conformations of the geminal dimethyl groups) and, save for the geminal dimethyl group in each pyrroline ring, would exhibit D_{2h} symmetry characteristic of the bacteriochlorin π framework. This synthetic route is concise, has been exploited to prepare a wide variety of substituted bacteriochlorins,³⁴ and accommodates numerous metal chelates.³⁵ These advances open the door to the use of the *de novo* synthetic route to prepare bacteriochlorins that bear site-specific isotopic substitution.

The sparsely substituted natural abundance bacteriochlorin **H₂BC-NA**, which contains no substituents other than the geminal dimethyl groups, was first prepared by debromination of the corresponding 3,13-dibromobacteriochlorin,³⁶ and more recently by condensation of the unsubstituted dihydrodipyrin–acetal.³⁴ The simple substitution pattern makes **H₂BC-NA** a valuable benchmark compound for fundamental spectroscopic studies.³⁶ Herein, we expanded the benchmark compound to include zinc and copper chelates (**ZnBC-NA** and **CuBC-NA**) with specific isotope substitution. The nature of the self-condensation of the dihydrodipyrin–acetal leads to introduction of isotopes in a pairwise manner. Our focus to date concerns the atoms that constitute the inner core of the bacteriochlorin, namely the 12 carbon and 4 nitrogen atoms. The inner core encompasses the entire π system excepting only the 4 β -pyrrolic carbons. Given pairwise isotopic substitution, there are eight resulting bacteriochlorins that are “double-stamped” with isotopic atoms (for usage of this term in a different context in tetrapyrrole chemistry, see Tsay *et al.*³⁷). Zinc chelates of

bacteriochlorins yield stable anion and cation radicals and therefore are suited for EPR spectroscopic analysis. Copper bacteriochlorins afford no detectable fluorescence, which otherwise causes interference in RR spectroscopy. Accordingly, we have synthesized eight free base bacteriochlorins with pairwise introduction of ^{13}C or ^{15}N atoms about the inner resonance frame, as well as the corresponding zinc and copper chelates. The structures of the synthetic bacteriochlorins – a pair of isotopomers with ^{15}N substitution, and six isotopomers with ^{13}C substitution – are shown in Chart 3.3. Here, we report the synthesis; studies of the physicochemical properties (vibrational analysis and spin density mapping) of the 24 bacteriochlorins will be reported elsewhere.

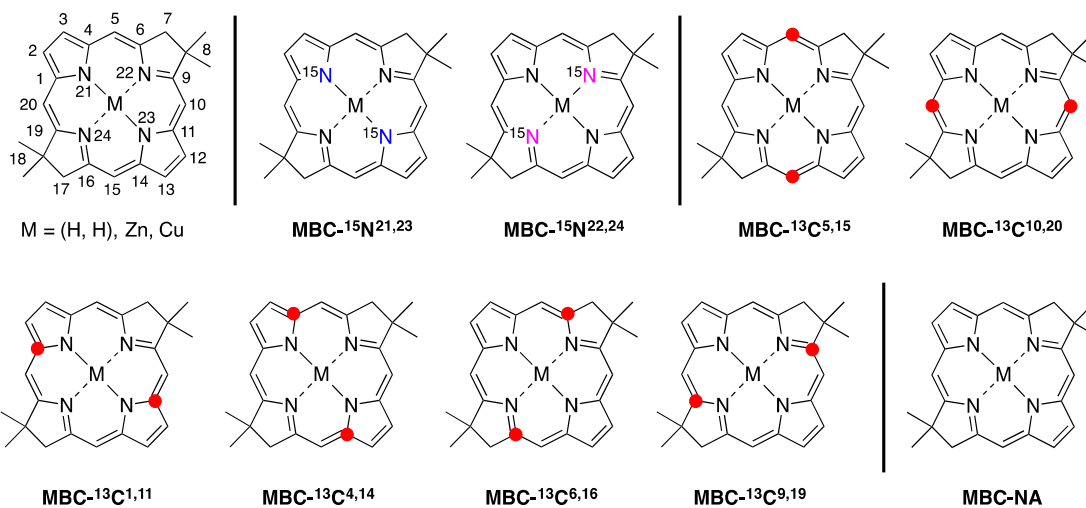


Chart 3.3. Isotopically substituted synthetic bacteriochlorins (• = ^{13}C).

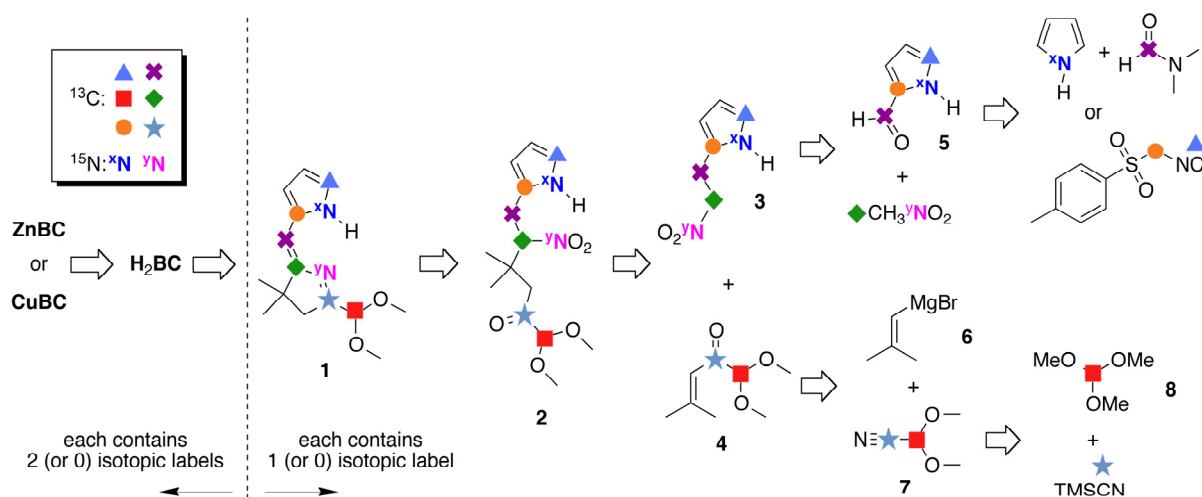
Results and Discussion

Throughout the chapter we employ IUPAC nomenclature and terminology for isotopic chemistry.^{38,39} Hereafter, we employ the use of brackets, {**X**}, to refer to a set of

isotopologues; **X-NA** for the natural abundance compound; and **X** to indicate a general structure regardless of any isotopic substitution.

(I) Retrosynthetic Analysis

The retrosynthesis of isotopically substituted metallobacteriochlorins is outlined in Scheme 3.2. The desired zinc and copper chelates are obtained by metalation of **H₂BC**,³⁵ which are created upon acid-catalyzed condensation of the dihydrodipyrin-acetal **1**.³⁴ The dihydrodipyrin-acetal is synthesized through a McMurry-type reductive cyclization of the nitrohexanone-pyrrole **2**, which in turn is derived from the nitroethylpyrrole **3** and the α,β -unsaturated ketone-acetal **4**.³⁴ The nitroethylpyrrole **3** is synthesized from nitromethane and pyrrole-2-carboxaldehyde **5** (for which multiple routes are available). The α,β -unsaturated ketone-acetal **4** is obtained upon reaction of Grignard reagent **6** with dimethoxyacetonitrile **7**, which in turn is prepared from trimethyl orthoformate **8** and TMSCN.⁴⁰

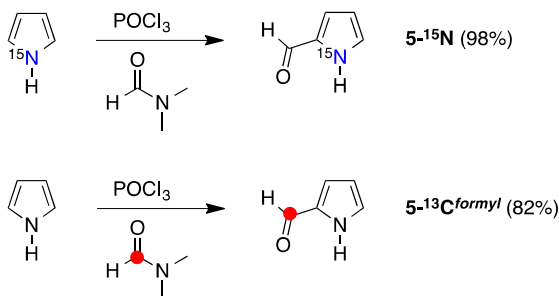


Scheme 3.2. Retrosynthesis of isotopically substituted bacteriochlorins.

(II) Synthesis

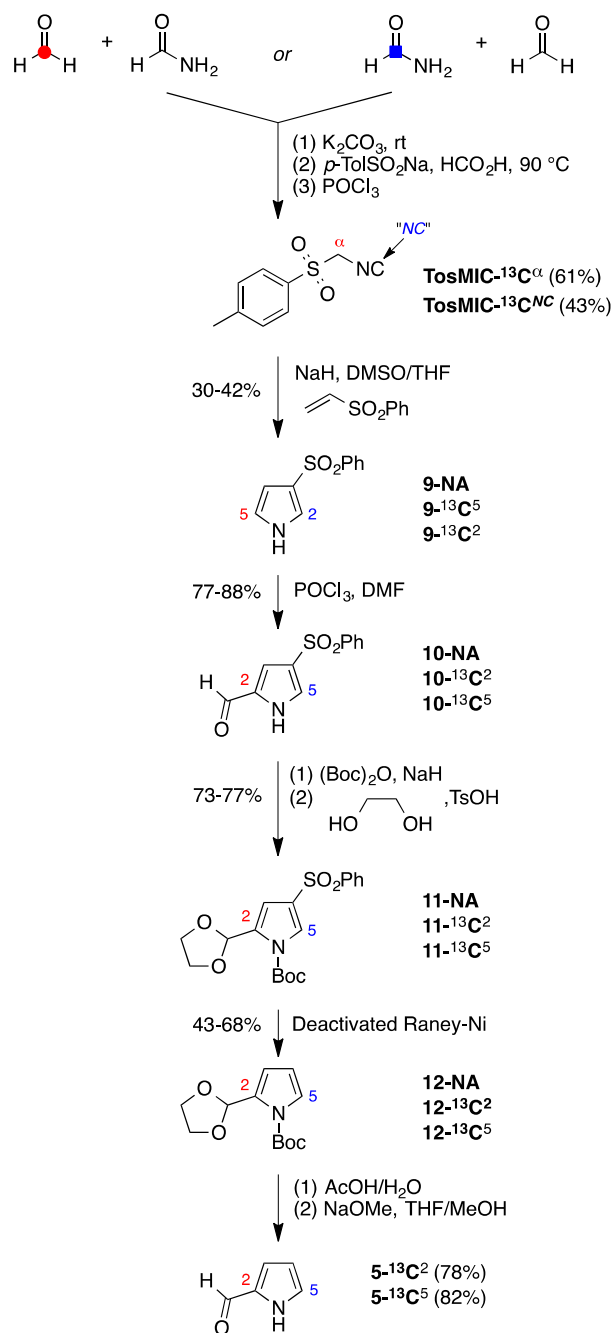
The synthesis of dihydrodipyrin–acetal **1-NA** has been reported twice^{34,41} during the development of routes to bacteriochlorin **H₂BC-NA**. The compound 2-(2-nitroethyl)pyrrole (**3-NA**) has served as a versatile intermediate in the synthesis of chlorins⁴²⁻⁴⁴ and bacteriochlorins.³⁴ Compound **3-NA** has been reported five times at different scales, in different degrees of purity, and with various extent of characterization given that in some cases the product was used directly in subsequent reactions.^{34,41-44} The prior syntheses were refined over the course of the work described herein to handle small quantities of expensive isotopically substituted reactants.

(A) Pyrrole-2-carboxaldehydes. Four isotopologues of **5** were synthesized: **5-¹⁵N**, **5-¹³C^{formyl}**, **5-¹³C²** and **5-¹³C⁵**. Pyrrole-2-carboxaldehyde **5-¹⁵N** was synthesized via Vilsmeier-Haack formylation⁴⁵ of pyrrole-(¹⁵N) with *N,N*-dimethylformamide. The synthesis of **5-¹³C^{formyl}** is known⁴⁶ and was carried out by the same reaction of pyrrole with *N,N*-dimethyl(¹³C)formamide (Scheme 3.3).



Scheme 3.3. Synthesis of isotopically substituted pyrrole-2-carboxaldehyde.

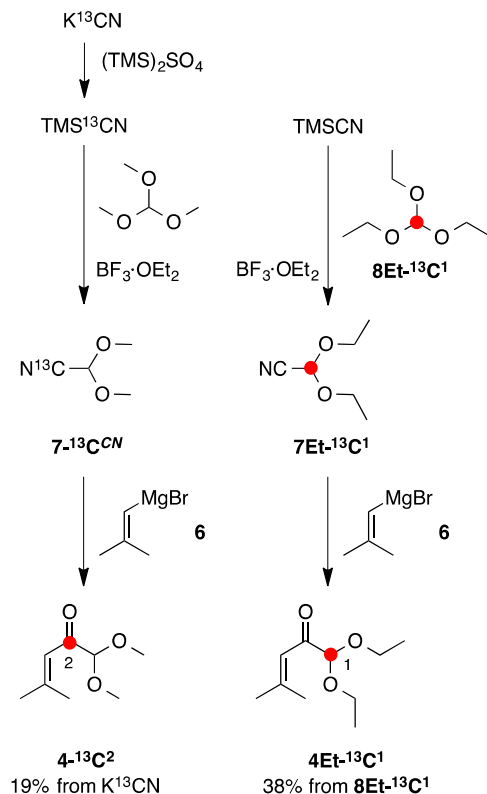
The syntheses of α - ^{13}C -substituted formyl-pyrroles **5- $^{13}\text{C}^2$** and **5- $^{13}\text{C}^5$** are seemingly straightforward yet challenging in practice. The difficulty stems from limited accessibility to sparsely substituted pyrroles with independent control over the 2- vs. 5-positions of the ^{13}C -atom and the site of formylation. Indeed, prior syntheses via Knorr,⁴⁷⁻⁵¹ Paal-Knorr,^{52,53} Hantzsch,⁵⁴ and other⁵⁵⁻⁵⁷ routes typically have afforded α - ^{13}C -substituted pyrroles that bear multiple substituents (e.g., alkyl, carboalkoxy); such substituents are not readily removed. In cases where all substituents could be removed, independent control over the 2- vs. 5- sites of the formyl group and the α - ^{13}C -atom is not available.^{49,53} One workaround entails rational synthesis of a pyrrole bearing an α -carbon protective group and the desired ^{13}C -atom at the same (α) or distinct (α , α') positions. In this regard, 2-(methylthio)(2- ^{13}C)pyrrole was synthesized and found to undergo electrophilic aromatic substitution at the 5-position.⁵⁸ The methylthio group was subsequently removed by treatment with Raney Nickel. While this approach offered potential, we turned to a route that relies on use of ^{13}C -substituted *p*-toluenesulfonylmethyl isocyanide (TosMIC)⁵⁹ to rationally construct the ^{13}C -substituted pyrroles.



Scheme 3.4. Syntheses of $\alpha\text{-}^{13}\text{C}$ -substituted pyrrole-2-carboxaldehydes (\bullet , \blacksquare = ^{13}C).

The two isotopomers can be synthesized by the same route via isotopologues of TosMIC. TosMIC is typically synthesized from three components: paraformaldehyde, formamide and sodium *p*-toluenesulfinate.⁶⁰ Swapping paraformaldehyde for the ¹³C-substituted reagent will make an α-¹³C-substituted TosMIC (**TosMIC-¹³C^α**). The same strategy has been exploited to make an α-¹⁴C-labeled TosMIC.⁶¹ Similarly, utilizing (¹³C)formamide in the reaction will make **TosMIC-¹³C^{NC}**. Thus, the corresponding ¹³C-substituted paraformaldehyde and formamide were mixed under basic conditions (K₂CO₃)⁶² for 2 h at room temperature prior to reaction with sodium *p*-toluenesulfinate in acetic acid.⁶⁰ This pre-mixing procedure helped reduce the required equivalents of ¹³C-substituted reagents. Subsequent dehydration with POCl₃ gave **TosMIC-¹³C^α** [from (¹³C)paraformaldehyde, 61%] and **TosMIC-¹³C^{NC}** [from (¹³C)formamide, 43%]. The structures of **TosMIC-¹³C^α** and **TosMIC-¹³C^{NC}** are shown in Scheme 3.4.

(B) α,β-Unsaturated Ketone-acetals. Two isotopologues of α,β-unsaturated ketone-acetal **4-NA** were synthesized: **4-¹³C²** and **4Et-¹³C¹**. Reaction of K¹³CN and bis(trimethylsilyl) sulfate afforded TMS¹³CN.⁷⁷ Following an established route,⁴⁰ reaction of TMS¹³CN with trimethyl orthoformate and catalytic BF₃·OEt₂ gave 1,1-dimethoxyacetonitrile **7-¹³C^{CN}**. Treatment of the latter with Grignard reagent **6** followed by hydrolysis gave the **4-¹³C²** in 19% overall yield (Scheme 3.5, left sequence).

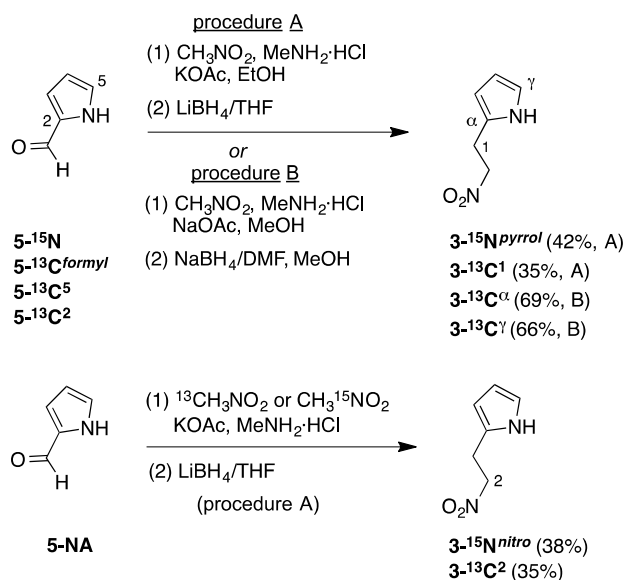


Scheme 3.5. Synthesis of isotopically substituted α,β -unsaturated ketone-acetal.

Introduction of the ^{13}C atom at position 1 requires use of trimethyl (^{13}C)orthoformate, which to our knowledge was not commercially available. Accordingly, the commercially available triethyl (^{13}C)orthoformate ($\text{8Et-}^{13}\text{C}^1$) was used instead leading ultimately to diethyl acetal 4Et-NA was obtained instead of 4-NA . The reaction sequence proceeded uneventfully, with conversion of $\text{8Et-}^{13}\text{C}^1$ to 1,1-diethoxy ($1\text{-}^{13}\text{C}$)acetonitrile $\text{7Et-}^{13}\text{C}^1$, which upon reaction with Grignard reagent **6** followed by hydrolysis gave $\text{4Et-}^{13}\text{C}^1$ in 38% overall yield (Scheme 3.5, right sequence).

(C) Nitroethylpyrroles. Four isotopologues **{5}** were transformed to the corresponding nitroethylpyrrole **{3}** via nitroaldol (Henry) condensation with CH_3NO_2 and

subsequent borohydride reduction (Scheme 3.6). Compounds **3**- $^{13}\text{C}^2$ (a known compound)⁷⁸ and **3**- $^{15}\text{N}^{nitro}$ were obtained by reaction of **5-NA** with $^{13}\text{CH}_3\text{NO}_2$ and $\text{CH}_3^{15}\text{NO}_2$, respectively. Drawing on prior syntheses of **3-NA**,^{34,43} two procedures that differ chiefly in reaction time and workup procedure were employed. Procedure A employed a 2.5 h Henry reaction and partially purified the nitrovinylpyrrole prior to LiBH_4 reduction (35–42% yields), whereas a longer reaction time (12 h) and direct addition of NaBH_4 to the nitrovinylpyrrole constituted procedure B (66, 69% yields).

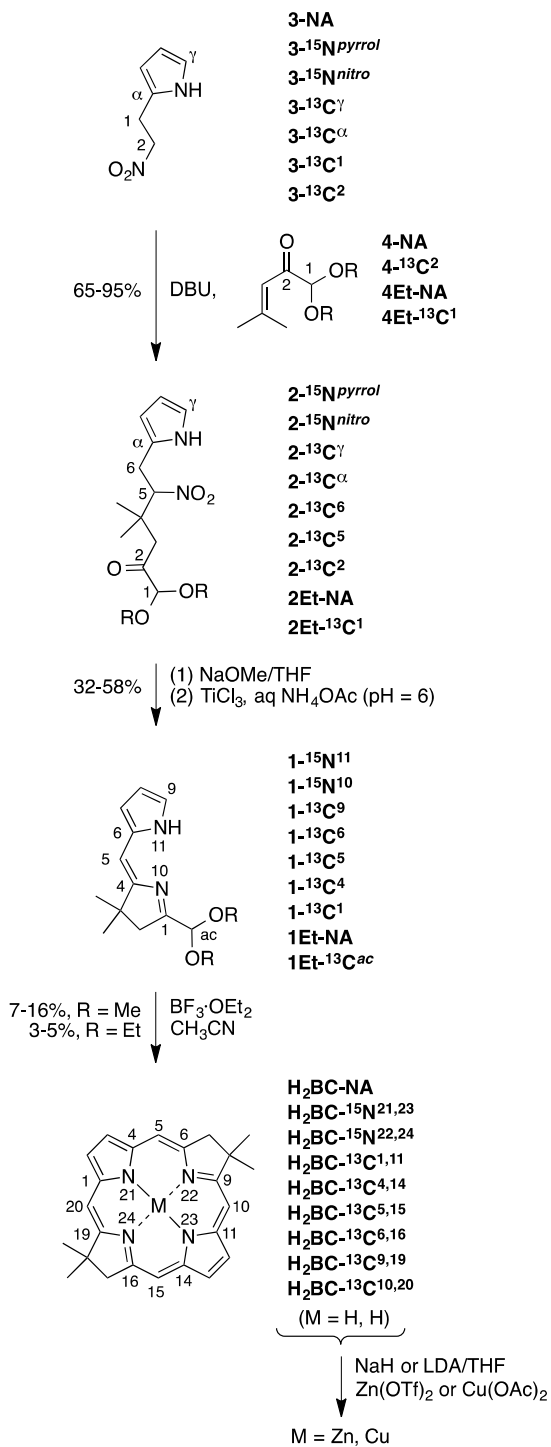


Scheme 3.6. Synthesis of various isotopically substituted nitroethylpyrroles.

(D) Dihydrodipyrin–acetals. Each nitroethylpyrrole isotopologue **{3}** was respectively reacted with α,β -unsaturated ketone **4-NA** via Michael addition⁴¹ to give the corresponding isotopologue of nitrohexanone–pyrrole **{2}** (Scheme 3.7). Conversely, **4**- $^{13}\text{C}^2$, **4Et**- $^{13}\text{C}^1$ or **4Et-NA** under the same condition with **3-NA** afforded nitrohexanone–pyrrole **2**- $^{13}\text{C}^2$, **2Et**- $^{13}\text{C}^1$ or **2Et-NA**, respectively. The prior synthesis of nitrohexanone–pyrrole **2-NA**

was achieved in 25% overall yield (upon three steps of nitro-aldol condensation, reduction, and Michael addition) from pyrrole-2-carboxaldehyde.³⁴ The procedural improvements herein (see Experimental section) gave overall yields ranging from 29% to 66% for conversion of pyrrole-2-carboxaldehyde isotopologues **{5}** to **{2}**.

Each of the eight resulting isotopologues **{2}** as well as **2Et-¹³C¹** and **2Et-NA** underwent McMurry-type cyclization to give the corresponding dihydrodipyrin–acetal isotopologues **{1}**, **1Et-¹³C^{ac}** and **1Et-NA**, respectively. The cyclization employs TiCl₃ in buffered aqueous/THF solution, which stem from conditions that were first described by McMurry for the synthesis of Δ^1 -pyrrolines,⁷⁹ adopted by Battersby for the synthesis of the 1-methyldihydrodipyrins in the preparation of the natural chlorin Bonellin,⁸⁰ and further modified by us for synthesis of (di- or tetra-) hydrodipyrins employed in routes to chlorins^{42,81} and dihydrodipyrins in routes to bacteriochlorins.^{31,34,82} The amount of buffer required depends on the nature of the TiCl₃ source (powder, 3% HCl solution, or 28% HCl solution),⁸² as described in the Experimental Section. We employed 6 equiv of TiCl₃ (20 wt % in 3% HCl solution) and 100–150 equiv of NH₄OAc per nitrohexanone–pyrrole **{2}**.



Scheme 3.7. Synthesis of isotopically substituted bacteriochlorins. See Chart 3.3 for individual bacteriochlorin structures.

(E) Bacteriochlorins. Bacteriochlorin formation is achieved by self-condensation of a dihydrodipyrin–acetal under acidic conditions. The condensation of two dihydrodipyrin–acetal molecules liberates three molecules of methanol and affords the mono-methoxybacteriochlorin.⁴⁰ We have carried out extensive studies of acid catalysis and identified mild conditions that afford the mono-methoxybacteriochlorin in reasonable yields (~40% or greater). On the other hand, the reaction in the presence of a strong acid typically affords the bacteriochlorin lacking any methoxy substituent in addition to the mono-methoxybacteriochlorin, and with lower total yields of macrocycles. Indeed, the only prior condensation of **1-NA** employed Bi(OTf)₃ in CH₂Cl₂ and afforded **H₂BC** (11%) and the monomethoxy-bacteriochlorin (9%).³⁴ Here, we employed catalysis by BF₃·OEt₂ in CH₃CN at room temperature³¹ to afford {**H₂BC**} and **H₂BC-NA** (from **1Et-NA**). In each case, the free base bacteriochlorin was readily obtained as an intense green band by a single chromatography procedure. Yields ranged from 7–16%, with little methoxybacteriochlorin detected for the lower-yielding reactions and only small quantities detected for the higher-yielding reactions. Regardless, the desired bacteriochlorin (lacking the methoxy substituent) was readily isolated. The scale of reaction typically afforded 20–70 mg of each free base bacteriochlorin. In the case of macrocycle formation from diethyl acetal **1Et-NA** or **1Et-¹³C^{ac}**, the reaction also gave the ethoxy-substituted bacteriochlorin **EtOBC-NA** or **EtOBC-¹³C^{5,15}** (not isolated), respectively (Chart 3.4). The yields of **H₂BC-NA** and **H₂BC-¹³C^{5,15}** from **1Et** and **1Et-¹³C^{ac}** are significantly lower (3–5%) than that from the corresponding dimethyl acetal **{1}** (7–16%).

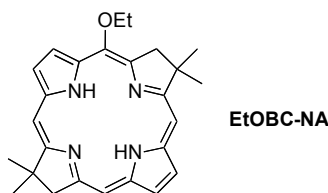


Chart 3.4. Structure of **EtOBC-NA**.

Bacteriochlorins are metalated with substantially greater difficulty than are chlorins or porphyrins.³⁵ The metalation of bacteriochlorins is facilitated by electron-withdrawing substituents. In the absence of any such substituents, metalation has recently been achieved by treatment of the bacteriochlorin with NaH or LDA followed by the metal salt.³⁵ Here, each free base macrocycle was treated with NaH (or LDA) in THF containing Cu(OAc)₂ or Zn(OTf)₂ to give the desired copper or zinc chelate. The metallochlorins were typically isolated in pure form without chromatography (Scheme 3.7). The metalation was readily observed by the bathochromic shift of the long-wavelength absorption (Q_y) band. The intensity ($\epsilon \sim 120,000 \text{ M}^{-1}\text{cm}^{-1}$) and sharpness (full-width-at-half-maximum, fwhm = 12 nm) of the Q_y band of the free base bacteriochlorin, and the shift from 713 nm to 723 nm (zinc chelate, fwhm = 14 nm) or 728 nm (copper chelate, fwhm = 19 nm) provided a very clear and reliable indicator of the completion of the metalation process.

(III) Chemical Characterization

Each {1}–{5}, {9}–{12}, {H₂BC} (as well as **EtOBC-NA**), {ZnBC} and {CuBC} was characterized by electrospray ionization mass spectroscopy (ESI-MS). Each isotopically substituted compound showed the correct molecular ion peak (except for 5-¹⁵N and

{**TosMIC**}). ESI-MS was also used to assess the integrity of isotopic incorporation at the designated sites of the bacteriochlorin isotopologues (vide infra).

Each {**1**}–{**5**}, {**9**}–{**12**} and {**H₂BC**} also was characterized by ¹H NMR and ¹³C NMR spectroscopy. Each isotopically substituted compound showed the expected splitting pattern upon ¹H NMR spectroscopy and an enhanced signal upon ¹³C NMR spectroscopy. All isotopologues {**ZnBC**} (as well as **EtOBC-NA**) were characterized by ¹H NMR spectroscopy and absorption spectroscopy. The isotopologues {**CuBC**} were not characterized by NMR spectroscopy given the paramagnetism of the copper chelate. The availability of the macrocycles with site-specific ¹³C substitution enables unambiguous determination of the NMR assignments for the bacteriochlorin skeleton. In bacteriochlorins the meso-protons and β-pyrrole protons resonate in a very narrow region (~8.73–8.83 for **H₂BC-NA**; 8.60–8.65 ppm for **ZnBC-NA**). While ¹H NMR assignments can be made without isotopic substitution, the ¹³C NMR assignments are far more challenging given the large number of quaternary carbons. The ¹H and ¹³C NMR chemical shift for each site of ¹³C-substitution in the isotopologues {**H₂BC**} are listed in Table 3.1. The ¹H NMR assignments also are provided for {**ZnBC**}.

The ¹⁵N-substituted compounds ({**1**}–{**3**} and {**H₂BC**}) were characterized by ¹⁵N NMR spectroscopy. The ¹⁵N chemical shifts (ppm, in THF-*d*₈ at 298 K referenced to external nitromethane) are characteristic for the distinct types of nitrogen-containing groups: ¹⁵N-pyrrole (**3**-¹⁵N^{pyrrol}, -228; **2**-¹⁵N^{pyrrol}, -228; **1**-¹⁵N¹¹, -229; **H₂BC**-¹⁵N^{21,23}, -249); ¹⁵N-nitroalkyl (**3**-¹⁵N^{nitro}, 6; **2**-¹⁵N^{nitro}, 10); and ¹⁵N-pyrroline (**1**-¹⁵N¹⁰, -58; **H₂BC**-¹⁵N^{22,24}, -82). The in-depth NMR analyses of each isotopologue {**H₂BC**} will be reported elsewhere.

Table 3.1. NMR chemical shifts of {H₂BC} and {ZnBC}.

Position	{H ₂ BC}		{ZnBC}
	¹ H NMR δ ^a	¹³ C NMR δ ^a	¹ H NMR δ ^b
<i>β</i> -positions			
2, 12	8.77	121.84	8.65
3, 13	8.73	121.73	8.61
7, 17	4.47	51.4	4.46
8, 18	1.97 ^c	46.0	1.98
<i>α</i> -positions			
1, 11	-- ^d	136.2	-- ^d
4, 14	-- ^d	135.3	-- ^d
6, 16	-- ^d	157.6	-- ^d
9, 19	-- ^d	169.6	-- ^d
<i>meso</i> -positions			
5, 15	8.83	98.7	8.60
10, 20	8.73	96.5	8.64
<i>NH</i> -positions			
21, 23	-2.38	-- ^d	-- ^d

^aIn CDCl₃ at 298 K. ^bIn THF-*d*₈ at 298 K. ^cChemical shifts of the geminal dimethyl protons. ^dNot available.

The bacteriochlorins {H₂BC} (as well as EtOBC-NA), {ZnBC} and {CuBC} were characterized by absorption spectroscopy, where each compound gave the characteristic bacteriochlorin features of strong bands in the near-UV and a strong band in the near-infrared spectral region.⁸ The copper bacteriochlorins gave λ_{abs} = 728 nm and also were examined by fluorescence spectroscopy to confirm the absence of fluorescence.

Integrity of Isotopic Incorporation. Free base bacteriochlorins typically afford peaks due to both the molecular ion (M^+) and the protonated molecule ($M + H^+$) upon ESI-MS analysis. On the other hand, the zinc and copper chelates of bacteriochlorins typically exhibit solely the molecular ion (M^+). Consequently, interpretation of the isotopic incorporation by ESI-MS is quite complicated for the free base bacteriochlorins but can be achieved for the zinc and copper chelates **{ZnBC}** and **{CuBC}**. Such comparisons are posited on the assumptions of (1) equal ionization efficiencies of isotopologues, and (2) peak intensities as a reliable measure of relative ion abundance.⁸³ The following presentation concerns data for the zinc chelates; the same findings were arrived at upon examination of the data for the copper chelates.

The zinc chelate of a tetrapyrrole macrocycle generally shows a characteristic isotope pattern upon ESI-MS analysis due to the natural abundance of five stable isotopes of zinc [⁶⁴Zn (48.9%), ⁶⁶Zn (27.8%), ⁶⁷Zn (4.1%), ⁶⁸Zn (18.6%) and ⁷⁰Zn (0.6%)].⁸⁴ For **ZnBC-NA**, the molecular formula is C₂₄H₂₄N₄Zn. The pattern owing to the zinc isotopes is superposed on that from the stable isotopes of ¹H (²H = 0.015%), ¹²C (¹³C = 1.11%) and ¹⁴N (¹⁵N = 0.37%) of the tetrapyrrole ligand.⁸⁴ For the ligand alone, the expected distribution of natural abundance ions is as follows:⁸⁵ (A+0), 75.9%; (A+1), 21.1%; (A+2), 2.8%; (A+3), 0.2%. Hence, the ESI-MS spectrum of a zinc bacteriochlorin is expected to exhibit multiple lines, with the monoisotopic (A+0) entity constituting the base peak.

The observed ESI mass spectrum of **ZnBC-NA** is shown in Figure 3.1 (panel A). The accurate monoisotopic mass for **ZnBC-NA** was found at 432.128 *m/z*. The observed spectrum for **ZnBC-¹³C^{1,11}** (panel B) shows a peak distribution essentially identical to that of

ZnBC-NA except for the expected shift to higher mass by 2 Da. In addition to the intense peak at 434.123 m/z , a tiny peak at 433.134 m/z corresponds to the monoisotopic mass of the bacteriochlorin substituted with only a single ^{13}C atom. No peak was observed for the monoisotopic species of the bacteriochlorin lacking any ^{13}C atoms. The spectrum of **ZnBC- $^{13}\text{C}^{1,11}$** is representative of those cases where the synthesis was performed without loss of isotopic integrity from that of the isotopically substituted reactant (>99% ^{13}C , >98% ^{15}N). Such examples also include **ZnBC- $^{13}\text{C}^{5,15}$** , **ZnBC- $^{13}\text{C}^{6,16}$** , **ZnBC- $^{13}\text{C}^{9,19}$** , **ZnBC- $^{13}\text{C}^{10,20}$** , and **ZnBC- $^{15}\text{N}^{21,23}$** .

On the other hand, the spectrum of **ZnBC- $^{13}\text{C}^{4,14}$** (Figure 3.1, panel C) shows the presence of a diagnostic ion peak at 433.134 or 432.130 m/z due to the monoisotopic mass of a bacteriochlorin bearing one or no ^{13}C -atoms, respectively. The overall isotopic enrichment for **ZnBC- $^{13}\text{C}^{4,14}$** was 87% (see Experiment section for method of calculation). The isotopic loss was also found in the earliest precursor **9- $^{13}\text{C}^2$** , which contains 13% of isotopically unsubstituted species. No further isotopic loss was found for the transformation of **9- $^{13}\text{C}^2$** to the corresponding dihydrodipyrin **1- $^{13}\text{C}^9$** . The isotopic loss apparently resulted upon formation of **TosMIC- $^{13}\text{C}^{NC}$** in the presence of formic acid as solvent, where formyl exchange between formic acid and (^{13}C)formamide may have occurred.

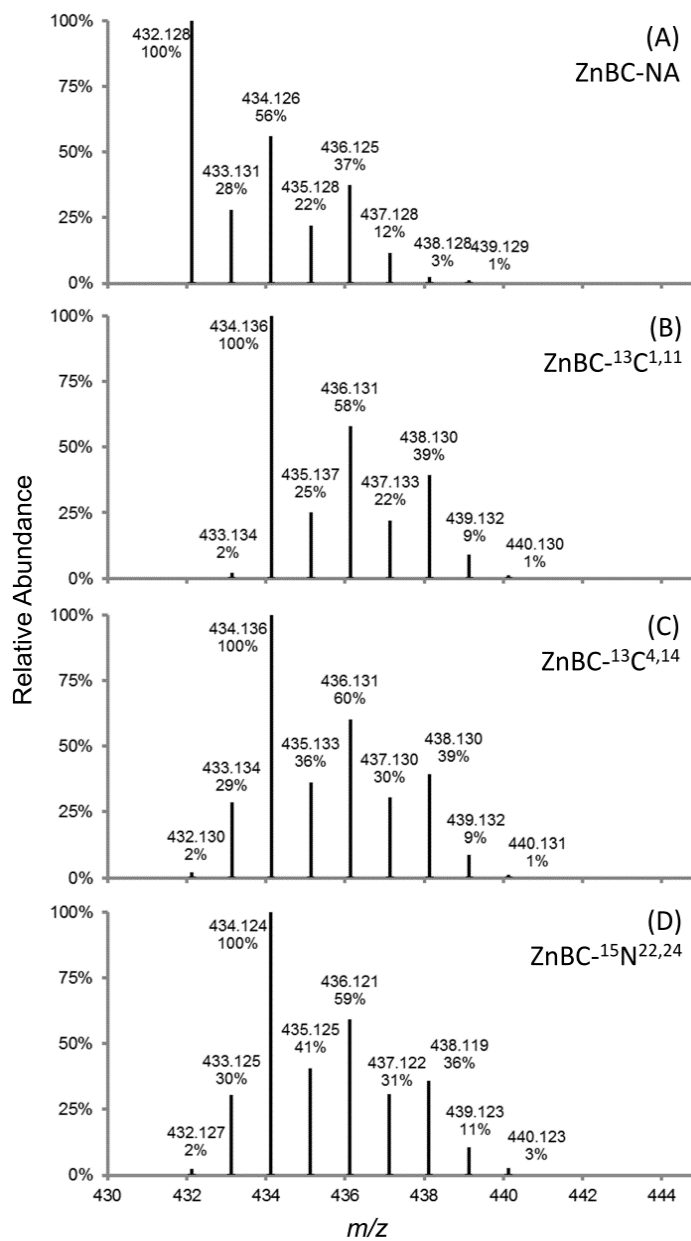
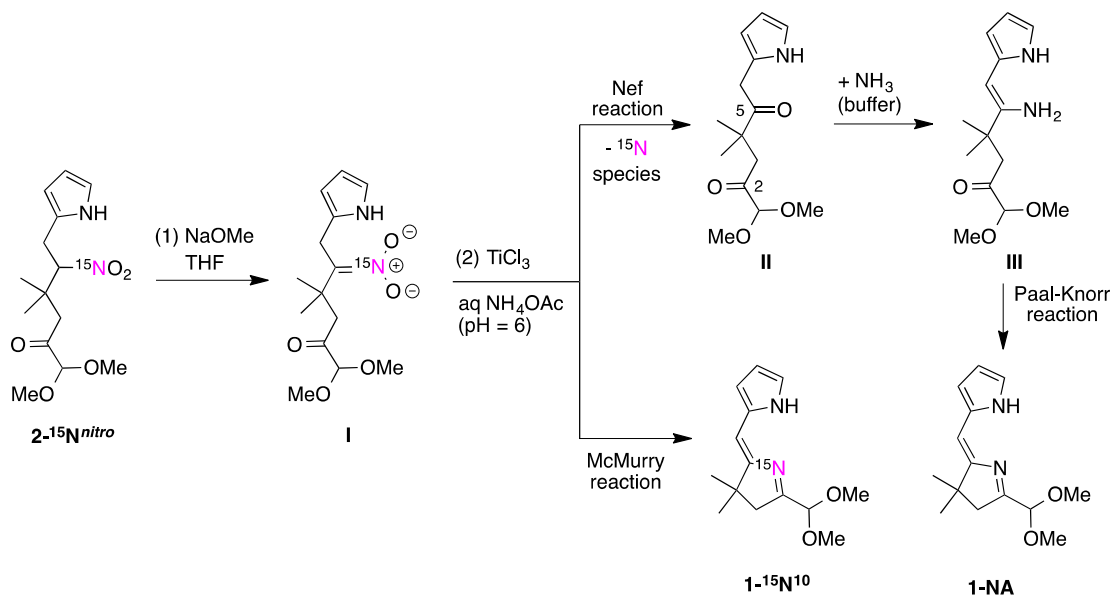


Figure 3.1. ESI-Mass spectra of ZnBC-NA, ZnBC-¹³C^{1,11} and ZnBC-¹³C^{4,14}.

The spectrum of ZnBC-¹⁵N^{22,24} (Figure 3.1, panel D) also shows a peak at 433.125 or 432.127 m/z corresponding to the monoisotopic mass of a bacteriochlorin that bears one and no ¹⁵N atoms, respectively. The overall isotopic enrichment was found to be 86%. The

precursor $2\text{-}^{15}\text{N}^{\text{nitro}}$ was found to contain only 1–2% of isotopically unsubstituted species, hence the isotopic loss must accrue during the reductive cyclization of $2\text{-}^{15}\text{N}^{\text{nitro}}$ to $1\text{-}^{15}\text{N}^{10}$ by exchange upon exposure to the large quantity of NH_4OAc used as buffer. The low quality of the mass spectrum of $1\text{-}^{15}\text{N}^{10}$ precluded an assessment of any isotopic loss at this step. A proposal for the origin of the isotopic loss upon formation of $1\text{-}^{15}\text{N}^{10}$ is shown in Scheme 3.8. Treatment of $2\text{-}^{15}\text{N}^{\text{nitro}}$ with NaOMe affords the ^{15}N -substituted nitronate anion **I**, which upon addition to the aqueous NH_4OAc buffer can undergo Nef reaction to give the natural-abundance 2,5-diketone (**II**) with loss of an ^{15}N -species (e.g., hyponitrous acid or hydroxylamine). Subsequent reaction with natural abundance NH_3 from the buffer at either ketone gives an imine or enamine (e.g., **III**), which undergoes Paal-Knorr⁸⁶ reaction with the second carbonyl group to form the pyrroline ring of **1-NA**. (Alternatively, direct attack of NH_3 may occur on the carbon of the nitronate **I** to displace an ^{15}N -species without the intermediacy of the 5-carbonyl group in **II**.) The isotopically enriched sample hence consists of an admixture of $1\text{-}^{15}\text{N}^{10}$ and **1-NA**. While the TiCl_3 -mediated Nef reaction is known,⁸⁷ the occurrence of the sequential Nef reaction, amination with NH_4OAc buffer, and Paal-Knorr reaction in parallel with the McMurry ring closure for this transformation was unknown prior to the isotopic studies reported herein.



Scheme 3.8. Proposed route for the loss of ¹⁵N upon McMurry reaction.

Conclusions

A *de novo* synthesis of stable bacteriochlorins has been exploited to incorporate pairs of ¹³C or ¹⁵N atoms in a site-specific manner. The concise nature of the synthesis enabled straightforward conversion of isotopically substituted small-molecule reactants [*N,N*-dimethyl(¹³C)formamide, (¹³C)paraformaldehyde, (¹³C)formamide, ¹³CH₃NO₂, K¹³CN and triethyl (¹³C)orthoformate, (¹⁵N)pyrrole, CH₃¹⁵NO₂] to a set of eight free base bacteriochlorins; subsequent metalation afforded the zinc and copper chelates. Each bacteriochlorin is stable by virtue of a geminal dimethyl group in each pyrroline ring. A rational synthetic route to 2- or 5-¹³C-substituted pyrrole-2-carboxaldehydes proceeded via the intermediacy of isotopically substituted TosMIC. The partial isotopic loss in two syntheses is proposed to stem from exchange processes with natural abundance species in the

reaction medium. The zinc and copper chelates of the bacteriochlorin isotopologues will be examined by EPR and RR spectroscopy, respectively, to provide spin-density and vibrational information germane to the function of the bacteriochlorin macrocycles in photosynthetic-like energy-transduction processes.

Experimental Section

A. General Methods. ^1H NMR (400 MHz) spectra and ^{13}C NMR spectra (100 MHz) were collected at room temperature in CDCl_3 unless noted otherwise. ^{15}N NMR spectroscopy (41 MHz) was performed at room temperature. The ^{15}N chemical shifts are reported relative to that of nitromethane (δ 0.0) as an indirect reference using pyrrole as a direct reference. An NMR microtube containing 8.0 M pyrrole- ^{15}N in $\text{THF-}d_8$ (70 μL) was placed in an NMR tube containing the samples in $\text{THF-}d_8$ (500 μL). The resonance of the pyrrole nitrogen was set to -230.1 ppm relative to nitromethane (δ 0.0 ppm). The description of signals includes: dt = doublet of triplets, dm = doublet of multiplets. All dipole-dipole coupling constants were reported as positive values (note that J_{NH} and J_{CN} values of pyrrole- ^{15}N have been studied and reported as negative,^{88,89} yet such detailed studies were not performed herein). Electrospray ionization mass spectrometry (ESI-MS) data are reported for the molecular ion or adduct ion. Absorption spectra were collected in toluene at room temperature.

The ^{15}N -substituted compounds [^{15}N]pyrrole, $\text{CH}_3^{15}\text{NO}_2$] exhibited $>98\%$ ^{15}N purity. The ^{13}C -substituted compounds [N,N -dimethyl(^{13}C)formamide, (^{13}C)paraformaldehyde, (^{13}C)formamide, $^{13}\text{CH}_3\text{NO}_2$, K^{13}CN and triethyl (^{13}C)orthoformate] exhibited 99% ^{13}C purity.

NaH (dry, 95%), LDA (2.0 M solution in heptanes/THF/ethylbenzene), and Raney Nickel (W.R. Grace and Co. Raney[®] 2800) were used as obtained commercially. Silica gel (40 μm average particle size) was used for column chromatography. All solvents were reagent grade and were used as received unless noted otherwise. THF was freshly distilled from sodium/benzophenone ketyl.

B. Noncommercial Compounds. Compounds **1-NA**,³⁴ **3-NA**,³⁴ **4-NA**,⁴⁰ **4Et-NA**,⁴⁰ **9-NA**,⁶³ **ZnBC-NA**,³⁵ and **CuBC-NA**³⁵ were prepared as described in the literature.

C. Pyrrole-2-carboxaldehydes {5}:

(¹⁵N)Pyrrole-2-carboxaldehyde (5-¹⁵N). Following a standard procedure,⁴⁵ *N,N*-dimethylformamide (1.61 g, 22.0 mmol) in an ice bath was slowly treated with POCl₃ (3.38 g, 22.0 mmol). The ice bath was removed, and the mixture was allowed to stir for 5 min. The ice bath was replaced, and anhydrous 1,2-dichloroethane (6.8 mL) was added, followed by a solution of (¹⁵N)pyrrole (1.25 g, 18.4 mol) in 1,2-dichloroethane (6.8 mL) over 30 min. The mixture was refluxed for 15 min and then allowed to cool to room temperature. A saturated aqueous NaOAc solution (6.9 g of NaOAc in 15 mL of deionized water) was added, and the mixture was refluxed for 15 min. The mixture was allowed to cool to room temperature and diluted with diethyl ether. The mixture was washed with saturated aqueous NaHCO₃ solution. The organic layer was dried (Na₂SO₄) and concentrated to yield a brown solid (1.73 g, 98%): mp 38–40 °C; ¹H NMR δ 6.34–6.37 (m, 1H), 7.01–7.04 (m, 1H), 7.18–7.20 (m, 1H), 9.51 (d, $J = 2.6$ Hz, 1H), 10.65 (dd, $J = 98.4$ Hz, $J = 24.0$ Hz, 1H); ¹³C NMR δ 111.3 (d, $J = 3.1$ Hz), 122.0, 127.1 (dd, $J = 14.1$ Hz, $J = 5.0$ Hz), 132.7 (d, $J = 14.5$ Hz), 179.5; the sample failed to show the correct *m/z* peak in ESI-MS possibly due to the limited

stability at room temperature while waiting in queue for analysis.

Pyrrole-2-(^{13}C)carboxaldehyde (5- $^{13}\text{C}^{\text{formyl}}$). The above procedure with *N,N*-dimethyl(^{13}C)formamide (1.00 g, 13.5 mmol) afforded the title compound (previously reported with limited data)⁴⁶ as a brown solid (1.07 g, 82%): mp 37–39 °C; ^1H NMR δ 6.36–6.37 (m, 1H), 7.01–7.02 (m, 1H), 7.18 (br s, 1H), 9.52 (d, $J = 176$ Hz, 1H), 10.28 (br s, 1H); ^{13}C NMR δ 111.3 (d, $J = 4.6$ Hz), 121.8 (d, $J = 8.4$ Hz), 126.6 (d, $J = 3.1$ Hz), 132.8 (d, $J = 65.6$ Hz), 179.4 (^{13}C); ESI-MS obsd 95.0331, calcd 95.0332 [(M – H) $^-$, M = C₄ $^{13}\text{CH}_5\text{NO}$].

D. Pyrrole-2-carboxaldehydes {5} via TosMIC:

***p*-Toluenesulfonyl(^{13}C)methyl isocyanide (TosMIC- $^{13}\text{C}^\alpha$).** Following a modified procedure,^{60,62} (^{13}C)paraformaldehyde (5.00 g, 161 mmol), formamide (22.5 g, 500 mmol) and K₂CO₃ (2.30 g, 16.7 mmol) was placed in a 250 mL round-bottom flask. Deionized water (~5 mL) was added to dissolve the solid materials on the wall of the flask. The mixture was stirred at room temperature for 2 h, whereupon formic acid (52.5 g, 1.14 mol) and sodium *p*-toluenesulfinate hydrate (62.5 g, 233 mmol) were added in an alternating portionwise fashion. The mixture was heated at 90 °C for another 2 h before being poured into an ice-salt bath (400 g of ice and 40 g of salt). The mixture was extracted with CH₂Cl₂. The organic phase was washed with saturated aqueous NaHCO₃ solution until neutral, dried (Na₂SO₄), and concentrated to a white solid. The crude solid was placed in a 1 L round-bottom flask, to which freshly distilled THF (60 ml), anhydrous ether (24 mL), and triethylamine (56 mL) were then added. The suspension was cooled to –5 °C in an ice-salt bath. Then, a solution of POCl₃ (25 g, 160 mmol) in freshly distilled THF (25 ml) was added dropwise by an addition funnel at a rate such that the temperature was maintained between –

5 °C and 0 °C. After stirring for 30 min at 0 °C, the mixture was poured into 1.5 L of ice-water with continuous stirring. The mixture was stirred for another 30 min. The resulting brown precipitate was collected by suction filtration and washed with cold water (100 mL). The collected wet product was dissolved in CH₂Cl₂, dried (NaSO₄) and concentrated to a brown solid (19.3 g, 61%), which was used directly in the next step without further purification: ¹H NMR δ 2.50 (s, 3H), 4.59 (d, *J* = 156 Hz, 2H), 7.46 (d, *J* = 8.1 Hz, 2H), 7.90 (d, *J* = 8.1 Hz, 2H); ¹³C NMR δ 21.8, 61.1 (¹³C), 129.4, 130.3, 146.9.

***p*-Toluenesulfonylmethyl (¹³C)isocyanide (TosMIC-¹³C^{NC}).** The above procedure with paraformaldehyde (3.66 g, 122 mmol), (¹³C)formamide (5.00 g, 109 mmol), K₂CO₃ (1.52 g, 11.0 mmol), formic acid (28.1 g, 611 mmol) and sodium *p*-toluenesulfinate hydrate (31.5 g, 122 mmol) afforded the title compound as a brown solid (9.20 g, 43%), which was used directly in the next step without further purification: ¹H NMR δ 2.50 (s, 3H), 4.58–4.59 (m, 2H), 7.46 (d, *J* = 8.4 Hz, 2H), 7.90 (d, *J* = 8.4 Hz, 2H); ¹³C NMR δ 21.8, 129.4, 130.4, 131.9, 146.9, 166.0 (¹³C).

3-Benzenesulfonyl(5-¹³C)pyrrole (9-¹³C⁵). Following a standard procedure,⁶³ phenyl vinyl sulfone (16.5 g, 98.5 mmol) and TosMIC-¹³C^α (19.3 g, 98.5 mmol) in THF/DMSO (450 mL, 2:1) were added via a cannula to a suspension of NaH (7.9 g, 60% in oil suspension, 0.20 mol) in 150 mL of THF. The reaction mixture was stirred at room temperature for 5 h. Water was added slowly, and the mixture was extracted with ethyl acetate. The organic extract was dried (Na₂SO₄) and concentrated. Column chromatography [silica, hexanes/ethyl acetate (2:3)] afforded a pale yellow solid (6.07 g, 30%): mp 137–140

°C; ^1H NMR δ 6.51–6.54 (m, 1H), 6.79–6.81 (dm, $J = 189$ Hz, 1H), 7.41–7.43 (m, 1H), 7.46–7.55 (m, 3H), 7.93–7.96 (m, 2H), 8.73 (br s, 1H); ^{13}C NMR δ 108.6 (d, $J = 67.9$ Hz), 120.1 (^{13}C), 126.8, 129.0, 132.5; ESI-MS obsd 209.0470, calcd 209.0466 [(M + H) $^+$, M = $\text{C}_9^{13}\text{CH}_9\text{NO}_2\text{S}$].

3-Benzenesulfonyl(2- ^{13}C)pyrrole (9- $^{13}\text{C}^2$). The above procedure with TosMIC- $^{13}\text{C}^{\text{NC}}$ (8.61 g, 43.9 mmol) afforded the title compound as a brown solid (3.82 g, 42%): mp 145–147 °C; ^1H NMR δ 6.51–6.54 (m, 1H), 6.78–6.82 (m, 1H), 7.41–7.43 (dm, $J = 193$ Hz, 1H), 7.46–7.55 (m, 3H), 7.93–7.96 (m, 2H), 8.73 (br s, 1H); ^{13}C NMR δ 108.6 (d, $J = 3.8$ Hz), 120.2 (d, $J = 4.6$ Hz), 122.4 (^{13}C), 125.4, 126.8, 129.0, 132.5; ESI-MS obsd 209.0457, calcd 209.0466 [(M + H) $^+$, M = $\text{C}_9^{13}\text{CH}_9\text{NO}_2\text{S}$].

4-Benzenesulfonyl-2-formylpyrrole (10-NA). Following a standard procedure,³⁴ a solution of 9-NA (8.56 g, 41.4 mmol) in DMF (190 mL) was treated with POCl_3 (6.0 mL, 64 mmol). The resulting mixture was stirred at 80 °C for 40 h, allowed to cool to room temperature, treated with a mixture of saturated aqueous sodium acetate/ CH_2Cl_2 (400 mL, 1:1), and then stirred for 1 h. The aqueous phase was separated and extracted with CH_2Cl_2 . The combined organic extract was washed with saturated brine, dried (Na_2SO_4), and concentrated. Column chromatography [silica, CH_2Cl_2 /ethyl acetate (3:2)] afforded a yellow solid (8.58 g, 88%): mp 152–155 °C; ^1H NMR δ 7.25 (d, $J = 1.5$ Hz, 1H), 7.50–7.61 (m, 3H), 7.66 (br s, 1H), 7.95–7.98 (m, 2H), 9.55 (d, $J = 1.1$ Hz, 1H), 10.1 (br s, 1H); ^{13}C NMR δ 118.9, 127.0, 127.84, 128.29, 129.3, 133.2, 133.5, 142.3, 179.8; ESI-MS obsd 236.0380, calcd 236.0381 [(M + H) $^+$, M = $\text{C}_{11}\text{H}_9\text{NO}_3\text{S}$].

4-Benzenesulfonyl-2-formyl-(2- ^{13}C)pyrrole (10- $^{13}\text{C}^2$). The above procedure with 9-

$^{13}\text{C}^5$ (6.07 g, 29.3 mmol) afforded the title compound as a yellow solid (5.33 g, 77%): mp 157–159 °C; ^1H NMR δ 7.25 (br s, 1H), 7.51–7.61 (m, 3H), 7.67 (d, $J = 7.0$ Hz, 1H), 7.95–7.98 (m, 2H), 9.54 (d, $J = 30.4$ Hz, 1H), 10.2 (br s, 1H); ^{13}C NMR δ 118.9 (d, $J = 65.6$ Hz), 127.0, 127.8 (d, $J = 5.3$ Hz), 128.3, 129.3, 133.2 (d, $J = 3.8$ Hz), 133.5 (^{13}C), 142.3, 179.8 (d, $J = 63.3$ Hz); ESI-MS obsd 237.0413, calcd 237.0409 [(M + H) $^+$, M = C $_{10}^{13}\text{CH}_9\text{NO}_3\text{S}$].

4-Benzenesulfonyl-2-formyl-(5- ^{13}C)pyrrole (10- $^{13}\text{C}^5$). The above procedure with **9- $^{13}\text{C}^2$** (5.84 g, 28.1 mmol) afforded the title compound as a yellow solid (5.17 g, 78%): mp 151–155 °C; ^1H NMR δ 7.25–7.28 (m, 1H), 7.51–7.62 (m, 3H), 7.67–7.68 (dm, $J = 194$ Hz, 1H), 7.95–7.98 (m, 2H), 9.54 (s, 1H), 10.2 (br s, 1H); ^{13}C NMR δ 119.0, 127.0, 127.95 (^{13}C), 129.3, 133.2, 142.3, 179.8 (d, $J = 2.3$ Hz); ESI-MS obsd 259.0230, calcd 259.0229 [(M + Na) $^+$, M = C $_{10}^{13}\text{CH}_9\text{NO}_3\text{S}$].

***tert*-Butyl 4-benzenesulfonyl-2-(1,3-dioxolan-2-yl)-pyrrole-1-carboxylate (11-NA).** Following standard procedures,^{64,65} a solution of **10-NA** (8.58 g, 36.5 mmol) in THF (230 mL) was slowly treated with NaH (1.75 g, 43.8 mmol, 60% dispersion in mineral oil) at room temperature under argon. After 1 h, Boc anhydride (8.30 g, 40.0 mmol) was added. After stirring for 24 h at room temperature, the reaction mixture was quenched by the addition of saturated aqueous NH_4Cl , and then extracted with ethyl acetate. The organic extract was concentrated to a dark red oil. The crude solid material was dissolved in benzene (730 mL) and then treated with ethylene glycol (50.8 mL, 91.1 mmol) and *p*-TsOH·H $_2\text{O}$ (0.83 g, 44 mmol). The reaction mixture was refluxed using a Dean-Stark apparatus for 1.5 h. After allowing to cool to room temperature, saturated aqueous NaHCO_3 (400 mL) was added, and the mixture was extracted with CH_2Cl_2 . The organic layer was washed with

saturated brine, dried (Na₂SO₄), and concentrated. Recrystallization from hot 2-propanol afforded a brown solid (7.86 g, 57%). The mother liquor was chromatographed [silica, CH₂Cl₂/ethyl acetate (4:1)] to obtain an additional 2.30 g of pale yellow product for a total of 10.16 g (73%): mp 135–137 °C; ¹H NMR δ 1.61 (s, 9H), 3.97–4.01 (m, 4H), 6.35 (s, 1H), 6.63–6.64 (m, 1H), 7.49–7.60 (m, 3H), 7.84 (d, *J* = 1.83 Hz, 1H), 7.94–7.97 (m, 2 H); ¹³C NMR δ 27.8, 65.0, 86.6, 97.6, 110.3, 125.9, 126.65, 127.18, 129.2, 133.0, 134.7, 142.0, 147.4; ESI-MS obsd 402.0990, calcd 402.0987 [(M + Na)⁺, M = C₁₈H₂₁NO₆S].

***tert*-Butyl 4-benzenesulfonyl-2-(1,3-dioxolan-2-yl)-(2-¹³C)pyrrole-1-carboxylate (11-¹³C²).** The above procedure with **10-¹³C²** (5.33 g, 22.6 mmol) afforded the title compound as a yellow solid (6.60 g, 77%): mp 142–144 °C; ¹H NMR δ 1.61 (s, 9H), 3.97–4.01 (m, 4H), 6.35 (d, *J* = 2.2 Hz, 1H), 6.62–6.64 (m, 1H), 7.49–7.60 (m, 3H), 7.84 (dd, *J* = 5.3 Hz, *J* = 2.0 Hz, 1H), 7.94–7.97 (m, 2 H); ¹³C NMR δ 27.8, 65.0, 86.6, 97.6 (d, *J* = 65.6 Hz), 110.3 (d, *J* = 71.7 Hz), 125.9 (d, *J* = 6.1 Hz), 127.2, 129.2, 133.0, 134.7 (¹³C), 142.0; ESI-MS obsd 403.1022, calcd 403.1016 [(M + Na)⁺, M = C₁₇¹³CH₂₁NO₆S].

***tert*-Butyl 4-benzenesulfonyl-2-(1,3-dioxolan-2-yl)-(5-¹³C)pyrrole-1-carboxylate (11-¹³C⁵).** The above procedure with **10-¹³C⁵** (4.20 g, 17.8 mmol) afforded the title compound as a yellow solid (4.73 g, 70%): mp 129–133 °C; ¹H NMR δ 1.61 (s, 9H), 3.97–4.01 (m, 4H), 6.35 (s, 1H), 6.62–6.64 (m, 1H), 7.49–7.60 (m, 3H), 7.83 (dd, *J* = 98.6 Hz, *J* = 1.8 Hz, 1H), 7.94–7.97 (m, 2 H); ¹³C NMR δ 27.8, 65.0, 86.6, 97.5, 110.3, 125.9 (¹³C), 127.2, 129.2, 133.0, 142.0; ESI-MS obsd 403.1013, calcd 403.1016 [(M + Na)⁺, M = C₁₇¹³CH₂₁NO₆S].

***tert*-Butyl 2-(1,3-dioxolan-2-yl)-pyrrole-1-carboxylate (12-NA).** Raney nickel

(~100 g, slurry in H₂O) was washed with deionized water (3 x 300 mL) and acetone (3 x 300 mL) before being poured into a three-necked, 1-L flask equipped with a mechanical stirrer and a condenser. A total of 150 mL of acetone was used to facilitate the transfer of Raney nickel into the flask. The Raney nickel–acetone mixture was deactivated at 50 °C with stirring for 2 h before the addition of a solution of **11-NA** (2.28 g, 6.00 mmol) in acetone (50 mL). The mixture was stirred at 50 °C for a further 18 h. The reaction mixture was filtered through a pad of Celite. The filter cake was washed with acetone. The filtrate was concentrated and chromatographed [silica, hexanes/ethyl acetate (3:1)] to yield a colorless liquid (648 mg, 44%): ¹H NMR δ 1.60 (s, 9H), 3.97–4.06 (m, 4H), 6.13 (t, *J* = 3.3 Hz, 1H), 6.41–6.43 (m, 1H), 6.45 (s, 1H), 7.24 (dd, *J* = 3.3 Hz, *J* = 1.8 Hz, 1H); ¹³C NMR δ 27.9, 64.8, 84.2, 98.4, 109.9, 112.5, 122.6, 132.0; ESI-MS obsd 262.1043, calcd 262.1050 [(M + Na)⁺, M = C₁₂H₁₇NO₄].

***tert*-Butyl 2-(1,3-dioxolan-2-yl)-(2-¹³C)pyrrole-1-carboxylate (12-¹³C²)**. Following the above procedure, Raney nickel (~150 g slurry in H₂O) was deactivated in acetone (450 mL) for 3.5 h before **11-¹³C²** (6.60 g, 17.4 mmol) in acetone (50 mL) was added. The mixture was stirred and heated at 50 °C for a further 20 h. Chromatography yielded the title compound as a colorless liquid (1.81 g, 43%). Further elution also recovered starting material **11-¹³C²** (1.65 g, 25%), which was combined with another batch and converted to the title compound in an average yield of 56%: ¹H NMR δ 1.60 (s, 9H), 3.97–4.07 (m, 4H), 6.13 (dt, *J* = 6.6 Hz, *J* = 3.3 Hz, 1H), 6.41–6.44 (m, 1H), 6.45 (s, 1H), 7.23–7.26 (m, 1H); ¹³C NMR δ 27.9, 64.8, 98.4 (d, *J* = 66.4 Hz), 109.9, 112.5 (d, *J* = 71.0 Hz), 122.7, 132.0 (¹³C); ESI-MS obsd 263.1085, calcd 263.1083 [(M + Na)⁺, M = C₁₁¹³CH₁₇NO₄].

***tert*-Butyl 2-(1,3-dioxolan-2-yl)-(5-¹³C)pyrrole-1-carboxylate (12-¹³C⁵)**. The above procedure with **11-¹³C⁵** (4.15 g, 10.9 mmol) afforded the title compound as a yellow solid (1.78 g, 68%): ¹H NMR δ 1.60 (s, 9H), 3.97–4.07 (m, 4H), 6.12 (dt, *J* = 8.7 Hz, *J* = 3.3 Hz, 1H), 6.40–6.44 (m, 1H), 6.45 (s, 1H), 7.24–7.25 (dm, *J* = 192.0 Hz, 1H); ¹³C NMR δ 27.9, 64.8, 98.4, 112.5, 122.6 (¹³C) ; ESI-MS obsd 263.1077, calcd 263.1083 [(M + Na)⁺, M = C₁₁¹³CH₁₇NO₄].

(2-¹³C)Pyrrole-2-carboxaldehyde (5-¹³C²). Following a standard procedure,⁷³ **12-¹³C²** (2.45 g, 10.2 mmol) in a 50-mL flask was treated with AcOH/H₂O (24 mL, 1:1). The reaction mixture was stirred at room temperature for 2 h. The reaction mixture was quenched by the slow addition of saturated aqueous NaHCO₃, and then extracted with CH₂Cl₂. The organic extract was dried (NaSO₄) and concentrated. The residue was dissolved in freshly distilled THF (40 mL) and treated with NaOMe (1.95 g, 36.1 mmol) in MeOH (6 mL). The reaction mixture was stirred for 15 min and then treated with water and diethyl ether. The organic extract was dried (NaSO₄) and concentrated to yield a brown solid (760 mg, 78%): mp 35–37°C; ¹H NMR δ 6.34–6.38 (m, 1H), 6.97–7.01 (m, 1H), 7.12–7.14 (m, 1H), 9.31 (br s, 1H), 9.53 (d, *J* = 29.0 Hz, 1H); ¹³C NMR δ 111.3 (d, *J* = 2.3 Hz), 120.1, 132.9 (¹³C), 179.2 (d, *J* = 65.6 Hz); ESI-MS obsd 97.0483, calcd 97.0478 [(M + H)⁺, M = C₄¹³CH₅NO].

(5-¹³C)Pyrrole-2-carboxaldehyde (5-¹³C⁵). The above procedure with **12-¹³C⁵** (3.45 g, 14.4 mmol) afforded the title compound as a brown solid (1.13 g, 82%): mp 33–37°C; ¹H NMR δ 6.35–6.38 (m, 1H), 6.98–7.02 (m, 1H), 7.15 (d, *J* = 186 Hz, 1H), 9.52 (s, 1H), 9.85 (br s, 1H); ¹³C NMR δ 111.3 (d, *J* = 62.6 Hz), 126.4 (¹³C), 179.3; ESI-MS obsd 97.0481, calcd 97.0478 [(M + H)⁺, M = C₄¹³CH₅NO].

E. Nitroethylpyrroles {3}:

2-(2-Nitroethyl)(¹⁵N)pyrrole (3-¹⁵N^{pyrrol}). Following a standard procedure³⁴ with slight modification (procedure A), a mixture of 5-¹⁵N (1.73 g, 18.0 mmol), potassium acetate (1.40 g, 14.3 mmol), and methylamine hydrochloride (0.97 g, 14 mmol) in absolute ethanol (6.3 mL) was treated with nitromethane (2.5 mL, 47 mmol) with stirring. The mixture was stirred for 2.5 h, whereupon water was added. The mixture was extracted with CH₂Cl₂. The organic layer was dried (NaSO₄) and concentrated to yield a dark yellow solid. The crude solid material was dissolved in freshly distilled THF (81 mL), and the solution was cooled to -10 °C. The solution was treated with LiBH₄ (0.48 g, 90%, 22 mmol) all-at-once under vigorous stirring. The reaction mixture was stirred for 25 min at -10 °C, whereupon the reaction mixture was quenched by slow addition of a cold saturated aqueous NH₄Cl solution. The mixture was extracted with ethyl acetate, and the organic layer was washed with brine, dried (Na₂SO₄), and concentrated. Column chromatography [silica, hexanes/ethyl acetate (3:1)] afforded an orange oil (1.07 g, 42%): ¹H NMR δ 3.31 (td, *J* = 6.8 Hz, *J* = 2.2 Hz, 2H), 4.60 (t, *J* = 6.8 Hz, 2H), 6.00–6.02 (m, 1H), 6.13–6.16 (m, 1H), 6.70–6.72 (m, 1H), 8.17 (dq, *J* = 95.3 Hz, *J* = 2.6 Hz, 1H); ¹³C NMR δ 25.5, 75.4, 106.9 (d, *J* = 5.3 Hz), 108.8 (d, *J* = 3.1 Hz), 117.8 (d, *J* = 13.0 Hz), 126.0; ¹⁵N NMR δ -228.1; ESI-MS obsd 140.0479, calcd 140.0483 [(M - H)⁻, M = C₆H₈N¹⁵NO₂].

2-[2-(¹⁵N)Nitroethyl]pyrrole (3-¹⁵N^{nitro}). Procedure A with 5-NA (1.74 g, 18.3 mmol) and CH₃¹⁵NO₂ (1.00 g, 16.1 mmol) afforded the title compound as an orange oil (863 mg, 38%): ¹H NMR δ 3.31 (td, *J* = 6.7 Hz, *J* = 3.5 Hz, 2H), 4.60 (td, *J* = 6.7 Hz, *J* = 2.3 Hz, 2H), 6.00–6.02 (m, 1H), 6.13–6.16 (m, 1H), 6.70–6.72 (m, 1H), 8.17 (br s, 1H); ¹³C NMR δ

25.5 (^{13}C), 75.3 (d, $J = 7.6$ Hz), 106.9, 108.8, 117.8, 126.0; ^{15}N NMR δ 5.9; ESI-MS obsd 142.0630, calcd 142.0629 [(M + H) $^+$, M = C₆H₈N¹⁵NO₂].

2-[2-Nitro(1- ^{13}C)ethyl]pyrrole (3- $^{13}\text{C}^1$). Procedure A with **5- $^{13}\text{C}^{\text{formyl}}$** (1.01 g, 10.5 mmol) afforded the title compound as an orange oil (513 mg, 35%): ^1H NMR δ 3.31 (dt, $J = 131$ Hz, $J = 6.7$ Hz, 2H), 4.60 (td, $J = 6.7$ Hz, $J = 3.3$ Hz, 2H), 6.01 (br s, 1H), 6.13–6.16 (m, 1H), 6.71 (br s, 1H), 8.17 (br s, 1H); ^{13}C NMR δ 25.4, 75.3 (d, $J = 35.9$ Hz), 106.9 (d, $J = 3.8$ Hz), 108.8 (d, $J = 3.1$ Hz), 117.8, 126.0 (d, $J = 52.6$ Hz); ESI-MS obsd 142.0690, calcd 142.0692 [(M + H) $^+$, M = C₅¹³CH₈N₂O₂].

2-[2-Nitro(2- ^{13}C)ethyl]pyrrole (3- $^{13}\text{C}^2$).⁷⁸ Procedure A with **5-NA** (2.72 g, 28.6 mmol) and $^{13}\text{CH}_3\text{NO}_2$ (1.77 g, 28.5 mmol) afforded the title compound as an orange oil (1.41 g, 35%): ^1H NMR δ 3.31 (td, $J = 6.7$ Hz, $J = 4.9$ Hz, 2H), 4.60 (dt, $J = 147$ Hz, $J = 6.7$ Hz, 2H), 6.01 (br s, 1H), 6.13–6.16 (m, 1H), 6.71–6.72 (m, 1H), 8.17 (br s, 1H); ^{13}C NMR δ 75.3 (^{13}C); ESI-MS obsd 140.0551, calcd 140.0547 [(M – H) $^-$, M = C₅¹³CH₈N₂O₂].

2-(2-Nitroethyl)(2- ^{13}C)pyrrole (3- $^{13}\text{C}^\alpha$). Following a standard procedure (procedure B),⁴³ **5- $^{13}\text{C}^2$** (1.76 g, 18.3 mmol) was dissolved in methanol (55 mL) and treated with nitromethane (2.96 mL, 55.2 mmol), sodium acetate (1.66 g, 20.0 mmol), and methylamine hydrochloride (1.66 g, 20.0 mmol). Stirring at room temperature for 12 h afforded a yellow/brown mixture. DMF (37 mL) and methanol (31 mL) were added to the reaction mixture. NaBH₄ (2.43 g, 63.9 mmol) was added portionwise. The reaction mixture was stirred at room temperature for 1 h, neutralized with acetic acid (~3 mL), and concentrated. The mixture was dissolved in CH₂Cl₂ and washed with water. The organic layer was dried

(Na₂SO₄), concentrated, and chromatographed [silica, hexanes/ethyl acetate (3:1)] to give an orange oil (1.70 g, 66%): ¹H NMR δ 3.32 (td, *J* = 6.6 Hz, *J* = 6.6 Hz, 2H), 4.60 (dt, *J* = 6.6 Hz, *J* = 4.4 Hz, 2H), 5.99–6.03 (m, 1H), 6.12–6.17 (m, 1H), 6.70–6.73 (m, 1H), 8.17 (br s, 1H); ¹³C NMR δ 25.4 (d, *J* = 52.6 Hz), 75.3, 106.9 (d, *J* = 68.7 Hz), 108.8 (d, *J* = 2.3 Hz), 117.8 (d, *J* = 7.6 Hz), 126.0; ESI-MS obsd 142.0693, calcd 142.0692 [(M + H)⁺, M = C₅¹³CH₈N₂O₂].

2-(2-Nitroethyl)(5-¹³C)pyrrole (3-¹³C^γ). Procedure B with **5-¹³C⁵** (1.60 g, 16.7 mmol) afforded the title compound as an orange oil (1.62 g, 69%): ¹H NMR δ 3.31 (t, *J* = 6.8 Hz, 2H), 4.60 (t, *J* = 6.8 Hz, 2H), 6.00–6.03 (m, 1H), 6.13–6.17 (m, 1H), 6.71–6.72 (dm, *J* = 185 Hz, 1H), 8.17 (br s, 1H); ¹³C NMR δ 25.4, 75.3, 106.9, 108.8 (d, *J* = 66.4 Hz), 117.8 (¹³C), 126.0; ESI-MS obsd 142.0694, calcd 142.0692 [(M + H)⁺, M = C₅¹³CH₈N₂O₂].

F. *α,β*-unsaturated ketone-acetals {4}:

1,1-Dimethoxy-4-methyl-3-(2-¹³C)penten-2-one (4-¹³C²). Following a standard procedure,⁷⁷ a round-bottomed flask equipped with a 10-cm Vigreux column and a short-path condenser was charged with bis(trimethylsilyl) sulfate (11.5 g, 47.2 mmol) and K¹³CN (4.30 g, 65.2 mmol). The reaction mixture was heated and distilled at 200 °C. The distillate was collected (40–60 °C at top of column) as a colorless liquid and found (by ¹H NMR spectroscopy) to contain TMS¹³CN (~2.48 g, ~38%) and silyl-containing species. The crude mixture was used without further purification: ¹H NMR δ 0.37 (d, *J* = 2.9 Hz). Following a standard procedure,⁴⁰ the crude mixture (containing ~2.48 g of TMS¹³CN, 24.8 mmol) was combined with trimethyl orthoformate (5.39 mL, 49.2 mmol) in a round-bottomed flask and

treated dropwise with $\text{BF}_3 \cdot \text{OEt}_2$ (0.50 ml, 4.0 mmol) under argon at room temperature. The reaction mixture was stirred for 3 h at room temperature whereupon saturated aqueous NaHCO_3 was added. The aqueous phase was extracted with diethyl ether. The organic phase was washed with saturated brine, dried (Na_2SO_4), and concentrated. The residue was placed in a round-bottom flask and treated dropwise with **6** (123 mL, 61.5 mmol, 0.5 M in THF) under argon at 0 °C, followed by stirring for 2 h at room temperature. The reaction mixture was treated with saturated aqueous NH_4Cl (500 mL) and vigorously stirred for 3 h. The aqueous phase was extracted with diethyl ether. The organic phase was washed with saturated brine, dried (Na_2SO_4), and concentrated. The resulting mixture was chromatographed [silica, hexanes/ethyl acetate (3:1)] to afford a pale-yellow liquid (2.02 g, 19% from K^{13}CN): ^1H NMR δ 1.96 (s, 3H), 2.21 (s, 3H), 3.42 (s, 6H), 4.49 (s, 1H), 6.36–6.38 (m, 1H); ^{13}C NMR δ 21.3 (d, $J = 1.5$ Hz), 28.1 (d, $J = 6.1$ Hz), 54.5 (d, $J = 2.3$ Hz), 104.5 (d, $J = 53.4$ Hz), 119.0 (d, $J = 56.5$ Hz), 160.2, 194.1 (^{13}C); ESI-MS obsd 182.0866, calcd 182.0869 [(M + Na) $^+$, M = $\text{C}_7^{13}\text{CH}_{14}\text{O}_3$].

1,1-Diethoxy-4-methyl-3-(1- ^{13}C)penten-2-one (4Et- $^{13}\text{C}^1$). Following a standard procedure,⁴⁰ a mixture of TMS-CN (1.25 mL, 1.70 mmol) and triethyl (^{13}C)orthoformate (1.50 g, 10.5 mmol) in a round-bottomed flask was treated dropwise with $\text{BF}_3 \cdot \text{OEt}_2$ (0.2 mL, 0.1 mmol) under argon at room temperature. The reaction mixture was stirred for 3 h at room temperature whereupon a solution of saturated aqueous NaHCO_3 was added. The aqueous phase was extracted with diethyl ether. The organic phase was washed with saturated brine, dried (Na_2SO_4), and concentrated. The residue was placed in a round-bottomed flask and treated dropwise under argon with **6** (32 mL, 16 mmol, 0.5 M in THF) at

0 °C, followed by stirring for 2 h at room temperature. The reaction mixture was treated with saturated aqueous NH₄Cl (150 mL) and vigorously stirred for 3 h. The aqueous phase was extracted with diethyl ether. The organic phase was washed with saturated brine, dried (Na₂SO₄), and concentrated. The resulting mixture was chromatographed [silica, hexanes/ethyl acetate (3:1)] to afford a pale-yellow liquid (742 mg, 38%): ¹H NMR δ 1.25 (t, *J* = 7.1 Hz, 6H), 1.95 (d, *J* = 1.1 Hz, 3H), 2.20 (d, *J* = 1.1 Hz, 3H), 3.54–3.74 (m, 4H), 4.58 (d, *J* = 161 Hz 1H), 6.40–6.41 (m, 1H); ¹³C NMR δ 15.1 (d, *J* = 3.1 Hz), 21.2, 28.1, 62.9, 103.1 (¹³C), 119.0 (d, *J* = 13.7 Hz), 159.8, 194.7 (d, *J* = 54.2 Hz); ESI-MS obsd 210.1176, calcd 210.1182 [(M + Na)⁺, M = C₉¹³CH₁₈O₃].

G. Nitrohexanone-pyrroles {2}:

1,1-Dimethoxy-4,4-dimethyl-5-nitro-6-[2-(1-¹⁵N)pyrrolyl]-2-hexanone (2-¹⁵N^{pyrrol}). Following a standard procedure⁴¹ with slight modification, a mixture of 3-¹⁵N^{pyrrol} (1.04 g, 7.38 mmol) and 4-NA (2.33 g, 14.8 mmol) was treated with DBU (3.3 mL, 22 mmol). Ethyl acetate (~2 mL) was added as required to completely dissolve the reaction mixture. The reaction mixture was stirred at room temperature for 16 h, diluted with ethyl acetate, and washed with saturated aqueous NH₄Cl solution and brine. The organic layer was dried (Na₂SO₄) and concentrated. The resulting mixture was chromatographed [silica, hexanes/ethyl acetate (3:1)] to afford a brown solid (1.95 mg, 88%): mp 65–68 °C; ¹H NMR δ 1.14 (s, 3H), 1.23 (s, 3H), 2.55, 2.77 (AB, ²*J* = 18.5 Hz, 2H), 3.01–3.06 (m, 1H), 3.30–3.39 (m, 1H), 3.43 (s, 3H), 3.44 (s, 3H), 4.36 (s, 1H), 5.15 (ABX, ³*J* = 2.2 Hz, ³*J* = 11.7 Hz, 1H), 5.97–5.99 (m, 1H), 6.08–6.11 (m, 1H), 6.65–6.67 (m, 1H), 8.08 (dm, *J* = 95.1 Hz, 1H); ¹³C NMR δ 24.17, 24.26, 26.6 (d, *J* = 2.3 Hz), 36.4, 45.0, 55.1, 94.7, 104.6, 107.2 (d, *J* = 4.6 Hz),

108.6 (d, $J = 3.8$ Hz), 117.7 (d, $J = 13.7$ Hz), 125.9 (d, $J = 13.7$ Hz), 203.6; ^{15}N NMR $\delta - 227.8$; ESI-MS obsd 322.1398, calcd 322.1391 [(M + Na) $^+$, M = C₁₄H₂₂N¹⁵NO₅].

1,1-Dimethoxy-4,4-dimethyl-5-(^{15}N)nitro-6-(2-pyrrolyl)-2-hexanone (2- $^{15}\text{N}^{nitro}$).

The above procedure with 3- $^{15}\text{N}^{nitro}$ (863 mg, 6.12 mmol) afforded the title compound as a brown solid (1.43 g, 78%): mp 73–74 °C; ^1H NMR δ 1.14 (s, 3H), 1.23 (s, 3H), 2.55, 2.77 (AB, $^2J = 18.5$ Hz, 2H), 3.03 (ABX, $^3J = 2.6$ Hz, $^2J = 15.4$ Hz, 1H, $^3J_{\text{NH}} = 6.6$ Hz), 3.36 (ABX, $^3J = 11.7$ Hz, $^2J = 15.4$ Hz, 1H, $^3J_{\text{NH}} = 1.6$ Hz), 3.43 (s, 3H), 3.44 (s, 3H), 4.36 (s, 1H), 5.15 (ABX, $^3J = 2.6$ Hz, $^3J = 11.7$ Hz, 1H, $^2J_{\text{NH}} = 1.2$ Hz), 5.97–5.99 (m, 1H), 6.08–6.11 (m, 1H), 6.65–6.67 (m, 1H), 8.08 (br s, 1H); ^{13}C NMR δ 24.18, 24.28, 26.6, 36.4, 45.0, 55.2, 94.8 (d, $J = 5.3$ Hz), 104.7, 107.2, 108.7, 117.7, 125.9, 203.6; ^{15}N NMR δ 10.3; ESI-MS obsd 300.1572, calcd 300.1567 [(M + H) $^+$, M = C₁₄H₂₂N¹⁵NO₅].

1,1-Dimethoxy-4,4-dimethyl-5-nitro-6-(2-pyrrolyl)-2-(6- ^{13}C)hexanone (2- $^{13}\text{C}^6$).

The above procedure with 3- $^{13}\text{C}^1$ (764 mg, 5.42 mmol) afforded the title compound as a brown solid (1.36 g, 84%): mp 70–72 °C; ^1H NMR δ 1.14 (s, 3H), 1.23 (s, 3H), 2.55, 2.77 (AB, $^2J = 18.5$ Hz, 2H), 3.03 (ABX, $^3J = 2.6$ Hz, $^2J = 15.4$ Hz, 1H, $^1J_{\text{CH}} = 128$ Hz), 3.36 (ABX, $^3J = 11.7$ Hz, $^2J = 15.4$ Hz, 1H, $^1J_{\text{CH}} = 131$ Hz), 3.43 (s, 3H), 3.44 (s, 3H), 4.36 (s, 1H), 5.15 (ABX, $^3J = 2.6$ Hz, $^3J = 11.7$ Hz, 1H, $^3J_{\text{CH}} = 2.6$ Hz), 5.97–5.99 (m, 1H), 6.08–6.11 (m, 1H), 6.65–6.67 (m, 1H), 8.08 (br s, 1H); ^{13}C NMR δ 24.10, 24.18, 26.6 (^{13}C), 36.3, 45.0, 55.1, 94.7 (d, $J = 37.4$ Hz), 104.5, 107.1 (d, $J = 3.8$ Hz), 108.6 (d, $J = 3.1$ Hz), 117.6, 125.9 (d, $J = 51.9$ Hz), 203.6; ESI-MS obsd 322.1457, calcd 322.1454 [(M + Na) $^+$, M = C₁₃¹³CH₂₂N₂O₅].

1,1-Dimethoxy-4,4-dimethyl-5-nitro-6-(2-pyrrolyl)-2-(5- ^{13}C)hexanone (2- $^{13}\text{C}^5$).

The above procedure with **3-¹³C²** (1.41 g, 10.0 mmol) afforded the title compound as a brown solid (2.48 g, 83%): mp 71–73 °C; ¹H NMR δ 1.14 (d, *J* = 4.0 Hz, 3H), 1.23 (d, *J* = 4.0 Hz, 3H), 2.55, 2.77 (AB, ²*J* = 18.5 Hz, ³*J*_{CH} = 3.8 Hz, 2H), 3.03 (m, 1H), 3.36 (ABX, ³*J* = 11.7 Hz, ²*J* = 15.4 Hz, 1H, ²*J*_{CH} = 7.0 Hz), 3.43 (s, 3H), 3.44 (s, 3H), 4.36 (s, 1H), 5.15 (ABX, ³*J* = 2.6 Hz, ³*J* = 11.7 Hz, 1H, ¹*J*_{CH} = 151 Hz), 5.97–5.99 (m, 1H), 6.08–6.11 (m, 1H), 6.65–6.67 (m, 1H), 8.08 (br s, 1H); ¹³C NMR δ 24.16, 24.26, 26.6 (d, *J* = 36.6 Hz), 36.4 (d, *J* = 32.8 Hz), 45.0, 55.1, 94.8 (¹³C), 104.6, 107.2, 108.6, 117.7, 125.9, 203.6; ESI-MS obsd 322.1444, calcd 322.1454 [(M + Na)⁺, M = C₁₃¹³CH₂₂N₂O₅].

1,1-Dimethoxy-4,4-dimethyl-5-nitro-6-(2-pyrrolyl)-2-(2-¹³C)hexanone (2-¹³C²).

The above procedure with **3-NA** (1.29 g, 9.21 mmol) and **4-¹³C²** (1.22 g, 7.67 mmol) afforded the title compound as a brown solid (1.50 g, 65%): mp 66–68 °C; ¹H NMR δ 1.14 (s, 3H), 1.23 (s, 3H), 2.55, 2.77 (AB, ²*J* = 18.5 Hz, 2H, ²*J*_{CH} = 6.0 Hz), 3.03 (ABX, ³*J* = 2.6 Hz, ²*J* = 15.4 Hz, 1H), 3.36 (ABX, ³*J* = 11.7 Hz, ²*J* = 15.4 Hz, 1H), 3.43 (s, 3H), 3.44 (s, 3H), 4.36 (s, 1H), 5.15 (ABX, ³*J* = 2.6 Hz, ³*J* = 11.7 Hz, 1H), 5.97–5.99 (m, 1H), 6.08–6.11 (m, 1H), 6.65–6.67 (m, 1H), 8.08 (br s, 1H); ¹³C NMR δ 24.04 (d, *J* = 1.5 Hz), 24.12, (d, *J* = 2.3 Hz), 26.6, 36.3, (d, *J* = 1.5 Hz), 44.9, (d, *J* = 39.7 Hz), 55.0, (d, *J* = 3.1 Hz), 94.7, 104.5 (d, *J* = 53.4 Hz), 107.0, 108.5, 117.6, 125.9, 203.6 (¹³C); ESI-MS obsd 300.1630, calcd 300.1635 [(M + H)⁺, M = C₁₃¹³CH₂₂N₂O₅].

1,1-Dimethoxy-4,4-dimethyl-5-nitro-6-[2-(2-¹³C)pyrrolyl]-2-hexanone (2-¹³C^α).

The above procedure with **3-¹³C^α** (1.70 g, 12.1 mmol) afforded the title compound as a brown solid (3.26 g, 91%): mp 70–72 °C; ¹H NMR δ 1.14 (s, 3H), 1.23 (s, 3H), 2.55, 2.77

(AB, $^2J = 18.5$ Hz, 2H), 3.03 (ABX, $^3J = 2.6$ Hz, $^2J = 15.5$ Hz, 1H, $^2J_{\text{CH}} = 7.1$ Hz), 3.36 (m, 1H), 3.43 (s, 3H), 3.44 (s, 3H), 4.36 (s, 1H), 5.15 (ABX, $^3J = 2.6$ Hz, $^3J = 11.7$ Hz, 1H, $^3J_{\text{CH}} = 2.6$ Hz), 5.96–6.00 (m, 1H), 6.08–6.12 (m, 1H), 6.64–6.68 (m, 1H), 8.08 (br s, 1H); ^{13}C NMR δ 24.20, 24.30, 26.6 (d, $^2J_{\text{CC}} = 52.6$ Hz), 36.4, 45.0, 55.2, 94.8, 104.7, 106.9, 108.9 (d, $J = 2.3$ Hz), 117.7 (d, $J = 7.6$ Hz), 126.0 (^{13}C), 203.6; ESI-MS obsd 300.1634, calcd 300.1635 [(M + H) $^+$, M = C $_{13}^{13}$ CH $_{22}$ N $_2$ O $_5$].

1,1-Dimethoxy-4,4-dimethyl-5-nitro-6-[2-(5- ^{13}C)pyrrolyl]-2-hexanone (2- $^{13}\text{C}^{\gamma}$).

The above procedure with 3- $^{13}\text{C}^{\gamma}$ (1.60 g, 11.3 mmol) afforded the title compound as a brown solid (3.20 g, 95%): mp 70–74 °C; ^1H NMR δ 1.14 (s, 3H), 1.23 (s, 3H), 2.55, 2.77 (AB, $^2J = 18.5$ Hz, 2H), 3.03 (ABX, $^3J = 2.6$ Hz, $^2J = 15.5$ Hz, 1H), 3.36 (m, 1H), 3.43 (s, 3H), 3.44 (s, 3H), 4.36 (s, 1H), 5.15 (ABX, $^3J = 2.6$ Hz, $^3J = 11.7$ Hz, 1H), 5.96–6.00 (m, 1H), 6.08–6.12 (m, 1H), 6.64–6.68 (dm, $J = 185$ Hz, 1H), 8.08 (br s, 1H); ^{13}C NMR δ 24.20, 24.30, 26.6, 36.4, 45.0, 55.2, 94.8, 104.7, 106.9, 117.7 (^{13}C), 203.6; ESI-MS obsd 300.1638, calcd 300.1635 [(M + H) $^+$, M = C $_{13}^{13}$ CH $_{22}$ N $_2$ O $_5$].

1,1-Diethoxy-4,4-dimethyl-5-nitro-6-(2-pyrrolyl)-2-hexanone (2Et-NA).

The above procedure with 3-NA (872 mg, 4.69 mmol) and 4Et-NA (656 mg, 3.53 mmol) afforded the title compound as a yellow liquid (1.22 g, 80%): ^1H NMR δ 1.15 (s, 3H), 1.22 (s, 3H), 1.25 (t, $J = 7.0$ Hz, 6H), 2.61, 2.78 (AB, $^2J = 18.3$ Hz, 2H), 3.04 (ABX, $^3J = 2.2$ Hz, $^2J = 15.4$ Hz, 1H), 3.36 (ABX, $^3J = 11.7$ Hz, $^2J = 15.4$ Hz, 1H), 3.54–3.62 (m, 2H), 3.76–3.77 (m, 2H), 4.47 (s, 1H), 5.17 (ABX, $^3J = 2.6$ Hz, $^3J = 11.8$ Hz, 1H), 5.97–5.99 (m, 1H), 6.08–6.11 (m, 1H), 6.65–6.67 (m, 1H), 8.07 (br s, 1H); ^{13}C NMR δ 15.1, 24.1, 24.4, 26.7, 36.5,

44.6, 63.8, 94.9, 103.2, 107.3, 108.7, 117.7, 204.1; ESI-MS obsd 349.1735, calcd 349.1734 [(M + Na)⁺, M = C₁₆H₂₆N₂O₅].

1,1-Diethoxy-4,4-dimethyl-5-nitro-6-(2-pyrrolyl)-2-(1-¹³C)hexanone (2Et-¹³C¹).

The above procedure with **3-NA** (634 mg, 4.53 mmol) and **4Et-¹³C¹** (706 mg, 3.78 mmol) afforded the title compound as a yellow liquid (928 mg, 75%): ¹H NMR δ 1.15 (s, 3H), 1.22 (s, 3H), 1.25 (t, *J* = 7.0 Hz, 6H), 2.61, 2.78 (AB, ²*J* = 18.3 Hz, 2H), 3.04 (ABX, ³*J* = 2.2 Hz, ²*J* = 15.4 Hz, 1H), 3.36 (ABX, ³*J* = 11.7 Hz, ²*J* = 15.4 Hz, 1H), 3.54–3.62 (m, 2H), 3.76–3.77 (m, 2H), 4.47 (d, *J* = 162 Hz, 1H), 5.17 (ABX, ³*J* = 2.6 Hz, ³*J* = 11.8 Hz, 1H), 5.97–5.99 (m, 1H), 6.08–6.11 (m, 1H), 6.65–6.67 (m, 1H), 8.07 (br s, 1H); ¹³C NMR δ 15.1, 24.1, 24.4, 26.7, 36.5, 44.6 (d, *J* = 11.4 Hz), 63.8, 94.9, 103.2 (¹³C), 107.3, 108.7, 117.7, 126.0, 204.1 (d, *J* = 54.2 Hz); ESI-MS obsd 350.1759, calcd 350.1767 [(M + Na)⁺, M = C₁₅¹³CH₂₆N₂O₅].

H. Synthesis of dihydrodipyrin–acetals {1}:

2,3-Dihydro-1-(1,1-dimethoxymethyl)-3,3-dimethyl(11-¹⁵N)dipyrin (1-¹⁵N¹¹)

Following a standard procedure³⁴ with increased amount of buffer (see the following section), a solution of **2-¹⁵N^{pyrrol}** (1.95 g, 6.52 mmol) in freshly distilled THF (15 mL) was treated with NaOMe (1.76 g, 32.6 mmol) at 0 °C. The reaction mixture was stirred and degassed with argon for 30 min (first flask). In a second flask, TiCl₃ (32.6 mL, 20 wt % TiCl₃ in 3% HCl, 55.6 mmol), THF (67 mL) and NH₄OAc (50.2 g, 652 mmol) were combined. The mixture was degassed with argon for 30 min. The mixture in the first flask was transferred via a cannula to the buffered TiCl₃ mixture. The resulting mixture was stirred at room temperature for 16 h. Then the mixture was quenched by addition of saturated aqueous NaHCO₃ and extracted with ethyl acetate. The organic extract was washed

with water, dried (NaSO₄), and concentrated. Chromatography (3 x 30 cm, ~80 g of neutral alumina, CH₂Cl₂) afforded a dark brown oil (939 mg, 58%): ¹H NMR δ 1.21 (s, 6H), 2.61 (s, 2H), 3.45 (s, 6H), 5.02 (s, 1H), 5.88 (d, *J* = 3.7 Hz, 1H), 6.15–6.16 (m, 2H), 6.83–6.85 (m, 1H), 10.65 (dm, *J* = 97.3, 1H); ¹³C NMR δ 29.1, 40.0, 48.1, 54.6, 102.8, 107.4, 108.4 (d, *J* = 3.1 Hz), 109.1 (d, *J* = 4.6 Hz), 119.4 (d, *J* = 13.0 Hz), 130.6 (d, *J* = 13.7 Hz), 159.2, 173.8; ¹⁵N NMR δ –229.0; ESI-MS obsd 272.1385, calcd 272.1387 [(M + Na)⁺, M = C₁₄H₂₀N¹⁵NO₂].

2,3-Dihydro-1-(1,1-dimethoxymethyl)-3,3-dimethyl(10-¹⁵N)dipyrrin (1-¹⁵N¹⁰)

The above procedure with 2-¹⁵N^{nitro} (1.43 g, 4.78 mmol) afforded the title compound as a dark brown oil (487 mg, 41%): ¹H NMR δ 1.20 (s, 6H), 2.60 (d, *J* = 2.2 Hz, 2H), 3.44 (s, 6H), 5.01 (s, 1H), 5.87 (d, *J* = 5.9 Hz 1H), 6.15–6.16 (m, 2H), 6.83–6.85 (m, 1H), 10.65 (br s, 1H); ¹³C NMR δ 29.0, 39.9, 48.0 (d, *J* = 1.5 Hz), 54.5, 102.7 (d, *J* = 9.2 Hz), 107.4 (d, *J* = 3.8 Hz), 108.4, 109.1, 119.3, 130.5, 159.1 (d, *J* = 1.5 Hz), 173.7 (d, *J* = 5.3 Hz); ¹⁵N NMR δ –58.3; ESI-MS obsd 272.1390, calcd 272.1387 [(M + Na)⁺, M = C₁₄H₂₀N¹⁵NO₂].

2,3-Dihydro-1-(1,1-dimethoxymethyl)-3,3-dimethyl(1-¹³C)dipyrrin (1-¹³C¹) The above procedure with 2-¹³C² (1.50 g, 5.02 mmol) afforded the title compound as a dark brown oil (720 mg, 58%): ¹H NMR δ 1.21 (s, 6H), 2.61 (d, *J* = 6.2 Hz, 2H), 3.45 (s, 6H), 5.01 (s, 1H), 5.88 (s, 1H), 6.15–6.16 (m, 2H), 6.83–6.85 (m, 1H), 10.65 (br s, 1H); ¹³C NMR δ 29.1, 48.1 (d, *J* = 35.1 Hz), 54.5, 102.8 (d, *J* = 64.1 Hz), 107.4 (d, *J* = 9.9 Hz), 108.5, 109.1, 119.4, 173.8 (¹³C); ESI-MS obsd 250.1632, calcd 250.1631 [(M + H)⁺, M = C₁₃¹³CH₂₀N₂O₂].

2,3-Dihydro-1-(1,1-dimethoxymethyl)-3,3-dimethyl(4-¹³C)dipyrrin (1-¹³C⁴) The above procedure with **2-¹³C⁵** (2.47 g, 8.33 mmol) afforded the title compound as a dark brown oil (1.16 mg, 56%): ¹H NMR δ 1.21 (d, *J* = 4.0 Hz, 6H), 2.61 (s, 2H), 3.45 (s, 6H), 5.01 (s, 1H), 5.88 (s, 1H), 6.15–6.16 (m, 2H), 6.83–6.85 (m, 1H), 10.65 (br s, 1H); ¹³C NMR δ 29.1, 48.1 (d, *J* = 4.6 Hz), 54.6, 102.8 (d, *J* = 9.9 Hz), 107.4 (d, *J* = 82.4 Hz), 108.5, 109.1 (d, *J* = 6.1 Hz), 119.4, 159.2 (¹³C); ESI-MS obsd 250.1631, calcd 250.1631 [(M + H)⁺, M = C₁₃¹³CH₂₀N₂O₂].

2,3-Dihydro-1-(1,1-dimethoxymethyl)-3,3-dimethyl(5-¹³C)dipyrrin (1-¹³C⁵) The above procedure with **2-¹³C⁶** (1.69 g, 5.65 mmol) afforded the title compound as a dark brown oil (463 mg, 33%): ¹H NMR δ 1.20 (s, 6H), 2.61 (s, 2H), 3.45 (s, 6H), 5.01 (s, 1H), 5.88 (d, *J* = 153 Hz, 1H), 6.15–6.16 (m, 2H), 6.83–6.85 (m, 1H), 10.64 (br s, 1H); ¹³C NMR δ 29.1, 40.0 (d, *J* = 5.3 Hz), 48.1, 54.5, 102.8, 107.4 (¹³C), 108.4 (d, *J* = 5.3 Hz), 109.1 (d, *J* = 4.6 Hz), 119.4, 130.6 (d, *J* = 66.4 Hz), 159.2 (d, *J* = 81.6 Hz), 173.8 (d, *J* = 9.2 Hz); ESI-MS obsd 272.1438, calcd 272.1451 [(M + Na)⁺, M = C₁₃¹³CH₂₀N₂O₂].

2,3-Dihydro-1-(1,1-dimethoxymethyl)-3,3-dimethyl(6-¹³C)dipyrrin (1-¹³C⁶) The above procedure with **2-¹³C^α** (1.00 g, 3.34 mmol) afforded the title compound as a dark brown oil (354 mg, 43%): ¹H NMR δ 1.21 (s, 6H), 2.61 (s, 2H), 3.45 (s, 6H), 5.01 (s, 1H), 5.87–5.88 (m, 1H), 6.15–6.17 (m, 2H), 6.83–6.85 (m, 1H), 10.65 (br s, 1H); ¹³C NMR δ 29.1, 40.0, 48.1, 54.5, 102.8, 107.4 (d, *J* = 66.4 Hz), 108.4, 109.1 (d, *J* = 67.1 Hz), 119.4 (d, *J* = 6.9 Hz), 130.6 (¹³C), 173.8; ESI-MS obsd 250.1628, calcd 250.1631 [(M + H)⁺, M = C₁₃¹³CH₂₀N₂O₂].

2,3-Dihydro-1-(1,1-dimethoxymethyl)-3,3-dimethyl(9-¹³C)dipyrin (1-¹³C⁹) The above procedure with **2-¹³C^γ** (1.50 g, 5.02 mmol) afforded the title compound as a dark brown oil (634 mg, 51%): ¹H NMR δ 1.21 (s, 6H), 2.61 (s, 2H), 3.45 (s, 6H), 5.01 (s, 1H), 5.88 (s, 1H), 6.15–6.16 (m, 2H), 6.83–6.85 (dm, *J* = 184 Hz, 1H), 10.65 (br s, 1H); ¹³C NMR δ 29.1, 40.0, 48.1, 54.6, 102.8, 107.4, 109.1, 119.4 (¹³C); ESI-MS obsd 250.1630, calcd 250.1631 [(M + H)⁺, M = C₁₃¹³CH₂₀N₂O₂].

2,3-Dihydro-1-(1,1-diethoxymethyl)-3,3-dimethyldipyrin (1Et-NA). The above procedure with **2Et-NA** (928 mg, 2.85 mmol) afforded the title compound as a dark brown oil (256 mg, 32%): ¹H NMR δ 1.20 (s, 6H), 1.26 (t, *J* = 7.1 Hz, 6H), 2.64 (s, 2H), 3.56–3.63 (m, 2H), 3.72–3.80 (m, 2H), 5.15 (s, 1H), 5.87 (s, 1H), 6.14–6.17 (m, 2H), 6.83–6.84 (m, 1H), 10.67 (br s, 1H); ¹³C NMR δ 15.2, 29.1, 40.0, 47.8, 62.9, 100.9, 107.1, 108.45, 108.97, 119.2, 130.8, 159.4, 174.8; ESI-MS obsd 299.1732, calcd 299.1730 [(M + Na)⁺, M = C₁₆H₂₄N₂O₂].

2,3-Dihydro-1-[1,1-diethoxy(¹³C)methyl]-3,3-dimethyldipyrin (1Et-¹³C^{ac}). The above procedure with **2Et-¹³C¹** (900 mg, 2.75 mmol) afforded the title compound as a dark brown oil (305 mg, 40%): ¹H NMR δ 1.21 (s, 6H), 1.26 (t, *J* = 7.1 Hz, 6H), 2.64 (s, 2H), 3.55–3.64 (m, 2H), 3.72–3.80 (m, 2H), 5.15 (d, *J* = 161 Hz, 1H), 5.87 (s, 1H), 6.14–6.17 (m, 2H), 6.83–6.84 (m, 1H), 10.67 (br s, 1H); ¹³C NMR δ 15.2, 29.1, 40.0, 62.9, 100.9 (¹³C), 107.1, 108.45, 108.97, 119.2, 130.8; ESI-MS obsd 278.1942, calcd 278.1194 [(M + H)⁺, M = C₁₅¹³CH₂₄N₂O₂].

I. Bacteriochlorins {H₂BC}: Note: employing anhydrous CH₃CN instead of HPLC-

grade CH₃CN as solvent resulted in higher yields (9–16% versus 7–8%).

8,8,18,18-Tetramethylbacteriochlorin (H₂BC-NA). Following a standard procedure,³⁶ a solution of **1-NA** (487 mg, 1.96 mmol, 5.0 mM) in HPLC-grade CH₃CN (390 mL) was treated dropwise with neat BF₃·OEt₂ (2.49 mL, 19.8 mmol, 50 mM) at room temperature. The reaction was allowed to proceed at room temperature for 16 h. TEA (3 mL) was added to the reaction mixture. The reaction mixture was then concentrated. Chromatography of the residue [silica, hexanes/CH₂Cl₂ (2:1)] afforded a green solid (28.4 mg, 8%): ¹H NMR δ –2.38 (br s, 2H), 1.97 (s, 12H), 4.47 (s, 4H), 8.72–8.74 (m, 2H), 8.73 (s, 2H), 8.76 (dd, *J* = 4.0 Hz, *J* = 1.8 Hz, 2H), 8.83 (s, 2H); ¹³C NMR δ 31.1, 46.0, 51.4, 96.5, 98.7, 121.73, 121.84, 135.3, 136.2, 157.6; ESI-MS obsd 371.2223, calcd 371.2230 [(M + H)⁺, M = C₂₄H₂₆N₄]; λ_{abs} (toluene) 340, 365, 489, 713 nm.

8,8,18,18-Tetramethyl(21,23-¹⁵N₂)bacteriochlorin (H₂BC-¹⁵N^{21,23}). The above procedure with **1-¹⁵N¹¹** (934 mg, 3.75 mmol) afforded the title compound as a green solid (46.7 mg, 7%): ¹H NMR δ –2.39 (dt, *J* = 99 Hz, *J* = 2.0 Hz, 2H), 1.97 (s, 12H), 4.47 (s, 4H), 8.72–8.74 (m, 2H), 8.73 (d, *J* = 4.0 Hz, 2H), 8.76–8.78 (m, 2H), 8.84 (d, *J* = 4.8 Hz, 2H); ¹³C NMR δ 31.1, 46.0, 51.4, 96.5, 98.6, 121.73 (d, *J* = 3.1 Hz), 121.84 (d, *J* = 3.8 Hz); ¹⁵N NMR δ –249.3; ESI-MS obsd 373.2179, calcd 373.2171 [(M + H)⁺, M = C₂₄H₂₆N₂¹⁵N₂]; λ_{abs} (toluene) 340, 365, 489, 713 nm.

8,8,18,18-Tetramethyl(22,24-¹⁵N₂)bacteriochlorin (H₂BC-¹⁵N^{22,24}). The above procedure with **1-¹⁵N¹⁰** (487 mg, 1.96 mmol) afforded the title compound as a green solid (28.4 mg, 8%): ¹H NMR δ –2.39 (br s, 2H), 1.97 (s, 12H), 4.47 (s, 4H), 8.72–8.74 (m, 4H),

8.76 (dd, $J = 4.4$ Hz, $J = 2.0$ Hz, 2H) 8.83 (d, $J = 4.8$ Hz, 2H); ^{13}C NMR δ 31.1, 51.4, 96.5 (d, $J = 3.8$ Hz), 98.6 (d, $J = 4.6$ Hz), 121.72, 121.83; ^{15}N NMR δ -82.0 ; ESI-MS obsd 372.2093, calcd 372.2093 (M^+ , $\text{M} = \text{C}_{24}\text{H}_{26}\text{N}_2^{15}\text{N}_2$); λ_{abs} (toluene) 340, 365, 489, 713 nm.

8,8,18,18-Tetramethyl(1,11- $^{13}\text{C}_2$)bacteriochlorin ($\text{H}_2\text{BC-}^{13}\text{C}^{1,11}$). The above procedure with **1- $^{13}\text{C}^6$** (460 mg, 1.85 mmol) afforded the title compound as a green solid (32.2 mg, 9%): ^1H NMR δ -2.38 (br s, 2H), 1.97 (s, 12H), 4.47 (s, 4H), 8.71–8.78 (m, 4H), 8.73 (d, $J = 2.2$ Hz, 2H), 8.84 (s, 2H); ^{13}C NMR δ 31.1, 46.0 (d, $J = 3.8$ Hz), 51.4, 96.5 (d, $J = 70.2$ Hz), 98.6, 121.72, 121.82 (d, $J = 58.0$ Hz), 135.3, 136.2 (^{13}C); ESI-MS obsd 373.2280, calcd 373.2297 [$(\text{M} + \text{H})^+$, $\text{M} = \text{C}_{22}^{13}\text{C}_2\text{H}_{26}\text{N}_4$]; λ_{abs} (toluene) 340, 365, 489, 713 nm.

8,8,18,18-Tetramethyl(4,14- $^{13}\text{C}_2$)bacteriochlorin ($\text{H}_2\text{BC-}^{13}\text{C}^{4,14}$). The above procedure with **1- $^{13}\text{C}^9$** (615 mg, 2.47 mmol) afforded the title compound as a green solid (57.5 mg, 13%): ^1H NMR δ -2.38 (br s, 2H), 1.98 (s, 12H), 4.48 (s, 4H), 8.72–8.79 (m, 4H), 8.74 (s, 2H), 8.83 (d, $J = 2.2$ Hz, 2H); ^{13}C NMR δ 31.1, 46.0, 51.4 (d, $J = 3.8$ Hz), 96.5, 98.6 (d, $J = 70.2$ Hz), 121.71 (d, $J = 58.0$ Hz), 121.83, 135.3 (^{13}C), 136.2; ESI-MS obsd 372.2227, calcd 372.2219 (M^+ , $\text{M} = \text{C}_{22}^{13}\text{C}_2\text{H}_{26}\text{N}_4$); λ_{abs} (toluene) 340, 365, 489, 713 nm.

8,8,18,18-Tetramethyl(6,16- $^{13}\text{C}_2$)bacteriochlorin ($\text{H}_2\text{BC-}^{13}\text{C}^{6,16}$). The above procedure with **1- $^{13}\text{C}^1$** (720 mg, 2.89 mmol) afforded the title compound as a green solid (74.9 mg, 14%): ^1H NMR δ -2.38 (br s, 2H), 1.98 (s, 12H), 4.48 (d, $J = 5.1$ Hz, 4H), 8.72–8.74 (m, 2H), 8.73 (s, 2H), 8.77 (dd, $J = 4.0$ Hz, $J = 1.8$ Hz, 2H), 8.84 (s, 2H); ^{13}C NMR δ 31.1, 51.4 (d, $J = 38.2$ Hz), 96.5 (d, $J = 8.4$ Hz), 98.6 (d, $J = 74.0$ Hz), 121.74 (d, $J = 6.1$ Hz),

121.84, 157.6 (^{13}C); ESI-MS obsd 373.2291, calcd 373.2297 [(M + H) $^+$, M = C₂₂¹³C₂H₂₆N₄]; λ_{abs} (toluene) 340, 365, 489, 713 nm.

8,8,18,18-Tetramethyl(9,19- $^{13}\text{C}_2$)bacteriochlorin ($\text{H}_2\text{BC-}^{13}\text{C}^{9,19}$). The above procedure with **1- $^{13}\text{C}^4$** (1.16 g, 4.66 mmol) afforded the title compound as a green solid (76.3 mg, 9%): ^1H NMR δ -2.38 (br s, 2H), 1.97 (d, J = 3.7 Hz, 12H), 4.47 (s, 4H), 8.72–8.74 (m, 2H), 8.73 (s, 2H), 8.77 (dd, J = 4.4 Hz, J = 1.8 Hz, 2H), 8.84 (s, 2H); ^{13}C NMR δ 31.1, 51.4 (d, J = 5.3 Hz), 96.5 (d, J = 74.5 Hz), 98.7 (d, J = 8.4 Hz), 121.73, 121.84 (d, J = 6.1 Hz), 135.3, 169.6 (^{13}C); ESI-MS obsd 373.2294, calcd 373.2297 [(M + H) $^+$, M = C₂₂¹³C₂H₂₆N₄]; λ_{abs} (toluene) 340, 365, 489, 713 nm.

8,8,18,18-Tetramethyl(10,20- $^{13}\text{C}_2$)bacteriochlorin ($\text{H}_2\text{BC-}^{13}\text{C}^{10,20}$). The above procedure with **1- $^{13}\text{C}^5$** (463 mg, 1.86 mmol) afforded the title compound as a green solid (54.8 mg, 16%): ^1H NMR δ -2.38 (br s, 2H), 1.97 (s, 12H), 4.47 (s, 4H), 8.73 (dd, J = 4.4 Hz, J = 1.8 Hz, 2H), 8.73 (d, J = 154 Hz, 2H), 8.75–8.78 (m, 2H), 8.83 (s, 2H); ^{13}C NMR δ 31.1, 54.4, 96.5 (^{13}C), 98.7, 121.73 (d, J = 4.6 Hz), 121.84 (d, J = 5.3 Hz); ESI-MS obsd 373.2297, calcd 373.2297 [(M + H) $^+$, M = C₂₂¹³C₂H₂₆N₄]; λ_{abs} (toluene) 340, 365, 489, 713 nm.

8,8,18,18-Tetramethylbacteriochlorin ($\text{H}_2\text{BC-NA}$) and 5-Ethoxy-8,8,18,18-tetramethylbacteriochlorin (EtOBC-NA) from **1Et.** The above procedure was carried out with **1Et** (256 mg, 928 μmol , 5.0 mM). Chromatography [silica, hexanes/ CH_2Cl_2 (1:1)] afforded two green bands, which in order of elution consisted of **H₂BC-NA** (9.2 mg, 5%) and **EtOBC-NA** (3.8 mg, 2%). The characterization data for **H₂BC-NA** were consistent with

those described above. Data for **EtOBC-NA**: ^1H NMR δ -2.27 (s, 1H), -2.14 (s, 1H), 1.84 (t, $J = 7.0$ Hz, 3H), 1.95 (s, 6H), 1.96 (s, 6H), 4.41 (s, 2H), 4.42 (s, 2H), 4.64 (q, $J = 7.0$ Hz, 2H), 8.66–8.69 (m, 3H), 8.66 (s, 1H), 8.70 (s, 1H), 8.74 (dd, $J = 4.6$ Hz, $J = 2.0$ Hz, 1H), 8.92 (dd, $J = 4.4$ Hz, $J = 1.8$ Hz, 1H); ESI-MS obsd 415.2494, calcd 415.2492 [(M + H)⁺, M = C₂₆H₃₀N₄O]; λ_{abs} (CH₂Cl₂) 344, 354, 366, 500, 710 nm.

8,8,18,18-Tetramethyl(5,15-¹³C₂)bacteriochlorin (H₂BC-¹³C^{5,15}). The above procedure with **1Et-¹³C^{acc}** (305 mg, 933 μmol) afforded the title compound as a green solid (5.8 mg, 3%); ^1H NMR δ -2.39 (br s, 2H), 1.97 (s, 12H), 4.47 (s, 4H), 8.72–8.84 (m, 2H), 8.73 (s, 2H), 8.77 (dd, $J = 4.4$ Hz, $J = 2.0$ Hz, 2H), 8.83 (d, $J = 155$ Hz, 2H); ^{13}C NMR δ 31.1, 51.4 (d, $J = 6.9$ Hz), 96.5, 98.7 (^{13}C), 121.73 (d, $J = 5.3$ Hz), 121.84 (d, $J = 4.6$ Hz); ESI-MS obsd 373.2292, calcd 373.2297 [(M + H)⁺, M = C₂₂¹³C₂H₂₆N₄]; λ_{abs} (toluene) 340, 365, 489, 713 nm.

J. Zinc bacteriochlorins {ZnBC}:

Zn(II)-8,8,18,18-tetramethyl(21,23-¹⁵N₂)bacteriochlorin (ZnBC-¹⁵N^{21,23}).

Following a standard procedure,³⁵ a solution of **H₂BC-¹⁵N^{21,23}** (5.8 mg, 16 μmol , 4 mM) in freshly distilled THF (4 mL) was treated with NaH (54 mg, 2.3 mmol, 150 equiv, 95%) and Zn(OTf)₂ (176 mg, 0.484 mmol, 30 equiv). The reaction mixture was heated at 60 °C for 16 h. The reaction mixture was diluted with CH₂Cl₂ and washed with saturated aqueous NaHCO₃ solution. The organic layer was dried (Na₂SO₄) and filtered. The filtrate was concentrated. The crude solid was treated with hexanes, sonicated in a benchtop sonication bath, centrifuged, and the supernatant discarded. A single repetition of the hexanes treatment

afforded a dark red solid (2.4 mg, 35%): ^1H NMR (THF- d_8) δ 1.97 (s, 12H), 4.46 (s, 4H), 8.60–8.62 (m, 4H), 8.64–8.66 (m, 4H); ESI-MS obsd 434.1212, calcd 434.1228 ($\text{C}_{24}\text{H}_{24}\text{N}_2^{15}\text{N}_2\text{Zn}$); λ_{abs} (toluene) 336, 375, 514, 723 nm. (A peak ~ 433 m/z was found in the ESI-mass spectrum yet did not match the exact mass of a bacteriochlorin bearing one ^{15}N atom. Given that the ESI-mass spectrum of the corresponding **CuBC- $^{15}\text{N}^{21,23}$** does not show a such peak, we consider no isotopic loss in **ZnBC- $^{15}\text{N}^{21,23}$** .)

Zn(II)-8,8,18,18-tetramethyl(22,24- $^{15}\text{N}_2$)bacteriochlorin (ZnBC- $^{15}\text{N}^{22,24}$). The above procedure with **H₂BC- $^{15}\text{N}^{22,24}$** (5.6 mg, 15 μmol) afforded the title compound as a dark red solid (4.6 mg, 71%): ^1H NMR (THF- d_8) δ 1.98 (s, 12H), 4.46 (s, 4H), 8.60–8.62 (m, 4H), 8.64–8.66 (m, 4H); ESI-MS obsd 434.1235, calcd 434.1228 ($\text{C}_{24}\text{H}_{24}\text{N}_2^{15}\text{N}_2\text{Zn}$); λ_{abs} (toluene) 336, 375, 514, 723 nm.

Zn(II)-8,8,18,18-tetramethyl(1,11- $^{13}\text{C}_2$)bacteriochlorin (ZnBC- $^{13}\text{C}^{1,11}$). The above procedure with **H₂BC- $^{13}\text{C}^{5,15}$** (3.7 mg, 10 μmol) afforded the title compound as a dark red solid (3.2 mg, 73%): ^1H NMR (THF- d_8) δ 1.97 (s, 12H), 4.46 (s, 4H), 8.59–8.66 (m, 8H); ESI-MS obsd 434.1362, calcd 434.1354 ($\text{C}_{22}^{13}\text{C}_2\text{H}_{24}\text{N}_4\text{Zn}$); λ_{abs} (toluene) 336, 375, 514, 723 nm.

Zn(II)-8,8,18,18-tetramethyl(4,14- $^{13}\text{C}_2$)bacteriochlorin (ZnBC- $^{13}\text{C}^{4,14}$). The above procedure with **H₂BC- $^{13}\text{C}^{4,14}$** (3.7 mg, 10 μmol) afforded the title compound as a dark red solid (2.2 mg, 50%): ^1H NMR (THF- d_8) δ 1.97 (s, 12H), 4.46 (br s, 4H), 8.59–8.67 (m, 6H), 8.60 (s, 2H); ESI-MS obsd 434.1359, calcd 434.1354 ($\text{C}_{22}^{13}\text{C}_2\text{H}_{24}\text{N}_4\text{Zn}$); λ_{abs} (toluene) 336, 375, 514, 723 nm.

Zn(II)-8,8,18,18-tetramethyl(5,15-¹³C₂)bacteriochlorin (ZnBC-¹³C^{5,15}). The above procedure with **H₂BC-¹³C^{5,15}** (2.9 mg, 7.8 μmol) afforded the title compound as a dark red solid (2.8 mg, 83%): ¹H NMR (THF-*d*₈) δ 1.98 (s, 12H), 4.46 (s, 4H), 8.60–8.62 (m, 4H), 8.64 (d, *J* = 152.5 Hz 2H), 8.65 (d, *J* = 4.1 Hz, 2H); ESI-MS obsd 434.1355, calcd 434.1354 (C₂₂¹³C₂H₂₄N₄Zn); λ_{abs} (toluene) 336, 375, 514, 723 nm.

Zn(II)-8,8,18,18-tetramethyl(6,16-¹³C₂)bacteriochlorin (ZnBC-¹³C^{6,16}). The above procedure with **H₂BC-¹³C^{6,16}** (5.8 mg, 16 μmol) afforded the title compound as a dark red solid (4.8 mg, 69%): ¹H NMR (THF-*d*₈) δ 1.97 (s, 12H), 4.46 (br s, 4H), 8.60–8.62 (m, 4H), 8.64–8.66 (m, 4H); ESI-MS obsd 434.1355, calcd 434.1354 (C₂₂¹³C₂H₂₄N₄Zn); λ_{abs} (toluene) 336, 375, 514, 723 nm.

Zn(II)-8,8,18,18-tetramethyl(9,19-¹³C₂)bacteriochlorin (ZnBC-¹³C^{9,19}). The above procedure with **H₂BC-¹³C^{9,19}** (5.8 mg, 16 μmol) afforded the title compound as a dark red solid (2.8 mg, 40%): ¹H NMR (THF-*d*₈) δ 1.97–1.98 (m, 12H), 4.46 (br s, 4H), 8.60–8.62 (m, 4H), 8.64–8.66 (m, 4H); ESI-MS obsd 434.1362, calcd 434.1354 (C₂₂¹³C₂H₂₄N₄Zn); λ_{abs} (toluene) 336, 375, 514, 723 nm.

Zn(II)-8,8,18,18-tetramethyl(10,20-¹³C₂)bacteriochlorin (ZnBC-¹³C^{10,20}). The above procedure with **H₂BC-¹³C^{10,20}** (5.8 mg, 16 μmol) afforded the title compound as a dark red solid (4.1 mg, 59%): ¹H NMR (THF-*d*₈) δ 1.97 (s, 12H), 4.46 (s, 4H), 8.60 (d, ¹*J*_{CH} = 151.4 Hz, 2H), 8.61 (d, *J* = 4.4 Hz, 2H), 8.64 (s, 2H), 8.65 (d, *J* = 4.4 Hz, 2H); ESI-MS obsd 434.1345, calcd 434.1354 (C₂₂¹³C₂H₂₄N₄Zn); λ_{abs} (toluene) 336, 375, 514, 723 nm.

K. Copper bacteriochlorins {CuBC}: The reaction is sensitive to moisture. In the

case that reaction was not complete in 16 h, a supplement of NaH (150 equiv) or LDA (10 equiv) was added and the reaction mixture was heated at 60 °C for a further 8–16 h. Use of Cu(OAc)₂ dried in an oven for 36 h at 100 °C before using significantly shortened the reaction time (usually <16 h). When LDA was used, the crude mixture was chromatographed [silica, hexanes/CH₂Cl₂ (1:2)] to afford the **CuBC**.

Cu(II)-8,8,18,18-tetramethyl(21,23-¹⁵N₂)bacteriochlorin (CuBC-¹⁵N^{21,23}).

Following a standard procedure,³⁵ a solution of **H₂BC-¹⁵N^{21,23}** (6.1 mg, 16 μmol, 4 mM) in freshly distilled THF (4 mL) was treated with NaH (54 mg, 2.3 mmol, 150 equiv, 95%) and Cu(OAc)₂ (90 mg, 0.49 mmol, 30 equiv). The reaction mixture was heated at 60 °C for 16 h. The reaction mixture was diluted with CH₂Cl₂ and washed with saturated aqueous NaHCO₃ solution. The organic layer was dried (Na₂SO₄) and filtered. The filtrate was concentrated. The crude solid was treated with hexanes, sonicated in a benchtop sonication bath, centrifuged, and the supernatant discarded. A single repetition of the hexanes treatment afforded a green solid (1.9 mg, 27%): ESI-MS obsd 433.1235, calcd 433.1232 (C₂₄H₂₄N₂¹⁵N₂Cu); λ_{abs} (toluene) 332, 378, 507, 728 nm.

Cu(II)-8,8,18,18-tetramethyl(22,24-¹⁵N₂)bacteriochlorin (CuBC-¹⁵N^{22,24}). The above procedure with **H₂BC-¹⁵N^{22,24}** (5.8 mg, 16 μmol) afforded the title compound as a green solid (3.4 mg, 49%): ESI-MS obsd 433.1234, calcd 433.1232 (C₂₄H₂₄N₂¹⁵N₂Cu); λ_{abs} (toluene) 332, 378, 507, 728 nm.

Cu(II)-8,8,18,18-tetramethyl(1,11-¹³C₂)bacteriochlorin (CuBC-¹³C^{1,11}). The above procedure with **H₂BC-¹³C^{1,11}** (5.8 mg, 16 μmol) afforded the title compound as a green solid (1.9 mg, 28%): ESI-MS obsd 433.1364, calcd 433.1359 (C₂₂¹³C₂H₂₄N₄Cu); λ_{abs} (toluene)

332, 378, 507, 728 nm.

Cu(II)-8,8,18,18-tetramethyl(4,14-¹³C₂)bacteriochlorin (CuBC-¹³C^{4,14}). The above procedure with **H₂BC-¹³C^{6,16}** (5.8 mg, 16 μmol) afforded the title compound as a green solid (2.0 mg, 30%): ESI-MS obsd 433.1358, calcd 433.1359 (C₂₂¹³C₂H₂₄N₄Cu); λ_{abs} (toluene) 332, 378, 507, 728 nm.

Cu(II)-8,8,18,18-tetramethyl(5,15-¹³C₂)bacteriochlorin (CuBC-¹³C^{5,15}). The above procedure with **H₂BC-¹³C^{5,15}** (5.8 mg, 16 μmol) afforded the title compound as a green solid (2.8 mg, 40%): ESI-MS obsd 433.1352, calcd 433.1359 (C₂₂¹³C₂H₂₄N₄Cu); λ_{abs} (toluene) 332, 378, 507, 728 nm.

Cu(II)-8,8,18,18-tetramethyl(6,16-¹³C₂)bacteriochlorin (CuBC-¹³C^{6,16}). The above procedure with **H₂BC-¹³C^{6,16}** (5.8 mg, 16 μmol) afforded the title compound as a green solid (5.3 mg, 77%): ESI-MS obsd 433.1362, calcd 433.1359 (C₂₂¹³C₂H₂₄N₄Cu); λ_{abs} (toluene) 332, 378, 507, 728 nm.

Cu(II)-8,8,18,18-tetramethyl(9,19-¹³C₂)bacteriochlorin (CuBC-¹³C^{9,19}). The above procedure with **H₂BC-¹³C^{9,19}** (5.8 mg, 16 μmol) afforded the title compound as a green solid (4.7 mg, 69%): ESI-MS obsd 433.1364, calcd 433.1359 (C₂₂¹³C₂H₂₄N₄Cu); λ_{abs} (toluene) 332, 378, 507, 728 nm.

Cu(II)-8,8,18,18-tetramethyl(10,20-¹³C₂)bacteriochlorin (CuBC-¹³C^{10,20}). The above procedure with **H₂BC-¹³C^{10,20}** (5.8 mg, 16 μmol) afforded the title compound as a green solid (5.3 mg, 77%): ESI-MS obsd 433.1343, calcd 433.1359 (C₂₂¹³C₂H₂₄N₄Cu); λ_{abs} (toluene) 332, 378, 507, 728 nm.

L. X-ray Crystal Structure of 10-NA

Data Collection and Processing. All X-ray measurements were made on a Bruker-Nonius X8 Kappa APEX II CCD system equipped with a graphite monochromator. The frames were integrated with the Bruker SAINT software package using a SAINT algorithm (V7.68 Bruker AXS Inc. 2009). The data are shown in Table 3.2.

Table 3.2. Summary of Crystal Data for 10-NA.

Formula	C ₁₁ H ₉ NO ₃ S
Formula Weight (g/mol)	235.25
Crystal Dimensions (mm)	0.28 × 0.24 × 0.24
Crystal Color and Habit	colorless block
Crystal System	monoclinic
Space Group H-M entry	P 1 21/c 1
Space Group Hall entry	-P 2ybc
Temperature, K	110
a, Å	12.5682(4)
b, Å	7.3873(2)
c, Å	11.2454(4)
α, °	90
β, °	98.1280(10)
γ, °	90
V, Å ³	1033.59(6)
Number of reflections to determine final unit cell	9938
Min and Max 2θ for cell determination, °	6.41 < 2θ < 66.4
Z	4
F(000)	488
ρ (g/cm ³)	1.512
λ, Å, (MoKα)	0.71073
μ, (cm ⁻¹)	0.302
Diffractometer Type	graphite
Scan Type(s)	phi and omega scans
Max 2θ for data collection, °	64.1
Measured fraction of data	0.999
Number of reflections measured	23042
Unique reflections measured	3584
R _{merge}	0.0222
Structure refined using	full matrix least-squares using F ²

Table 3.2. Continued.

Weighting Scheme	calca
Number of parameters in least-squares	203
R ₁	0.0322
wR ₂	0.0883
R ₁ (all data)	0.0359
wR ₂ (all data)	0.0914
GOF	1.079
Maximum shift/error	0.001
Min & Max peak heights on final ΔF Map ($e^-/\text{\AA}$)	-0.371, 0.808

^a $w=1/[\sigma^2(F_o^2) + (0.0462P)^2 + 0.4245P]$ where $P=(F_o^2 + 2F_c^2)/3$

Structure Solution and Refinement. The structures were solved by direct methods using XS. Additional positions for disordered atoms were found in subsequent difference maps during multiple rounds of refinement. The hydrogen atom positions were placed at idealized positions and were allowed to ride on the parent atom with isotropic displacement parameters of 1.2 or 1.5 times the parent. Modeling of the disordered component of this structure required that atom be constrained to give reasonable anisotropic refinement. The calculated structure factors included corrections for polarization, and an absorption correction using SADABS. The structure was refined using the SHELXL program from the SHELX2013 package,⁹⁰ and graphic plots were produced using OLEX2 crystallographic package.⁹¹ The ORTEP drawing is provided in Figure 3.2.

M. Comparison of Syntheses of Nitrohexanone–pyrrole 2

The known nitrohexanone–pyrrole **2-NA** was prepared previously by the following route.³⁴ Pyrrole-2-carboxaldehyde (**5-NA**) was converted to nitroethylpyrrole **3-NA** via procedure A (see the above section) without purification by column chromatography, whereupon the product exhibited ~90% purity as estimated by ¹H NMR spectroscopy.

Nitroethylpyrrole **3-NA** so obtained was directly used in a solventless Michael addition with **4-NA** in DBU. Nitrohexanone–pyrrole **2-NA** was obtained after column chromatography in 25% overall yield (upon three steps of nitro-aldol condensation, reduction, and Michael addition). This procedure is referred to herein as **A/-Chr/I**.

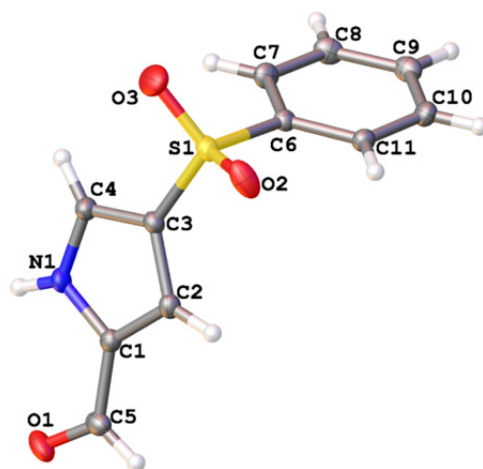


Figure 3.2. ORTEP drawing of **10-NA**. Ellipsoids are at the 50% probability level, and hydrogen atoms are drawn with arbitrary radii for clarity.

We carried out the synthesis of **{2}** via two procedures referred to as **A/+Chr/II** and **B/+Chr/II**. **A/+Chr/II** employed Procedure A with isolation by column chromatography to afford **{3}** in 35–42% yield. Nitrohexanone–pyrrole **{2}** was obtained in 65–88% yield via the Michael addition with inclusion of ethyl acetate (~2 mL) as required to completely dissolve the reaction mixture. The overall yields of **{2}** from **{5}** were 29–37%.

B/+Chr/II employed procedure B to afford two isotopologues **{3}** in 66 or 69% yield. Nitrohexanone–pyrrole **{2}** was then obtained in 91 or 95% yield via the Michael addition as described in **A/+Chr/II**. The overall yields of **{2}** from **{5}** were 60 or 66%.

A comparison of procedures for nitrohexanone–pyrrole **2** from pyrrole-2-carboxaldehyde **5** is shown in Table 3.3. Procedure **A/-Chr/I** requires three workup procedures and only one column chromatography yet gives the lowest yield. Procedure **A/+Chr/II** requires one more column chromatography and gives slightly improved yields versus that of procedure **A/-Chr/I**. Procedure **B/+Chr/II** gives the highest yields, however, at expense of a lengthy reaction time (29 h versus ~18 h for procedure **A/-Chr/I** and **A/+Chr/II**).

The procedure for reductive cyclization of nitrohexanone–pyrrole **{2}** to give the corresponding dihydrodipyrin–acetal **{1}** was identical to the previous reported³⁴ with modification in the amount of buffer employed. A thorough rationale for the amount of buffer is described in the next section. In general, the modified procedure gives slightly-to-moderately improved yields (32-58%) than that previously reported (29%).

Table 3.3. Procedures for pyrrole-2-carboxaldehyde **5** → nitrohexanone–pyrrole **2**.

<u>Route</u>	A/-Chr/I	A/+Chr/II	B/+Chr/II
Nitro-aldol condensation	KOAc, MeNH ₃ Cl, CH ₃ NO ₂ in EtOH rt, 2 h workup by extraction	KOAc, MeNH ₃ Cl, CH ₃ NO ₂ in EtOH rt, 2.5 h workup by extraction	NaOAc, MeNH ₃ Cl, CH ₃ NO ₂ in MeOH rt, 12 h workup not required
Reduction	LiBH ₄ in THF -10 °C, 15 min workup by extraction no chromatography	LiBH ₄ in THF -10 °C, 25 min workup by extraction column chromatography	NaBH ₄ in DMF/MeOH rt, 1 h workup by extraction column chromatography
Michael addition	solventless in DBU rt, 16 h column chromatography	DBU, ethyl acetate (~2 mL) rt, 16 h column chromatography	DBU, ethyl acetate (~2 mL) rt, 16 h column chromatography
Overall yield	25%	29–37%	60 or 66%

N. pH Estimation in the Reductive Cyclization with Buffered TiCl₃

The reductive cyclization of the nitrohexanone–pyrrole (**2**) is carried out with TiCl₃ in a buffered aqueous–organic medium to give the corresponding dihydrodipyrin–acetal (**1**). The general reaction with various substrates to form dihydrodipyrins has been employed over the years dating at least to the work of Battersby (ca. 1980).⁸⁰ The nature of the TiCl₃ source has varied over this >30-year period depending on commercial availability, worker, substrate, and reaction scale. Typical sources that we have employed include TiCl₃ (8.6 wt

% TiCl_3 in 28 wt % HCl solution),³¹ TiCl_3 (20 wt % in 3% HCl solution),³⁴ and TiCl_3 in powder form.⁸² The reaction is carried out with the TiCl_3 source and the reactant in a solution composed of aqueous buffer and THF. During workup of the reductive cyclization reaction (with 20 wt % TiCl_3 in 3% HCl solution),³⁴ rapid gas evolution was invariably observed upon quenching the reaction by addition of aqueous NaHCO_3 solution to the reaction mixture. Assuming such gas evolution to consist of CO_2 implies the reaction mixture must be quite acidic. The objective of using a buffer is to hold the reaction pH at ~ 6 . In practice, estimating the pH of the TiCl_3 mixture by use of pH paper is difficult because the presence of NH_4OAc and other species typically afford a rather thick slurry (dark green). The following calculations are presented to understand the amount of buffer required for the reaction.

The amount of buffer required entails consideration of (i) the amount of TiCl_3 and possible hydrolysis of TiCl_3 to give $\text{Ti}(\text{OH})_3$ (or other species) and 3 HCl; (ii) the amount of HCl in the TiCl_3 source, if any; and (iii) the amount of NaOMe used in the prior treatment of the nitrohexanone–pyrrole (**2**). The dihydrodipyrin product (**1**) is expected to be protonated and hence provide one molar equiv of buffering agent, but this can be ignored given the typically large quantities of TiCl_3 and HCl. Indeed, the reductive cyclization typically is carried out with 6 molar equiv of TiCl_3 per mole of nitrohexanone–pyrrole. Considering the lability of dihydrodipyrin–acetal **1** to acids (i.e., self-condensation to form the bacteriochlorin), it is worthwhile to scrutinize the pH change during the reaction.

Calculations of pH values were performed by assuming the volumes are additive and by considering only HCl and NH_4OAc in the solution (vide infra). Titration curves for 67,

100, 200 equiv of NH_4OAc versus 0–120 equiv of HCl are shown in Figure 3.3. The initial NH_4OAc solution is neutral but does not maintain at $\text{pH} = 7$ upon addition of HCl . The pH value immediately drops below 6 upon addition of 4, 6 and 11 equiv of HCl for solutions with 67, 100 and 200 equiv NH_4OAc , respectively. The buffer solutions (67, 100, 200 equiv of NH_4OAc) then maintain at $\text{pH} \sim 4.75$ (pK_a of AcOH) for ~ 40 equiv of HCl . The three solutions each drop to $\text{pH} < 4$ upon addition of 56, 85 and 167 equiv HCl , respectively.

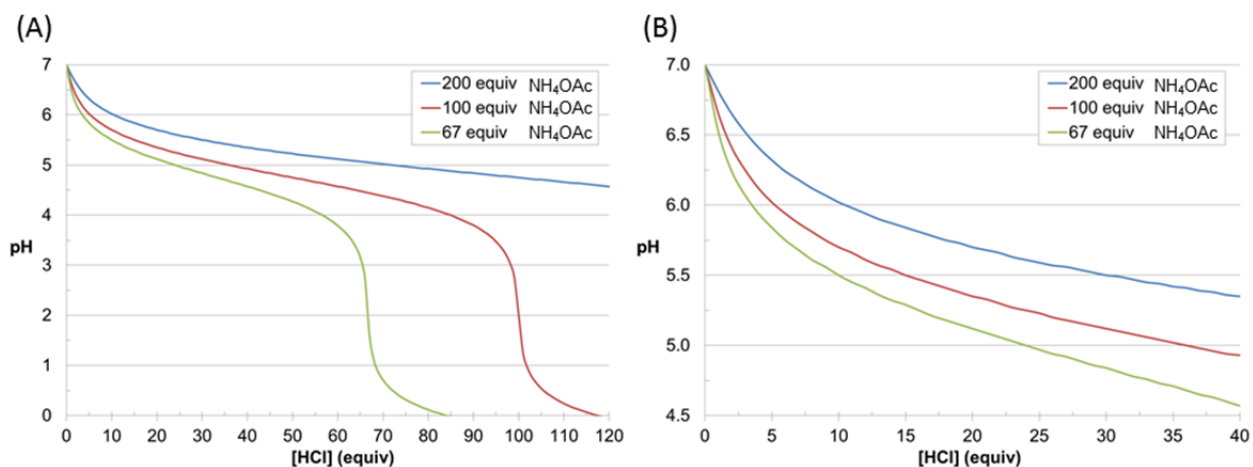


Figure 3.3. Calculated titration curves for NH_4OAc solutions (67, 100, 200 equiv) versus 0–120 equiv of HCl (panel A). An expansion of the graph is shown in panel B. Note the different pH scales in (A) and (B).

The most recent procedure employed TiCl_3 (20 wt % in 3% HCl solution) with a modest buffer requirement.³⁴ A such buffered TiCl_3 solution contains:

(1) nitrohexanone–pyrrole (**2**): 57 mM;

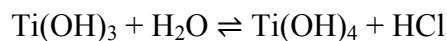
(2) MeONa: 0.17 M, 3.0 equiv;

(3) TiCl_3 : 0.45 M, 8.0 equiv;

(4) HCl: 0.24 M, 4.1 equiv; and

(5) NH_4OAc : 3.81 M, 67 equiv.

Initially, (1) and (2) react separately to give the nitronate **I** (Scheme 3.8) and then the reaction mixture was transferred into the buffer solution containing (3)-(5). Three equiv of MeONa were employed in practice to facilitate the reaction. We assume that two equiv of MeONa remain in the reaction mixture and were transferred to the buffer solution. Thus, the initial $[\text{HCl}] = 4.1 - 2 = 2.1$ (equiv). We then consider the following equilibria:



Hence, four equiv of HCl per TiCl_3 are released to the solution. Thus, the final $[\text{HCl}] = 2.1 + 8 \times 4 = 34.1$ (equiv). Therefore, the $[\text{HCl}]$ shifts from 2.1 to 34.1 equiv during the reaction, in turn causing the pH value of a solution containing 67 equiv of NH_4OAc to drop from 6.22 to 4.73 according to the calculated titration curve. The shifts in pH value calculated from selected buffered conditions in reference 34 are listed in Table 3.4. In most conditions, the pH value shifts from ~6 to ~4. In the final entry of Table 3.4 (procedure for **1-T**), a different source of TiCl_3 (8.6 wt % TiCl_3 in 28 wt % HCl) was employed. Because a

large excess of NH₄OAc (400 equiv) was used, the condition gives the most stable pH value of ~5.5.

Herein, we employed TiCl₃ (20 wt % in 3% HCl solution) for the reductive cyclization. According to the calculated titration curve, to better maintain the pH value the buffered solution requires 200 equivalents of NH₄OAc, which gives pH > 5.5 during the reaction. In practice, a high concentration of NH₄OAc forms a thick material and causes difficulty in stirring; a supplement of water or THF typically is required to efficiently stir the reaction mixture. For procedures described above, 100–150 equivalents of NH₄OAc were used and argon-bubbled THF (~30mL) was added to facilitate the stirring.

Table 3.4. Calculated pH values of buffered solutions in reference 34

Procedure ^a	[2] (mM)	[TiCl ₃] (M)	[NH ₄ OAc] (M)	[HCl] (M) ^c	pH shift
1-H	57	0.46	3.81	0.12 → 1.94	6.22 → 4.73
1-EtEs	62	0.39	3.24	0.08 → 1.65	6.33 → 4.73
1-EtEt	55	0.47	3.01	0.14 → 2.03	6.06 → 4.43
1-EsEs	57	0.44	3.67	0.12 → 1.89	6.21 → 4.72
1-Es	51	0.45	2.80	0.12 → 1.91	6.09 → 4.42
1-Py	27	0.39	2.39	0.15 → 1.71	5.92 → 4.35
1-T^b	17	0.08	6.62	0.88 → 1.21	5.56 → 5.40

^aThe compounds listed are the products of the various reactions.³⁴ The procedure employed TiCl₃ (20 wt % in 3% HCl solution) unless noted otherwise. ^bThe procedure was as follows:³⁴ “TiCl₃ (8.6 wt % TiCl₃ in 28 wt % HCl, 14.9 mL, 10. mmol) and water (80 mL) were mixed and bubbled with argon for 15 min.” ^cThe initial and final [HCl] are given.

Derivation of equations

Suppose $[\text{HCl}] = A$ M in $[\text{NH}_4\text{OAc}] = S$ M solution,

Definition:



Mass balance:

$$\text{Initial } [\text{NH}_4\text{OAc}] = S = [\text{NH}_3] + [\text{NH}_4^+] = [\text{HOAc}] + [\text{OAc}^-]$$

$$\text{So } [\text{NH}_3] = S - [\text{NH}_4^+] \text{ and } [\text{HOAc}] = S - [\text{OAc}^-]$$

replace $[\text{NH}_3]$ and $[\text{HOAc}]$ in equation (1) and (2):

$$\begin{aligned} K_a &= \frac{[\text{H}^+](S - [\text{NH}_4^+])}{[\text{NH}_4^+]} \\ [\text{NH}_4^+]K_a &= [\text{H}^+]S - [\text{H}^+][\text{NH}_4^+] \\ [\text{NH}_4^+](K_a + [\text{H}^+]) &= [\text{H}^+]S \\ [\text{NH}_4^+] &= \frac{[\text{H}^+]S}{(K_a + [\text{H}^+])} \end{aligned} \quad (3)$$

$$\text{similarly, } [\text{OAc}^-] = \frac{S[\text{OH}^-]}{(K_b + [\text{OH}^-])} \quad (4)$$

$$\text{Charge balance: } [\text{NH}_4^+] + [\text{H}^+] = [\text{OAc}^-] + [\text{OH}^-] + [\text{Cl}^-]$$

assuming $[\text{Cl}^-]$ remains constant ($= A$ M) when equilibrium is attained, replace $[\text{NH}_4^+]$ and $[\text{OAc}^-]$ by equations (3) and (4) gives

$$\frac{[\text{H}^+]S}{(K_a + [\text{H}^+])} + [\text{H}^+] = \frac{S[\text{OH}^-]}{(K_b + [\text{OH}^-])} + [\text{OH}^-] + A \quad (5)$$

$$\text{And } [\text{H}^+][\text{OH}^-] = K_w \quad (6)$$

Equations (5) and (6) can be solved by a Matlab program:

Matlab script example:

```
clearvars
i = 1;
for a = 0:120;                                % [HCl](equiv)
x = sym('x','real');
y = sym('y','real');
pka = 9.25;                                    % pKa of NH4
pkb = 9.25;                                    % pKb of OAc-
s = 200;                                       % [NH4OAc] (equiv)
kw = 1e-14;
ka = 10^-pka;
kb = 10^-pkb;
Ans = solve(x*s/(ka + x) + x - y*s/(kb + y) - y - a , kw - x*y);
Ans = [Ans.x, Ans.y];
Ans = -log10(abs(Ans));
Ans = double(Ans);
Ans = roundn(Ans, -2);
pH(i) = Ans(1,1);
i = i + 1;
end
Heq = 0:120;
plot (Heq, pH)
```

O. NMR Chemical Shift Assignments

The results are summarized in Table 3.1 in the above section. Assignments of the ¹H NMR chemical shifts of {H₂BC} and {ZnBC} are based on the following observations:

(1) The NOESY spectra of H₂BC-NA showed a clear coupling between methylene protons of pyrroline rings and a singlet *meso*-proton resonance. The singlet β-proton resonance at 8.83 ppm was then assigned to H⁵,H¹⁵. The other singlet resonance at 8.73 ppm was assigned to H¹⁰,H²⁰.

(2) By examining the ¹H NMR spectra of H₂BC-¹³C^{10,20}, the β-proton resonances were assigned (Figure 3.4). The ¹H NMR spectrum of H₂BC-¹³C^{10,20} revealed one upfield β-proton resonance in a doublet of doublets and the other downfield β-proton resonances in a

similar, yet broadened doublets (Figure 3.4). The broadening of the downfield resonances was not found in the spectra of $\text{H}_2\text{BC-NA}$ and $\text{H}_2\text{BC-}^{13}\text{C}^{5,15}$ and therefore must result from the coupling with $^{13}\text{C}^{10,20}$. The downfield resonances at 8.77 ppm are then assigned to $\text{H}^{2,12}$ and the upfield resonances at 8.74 ppm are assigned to $\text{H}^{3,13}$.

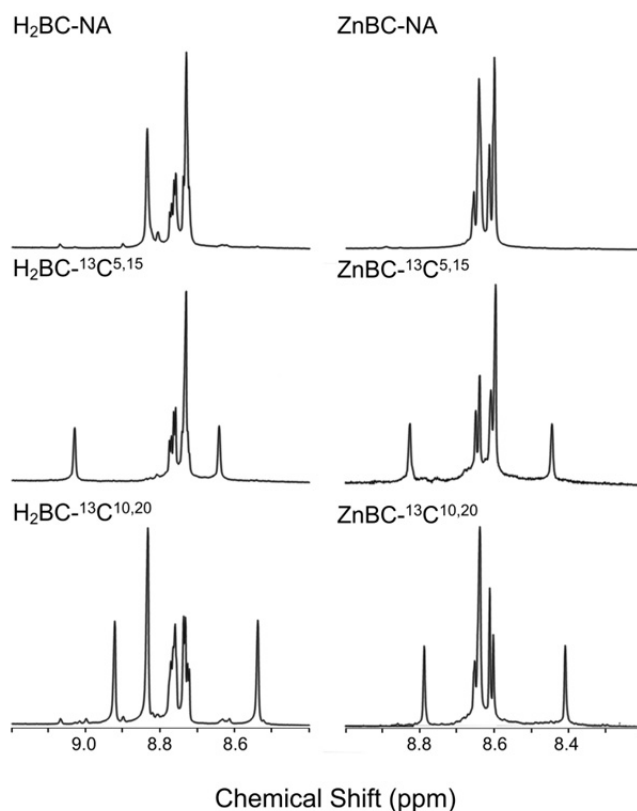


Figure 3.4. ^1H NMR spectra of $\{\text{H}_2\text{BC}\}$ (in CDCl_3) and $\{\text{ZnBC}\}$ (in $\text{THF-}d_8$) at 298 K (recorded at 400 MHz except for ZnBC-NA at 300 MHz).

(3) The resonances of $\{\text{ZnBC}\}$ show a coupling pattern similar to those of $\{\text{H}_2\text{BC}\}$. The resonances of the *meso*-protons of $\{\text{ZnBC}\}$ are assigned based on the splitting in the ^1H

NMR spectra of **ZnBC-¹³C^{5,15}** and **ZnBC-¹³C^{10,20}**. Assignment of β -proton resonances of **{ZnBC}** follows the β -proton resonances of **{H₂BC}** with downfield resonances to H^{2,12} and upfield resonances to H^{3,13}.

Assignments of the ¹³C NMR chemical shifts of **{H₂BC}** are based on the following observations:

(1) Information from HSQC and HMBC spectra of **H₂BC-NA** were used to assign the resonances of C^{7,17}, C^{8,18}, C^{10,20} and the geminal dimethyl carbons given the proton assignments as described above.

(2) By examining the ¹³C NMR spectra of isotopologues **{H₂BC}**, the resonances of C^{1,11}, C^{4,14}, C^{5,15}, C^{6,16}, C^{9,19} were assigned directly.

(3) A remaining set of closely spaced resonances at 121.84 and 121.73 were assigned to C^{2,12} and C^{3,13} respectively, on the basis of the coupling pattern in the ¹³C NMR spectra of **H₂BC-¹³C^{1,11}** and **H₂BC-¹³C^{4,14}**.

P. Method for Determination of Isotopic Enrichment

The isotopic enrichment of bacteriochlorins was determined by assessing the abundance of three species:

- (I) bacteriochlorins containing no ¹³C/¹⁵N atom,
- (II) bacteriochlorins containing one ¹³C/¹⁵N atom at either one of the designated sites,
- and (III) bacteriochlorins containing a ¹³C/¹⁵N atom at both target sites.

The following discussion concerns the **ZnBC-¹³C^{4,14}** sample. The ESI-mass spectrum of **ZnBC-¹³C^{4,14}** is listed in Table 3.5. The peak at nominal mass 432 (432.130 *m/z*) originates solely from the (A+0) species of I, whereas the peak at nominal mass 433

(433.134 m/z) stems from both the (A+0) species of II and the (A+1) species of I (due to natural isotopic abundance). The peak at nominal mass 434 (434.136 m/z) stems from the monoisotopic (A+0) species of III, the (A+1) species of II, and the (A+2) species of I.

Table 3.5. Selected peaks from the ESI-mass spectrum of **ZnBC-¹³C^{4,14}**

Nominal m/z	Relative abundance (%)	Composition
432	1.99	I (A+0)
433	28.7	II (A+0) + I (A+1)
434	100	III (A+0) + II (A+1) + III (A+2)

For **ZnBC-NA**, which has molecular formula $C_{24}H_{24}N_4Zn$, the measured ratio of the (A+1)/(A+0) peaks is 0.28, whereas the ratio of the (A+2)/(A+0) peaks is 0.56. The measured ratios are in accord (within ~10%) of that of the calculated ratios, as shown in Table 3.6.

The isotopic enrichment = (actual # of ¹³C summed over all target sites)/(theoretical # of ¹³C summed over all target sites)

Thus,

$$\text{Corrected abundance of (I)} = 1.99$$

$$\text{Corrected abundance of (II)} = 28.7 - (1.99 \times 0.28) = 28.14$$

$$\text{Corrected abundance of (III)} = 100 - (28.7 \times 0.28) - (1.99 \times 0.56) = 90.85$$

Accordingly, the isotopic enrichment of **ZnBC-¹³C^{4,14}** =

$$[(28.14 \times 1) + (90.85 \times 2)] / [2 \times (1.99 + 28.14 + 90.85)] \times 100 = 87\%$$

Table 3.6. Isotopic pattern for **ZnBC-NA**

Nominal masses	Relative abundance of ions	
	Calculated	Measured
432	100.00	100
433	27.72	28.01
434	60.98	56.04
435	24.43	22.14
436	42.60	37.41
437	10.85	11.69
438	2.51	2.52
439	0.33	1.26

References

- (1) Scheer, H. In *Chlorophylls and Bacteriochlorophylls: Biochemistry, Biophysics, Functions and Applications*; Grimm, B.; Porra, R. J.; Rüdiger, W.; Scheer, H., Eds.; Springer: Dordrecht, The Netherlands, 2006, pp 1–26.
- (2) Alben, J. O. In *The Porphyrins*, Vol. III, Dolphin, D., Ed.; Academic Press: New York, 1978, pp 323–345.
- (3) Felton, R. H.; Yu, N.-T. In *The Porphyrins*, Vol. III, Dolphin, D., Ed.; Academic Press: New York, 1978, pp 347–393.
- (4) Norris, J. R.; Scheer, H.; Katz, J. J. In *The Porphyrins*, Vol. IV, Dolphin, D., Ed.; Academic Press: New York, 1979, pp 159–195.
- (5) Fajer, J.; Davis, M. S. In *The Porphyrins*, Vol. IV, Dolphin, D., Ed.; Academic Press: New York, 1979, pp 197–256.
- (6) Schick, G. A.; Bocian, D. F. *Biochim. Biophys. Acta* **1987**, *895*, 127–154.
- (7) Lutz, M.; Robert, B. In *Biological Applications of Raman Spectroscopy*; Spiro, T. G., Ed.; Wiley: New York, 1988; Vol. 3, pp 347–411.
- (8) Kobayashi, M.; Akiyama, M.; Kano, H.; Kise, H. In *Chlorophylls and Bacteriochlorophylls: Biochemistry, Biophysics, Functions and Applications*; Grimm, B.; Porra, R. J.; Rüdiger, W.; Scheer, H. Springer: Dordrecht, The Netherlands, 2006, pp 79–94.
- (9) Chen, Y.; Li, G.; Pandey, R. K. *Curr. Org. Chem.* **2004**, *8*, 1105–1134.
- (10) Fajer, J.; Borg, D. C.; Forman, A.; Felton, R. H.; Dolphin, D.; Vegh, L. *Proc. Natl. Acad. Sci. USA* **1974**, *71*, 994–998.

- (11) Donohoe, R. J.; Atamian, M.; Bocian D. F. *J. Phys. Chem.* **1989**, *93*, 2244–2252.
- (12) Hu, S.; Mukherjee, A.; Spiro, T. G. *J. Am. Chem. Soc.* **1993**, *115*, 12366–12377.
- (13) Lin, C.-Y.; Spiro, T. G. *J. Phys. Chem. B* **1997**, *101*, 472–482.
- (14) Lin, C.-Y.; Blackwood, M. E., Jr.; Kumble, R.; Hu, S.; Spiro, T. G. *J. Phys. Chem. B* **1997**, *101*, 2372–2380.
- (15) Whitlock, H. W., Jr.; Hanauer, R.; Oester, M. Y.; Bower, B. K. *J. Am. Chem. Soc.* **1969**, *91*, 7485–7489.
- (16) Chang, C. K. *Biochemistry* **1980**, *19*, 1971–1976.
- (17) Porra, R. J.; Scheer, H. *Photosyn. Res.* **2000**, *66*, 159–175.
- (18) Shrestha-Dawadi, P. B.; Lugtenburg, J. *Eur. J. Org. Chem.* **2003**, 4654–4663.
- (19) Dawadi, P. B. S.; Schulten, E. A. M.; Lugtenburg, J. *J. Labelled Compd. Radiopharm.* **2009**, *52*, 341–349.
- (20) Prakash, S.; Alia, A.; Gast, P.; de Groot, H. J. M.; Jeschke, G.; Matysik, J. *Biochemistry* **2007**, *46*, 8953–8960.
- (21) Brückner, C.; Samankumara, L.; Ogikubo, J. in *Handbook of Porphyrin Science*, Vol. 17; Kadish, K. M.; Smith, K. M.; Guillard, R. Eds.; World Scientific Publishing Co.: Singapore, 2012, pp 1–112.
- (22) Sasaki, S.-I.; Tamiaki, H. *J. Org. Chem.* **2006**, *71*, 2648–2654.
- (23) Grin, M. A.; Mironov, A. F.; Shtil, A. A. *Anti-Cancer Agents Med. Chem.* **2008**, *8*, 683–697.
- (24) Tomé, A. C.; Neves, M. G. P. M. S.; Cavaleiro, J. A. S. *J. Porphyrins Phthalocyanines* **2009**, *13*, 408–414.

- (25) Singh, S.; Aggarwal, A.; Thompson, S.; Tomé, J. P. C.; Zhu, X.; Samaroo, D.; Vinodu, M.; Gao, R.; Drain, C. M. *Bioconjugate Chem.* **2010**, *21*, 2136–2146.
- (26) Pereira, M. M.; Monteiro, C. J. P.; Simões, A. V. C.; Pinto, S. M. A.; Abreu, A. R.; Sa, G. F. F.; Silva, E. F. F.; Rocha, L. B.; Dabrowski, J. M.; Formosinho, S. J.; Simoes, S.; Arnaut, L. G. *Tetrahedron* **2010**, *66*, 9545–9551.
- (27) Samankumara, L. P.; Wells, S.; Zeller, M.; Acuña, A. M.; Röder, B.; Brückner, C. *Angew. Chem. Int. Ed.* **2012**, *51*, 5757–5760.
- (28) Pereira, M. M.; Abreu, A. R.; Goncalves, N. P. F.; Calvete, M. J. F.; Simões, A. V. C.; Monteiro, C. J. P.; Arnaut, L. G.; Eusébio, M. E.; Canotilho, J. *Green Chem.* **2012**, *14*, 1666–1672.
- (29) Minehan, T. G.; Cook-Blumberg, L.; Kishi, Y.; Prinsep, M. R.; Moore, R. E. *Angew. Chem. Int. Ed.* **1999**, *38*, 926–928.
- (30) Wang, W.; Kishi, Y. *Org. Lett.* **1999**, *1*, 1129–1132.
- (31) Kim, H.-J.; Lindsey, J. S. *J. Org. Chem.* **2005**, *70*, 5475–5486.
- (32) Yu, Z.; Ptaszek, M. *Org. Lett.* **2012**, *14*, 3708–3711.
- (33) Alexander, V. M.; Sano, K.; Yu, Z.; Nakajima, T.; Choyke, P. L.; Ptaszek, M.; Kobayashi, H. *Bioconjugate Chem.* **2012**, *23*, 1671–1679.
- (34) Krayner, M.; Ptaszek, M.; Kim, H.-J.; Meneely, K. R.; Fan, D.; Secor, K.; Lindsey, J. S. *J. Org. Chem.* **2010**, *75*, 1016–1039.
- (35) Chen, C.-Y.; Sun, E.; Fan, D.; Taniguchi, M.; McDowell, B. E.; Yang, E.; Diers, J. R.; Bocian, D. F.; Holten, D.; Lindsey, J. S. *Inorg. Chem.* **2012**, *51*, 9443–9464.
- (36) Taniguchi, M.; Cramer, D. L.; Bhise, A. D.; Kee, H. L.; Bocian, D. F.; Holten, D.;

- Lindsey, J. S. *New J. Chem.* **2008**, *32*, 947–958.
- (37) Tsay, O. G.; Kim, B.-W.; Luu, T. L.; Kwak, J.; Churchill, D. G. *Inorg. Chem.* **2013**, *52*, 1991–1999.
- (38) Fox, R. B.; Powell, W. H. *Nomenclature of Organic Compounds*; American Chemical Society and Oxford University Press: New York, 2001, pp 359–370.
- (39) *IUPAC Compendium of Chemical Terminology – Gold Book*, version 2.3.2: <http://goldbook.iupac.org> (accessed Nov 4, 2013).
- (40) Mass, O.; Lindsey, J. S. *J. Org. Chem.* **2011**, *76*, 9478–9487.
- (41) Kim, H.-J.; Dogutan, D. K.; Ptaszek, M.; Lindsey, J. S. *Tetrahedron* **2007**, *63*, 37–55.
- (42) Strachan, J.-P.; O’Shea, D. F.; Balasubramanian, T.; Lindsey, J. S. *J. Org. Chem.* **2000**, *65*, 3160–3172.
- (43) Taniguchi, M.; Kim, H.-J.; Ra, D.; Schwartz, J. K.; Kirmaier, C.; Hindin, E.; Diers, J. R.; Prathapan, S.; Bocian, D. F.; Holten, D.; Lindsey, J. S. *J. Org. Chem.* **2002**, *67*, 7329–7342.
- (44) Ptaszek, M.; Bhaumik, J.; Kim, H.-J.; Taniguchi, M.; Lindsey, J. S. *Org. Process Res. Dev.* **2005**, *9*, 651–659.
- (45) Silverstein, R. M.; Ryskiewicz, E. E.; Willard, C.; Koehler, R. C. *J. Org. Chem.* **1955**, *20*, 668–672.
- (46) Martyn, D. C.; Vernall, A. J.; Clark, B. M.; Abell, A. D. *Org. Biomol. Chem.* **2003**, *1*, 2103–2110.
- (47) Wray, V.; Gossauer, A.; Grüning, B.; Reifensahl, G.; Zilch, H. *J. Chem. Soc. Perkin Trans. 2* **1979**, 1558–1567.

- (48) Battersby, A. R.; Fookes, C. J. R.; Meegan, M. J.; McDonald, E.; Wurziger, H. K. W. *J. Chem. Soc. Perkin Trans. 1* **1981**, 2786–2799.
- (49) Mispelter, J.; Momenteau, M.; Lhoste, J.-M. *J. Chem. Soc. Dalton Trans.* **1981**, 1729–1734.
- (50) Schlabach, M.; Limbach, H.-H.; Bunnenberg, E.; Shu, A. Y. L.; Tolf, B.-R.; Djerassi, C. *J. Am. Chem. Soc.* **1993**, *115*, 4554–4565.
- (51) Iida, K.; Ohtaka, K.; Komatsu, T.; Makino, T.; Kajiwara, M. *J. Label. Compd. Radiopharm.* **2008**, *51*, 167–169.
- (52) Woo, P. W. K.; Hartman, J.; Hicks, J.; Hayes, R.; *J. Label. Compd. Radiopharm.* **1999**, *42* 135–145.
- (53) Almeida, M.; Johannesson, P.; Boman, A.; Lundstedt, T. *J. Label. Compd. Radiopharm.* **2005**, *48*, 621–627.
- (54) Skaddan, M. B. *J. Label. Compd. Radiopharm.* **2010**, *53*, 73–77.
- (55) Bak, B.; Pedersen, T.; Sørensen, G. O. *Acta Chem. Scand.* **1964**, *18*, 275–276.
- (56) Evans, J. N. S.; Fagerness, P. E.; Mackenzie, N. E.; Scott, A. I. *Magn. Reson. Chem.* **1985**, *23*, 939–944.
- (57) Williams, S. R.; Maynard, H. D.; Chmelka, B. F. *J. Label. Compd. Radiopharm.* **1999**, *42*, 927–936.
- (58) Muresan, A. Z.; Thamyongkit, P.; Diers, J. R.; Holten, D.; Lindsey, J. S.; Bocian, D. *F. J. Org. Chem.* **2008**, *73*, 6947–6959.
- (59) Gossauer, A; Suhl, K. *Helv. Chim. Acta* **1976**, *59*, 1698–1704.

- (60) Chen, Q.; Huggins, M. T.; Lightner, D. A.; Norona, W.; McDonagh, A. F. *J. Am. Chem. Soc.* **1999**, *121*, 9253–9264.
- (61) Oldenziel, O. H.; van Leusen, D.; van Leusen, A. M. *J. Org. Chem.* **1977**, *42*, 3114–3118.
- (62) Hartung, R.; Golz, G.; Schlaf, S.; Silvennoinen, G.; Polborn, K.; Mayer, P.; Pfaendler, R. H. *Synthesis* **2009**, 495–501.
- (63) Padmavathi, V.; Reddy, B. J. M.; Sarma, M. R.; Thriveni, P. *J. Chem. Res.* **2004**, 79–80.
- (64) Waser, J.; Gaspar, B.; Nambu, H.; Carreira, E. M. *J. Am. Chem. Soc.* **2006**, *128*, 11693–11712.
- (65) Okabe, K.; Natsume, M. *Tetrahedron* **1991**, *47*, 7615–7624.
- (66) Spero, G. B.; McIntosh, A. V., Jr.; Levin, R. H. *J. Am. Chem. Soc.* **1948**, *70*, 1907–1910.
- (67) Mazingo, R. *Org. Synth.* **1941**, *21*, 15–22.
- (68) MacDonald, S. F.; Stedman, R. J. *Can. J. Chem.* **1954**, *32*, 812–813.
- (69) Antonio, Y.; de la Cruz, M. E.; Galeazzi, E.; Guzman, A.; Bray, B. L.; Greenhouse, R.; Kurz, L. J.; Lustig, D. A.; Maddox, M. L.; Muchowski, J. M. *Can. J. Chem.* **1994**, *72*, 15–22.
- (70) Maassarani, F.; Pfeffer, M.; Spencer, J.; Wehman, E. *J. Organomet. Chem.* **1994**, *466*, 265–271.
- (71) Campetella, S.; Palmieri, A.; Petrini, M. *Eur. J. Org. Chem.* **2009**, 3184–3188.

- (72) Shibasaki, T.; Ooishi, T.; Yamanouchi, N.; Murafuji, T.; Kurotobi, K.; Sugihara, Y. *J. Org. Chem.* **2008**, *73*, 7971–7977.
- (73) Hasan, I.; Marinelli, E. R.; Lin, L.-C. C.; Fowler, F. W.; Levy, A. B. *J. Org. Chem.* **1981**, *46*, 157–164.
- (74) Sessler, J. L.; Mozaffari, A.; Johnson, M. R. *Org. Synth.* **1991**, *70*, 68–77.
- (75) Artico, M. In *Pyrroles, Part One: The Synthesis and the Physical and Chemical Aspects of the Pyrrole Ring*; Jones, R. A., Ed.; John Wiley & Sons, Inc.: Hoboken, NJ, USA, 1990, pp 383–395.
- (76) Anderson, H. J.; Clase, J. A.; Loader, C. E. *Synth. Commun.* **1987**, *17*, 401–407.
- (77) Mehrsheikh, A. *J. Labelled Compd. Radiopharm.* **1996**, *38*, 631–636.
- (78) Nieves-Bernier, E. J.; Taniguchi, M.; Diers, J. R.; Holten, D.; Bocian, D. F.; Lindsey, J. S. *J. Org. Chem.* **2010**, *75*, 3193–3202.
- (79) McMurry, J. E.; Melton, J. *J. Org. Chem.* **1973**, *38*, 4367–4373.
- (80) Battersby, A. R.; Dutton, C. J.; Fookes, C. J. R. *J. Chem. Soc. Perkin Trans. 1* **1988**, 1569–1576.
- (81) Taniguchi, M.; Ra, D.; Mo, G.; Balasubramanian, T.; Lindsey, J. S. *J. Org. Chem.* **2001**, *66*, 7342–7354.
- (82) Krayner, M.; Balasubramanian, T.; Ruzié, C.; Ptaszek, M.; Cramer, D. L.; Taniguchi, M.; Lindsey, J. S. *J. Porphyrins Phthalocyanines* **2009**, *13*, 1098–1110.
- (83) Murray, K. K.; Boyd, R. K.; Eberlin, M. N.; Langley, G. J.; Li, L.; Naito, Y. *Pure Appl. Chem.* **2013**, *85*, 1515–1609.

- (84) *Handbook of Chemistry and Physics*, 52nd ed. ; Weast, R. C.; Ed.; The Chemical Rubber Co.: Cleveland, OH, 1971.
- (85) McLafferty, F. W. *Interpretation of Mass Spectra*, 3rd ed.; University Science Books: Mill Valley, CA, 1980.
- (86) Bean, G. P. In *Pyrroles, Part One. The Synthesis and the Physical and Chemical Aspects of the Pyrrole Ring*; Jones, R. A., Ed.; John Wiley & Sons: New York, 1990, pp 206–234.
- (87) Ballini, R.; Petrini, M. *Tetrahedron* **2004**, *60*, 1017–1047.
- (88) Briggs, J. M.; Rahkamaa, E.; Randall, E. W. *J. Magn. Reson.* **1973**, *12*, 40–47.
- (89) Bundgaard, T.; Jakobsen, H. J.; Rahkamaa, E. J. *J. Magn. Reson.* **1975**, *19*, 345–356.
- (90) Sheldrick, G. M. *Acta Cryst.* **2008**, *A64*, 112–122.
- (91) Dolomanov, O. V.; Bourhis, L. J.; Gildea, R. J.; Howard, J. A. K.; Puschmann, H. *J. Appl. Cryst.* **2009**, *42*, 339–341.

CHAPTER 4

Tapping the Near-Infrared Spectral Region with Bacteriochlorin Arrays

Preamble. The contents of this chapter have been published⁴⁰ with contributions from Olga Mass.

Introduction

Bacteriochlorophylls play an essential role in Nature as the chief light-absorbing pigment in photosynthetic bacteria, yet have been substantially less studied than other members of the class of tetrapyrrole macrocycles. Bacteriochlorophylls are distinguished by an intense long-wavelength absorption band located in the NIR (700–1000 nm) region, appearing at 772, 794, and 767 nm for **Bchl a**, **b**, and **g**, respectively, in diethyl ether solution.¹ The intense NIR absorption of **Bchl a** (Figure 4.1) is compared with the red absorption (600–700 nm) characteristic of chlorophylls (e.g., **Chl a**, **b**), and the absence of either red or NIR absorption of porphyrins (e.g., magnesium octaethylporphyrin, **MgOEP**).² The profound change in absorption stems from the nature of the π framework in the respective tetrahydroporphyrin (bacteriochlorins **Bchl a**, **b**, and **g**), dihydroporphyrin (chlorins **Chl a** and **b**), and porphyrin (**MgOEP**) macrocycles. *In vivo*, where bacteriochlorophyll dimers or more extensive aggregates are present, the absorption band appears at ~780–1020 nm.¹ The position of the long-wavelength absorption band is important not only with regards to light absorption but also in determining the energy of the resulting excited state.

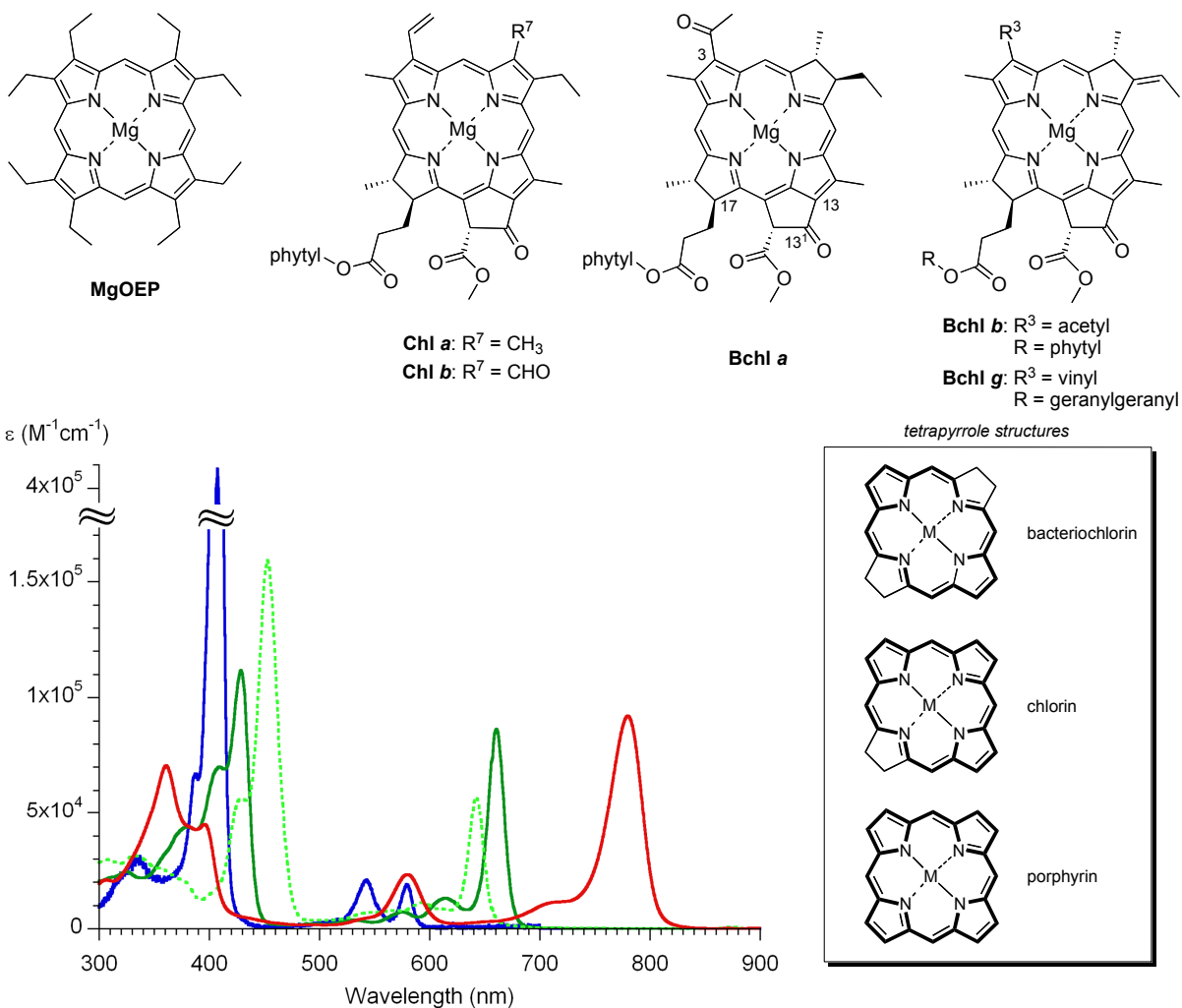


Figure 4.1. Absorption spectra of magnesium tetrapyrroles **MgOEP** (blue line), **Chl a** (solid green line), **Chl b** (dashed green line), and **Bchl a** (red line).² The spectra of **Bchl b** and **g** (not shown) closely resemble that of **Bchl a**. The box at right highlights the generic porphyrin, chlorin, and bacteriochlorin π framework.

Light in the NIR spectral region (i) is abundant in solar radiation, (ii) penetrates soft animal tissue more deeply than visible or UV light, and (iii) has been relatively little explored

for fundamental photochemistry versus that in the visible or UV regions. The NIR region has been comparatively little used in clinical diagnostics and biomedical imaging, hence, bacteriochlorins, which appear to be Nature's chosen absorbers in this spectral region, warrant extensive examination.³

Spectroscopic studies have been performed of bacteriochlorins in a variety of assemblies and architectures including solution⁴ or crystalline⁵ aggregates, monolayers and thin films,⁶ micelles,⁷ and with a 24-residue polypeptide in micelles.⁸ Bacteriochlorins also have been examined upon site-isolation in apoproteins⁹ and in mesoporous silica.¹⁰ Such non-covalent assemblies typically lack the structural control that is possible with covalent architectures where the constituents of interest are held at defined distances and orientations.

Building synthetic, covalently linked architectures (i.e., arrays) of tetrapyrrole macrocycles has proved to be invaluable for a host of fundamental studies and applications. Indeed, arrays containing >100 porphyrins have been prepared, and the number of porphyrin-containing arrays that have been reported must exceed one thousand.^{11,12} By contrast, relatively few bacteriochlorin-containing arrays have been prepared, and all such arrays are dyads (i.e., contain only two constituents, at least one of which is a bacteriochlorin).¹³⁻²⁹ Of course, the proteins of bacteriochlorophyll-containing light-harvesting complexes³⁰ and reaction centers³¹ can be tailored to some extent, yet such assemblies tend to be elaborate, not amenable to extensive structural modification, and limited with regards to the range of physicochemical conditions under which studies can be performed. Synthetic arrays offer the opportunity to exercise control over 3-dimensional structure (distance, orientation),

number of interacting constituents, types of constituents (and their respective energetics and photophysical properties), and pathways for inter-chromophore electronic communication.

The scientific motivation for the preparation of bacteriochlorin-containing arrays includes the following: (i) investigate spectral effects as a function of relative 3-dimensional organization of the constituents in the array, (ii) investigate mechanisms of electron transfer and energy transfer; (iii) build artificial photosynthetic architectures that absorb light, funnel energy, and convert energy into redox-stabilized species; (iv) study relatively low energy photochemical processes, given that absorption in the 700–900 nm region entails an excited state of at most 1.76 – 1.37 eV, and (v) develop probes for use in biomedicine including as fluorescent labels (with strong effective Stokes shifts), imaging agents, and tandem diagnostic/therapeutic agents.

In this chapter, we first outline the three distinct synthetic routes that have been employed to gain access to bacteriochlorin arrays. We then comprehensively survey known bacteriochlorin arrays, highlighting the motivation for their preparation and selected results. Consideration is given to design criteria for light-harvesting arrays composed of porphyrins versus bacteriochlorins. The chapter finishes with an outline of challenges to the broader implementation of bacteriochlorins in synthetic arrays.

Bacteriochlorin building blocks

A number of routes are available for the preparation of bacteriochlorins.³² Of these, three distinct approaches have been employed for the incorporation of bacteriochlorins in arrays (Figure 4.2).

(A) The most prevalent route entails modification of **Bchl a**, including demetalation/remetalation, esterification of the 17-propionate moiety, derivatization of the 3-acetyl group, or transformation of the isocyclic ring into the six-membered imide and elaboration at the *N*-imide site.^{33,34}

(B) Hydrogenation of a porphyrin, typically with diimide, affords the corresponding bacteriochlorin. Limitations of this approach typically include (i) formation of a mixture of porphyrin, chlorin, and bacteriochlorin, which can present separation challenges, (ii) formation of regioisomers depending on the macrocycle substitution pattern, and (iii) susceptibility of the bacteriochlorin to adventitious dehydrogenation leading to the chlorin and porphyrin.

(C) A recent *de novo* synthesis affords bacteriochlorins wherein a geminal-dimethyl group is present in each of the reduced rings to confer stability toward oxidation.^{3,35} Subsequent elaboration (e.g., Pd-mediated coupling reactions, aldol condensations, regioselective 15-bromination) enables wavelength tunability across a set of diverse bacteriochlorins ($\lambda_{\text{max}} \sim 720\text{--}820$ nm).^{36,37} This approach is perhaps most versatile but has only been employed to date for the preparation of two dyads.²⁷⁻²⁹

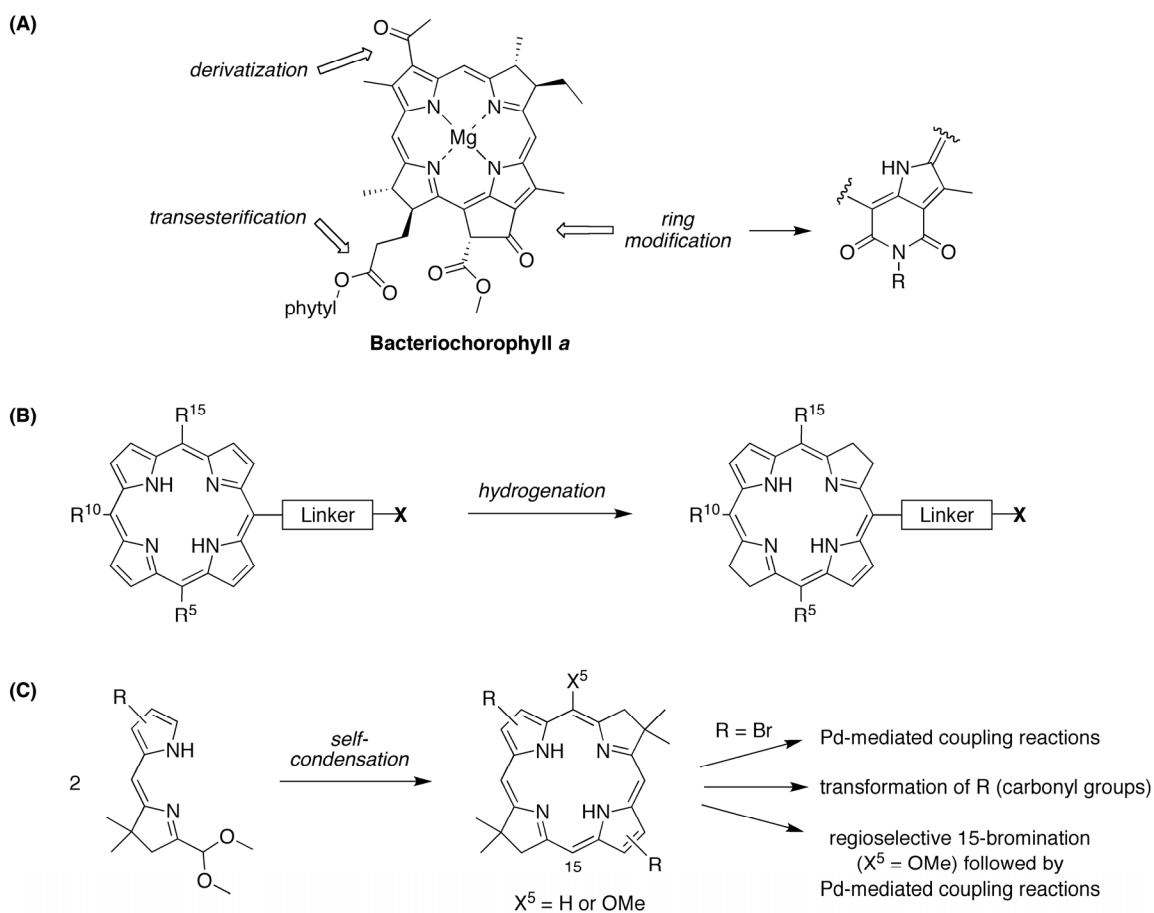
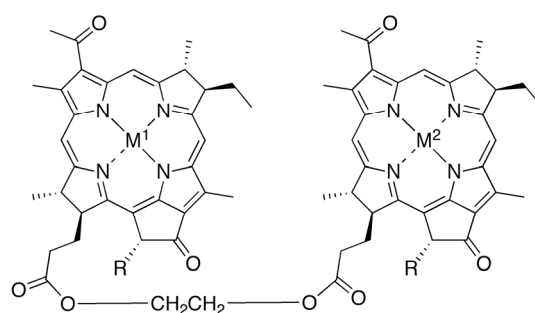


Figure 4.2. Routes to bacteriochlorins for incorporation in dyads: (A) modification of natural bacteriochlorophylls; (B) hydrogenation of porphyrins; and (C) *de novo* synthesis of bacteriochlorins.

Bacteriochlorin-containing dyads

The special pair of bacteriochlorophylls (P865) in the photosynthetic reaction center of purple bacteria is a low energy trap for electronic excitation delivered from the bacteriochlorophyll-containing antenna complex following light absorption. Wasielewski reported the first dyads (**1a**, **2a** and **2b**) containing bacteriochlorin macrocycles as a mimic of

P865.^{13,14} The ethylene glycol linker in **1a**, **2a** and **2b** was introduced via sequential esterification of the free base pigment bacterioopheophorbide *a* (Figure 4.3). Mild condensing methods (benzotriazole-1-methanesulfonate^{13,14} or dicyclohexylcarbodiimide¹⁸) provided compatibility with the 13²-carbomethoxy motif and the bacteriochlorin macrocycle. Treatment of **1a** with a hindered Grignard reagent afforded the mono- and bis-magnesium chelates **2a** and **2b**, respectively.



Dyad	R	M ¹	M ²	Ref.
1a	CO ₂ Me	H, H	H, H	14
1b	H	H, H	H, H	18
2a	CO ₂ Me	H, H	Mg	14
2b	CO ₂ Me	Mg	Mg	13,14

Figure 4.3. Bacteriochlorin–bacteriochlorin dyads (naturally derived constituents).

The all-magnesium dimer (**2b**) is an early example of what are now regarded as *foldamers*. In benzene saturated with water, **2b** self-folds owing to hydrogen-bonding of the 13¹-oxo moiety with the water ligated to the central magnesium (Figure 4.4), accompanied

by a spectral shift from 780 to 803 nm. Photooxidation of **2b** gave a cation radical delocalized over the two macrocycles, mimicking the reaction center.¹³

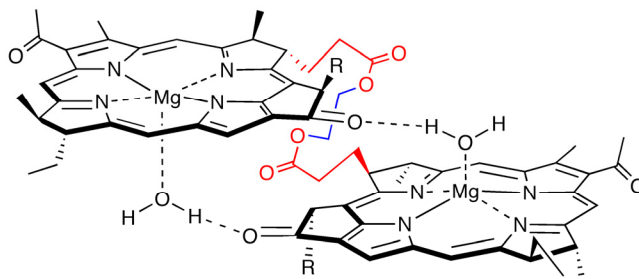
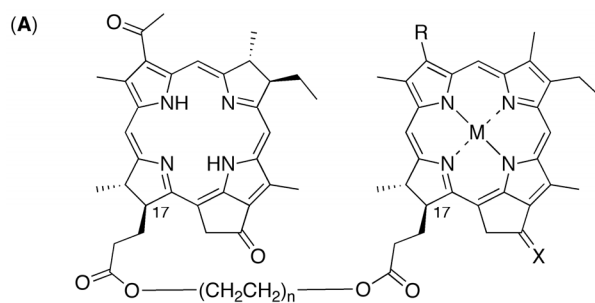


Figure 4.4. Proposed ntramolecular folding-up of bacteriochlorin dimer **2b** (R = CO₂Me) with linker provided by the 17-propionate (red) and ethylene groups (blue).¹³

In dimers, energy transfer between the constituent monomers is difficult to detect owing to the absence of a distinguishing spectroscopic signature. In bacteriochlorin–chlorin dyads (Figure 4.5), however, the energy transfer is unidirectional due to the difference in excitation energies of the two constituents. Constructs **3-10** were prepared by esterification processes analogous to those described above.^{16-18,21} The chlorin could be selectively metalated in the presence of the free base bacteriochlorin. The absorption spectra of bacteriochlorin–chlorin dyads (**3**, **5b**, **7** and **10b**) typically represent the sum of the spectra of the corresponding monomers indicating the lack of strong interaction between the chromophores in the ground state. On the other hand, the fluorescence spectra showed emission characteristic of the bacteriochlorin (~760 nm) at the expense of that from the chlorin. In general, the dyads exhibit fast and efficient energy transfer (e.g., $k_{\text{trans}} = 4.5 \times 10^{10} \text{ s}^{-1}$, $\Phi_{\text{trans}} > 99\%$ for **3**),¹⁷ which is consistent with the Förster mechanism of resonant coupling

of the excited-state donor and ground-state absorber. Dyads **5-10** were examined as traps of excitation energy transfer among self-assembled zinc chlorins, where the chlorin of the dyad was envisaged to incorporate in the zinc-chlorin assembly.^{18,21} Bacteriochlorin dimer **1b** (Figure 4.3) was examined similarly.¹⁸

Naturally derived bacteriochlorins and synthetic, electron-acceptor moieties have been joined to give hybrid dyads for studies in artificial photosynthesis. Dyad **11** incorporates a C₆₀ fullerene attached to the 17³-position of a naturally derived bacteriochlorin (Figure 4.6).²⁰ Upon mixing with an assembly of zinc-chlorins, the bacteriochlorin moiety of **11** served as energy acceptor (from the chlorin assembly) as well as electron donor (to C₆₀) to yield the charge-separated state.²³ The 3-acetyl group of a naturally derived bacteriochlorin was employed to attach a pyromellitimide group *via* an acetal linkage (Figure 4.6). The resulting bacteriochlorin–pyromellitimide dyad (**12**) constitutes a donor-acceptor construct for studies of electron-transfer reactions.¹⁵



Dyad	M	X	R	n	Ref.
3	H, H	O	CHCH ₂	1	17
4	H, H	O	CHO	1	18
5a	H, H	O	CH ₂ OH	1	18
5b	Zn	O	CH ₂ OH	1	16,18,21
6a	H, H	H, H	CH ₂ OH	1	18
6b	Zn	H, H	CH ₂ OH	1	18
7	Zn	O	CH ₂ OH	3	18
8a	H, H	O	CH ₂ CH ₃	1	18
8b	Zn	O	CH ₂ CH ₃	1	18
8c	Cu	O	CH ₂ CH ₃	1	18
9a	H, H	H, H	CH ₂ CH ₃	1	18
9b	Zn	H, H	CH ₂ CH ₃	1	18

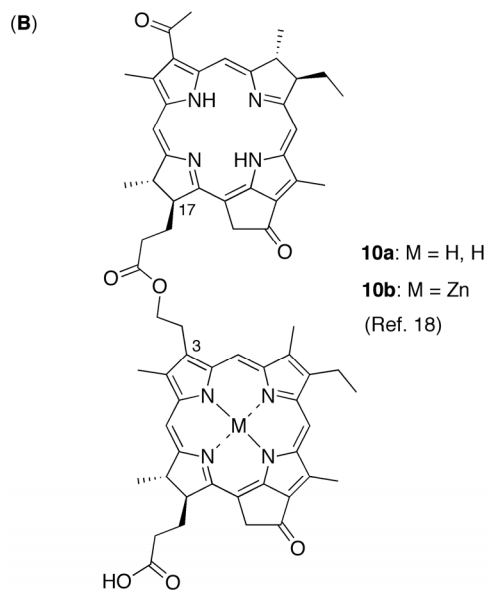


Figure 4.5. Bacteriochlorin–chlorin dyads (naturally derived constituents) linked at the (A) 17-17 or (B) 17-3 positions.

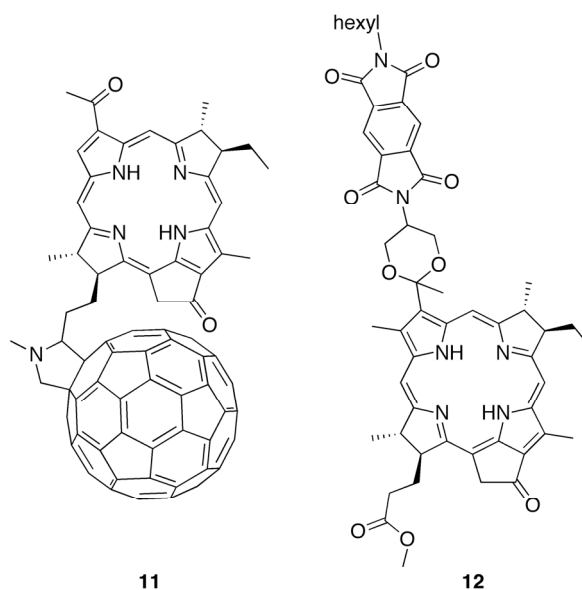


Figure 4.6. Hybrid dyads containing a naturally derived bacteriochlorin and a synthetic, electron-acceptor moiety.

Modification of the isocyclic ring of a bacteriochlorophyll can afford a bacteriochlorin bearing a six-membered imide ring. The imide stabilizes the macrocycle toward oxidation, shifts the long-wavelength absorption bathochromically by ~20-30 nm, and provides a new site for linkage. Dyads **13-15** incorporate linkers via the *N*-imide site (Figure 4.7). Dyad **13** comprises a C₆₀ moiety and a bacteriochlorin-imide with a short intervening linker.²² Excitation of **13** affords the radical ion pair, which decays rapidly to the bacteriochlorin triplet excited state. The bathochromic shift of the long-wavelength absorption band of bacteriochlorin-imides is attractive for photodynamic therapy (PDT). Dyads **14a,b**, designed for fluorescence diagnostics and PDT, showed absorption from 821–838 nm.²⁵ Dyads **15a,b** were designed for combined PDT and boron neutron capture

therapy.^{24,26} Bacteriochlorin-imides can now be created by *de novo* synthesis but have not yet been employed in arrays.³⁷

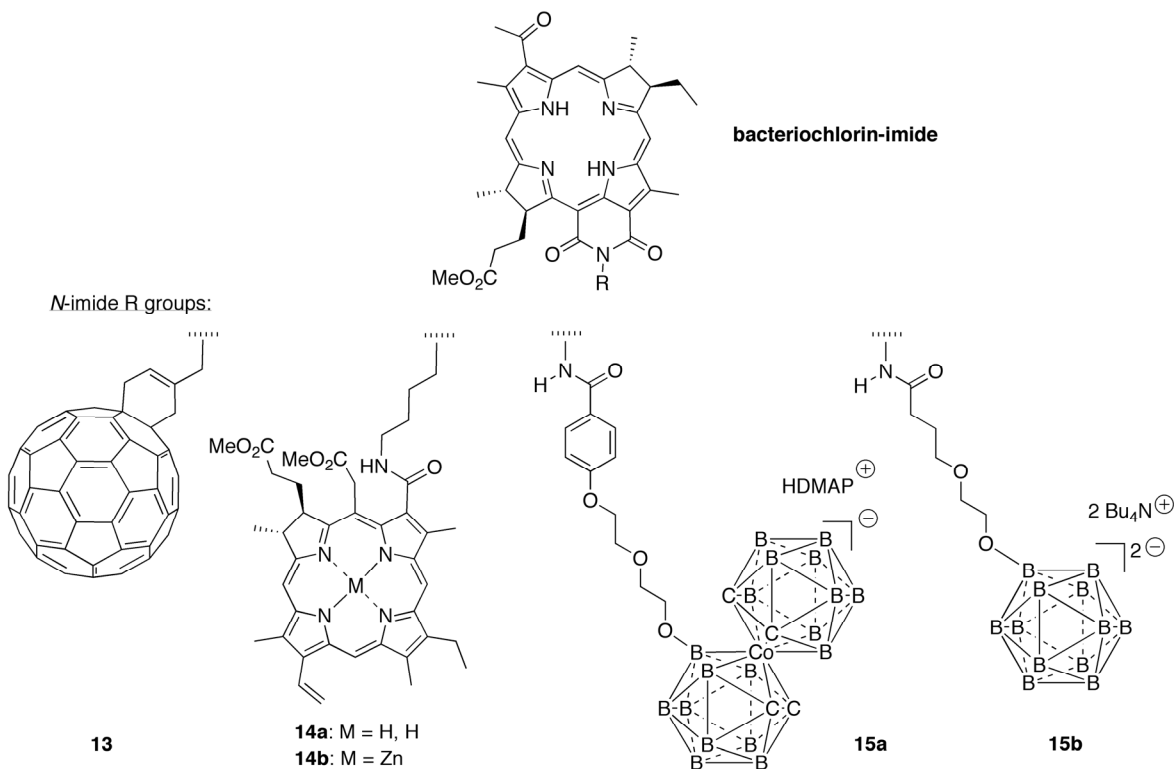


Figure 4.7. Dyads built around naturally derived bacteriochlorin-imides.

Synthetic dyads with a quinone attached directly (**16**) or via a 1,4-cyclohexylene linker (**17**) were prepared by diimide reduction of the corresponding porphyrin–hydroquinone followed by oxidation of the hydroquinone with *p*-benzoquinone (Figure 4.8). The bacteriochlorin cation radical and the quinone anion radical of **16** were each studied by electron paramagnetic resonance spectroscopy together with molecular orbital calculations,

which showed that the quinone had an insignificant effect on the electronic structure of the bacteriochlorin.¹⁹

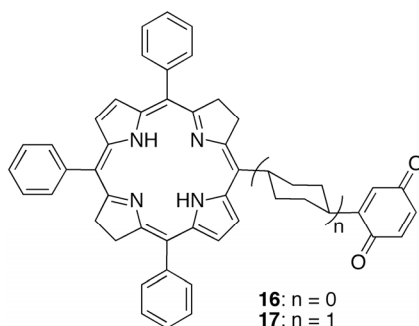


Figure 4.8. Synthetic bacteriochlorin–quinone dyads.

Monomers **18** and **19** were synthesized by *de novo* routes established for chlorins and bacteriochlorins, respectively.²⁷ A copper-free, Pd-mediated Sonogashira coupling of ethynylphenylchlorin **18** and bromobacteriochlorin **19** afforded phenylethyne-linked dyad **20a** (Figure 4.9). Treatment with zinc acetate gave selective metalation of the chlorin to afford the zinc-chlorin – free base bacteriochlorin (**20b**).²⁸ This result again highlights the ease of metalation in order of porphyrin > chlorin >> bacteriochlorin.

The chlorin and bacteriochlorin species in dyads **20a** and **20b** exhibit relatively narrow long-wavelength spectral bands (Figure 4.10). The absorption spectra of both dyads are essentially the sum of the spectra of the respective individual chromophores. Upon excitation of the (zinc or free base) chlorin, fast and efficient energy transfer ($k_{\text{trans}} \sim 2 \times 10^{11} \text{ s}^{-1}$, $\Phi_{\text{trans}} > 99\%$) occurred to the bacteriochlorin.^{27,28} The energy-transfer process is relatively insensitive to solvent polarity.^{28,29} The fluorescence emission of each dyad is nearly identical

with that of the bacteriochlorin monomer. Thus, each dyad behaves, operationally, as a single chromophore with large Stokes shift (85 nm for **20a**, 110 nm for **20b**). Large Stokes shifts together with narrow spectral bandwidths suggest the utility of such architectures for selective and multicolor NIR molecular imaging.^{28,29}

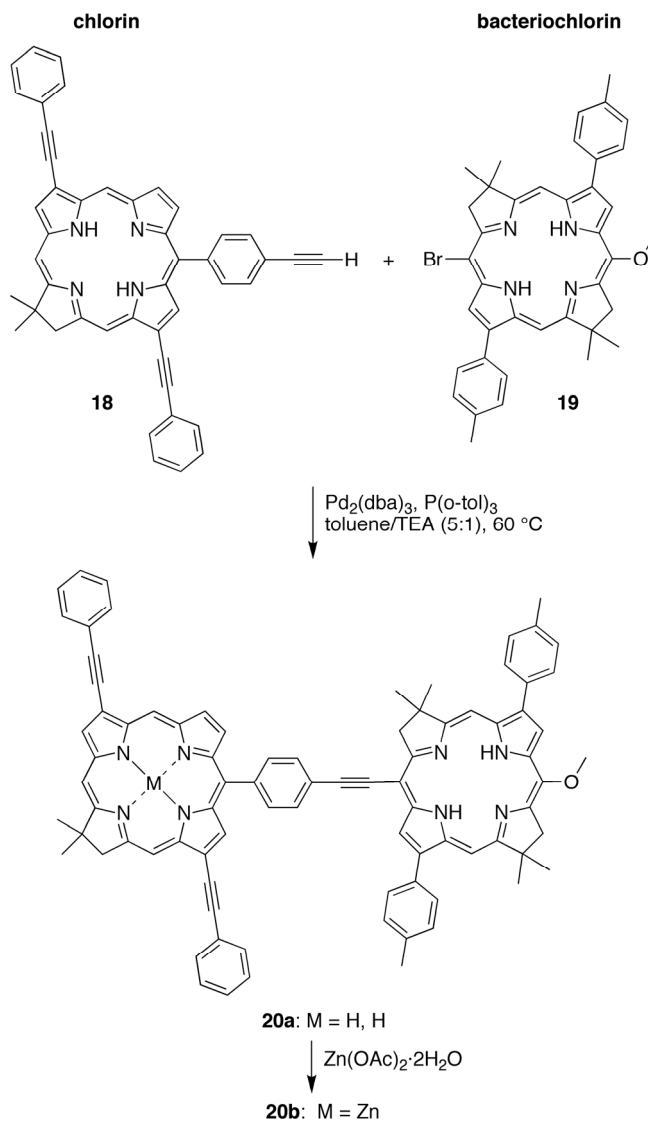


Figure 4.9. Bacteriochlorin–chlorin dyads prepared via *de novo* synthesis.

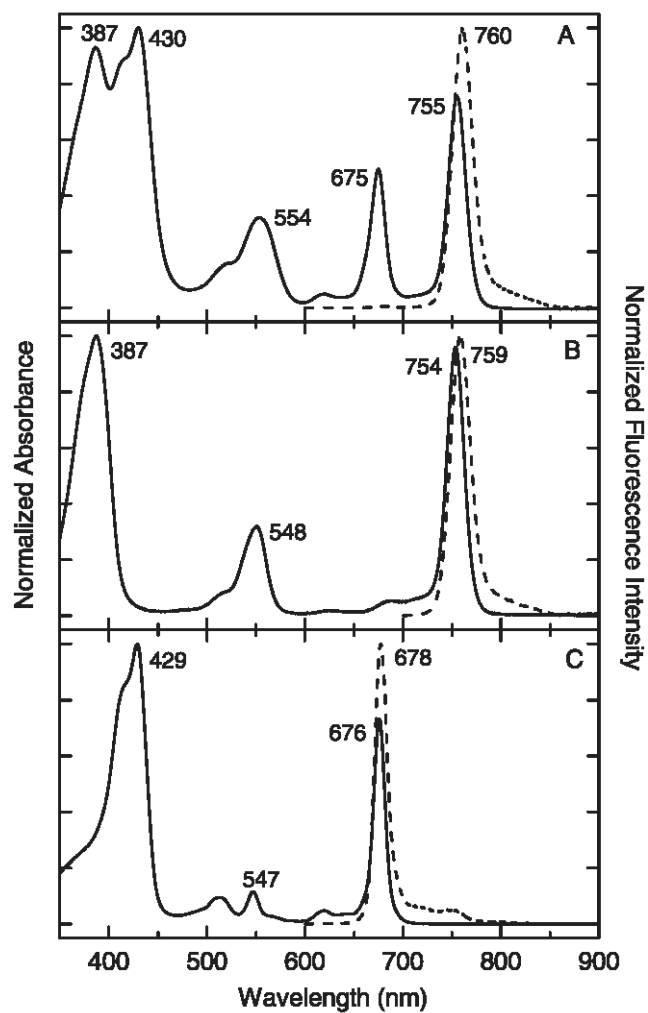


Figure 4.10. Normalized absorption spectra (solid) and fluorescence spectra (dashed) for (A) dyad **20a**, (B) benchmark bacteriochlorin monomer ($\lambda_{\text{exc}} = 548$ nm) and (C) benchmark chlorin monomer ($\lambda_{\text{exc}} = 550$ nm) in toluene at room temperature. Excitation of the dyad at 554 nm results in emission almost exclusively from the bacteriochlorin (760 nm).²⁷

Energy transfer in porphyrin versus hydroporphyrin arrays

Energy transfer is a central feature of light-harvesting arrays, enabling migration of the excited state among constituent chromophores. Extensive studies of porphyrin-containing arrays have revealed that fast and efficient energy transfer can be achieved despite a weak Förster, through-space (TS) coupling of the porphyrin chromophores.³⁸ The inefficient TS process stems from the typically weak transition dipoles characteristic of porphyrins (i.e., the low intensity of the long wavelength absorption band). The TS process can be complemented by a through-bond (TB) coupling mediated by the covalent linker; the observed energy-transfer process is the sum of the two mechanisms. The efficacy of the TB mechanism depends on a number of specific molecular design constraints, including electronic properties of the linker and conjugation of the linker with sites on the chromophores where the frontier molecular orbitals have high electron density.

The chlorin–bacteriochlorin dyads **20a** and **20b** undergo fast and efficient energy transfer, which could be fully explained by a TS (Förster) process despite the presence of a (phenylethyne) linker that is known to enable TB communication upon use in porphyrin arrays.²⁷ The strong TS process is not surprising given the magnitude of the respective hydroporphyrin transition dipoles. (In chlorin–chlorin dyads, where the chlorins have transition dipole strengths between those of porphyrins and bacteriochlorins, the TS and TB contributions can afford rates of comparable magnitude.³⁹) Although the magnitude of any TB contribution to energy transfer in bacteriochlorin arrays is not known, the apparently dominant TS mechanism affords versatility in the design of bacteriochlorin versus porphyrin arrays. Thus, in arrays wherein TB transfer is dominant (e.g., with porphyrins), the linker

must serve both architectural and electronic functions. By contrast, in arrays wherein TS transfer is dominant (e.g., with bacteriochlorins), the linker serves predominantly as an architectural unit and, therefore, can be chosen with considerable latitude with regards to molecular structure and site of chromophore attachment.

Outlook

Only about twenty bacteriochlorin dyads have been reported since the first such dyad over 30 years ago, yet studies of the bacteriochlorin dyads have expanded our knowledge related to photobiological phenomena and provided an enticing glimpse of potential photochemical applications. The dearth of dyads undoubtedly has stemmed from synthetic limitations, causing use of the structurally related porphyrins as synthetically accessible surrogates despite (i) their total lack of NIR absorption, and (ii) different molecular design criteria for light-harvesting. The recent advances in *de novo* routes to stable, tailorable, wavelength-tunable bacteriochlorins enables access to diverse bacteriochlorins for incorporation into arrays. Still, the elaboration of bacteriochlorin arrays of performance and architectural complexity rivaling existing porphyrin arrays requires a number of advances in synthetic chemistry and molecular design, including learning to: (1) introduce complex patterns of non-identical substituents about the perimeter of the macrocycle, (2) metalate bacteriochlorins (so as to alter spectra, tune energy levels, and enable ligand coordination); and (3) introduce motifs that shift the long-wavelength absorption deeper into the NIR (>850 nm) spectral region.

References

- (1) Scheer, H. In *Chlorophylls and Bacteriochlorophylls: Biochemistry, Biophysics, Functions and Applications*; Grimm, B.; Porra, R. J.; Rüdiger, W.; Scheer, H., Eds.; Springer: Dordrecht, The Netherlands, 2006, pp 1–26.
- (2) Dixon, J. M.; Taniguchi, M.; Lindsey, J. S. *Photochem. Photobiol.* **2005**, *81*, 212–213.
- (3) Taniguchi, M.; Cramer, D. L.; Bhise, A. D.; Kee, H. L.; Bocian, D. F.; Holten, D.; Lindsey, J. S. *New J. Chem.* **2008**, *32*, 947–958.
- (4) de Wilton, A. C.; Koningstein, J. A. *J. Am. Chem. Soc.* **1984**, *106*, 5088–5093.
- (5) Gottfried, D. S.; Boxer, S. G. *J. Luminescence* **1992**, *51*, 39–50.
- (6) Hanke, T.; Korth, O.; Rückmann, I.; Röder, B.; *Thin Solid Films* **1997**, *299*, 152–160.
- (7) Scherz, A.; Parson, W. W. *Biochim. Biophys. Acta* **1984**, *766*, 653–665.
- (8) Noy, D.; Dutton, P. L. *Biochemistry (A.C.S.)* **2006**, *45*, 2103–2113.
- (9) Wright, K. A.; Boxer, S. G. *Biochemistry (A.C.S.)* **1981**, *20*, 7546–7556.
- (10) Dandler, J.; Scheer, H. *Langmuir* **2009**, *25*, 11988–11992.
- (11) Harvey, P. D. In *The Porphyrin Handbook*; Kadish, K. M., Smith, K. M., Guillard, R., Eds.; Academic Press: San Diego, CA, 2003; Vol. 18, pp 63–250.
- (12) Aratani, N.; Osuka, A. In *Handbook of Porphyrin Science*; World Scientific Publishing Co.: Singapore, 2010, Vol. 1, ch. 1, pp. 1–132.
- (13) Wasielewski, M. R.; Smith, U. H.; Cope, B. T.; Katz, J. J. *J. Am. Chem. Soc.* **1977**, *99*, 4172–4173.
- (14) Wasielewski, M. R.; Svec, W. A. *J. Org. Chem.* **1980**, *45*, 1969–1974.

- (15) Osuka, A.; Marumo, S.; Wada, Y.; Yamazaki, I.; Yamazaki, T.; Shirakawa, Y.; Nishimura, Y. *Bull. Chem. Soc. Jpn.* **1995**, *68*, 2909–2915.
- (16) Tamiaki, H.; Miyatake, T.; Tanikaga, R.; Holzwarth, A. R.; Schaffner, K. *Angew. Chem. Int. Ed. Engl.* **1996**, *35*, 772–774.
- (17) Osuka, A.; Wada, Y.; Maruyama, K.; Tamiaki, H. *Heterocycles* **1997**, *44*, 165–168.
- (18) Miyatake, T.; Tamiaki, H.; Holzwarth, A. R.; Schaffner, K. *Photochem. Photobiol.* **1999**, *69*, 448–456.
- (19) Mössler, H.; Wittenberg, M.; Niethammer, D.; Mudrassagam, R. K.; Kurreck, H.; Huber, M. *Magn. Reson. Chem.* **2000**, *38*, 67–84.
- (20) Holzwarth, A. R.; Katterle, M.; Müller, M. G.; Ma, Y.-Z.; Prokhorenko, V. *Pure Appl. Chem.* **2001**, *73*, 469–474.
- (21) Prokhorenko, V. I.; Holzwarth, A. R.; Müller, M. G.; Schaffner, K.; Miyatake, T.; Tamiaki, H. *J. Phys. Chem. B* **2002**, *106*, 5761–5768.
- (22) Ohkubo, K.; Imahori, H.; Shao, J.; Ou, Z.; Kadish, K. M.; Chen, Y.; Zheng, G.; Pandey, R. K.; Fujitsuka, M.; Ito, O.; Fukuzumi, S. *J. Phys. Chem. A* **2002**, *106*, 10991–10998.
- (23) Katterle, M.; Prokhorenko, V. I.; Holzwarth, A. R.; Jesorka, A. *Chem. Phys. Lett.* **2007**, *447*, 284–288.
- (24) Grin, M. A.; Semioshkin, A. A.; Titeev, R. A.; Nizhnik, E. A.; Grebenyuk, J. N.; Mironov, A. F.; Bregadze, V. I. *Mendeleev Commun.* **2007**, *17*, 14–15.

- (25) Grin, M. A.; Lonin, I. S.; Fedyunin, S. V.; Tsiprovskiy, A. G.; Strizhakov, A. A.; Tsygankov, A. A.; Krasnovsky, A. A.; Mironov, A. F. *Mendeleev Commun.* **2007**, *17*, 209–211.
- (26) Grin, M. A.; Titeev, R. A.; Bakieva, O. M.; Brittal, D. I.; Lobanova, I. A.; Sivaev, I. B. Bregadze, V. I.; Mironov, A. F. *Russ. Chem. Bull. Int. Ed.* **2008**, *57*, 2230–2232.
- (27) Muthiah, C.; Kee, H. L.; Diers, J. R.; Fan, D.; Ptaszek, M.; Bocian, D. F.; Holten, D.; Lindsey, J. S. *Photochem. Photobiol.* **2008**, *84*, 786–801.
- (28) Kee, H. L.; Nothdurft, R.; Muthiah, C.; Diers, J. R.; Fan, D.; Ptaszek, M.; Bocian, D. F.; Lindsey, J. S.; Culver, J. P.; Holten, D. *Photochem. Photobiol.* **2008**, *84*, 1061–1072.
- (29) Kee, H. L.; Diers, J. R.; Ptaszek, M.; Muthiah, C.; Fan, D.; Lindsey, J. S.; Bocian D. F.; Holten, D. *Photochem. Photobiol.* **2009**, *85*, 909–920.
- (30) Silber, M. V.; Gabriel, G.; Strohmam, B.; Garcia-Martin, A.; Robert, B.; Braun, P. *Photosynth. Res.* **2008**, *96*, 145–151.
- (31) Chuang, J. I.; Boxer, S. G.; Holten, D.; Kirmaier, C. *J. Phys. Chem. B* **2008**, *112*, 5487–5499.
- (32) Galezowski, M.; Gryko, D. T. *Curr. Org. Chem.* **2007**, *11*, 1310–1338.
- (33) Grin, M. A.; Mironov, A. F.; Shtil, A. A. *Anti-Cancer Agents Med. Chem.* **2008**, *8*, 683–697.
- (34) Chen, Y.; Li, G.; Pandey, R. K. *Curr. Org. Chem.* **2004**, *8*, 1105–1134.
- (35) Kim, H.-J.; Lindsey, J. S. *J. Org. Chem.* **2005**, *70*, 5475–5486.

- (36) Krayner, M.; Ptaszek, M.; Kim, H.-J.; Meneely, K. R.; Fan, D.; Secor, K.; Lindsey, J. *S. J. Org. Chem.* **2010**, *75*, 1016–1039.
- (37) Krayner, M.; Yang, E.; Diers, J. R.; Bocian, D. F.; Holten, D.; Lindsey, J. S. *New J. Chem.* **2011**, *35*, 587-601.
- (38) Holten, D.; Bocian, D. F.; Lindsey, J. S. *Acc. Chem. Res.* **2002**, *35*, 57–69.
- (39) Taniguchi, M.; Ra, D.; Kirmaier, C.; Hindin, E. K.; Schwartz, J. K.; Diers, J. R.; Bocian, D. F.; Lindsey, J. S.; Knox, R. S.; Holten, D. *J. Am. Chem. Soc.* **2003**, *125*, 13461–13470.
- (40) Lindsey, J. S.; Mass, O.; Chen, C.-Y. *New J. Chem.* **2011**, *35*, 511–516.